TARGETING INFLAMMATION IN ATHEROSCLEROSIS AND MYOCARDIAL INFARCTION

JELTE ELLENBROEK

Targeting inflammation in atherosclerosis and myocardial infarction

ISBN/EAN 9789462336803
Cover design Kriti Verma
Layout Wendy Schoneveld || wenz iD.nl
Printing Gildeprint – Enschede

Targeting inflammation in atherosclerosis and myocardial infarction

Beïnvloeding van de ontstekingsreactie
in slagaderverkalking en hartinfarct

(met een samenvatting in het Nederlands)

Proefschrift

ter verkrijging van de graad van doctor aan de Universiteit Utrecht
op gezag van de rector magnificus, prof.dr. G.J. van der Zwaan,
ingevolge het besluit van het college voor promoties in het openbaar
te verdedigen op donderdag 14 september 2017 des middags te 2.30 uur

door

Guilielmus Hendrikus Johanna Maria Ellenbroek

geboren op 20 december 1988 te Heerlen

Promotoren: Prof.dr. G. Pasterkamp
Prof.dr. P.A.F.M. Doevendans

Copromotoren: Dr. I.E. Hoefer
Dr. L. Timmers

Financial support by the Dutch Heart Foundation for the publication of this thesis is gratefully acknowledged.

Financial support by AstraZeneca, International Cardio Corporation, OrbusNeich Medical and Silver Creek Pharmaceuticals is also greatly acknowledged.

Additional financial support was granted by Chipsoft B.V., Fujifilm VisualSonics Inc., Heart & Lung foundation Utrecht, Servier Nederland Farma B.V., Sanofi, Stichting Cardiovasculaire Biologie and Transonic Europe B.V.

Voor mijn ouders

TABLE OF CONTENTS

PART THREE SUMMARY AND DISCUSSION

PART FOUR ADDENDUM

CHAPTER 1

Introduction and thesis outline

BURDEN OF ISCHEMIC HEART DISEASE

Ischaemic heart disease (IHD), also known as coronary artery disease (CAD), is one of the major causes of morbidity and mortality worldwide, with an estimated death rate of 7.4 million in 2012.[1] The growing incidence of cardiovascular risk factors such as obesity, diabetes, hypertension and physical inactivity warrants an increase in CAD[2], especially in developing countries.[3] CAD is caused by the accumulation of lipids and inflammatory cells in the arterial walls that form atherosclerotic plaques.[4] Unstable coronary plaques are prone to erosion or rupture, obstructing coronary blood flow and causing an acute myocardial infarction (MI).[5] Despite optimal medical treatment, the risk of recurrent major adverse cardiovascular events (MACE) in these patients remains substantial[6], emphasizing the need for additional treatment options.

Although the detection and treatment of MI have improved over the years, still 5% of patients die within the first month after MI.[3,7] Moreover, approximately one in four patients surviving an MI develops heart failure (HF)[8], with a 5-year survival of less than 50%.[9] HF comes with the largest increase in loss of productivity and direct medical costs in the next 20 years[10], stressing the need for novel therapies to target both, atherosclerosis and the development of HF after MI.

Inflammation in atherosclerosis

Atherosclerosis has long been thought to be a disease primarily caused by lipids.[11] However, from the last decades of the 20th century onward, there have been a rising number of publications suggesting a key role for the immune system in this process, and particularly in CAD.[12] Specifically, monocytes[13,14] and T-lymphocytes[15] play an important role and their numbers are strongly related to the risk of CAD.[16,17]

In addition to leukocyte counts, their activation status greatly affects atherosclerotic plaque formation, progression and destabilization. Important leukocyte activators are pattern recognition receptors (PRR)[18], in particular the highly conserved Toll-like receptors (TLRs).[19] TLRs recognize pathogen- and danger-associated molecular patterns (PAMPs/DAMPs)[20,21], signalling molecules (e.g. LPS, oxidized LDL) that are present in atherosclerotic plaques and are released in the circulation upon vascular injury.[22] Binding of PAMPs or DAMPs to TLRs enables nuclear translocation of their main transcription factor NFκB and subsequent release of pro-inflammatory cytokines like interleukin-6 and TNF-α.[23,24] In general, TLR–mediated leukocyte activation has been shown to accelerate the process of atherosclerosis.[25]

Amongst others, TLRs facilitate the recruitment and activation of inflammatory cells to the plaque and exert detrimental effects upon activation. An important conduit for inflammatory cell recruitment in atherosclerosis is through the adventitial vasa vasorum.

Vasa vasorum not only supply the vessel wall with oxygen and nutrients, but also highly correlate with inflammatory cell density in the plaque and their reduction reduces macrophage influx.[26] Moreover, immature and leaky neovessels arising from the vasa vasorum are the major source of intraplaque haemorrhage, key in plaque destabilization.[27] Current interventional strategies for atherosclerosis aim at maintaining luminal patency by percutaneous coronary intervention (PCI). A major drawback from plain old balloon angioplasty (POBA) and stent implantation is the induction of an inflammatory response that leads to smooth muscle cell (SMC) proliferation and restenosis.[28] Although drug-eluting stents (DES) with an anti-proliferative coating increase patency rates[29], concomitant non-specific anti-proliferative effects hamper endothelial coverage.[30] Impaired endothelial strut coverage increases the stent strut's exposure to blood cells, thus increasing the deposition of inflammatory cells and platelets. This tightly linked process of inflammation and coagulation increases the risk for stent thrombosis[31], that could be prevented by stent endothelialisation.

Myocardial infarction and ischemia-reperfusion injury

Rupture or erosion of an atherosclerotic plaque induces thrombotic clot formation and blocks the coronary artery, depriving the corresponding myocardium of oxygen and nutrients.[32] Cardiomyocytes will then change to an anaerobic metabolism, which leads to intracellular accumulation of hydrogen ions (H^+) and decreased pH. This activates the Na^+/H^+ exchanger, which increases intracellular [Na^+]. In turn, increased intracellular [Na^+] activates the $2Na^+/Ca^{2+}$ exchanger, which increases intracellular [Ca^{2+}], leading to hypercontracture, membrane rupture and (eventually) cell death. Over time, this "wave front" of cell death spreads from subendocardium to epicardium.[33]

Infarct size is the main determinant of adverse left ventricular (LV) remodelling and subsequent HF.[34] Since adverse remodelling is strongly associated with increased morbidity and mortality rates[35], restoration of myocardial blood flow (reperfusion) is essential to salvage myocardial tissue and to preserve cardiac function.[36] Paradoxically, reperfusion itself also induces myocardial injury (ischemia-reperfusion injury).[37,38] Abrupt reoxygenation of previously ischemic cardiac tissue will induce the switch of cardiomyocytes to an aerobic metabolism. Similar to the processes described above, activation of the H^+/Na^+ and $2Na^+/Ca^{2+}$ exchanger will eventual increase intracellular [Ca^{2+}] and induce hypercontracture and cell death.

In addition, the previously damaged cardiac tissue is unable to adequately reduce normalized oxygen levels, which leads to an enormous increase in the production of highly reactive molecules and radicals called reactive oxygen species (ROS).[39] Although low concentrations of ROS are important in cell signalling, excessive ROS is detrimental for protein function and membrane permeability, leading to cellular destruction.

Inflammation in ischemia-reperfusion injury and cardiac remodelling

ROS and DAMPs from damaged myocardial cells increase the secretion of chemokines/cytokines in the bloodstream and the expression of adhesion molecules on the endothelium.[39–41] Cardiomyocytes, cardiofibroblasts and infiltrated inflammatory cells are activated by binding of DAMPs to PRRs, that can be either located at the cell membrane (*e.g.* the majority of TLRs) or in the cytosol (*e.g.* NOD-like receptors (NLRs)).[24,42] Activating cardiomyocyte and leukocyte receptors are key in pro-inflammatory signalling and leukocyte recruitment.[42–44] Although leukocytes are to some extent necessary for dead tissue clearance to allow for subsequent cardiac repair, their excessive infiltration and deposition is considered detrimental.[24] Of the recruited leukocytes, neutrophils are the first to enter, followed by monocytes.[45–47] They are known to be an important source of ROS as well as lysosomal proteolytic enzymes[48], responsible for additional cardiomyocyte death and an increase in infarct size.

In addition to their effect on infarct size, leukocytes play an important role in adverse LV remodelling.[49–51] In the first days after MI, secretion of serine proteases and matrix metalloproteinases (MMPs) leads to degradation of intermyocyte collagen struts.[52] Together with the loss in functional myocardium, wall stress increases and results in progressive cardiomyocyte slippage in the border zone and the remote part, resulting in wall thinning and ventricular dilatation.[53] Various neurohumoral pathways are then initiated and induce myocyte hypertrophy and fibrosis to redistribute wall stress more evenly, to counteract the distending forces and to prevent further ventricular dilatation.

THESIS OUTLINE

The great impact that atherosclerosis and ischemic heart disease still have on individual patients and on society stresses the need for the advent of novel treatments. Despite introduction of evidence-based medical therapy, ischemic heart disease remains the leading cause of death worldwide.[54] Improved targeting of atherosclerotic plaque burden and vulnerability could prevent the occurrence of MI and concomitant morbidity and mortality. To further improve outcome after MI, treatments to decrease infarct size and optimize myocardial healing are required. Inflammation has been shown to be key in all of the above (overlapping) processes. The current thesis therefore aims to decrease the burden of ischemic heart disease by targeting inflammation in atherosclerosis and myocardial infarction.

The first part of this thesis deals with inflammation in atherosclerosis and a variety of targets for treatment thereof. In chapter 2, the effect of hematopoietic TLR5 deficiency on plaque formation in mice is investigated. Chapter 3 evaluates the safety and feasibility of

radiofrequency ablation (RFA) in atherosclerotic plaques in rabbits. The effect of anti-CD34 coated stents on endothelialisation in rabbits is shown in chapter 4.
The second part of this thesis deals with inflammation in MI, one of the most detrimental consequences of atherosclerosis. Chapter 5 evaluates the regulation of LAIR-1 upon MI in patients and further investigates the effect of the LAIR-1 deficiency in a murine model of ischemia-reperfusion injury and remodelling. In chapter 6, we provide a detailed overview of some of the primary outcome measurements in the evaluation of novel treatments for acute MI in pigs. The inhibition of myeloperoxidase (MPO) and its effect on infarct size and ischemia-reperfusion injury is discussed in chapter 7. In a similar pig model of ischemia-reperfusion injury we studied the effect of NLRP3 inflammasome inhibition in chapter 8. In the chapters 9 and 10, the results and conclusions of the previous chapters are discussed, including future perspectives for translational research with respect to inflammation in atherosclerosis and MI.

REFERENCES

1. WHO. Causes of death, 2000-2012 [Internet]. 2012 [cited 2015 Apr 11];Available from: http://www.who.int/mediacentre/factsheets/fs310/en/
2. Mozaffarian D, Benjamin EJ, Go AS, Arnett DK, Blaha MJ, Das SR, Ferranti S De, Després J, Fullerton HJ, Howard J, Huffman MD, Isasi CR, Jiménez MC, Judd SE, Brett M, Lichtman JH, Lisabeth LD, Liu S, Mackey RH, Magid DJ, Mcguire DK, Mohler ER, Moy CS, Muntner P, Mussolino ME, Nasir K, Neumar RW, Nichol G, Palaniappan L, Pandey DK, Mathew J, Rodriguez CJ, Rosamond W, Sorlie PD, Stein J, Towfighi A, Turan N, Virani SS, Woo D, Yeh RW, Turner MB. Heart Disease and Stroke Statistics—2016 Update: A Report From the American Heart Association. *Circulation*. 2016;1–668.
3. Gaziano TA, Bitton A, Anand S, Abrahams-Gessel S, Murphy A. Growing Epidemic of Coronary Heart Disease in Low- and Middle- Income Countries. *Currative Probl Cardiol*. 2011;35:72–115.
4. Hansson GK. Inflammation and coronary artery disease. *N Engl J Med*. 2005;352:1685–95.
5. Finn A V., Nakano M, Narula J, Kolodgie FD, Virmani R. Concept of vulnerable/unstable plaque. *Arterioscler Thromb Vasc Biol*. 2010;30:1282–1292.
6. Udell JA, Bonaca MP, Collet J, Lincoff AM, Kereiakes DJ, Costa F, Lee CW, Mauri L, Valgimigli M, Park S, Montalescot G, Sabatine MS, Braunwald E, Bhatt DL. Long-term dual antiplatelet therapy for secondary prevention of cardiovascular events in the subgroup of patients with previous myocardial infarction : a collaborative meta-analysis of randomized trials. *Eur Heart J*. 2016;37:390–399.
7. Roe MT, Messenger JC, Weintraub WS, Cannon CP, Fonarow GC, Dai D, Chen AY, Klein LW, Masoudi FA, McKay C, Hewitt K, Brindis RG, Peterson ED, Rumsfeld JS. Treatments, trends, and outcomes of acute myocardial infarction and percutaneous coronary intervention. *J Am Coll Cardiol*. 2010;56:254–263.
8. Jhund PS, McMurray JJ V. Heart failure after acute myocardial infarction: a lost battle in the war on heart failure? *Circulation*. 2008;118:2019–2021.
9. Roger VL. Epidemiology of heart failure. *Circ Res*. 2013;113:646–659.
10. Heidenreich PA, Trogdon JG, Khavjou OA, Butler J, Dracup K, Ezekowitz MD, Finkelstein EA, Hong Y, Johnston SC, Khera A, Lloyd-Jones DM, Nelson SA, Nichol G, Orenstein D, Wilson PWF, Woo YJ. Forecasting the future of cardiovascular disease in the United States: A policy statement from the American Heart Association. *Circulation*. 2011;123:933–944.
11. Kannel WB, McGee D, Gordon T. A General Cardiovascular Risk Profile: The Framingham Study. *Am J Cardiol*. 1976;36:46–51.
12. Libby P. History of Discovery: Inflammation in Atherosclerosis. *Arter Thromb Vasc Biol*. 2012;32:2045–2051.
13. Woollard KJ, Geissmann F. Monocytes in atherosclerosis: subsets and functions. *Nat Rev Cardiol*. 2010;7:77–86.
14. Ghattas A, Griffiths HR, Devitt A, Lip GYH, Shantsila E. Monocytes in coronary artery disease and atherosclerosis: where are we now? *J Am Coll Cardiol*. 2013;62:1541–1551.
15. Hedrick CC. Lymphocytes in Atherosclerosis. *Arterioscler Thromb Vasc Biol*. 2015;35:253–257.
16. Madjid M, Awan I, Willerson JT, Casscells SW. Leukocyte count and coronary heart disease: Implications for risk assessment. *J Am Coll Cardiol*. 2004;44:1945–1956.
17. Núñez J, Miñana G, Bodí V, Núñez E, Sanchis J, Husser O, Llàcer A. Low lymphocyte count and cardiovascular diseases. *Curr Med Chem*. 2011;18:3226–33.
18. Mogensen TH. Pathogen recognition and inflammatory signaling in innate immune defenses. *Clin Microbiol Rev*. 2009;22:240–273.
19. Medzhitov R. Toll-like receptors and innate immunity. *Nat Rev Immunol*. 2001;1:135–145.
20. Seong S-Y, Matzinger P. Hydrophobicity: an ancient damage-associated molecular pattern that initiates innate immune responses. *Nat Rev Immunol*. 2004;4:469–478.
21. O'Neill LAJ. The interleukin-1 receptor/Toll-like receptor superfamily: 10 Years of progress. *Immunol Rev*. 2008;226:10–18.
22. Zheng Y, Gardner SE, Clarke MCH. Cell death, damage-associated molecular patterns, and sterile inflammation in cardiovascular disease. *Arterioscler Thromb Vasc Biol*. 2011;31:2781–2786.
23. Ikeda U, Ohkawa F, Seino Y, Yamamoto K, Hidaka Y, Kasahara T, Kawai T, Shimada K. Serum interleukin 6 levels become elevated in acute myocardial infarction. *J Mol Cell Cardiol*. 1992;24:579–84.
24. Frangogiannis NG. The inflammatory response in myocardial injury, repair, and remodelling. *Nat Rev Cardiol*. 2014;11:255–265.
25. Falck-hansen M, Kassiteridi C. Toll-Like Receptors in Atherosclerosis. *Int J Mol Sci*. 2013;14:14008–14023.
26. Moulton KS, Vakili K, Zurakowski D, Soliman M, Butterfield C, Sylvin E, Lo K-M, Gillies S, Javaherian K, Folkman J. Inhibition of plaque neovascularization reduces macrophage accumulation and progression of advanced atherosclerosis. *Proc Natl Acad Sci U S A*. 2003;100:4736–41.
27. Kolodgie FD, Gold HK, Burke AP, Fowler DR, Kruth HS, Weber DK, Farb A, Guerrero LJ, Hayase M, Kutys R, Narula J, Finn A V, Virmani R. Intraplaque hemorrhage and progression of coronary atheroma. *N Engl J Med*. 2003;349:2316–2325.
28. Alfonso F, Byrne RA, Rivero F, Kastrati A. Current treatment of in-stent restenosis. *J Am Coll Cardiol*. 2014;63:2659–2673.
29. Nakazawa G, Finn A V., Virmani R. Vascular pathology of drug-eluting stents. *Herz*. 2007;32:274–80.

30. Joner M, Finn A V., Farb A, Mont EK, Kolodgie FD, Ladich E, Kutys R, Skorija K, Gold HK, Virmani R. Pathology of drug-eluting stents in humans: delayed healing and late thrombotic risk. *J Am Coll Cardiol*. 2006;48:193–202.
31. Lüscher TF, Steffel J, Eberli FR, Joner M, Nakazawa G, Tanner FC, Virmani R. Drug-eluting stent and coronary thrombosis: biological mechanisms and clinical implications. *Circulation*. 2007;115:1051–8.
32. Tarantini G, Cacciavillani L, Corbetti F, Ramondo A, Marra MP, Bacchiega E, Napodano M, Bilato C, Razzolini R, Iliceto S. Duration of ischemia is a major determinant of transmurality and severe microvascular obstruction after primary angioplasty: a study performed with contrast-enhanced magnetic resonance. *J Am Coll Cardiol*. 2005;46:1229–35.
33. Hausenloy D, Yellon D. Myocardial ischemia-reperfusion injury: a neglected therapeutic target. *J Clin Invest*. 2013;123:92–100.
34. Chareonthaitawee P, Christian TF, Hirose K, Gibbons RJ, Rumberger JA. Relation of initial infarct size to extent of left ventricular remodeling in the year after acute myocardial infarction. *J Am Coll Cardiol*. 1995;25:567–73.
35. Burns RJ, Gibbons RJ, Yi Q, Roberts RS, Miller TD, Schaer GL, Anderson JL, Yusuf S. The relationships of left ventricular ejection fraction, end-systolic volume index and infarct size to six-month mortality after hospital discharge following myocardial infarction treated by thrombolysis. *J Am Coll Cardiol*. 2002;39:30–36.
36. Domburg RT, Hendriks JM, Kamp O, Smits P, Melle M, Schenkeveld L, Bax JJ, Simoons ML. Three life years gained after reperfusion therapy in acute myocardial infarction: 25-30 years after a randomized controlled trial. *Eur J Prev Cardiol*. 2012;19:1316–1323.
37. Yellon DM, Hausenloy DJ. Myocardial reperfusion injury. *N Engl J Med*. 2007;357:1221–35.
38. Ibáñez B, Heusch G, Ovize M, Van De Werf F. Evolving therapies for myocardial ischemia/reperfusion injury. *J Am Coll Cardiol*. 2015;65:1454–1471.
39. Braunersreuther V, Jaquet V. Reactive Oxygen Species in Myocardial Reperfusion Injury: From Physiopathology to Therapeutic Approaches. *Curr Pharm Biotechnol*. 2012;13:97–114.
40. Mulligan MS, Varani J, Warren JS, Till GO, Smith CW, Anderson DC, Todd RF, Ward P a. Roles of beta 2 integrins of rat neutrophils in complement- and oxygen radical-mediated acute inflammatory injury. *J Immunol*. 1992;148:1847–57.
41. Tang T-T, Yuan J, Zhu Z-F, Zhang W-C, Xiao H, Xia N, Yan X-X, Nie S-F, Liu J, Zhou S-F, Li J-J, Yao R, Liao M-Y, Tu X, Liao Y-H, Cheng X. Regulatory T cells ameliorate cardiac remodeling after myocardial infarction. *Basic Res Cardiol*. 2012;107:1–17.
42. van Hout GPJ, Arslan F, Pasterkamp G, Hoefer IE. Targeting danger-associated molecular patterns after myocardial infarction. *Expert Opin Ther Targets*. 2016;20:223–239.
43. Arslan F, de Kleijn DP, Pasterkamp G. Innate immune signaling in cardiac ischemia. *Nat Rev Cardiol*. 2011;8:292–300.
44. Kubota A, Hasegawa H, Tadokoro H, Hirose M, Kobara Y, Yamada-Inagawa T, Takemura G, Kobayashi Y, Takano H. Deletion of CD28 Co-stimulatory Signals Exacerbates Left Ventricular Remodeling and Increases Cardiac Rupture After Myocardial Infarction. *Circ J*. 2016;80:9171–1979.
45. Baxter GF. The neutrophil as a mediator of myocardial ischemia-reperfusion injury: Time to move on. *Basic Res Cardiol*. 2002;97:268–275.
46. Van Der Laan AM, Ter Horst EN, Delewi R, Begieneman MP V, Krijnen PAJ, Hirsch A, Lavaei M, Nahrendorf M, Horrevoets AJ, Niessen HWM, Piek JJ. Monocyte subset accumulation in the human heart following acute myocardial infarction and the role of the spleen as monocyte reservoir. *Eur Heart J*. 2014;35:376–385.
47. Frangogiannis N. The inflammatory response in myocardial infarction. *Cardiovasc Res*. 2002;53:31–47.
48. Vinten-Johansen J. Involvement of neutrophils in the pathogenesis of lethal myocardial reperfusion injury. *Cardiovasc Res*. 2004;61:481–497.
49. Hong YJ, Jeong MH, Ahn Y, Yoon NS, Lee SR, Hong SN, Moon JY, Kim KH, Park HW, Kim JH, Cho JG, Park JC, Kang JC. Relationship between peripheral monocytosis and nonrecovery of left ventricular function in patients with left ventricular dysfunction complicated with acute myocardial infarction. *Circ J*. 2007;71:1219–24.
50. Westermann D, Lindner D, Kasner M, Zietsch C, Savvatis K, Escher F, von Schlippenbach J, Skurk C, Steendijk P, Riad A, Poller W, Schultheiss H-P, Tschöpe C. Cardiac inflammation contributes to changes in the extracellular matrix in patients with heart failure and normal ejection fraction. *Circ Hear Fail*. 2011;4:44–52.
51. Seropian IM, Toldo S, Van Tassell BW, Abbate A. Anti-inflammatory strategies for ventricular remodeling following St-segment elevation acute myocardial infarction. *J Am Coll Cardiol*. 2014;63:1593–1603.
52. Cleutjens JPM, Kandala JC, Guarda E, Guntaka R V., Weber KT. Regulation of collagen degradation in the rat myocardium after infarction. *J Mol Cell Cardiol*. 1995;27:1281–1292.
53. Sutton SJ, Sharpe N. Left Ventricular Remodeling After Myocardial Infarction Pathophysiology and Therapy. *Circulation*. 2000;101:2981–2988.
54. GBD 2013 Mortality and Causes of Death Collaborators*. Global, regional, and national age – sex specific all-cause and cause-specific mortality for 240 causes of death, 1990 – 2013: a systematic analysis for the Global Burden of Disease Study 2013. *Lancet*. 2014;385:117–171.

PART ONE
TARGETING INFLAMMATION IN ATHEROSCLEROSIS

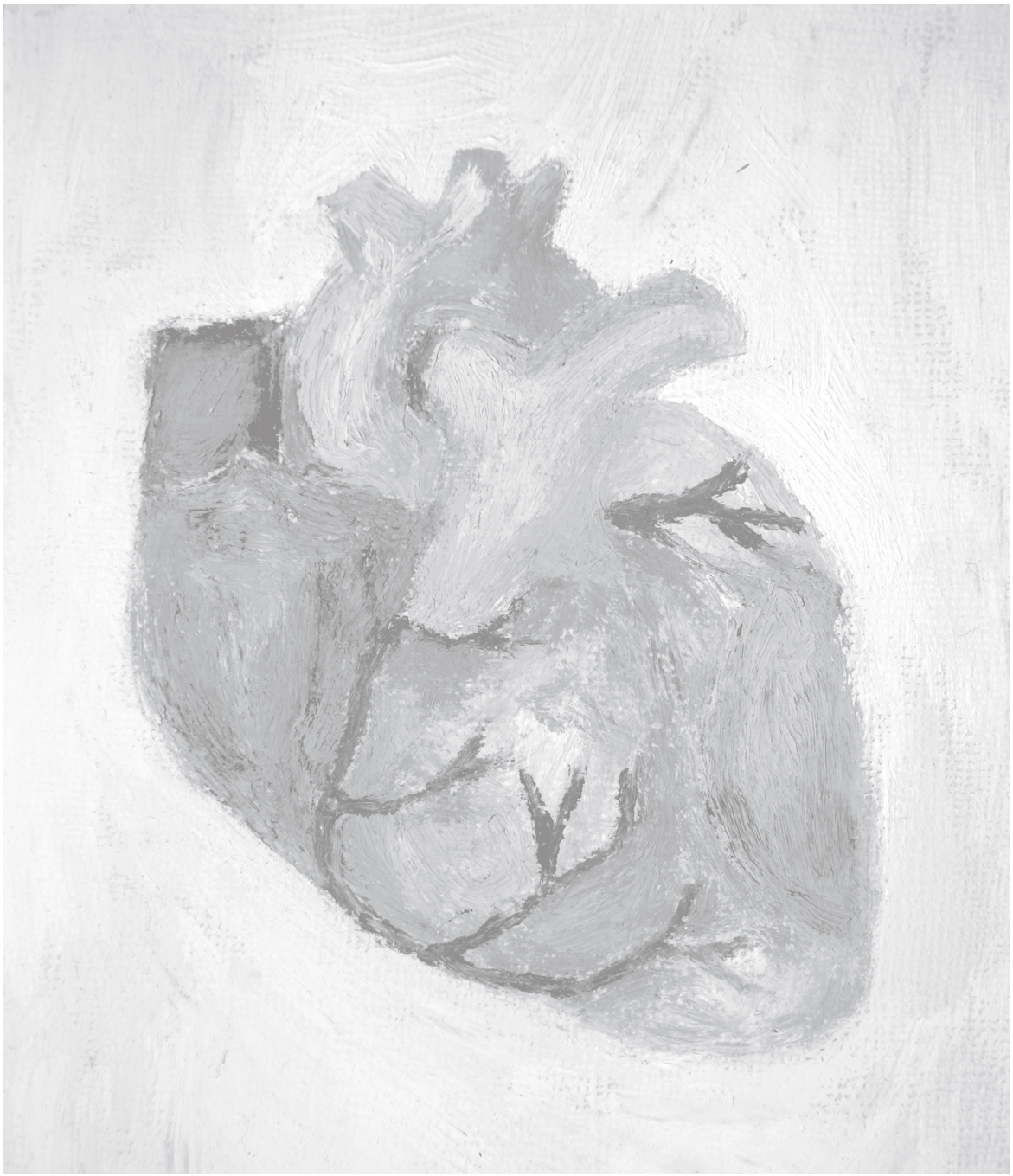

CHAPTER 2

Leukocyte TLR5 deficiency inhibits atherosclerosis by reduced macrophage recruitment and defective T-cell responsiveness

G.H.J.M. Ellenbroek[1], G.H.M. van Puijvelde[2], A.A. Anas[3], M. Bot[2], M. Asbach[2], A. Schoneveld[1], P.J. van Santbrink[2], A.C. Foks[2], L. Timmers[4], P.A.F.M. Doevendans[4], G. Pasterkamp[1,5], I.E. Hoefer[1,5], T. van der Poll[3], J. Kuiper[2], S.C.A. de Jager[1,2]

[1] Laboratory of Experimental Cardiology, University Medical Center Utrecht, The Netherlands
[2] Division of Biopharmaceutics, Leiden Academic Center for Drug Research, The Netherlands
[3] Center for Experimental and Molecular Medicine, Academic Medical Center, University of Amsterdam, The Netherlands
[4] Department of Cardiology, University Medical Center Utrecht, The Netherlands
[5] Laboratory of Clinical Chemistry and Hematology, University Medical Center Utrecht, The Netherlands

Scientific Reports 2017; 7: 1-10

ABSTRACT

Toll-like receptors (TLR) provide a critical link between innate and adaptive immunity, both important players in atherosclerosis. Since evidence for the role of TLR5 is lacking, we aimed to establish this in the immune axis of atherosclerosis. We assessed the effect of the TLR5-specific ligand Flagellin on macrophage maturation and T-cell polarisation. Next, we generated $TLR5^{-/-}LDLr^{-/-}$ chimeras to study the effect of hematopoietic TLR5 deficiency on atherosclerosis formation. Flagellin stimulation did not influence wildtype or $TLR5^{-/-}$ macrophage maturation. Only in wildtype macrophages, Flagellin exposure increased MCP-1 and IL6 expression. Flagellin alone reduced T-helper 1 proliferation, which was completely overruled in the presence of T-cell receptor activation. *In vivo*, hematopoietic TLR5 deficiency attenuated atherosclerotic lesion formation by ≈25% ($1030*10^3 \pm 63*10^3$ vs. $792*10^3 \pm 61*10^3$ μm^2; p=0.013) and decreased macrophage area (81.3±12.0 vs. 44.2±6.6 μm^2; p=0.011). In $TLR5^{-/-}$ chimeric mice, we observed lower IL6 plasma levels (36.4±5.6 vs. 15.1±2.2 pg/mL; p=0.003), lower (activated) splenic $CD4^+$ T-cell content (32.3±2.1 vs. 21.0±1.2%; p=0.0018), accompanied by impaired T-cell proliferative responses. In conclusion, hematopoietic TLR5 deficiency inhibits atherosclerotic lesion formation by attenuated macrophage accumulation and defective T-cell responsiveness.

INTRODUCTION

Atherosclerosis is a progressive multi-factorial disease affecting middle-sized and large arteries. It is the main culprit in the development of ischemic heart and cerebrovascular disease, together responsible for 29% of all deaths worldwide in 2013.[1] Although initially thought to be exclusively caused by lipids and risk factors such as diabetes, hypertension and smoking[2], it is now generally acknowledged that inflammation plays a critical role in atherosclerosis.[3,4] Migration of leukocytes into the vessel wall is an essential step in atherosclerotic lesion initiation and progression.[5,6] Hence, inhibition or prevention of leukocyte recruitment towards the vessel wall may prevent or reduce plaque development. In addition to the recruitment of leukocytes, it has been shown that immune cell activation plays an important role in lesion development.[7] Best known leukocyte activators are the highly conserved toll-like receptors (TLR), which are expressed on both immune and non-immune cells.[8] Several TLR subfamilies have been linked to atherosclerotic lesion initiation and progression, of which TLR2 and TLR4 have been the most extensively studied.[9] Although TLR5 has been linked to inflammation in a variety of inflammatory diseases including atherosclerosis[10–13], the role of hematopoietic TLR5 deficiency in atherosclerotic plaque formation remains unclear.

TLR5 is an extracellular receptor for bacterial Flagellin and ubiquitously expressed in almost all tissue types.[14] In addition to one or more exogenous stimuli, most TLRs also respond to specific endogenous ligands.[15] Whereas a broad variety of endogenous ligands have been described for most TLRs[9], an equivalent for TLR5 is lacking. Since many exogenous TLR ligands are expressed in (human) atherosclerotic lesions[16], Flagellin may also have a role in the development of atherosclerosis in the current study.[17] However, since TLR5 is an important contributor in diseases characterized by sterile inflammation (like cardiac ischemia-reperfusion injury[11] and rheumatoid artritis[18]), it is to be expected that both endogenous as well as exogenous ligands can lead to TLR5-dependent inflammation.

In addition to specific tissue cells, TLR5 is also present on different immune cells[19–21], of which macrophages and T-cells are of main importance in the context of atherosclerosis. Upon activation of the TLR5 receptor, MyD88 recruitment and activation of different intracellular kinases eventually leads to nuclear localization of NF-κB, resulting in a pro-inflammatory respons.[22] Since imbalanced inflammation is key in the development and progression of atherosclerosis, we investigated whether monocytes and T-cells lacking TLR5 differ in migratory and inflammatory behavior and whether hematopoietic TLR5 deficiency influences atherosclerotic plaque formation in vivo.

MATERIALS AND METHODS

Animals

LDLr$^{-/-}$ mice were obtained from the local animal breeding facility, C57Bl6 mice from Charles River (Maastricht, The Netherlands) and TLR5 deficient (TLR5$^{-/-}$) mice from Oriental Bioservices (Kyoto, Japan). Mice were maintained on sterilized regular chow (RM3; Special Diet Services, Essex, U.K.), drinking water was supplied ad libitum.

A blinded observer performed data acquisition and measurements. Animal experiments were performed at the animal facility of either the Gorlaeus laboratory, Leiden University or the Laboratory of Experimental Cardiology, University Medical Center Utrecht. All animal experiments were approved by the Ethical Committee on Animal Experimentation of Leiden University (Leiden, the Netherlands) or the University Medical Center Utrecht (Utrecht, the Netherlands) and conform to the 'Guide for the care and use of laboratory animals'.

Bone marrow transplantation

To induce bone marrow aplasia, female LDLr$^{-/-}$ recipient mice were exposed to a single dose of 9 Gy (0.19 Gy/min, 200 kV, 4 mA) total body irradiation using an Andrex Smart 225 Röntgen source (YXLON International) with a 6 mm aluminum filter. The day after, donor bone marrow was isolated from male WT and TLR5$^{-/-}$ littermates by flushing the femurs and tibias. Irradiated female recipients received 0.5x10^{7} bone marrow cells by tail vein injection. Drinking water was supplied ad libitum and supplemented with antibiotics (83 mg/L ciprofloxacin and 67 mg/L polymyxin B sulfate and 6.5 g/L sucrose) for 14 days, after which repopulation of the bone marrow has been completed.

After a recovery period of 6 weeks, animals were placed on a Western-type diet containing 0.25% cholesterol and 15% cacao butter (SDS) for 12 weeks, after which they were sacrificed.

Stimulation of bone marrow derived macrophages

Bone marrow cells were isolated from the tibias and femurs of male TLR5$^{-/-}$ and C57Bl/6 mice. To obtain bone marrow-derived macrophages, cells were cultured for 7 days in RPMI supplemented with 10% FCS, 100 U/mL penicillin/streptomycin, 0.1 mM nonessential amino acids, 1% pyruvate and 2 mM L-glutamine (Thermo Fisher Scientific) in the presence of 10 ng/mL macrophage colony-stimulating factor.

For in vitro stimulation, 0.5x10^{6} macrophages were added per well (24-well cell culture plates (Greiner Bio-One)). Cells were stimulated with 1 ng/mL Flagellin Ultrapure (Invivogen, Toulouse, France) or 1 ng/mL LPS (Sigma Aldrich, Zwijndrecht, the Netherlands) as a positive control. After 24 hours, cells were harvested for RNA isolation.

RT-PCR

Total RNA was isolated from the stimulated WT and TLR5$^{-/-}$ macrophages using Trizol reagent according to manufacturer's instructions (Invitrogen, Breda, the Netherlands). RNA was reverse transcribed using M-MuLV reverse transcriptase (RevertAid, MBI Fermentas, Leon-Roth). The expression levels of inducible nitric oxide synthase (iNOS), Arginase-1, monocyte chemoattractant protein-1 (MCP-1), C-C chemokine receptor type 2 (CCR2), and interleukin 6 (IL6) were analyzed by real time polymerase chain reaction (RT-PCR, Taqman, Applied Bioscience). Primer sequences are depicted in table 1. The mRNA expression was determined relative to the average expression of three household genes: acidic ribosomal phosphoprotein PO (36B4), hypoxanthine phosphoribosyltransferase (HPRT) and 60S ribosomal protein L27 (Rpl27).

Table 1. Primer sequences

Gene	Forward	Reverse
iNOS	CCTGGTACGGGCATTGCT	GCTCATGCGGCCTCCTTT
Arginase-1	TGGCAGAGGTCCAGAAGAATGG	GTGAGCATCCACCCAAATGACAC
MCP-1	AGGTCCCTGTCATGCTTCTG	TCTGGACCCATTCCTTCTTG
CCR2	AGAGAGCTGCAGCAAAAAGG	GGAAAGAGGCAGTTGCAAAG
IL6	AGACAAAGCCAGAGTCCTTCAGAGA	GGAGAGCATTGGAAATTGGGGTAGG
36B4	CTGAGTACACCTTCCCACTTACTGA	CGACTCTTCCTTTGCTTCAGCTTT
HPRT	TACAGCCCCAAAATGGTTAAGG	AGTCAAGGGCATATCCAACAAC
Rpl27	CGCCAAGCGATCCAAGATCAAGTCC	AGCTGGGTCCCTGAACACATCCTTG

iNOS: inducible Nitric Oxide Synthase, MCP-1: monocyte chemoattractant protein-1, CCR2: C-C chemokine receptor type 2 (CCR2), IL6: interleukin 6, 36B4: acidic ribosomal phosphoprotein PO, HPRT: hypoxanthine phosphoribosyltransferase, Rpl27: 60S ribosomal protein L27

Luminex

Circulating levels of IL6, IL17A and interferon-γ (IFN-γ) were determined by luminex according to the manufacturers protocol. A multiplex panel (eBioscience Mouse Th1/Th2 essential 6-plex and Mouse IL17A Simplex) was used in combination with the "Bio-Plex Multiplex system (Bio-Rad)" to perform luminex analyses.

Ex vivo proliferation and T-cell polarisation

Spleens were isolated from WT and TLR5$^{-/-}$ chimeras to assess ex vivo proliferation or C57Bl/6 WT mice to assess T-cell polarization. Spleens were gently squeezed through a 70 μm mesh cell strainer (Becton Dickinson, San Diego, CA, USA) to obtain a single cell suspension. Cells were washed and resuspended in RPMI1640 (supplemented with 10%

FCS, 20 mM L-glutamine, 100 U/ml penicillin and 100 µg/mL streptomycin) and seeded at a density of $3x10^5$ cells/well in a 96 well u-bottom cell culture plate (Greiner Bio One, Alphen aan den Rijn, the Netherlands). Cells were stimulated for 72 hours with medium alone, 1 ng/mL Flagellin Ultrapure, 1 ng/mL Flagellin Ultrapure in combination with 2 µg/mL anti-CD3 (eBioscience) or 2 µg/mL anti-CD3 in combination with 2 µg/mL anti-CD28 as a positive control. To assess proliferation, cells were incubated with 0.5 µCi [3H] Thymidine during the last 16 hours of 3 days in culture. To quantify thymidine incorporation the cells were washed with PBS and lysed with 0.1M NaOH and cell-associated radioactivity was determined by liquid scintillation counting. To assess T-cell polarisation, after 72 hours of stimulation, 10 µg/mL Brefeldin-A was added overnight to retain the proteins inside the cell. The next morning cells were harvested for flow cytometric analysis.

Intracellular flow cytometry

Cultured T-cells were harvested, centrifuged and resuspended for intracellular staining according to the manufacturers protocol (eBioscience). In short, cells were resuspended in PBS supplemented with 1% normal mouse serum and stained for the cell surface marker CD4 (BD Biosciences) for 30 minutes in the dark at 4°C. Cells were washed to remove unbound antibody and resuspended in IC fixation buffer. After 30 minutes, permeabilisation buffer was added, cells were centrifuged (1500rpm, 5 min) and resuspended in permeabilisation buffer. Antibodies for intracellular antigens Tbet, IFN-γ, RORγt, IL17A and Foxp3 (eBioscience) were added and incubated for 45 minutes at room temperature in the dark. Cells were washed twice in permeabilisation buffer and resuspended in flow cytometry staining buffer for cell acquisition (FACSCanto, BD Biosciences).

Flow cytometry

Blood, spleen and bone marrow cells were isolated from WT and $TLR5^{-/-}$ mice that had been fed a Western-type diet for 1 week. Bone marrow was isolated by flushing the femurs and tibias of WT and $TLR5^{-/-}$ mice with PBS. Subsequently, the cell suspension was gently filtered through a 70µm cell strainer to obtain a single cell suspension (70 µm pores, BD Bioscience). Spleens were harvested and single-cell suspensions of splenocytes were prepared by gently mincing the spleen through a cell strainer (70µm pores, BD Bioscience). Bone marrow cells and splenocytes were incubated at 4°C with erythrocyte lysis buffer (155 mM NH_4CL in 10 mM Tris/HCL, pH 7.2) for 5 minutes. Cells were centrifuged for 5 minutes at 1500 rpm and then resuspended in lysis buffer to remove residual erythrocytes. Cells were washed twice with PBS. 50 µL whole blood, bone marrow (300.000 cells), or spleen cell suspensions (300.000 cells) were stained for the surface markers CD11B (eBioscience), Ly6G (1A8) (Biolegend), Ly6C (Biolegend) and CCR2 (R&D Systems) and incubated for 30 minutes in

the dark. Subsequently cells were either washed in PBS and subjected to flow cytometric analyses (Gallios, Beckman Coulter) or prepared for intracellular staining.
For intracellular assessment of cytokine content, cells were washed to remove unbound antibody and resuspended in IC fixation buffer (4° Celsius). After 60 minutes, cells were centrifuged (1500 rpm, 5 min) and resuspended in permeabilisation buffer, washed once more and resuspended in permeabilisation buffer. Antibodies for intracellular antigens IL10 and IL12 (eBioscience, San Diego, CA, USA) were added and incubated for 30 minutes at room temperature in the dark. Cells were washed twice in permeabilisation buffer and resuspended in flow cytometry staining buffer for cell acquisition (Gallios, Beckman Coulter). FACS data were analyzed with Kaluza software (Beckman Coulter) and gated according to the strategy depicted in supplemental figure 1.

Histological analyses

Cryosections of the aortic root (10 mm) were collected and stained with Oil-red-O for morphometric analyses. Corresponding sections on separate slides were used for immunohistochemical stainings. Macrophages were stained with an antibody directed against MOMA-2 (monoclonal rat IgG2b, dilution 1:50; Serotec, Oxford, United Kingdom). Goat anti-rat IgG-AP (dilution 1:100; Sigma, St. Louis, MO) was used as a secondary antibody and NBT-BCIP (Dako, Glostrup, Denmark) as an enzyme substrate. $CD4^+$ T-cells were stained using CD4 (monoclonal rabbit, dilution 1:50; Cell Marque, Darmstadt, Germany). BrightVision poly-AP anti-rabbit (Immunologic, Duiven, The Netherlands) was used as a secondary antibody and liquid permanent red (DAKO) as an enzyme substrate. $CD8^+$ T-cells were stained using CD8a (monoclonal rat IgG2a,λ, dilution 1:50, eBioscience). The ImmPRESS HRP anti-Rat IgG, Mouse adsorbed (Peroxidase) Polymer Detection Kit (Vector, Burlingame, CA, USA) was used as a secondary antibody and DAB (Sigma, St. Louis, MO, USA) as an enzyme substrate. Collagen was visualized by a Masson's trichrome staining (Sigma). The section with the largest lesion and at least four flanking sections were used to determine lesion size. At least two flanking sections were used to analyse macrophage, T-cell and collagen content. The percentage of macrophages and collagen in the lesions was determined by dividing the area positive for MOMA-2 or collagen by the total lesion surface area. Necrotic core size was determined in the Oil-red-O stained sections and defined as an a-cellular, lipid-poor region. $CD4^+$ and $CD8^+$ T-cells were manually counted and expressed as counts/mm^2.
Histological analyses were performed in a blinded fashion using a Leica DMRE Microscope equipped with a Leica DC500 camera and Qwin quantification software (Leica, Rijswijk, the Netherlands). Histological analyses of $CD4^+$ and $CD8^+$ T-cell quantification were performed on an Olympus BX53 microscope equipped with a DP71 camera and CellSens quantification software (Olympus Corporation, Tokyo, Japan).

Statistical analysis

Data are expressed as mean ± standard error of the mean (SEM). Data distribution was evaluated using a Shapiro-Wilk test. A two-tailed student's t-test was used to compare individual groups if data were normally distributed, whereas non-parametric data were analyzed using a Mann-Whitney U test. Multiple groups were compared by one-way ANOVA with a post-hoc two-tailed student's t-test between significantly different groups. A level of $p<0.05$ was considered significant. Statistical analyses were performed using GraphPad Prism 6.

RESULTS

Absence of TLR5 affects migratory potential of macrophages in vitro

To study the effect of TLR5 signaling on immune cells, bone marrow derived macrophages from WT and TLR5$^{-/-}$ mice were stimulated *ex vivo* with the TLR5 ligand Flagellin. Cells stimulated with LPS served as a positive control. As measured by iNOS and Arginase I expression, no preferential skewing towards either M1 ($8.0*10^{-5}\pm4.7*10^{-5}$ vs. $6.0*10^{-5}\pm7.3*10^{-6}$; p=0.69, figure 1A) or M2 ($8.0*10^{-5}\pm8.9*10^{-6}$ vs. $7.0*10^{-5}\pm1.8*10^{-5}$; p=0.32, figure 1B) phenotype was observed upon stimulation with Flagellin. Already at baseline, TLR5$^{-/-}$ macrophages showed a lower expression of the potent monocyte chemoattractant MCP-1 (0.103±0.015 in WT vs. 0.046±0.014 A.U. in TLR5$^{-/-}$; p=0.013, figure 1C). Upon stimulation with Flagellin, the expression of MCP-1 increased only in WT macrophages (0.249±0.071 in WT vs. 0.070±0.013 A.U. in TLR5$^{-/-}$; p=0.0025). The expression of the MCP-1 receptor CCR2 was also lower in TLR5$^{-/-}$ macrophages at baseline ($6.0*10^{-4}\pm4.8*10^{-5}$ in WT vs. $2.3*10^{-4}\pm7.8*10^{-5}$ A.U. in TLR5$^{-/-}$; p=0.0069, figure 1D), but showed no further increase upon exposure to Flagellin in either WT ($6.0*10^{-4}\pm4.8*10^{-5}$ vs. $7.1*10^{-4}\pm3.9*10^{-5}$ A.U.; p=0.13) or TLR5$^{-/-}$ macrophages ($2.3*10^{-4}\pm7.8*10^{-5}$ vs. $2.4*10^{-4}\pm5.3*10^{-5}$ A.U.; p=0.92). In addition, expression levels of IL6 were significantly higher in WT macrophages at baseline ($1.4*10^{-4}\pm9.5*10^{-6}$ in WT vs. $6.0*10^{-5}\pm5.1*10^{-6}$ A.U. in TLR5$^{-/-}$; p=0.0003, figure 1E) and did marginally increase upon Flagellin stimulation in WT macrophages ($1.4*10^{-4}\pm9.5*10^{-6}$ vs. $2.1*10^{-4}\pm2.9*10^{-5}$ A.U.; p=0.06).

In vitro TLR5 stimulation induces regulatory T-cell differentiation

In addition to cells of the myeloid lineage, we observed expression of TLR5 in ≈14% of CD4^{+} T-cells, 44% of activated T-cells and 60% of the regulatory T-cells (data not shown). The effect of TLR5 signaling on CD4^{+} T-cell polarisation was studied by stimulating C57Bl/6 derived T-cells with Flagellin in the absence or presence of αCD3. Stimulation with a combination of αCD3 and αCD28 served as a positive control. The number of regulatory T-cells was mildly induced upon exposure to Flagellin alone (2455±74 vs.

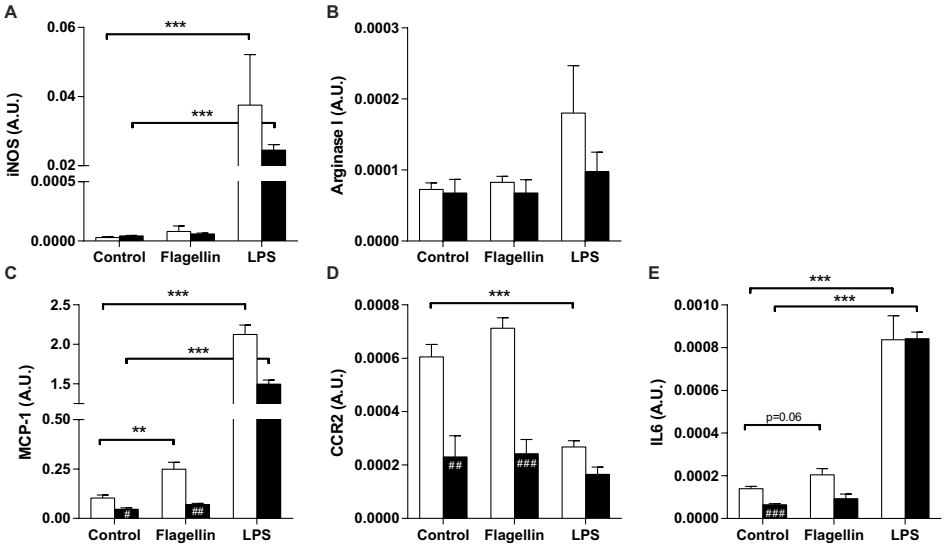

Figure 1. In vitro polarisation and migratory potential of macrophages
Stimulation of WT and TLR5$^{-/-}$ MCSF-derived macrophages with Flagellin or LPS did not induce significant differences in iNOS (A) and Arg-1 (B) gene expression between both groups. Already at baseline, WT macrophages showed higher mRNA levels of MCP-1 (C), CCR2 (D) and IL6 (E), of which the expression of MCP-1 and IL6 increased upon Flagellin stimulation. No such increase was observed in TLR5$^{-/-}$ macrophages upon stimulation with Flagellin. The expression of CCR2 was also different at baseline between both groups, but no change in expression level was observed after stimulation with Flagellin (D); n=4 per group. *WT: wildtype, TLR5$^{-/-}$: toll-like receptor 5 knockout, #: p<0.05, ##: p<0.01, ###: p<0.001, **: p<0.01, ***: p<0.001*

2807±109; p=0.056, figure 2A) or in combination with αCD3 (2448±306 vs. 3100±124; p=0.14). The number of T-helper 1 (Th1) cells decreased upon Flagellin stimulation alone (22196±203 vs. 19552±150; p=0.0005), figure 2B), but increased when exposed to a combination of Flagellin and αCD3 (181764±2777 vs. 279000±4879; p<0.0001). Exposing CD4^{+} T-cells to Flagellin alone did not affect the number of T-helper 17 (Th17) cells (23064±86 vs. 22385±522; p=0.27, figure 2C), but when exposed to a combination of Flagellin and αCD3 the number of Th17-cells robustly increased (160854±1439 vs. 199392±4142; p=0.0001).

Hematopoietic TLR5 deficiency reduces plaque size, macrophage area and necrotic core in LDLr$^{-/-}$ mice

To assess the effect of hematopoietic TLR5 deficiency on atherosclerotic lesion development, TLR5$^{-/-}$ bone marrow chimeras were generated. Plasma cholesterol and body weight were monitored during the experiment and did not significantly differ between WT and TLR5$^{-/-}$chimeras (data not shown). After 12 weeks of high fat diet feeding, mice were sacrificed

and atherosclerotic lesion size in the aortic root was analyzed. In TLR5$^{-/-}$ chimeras, lesion size was markedly reduced by ≈25% (1030*10^3±63*10^3 in WT vs. 792*10^3±61*10^3 μm^2 in TLR5$^{-/-}$; p=0.013, figure 3A), whereas collagen content as a percentage of total plaque area was not different between both groups (24.0±2.0 in WT vs. 24.0±1.2% in TLR5$^{-/-}$; p=0.99, figure 3B). The decrease in lesion size was accompanied by a reduction in macrophage area (81.3±12.0 in WT vs. 44.2±6.6 μm^2 in TLR5$^{-/-}$; p=0.011, figure 3C), however lesions in TLR5$^{-/-}$ chimeras did not show a difference with respect to the percentage of macrophage area (7.4±1.1 in WT vs. 5.2±0.8% in TLR5$^{-/-}$; p=0.10, figure 3D). Despite the observed decrease in splenic T-cell content we did not observe a difference in the number of CD4$^+$ T-cells accumulated in the plaques of TLR5$^{-/-}$ mice (309±89 in WT vs. 498±338 /mm2 in TLR5$^{-/-}$; p=0.17, figure 3E). Similarly, no difference was observed in the number of CD8$^+$ T-cells (38±30 in WT vs. 69±40 /mm2 in TLR5$^{-/-}$; p=0.16, figure 3F). In agreement with smaller lesion size, necrotic core size was reduced (21.6±2.7 in WT vs. 14.7±1.9% in TLR5$^{-/-}$; p=0.046, figure 3G).

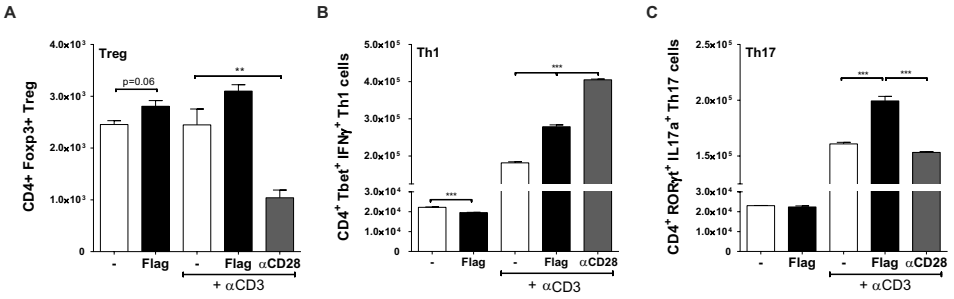

Figure 2. In vitro polarisation of T-cells
Exposure of Flagellin to WT CD4$^+$ T-cells either in the presence or absence of αCD3 resulted in a mild but insignificant induction in the number of Tregs (A). The number of Th1-cells decreased upon Flagellin stimulation only (B), whereas no change was observed in Th17-cells (C). In the presence of both Flagellin and αCD3, the induction of Th1- and Th17-cells robustly increased (B-C); n=3 per group. *WT: wildtype, Tregs: regulatory T-cells, Th1-cells: T helper type 1 cells, Th17: T helper type 17 cells, **: p<0.01, ***: p<0.001*

The numbers of circulating monocytes, T-cells and their subsets are influenced by TLR5 deficiency

One week after feeding WT and TLR5$^{-/-}$ mice a Western-type diet, flow cytometry was used to assess several monocyte subsets and receptor expression on blood and bone marrow. We observed that TLR5$^{-/-}$ mice displayed a decreased number of circulating pro-inflammatory Ly6C^{high} monocytes (498±75 in WT vs. 367±57 cells/uL in TLR5$^{-/-}$; p=0.01, table 2). In addition, TLR5$^{-/-}$ circulating monocytes showed a decrease in pro-inflammatory

IL12 staining (140±55 in WT vs. 38±8 cells/uL in TLR5$^{-/-}$; p=0.003, table 2). In the bone marrow, we observed a decrease in the number of monocytes as a percentage of all viable cells (11.4±0.5 in WT vs. 9.1±0.5% in TLR5$^{-/-}$; p<0.0001, table 2) and specifically, a decrease in Ly6C^{high} monocytes (10.1±0.7 in WT vs. 7.7±0.4% in TLR5$^{-/-}$; p=0.003, table 2). Both, blood and bone marrow showed a decrease in the percentage of CCR2^{+} cells.

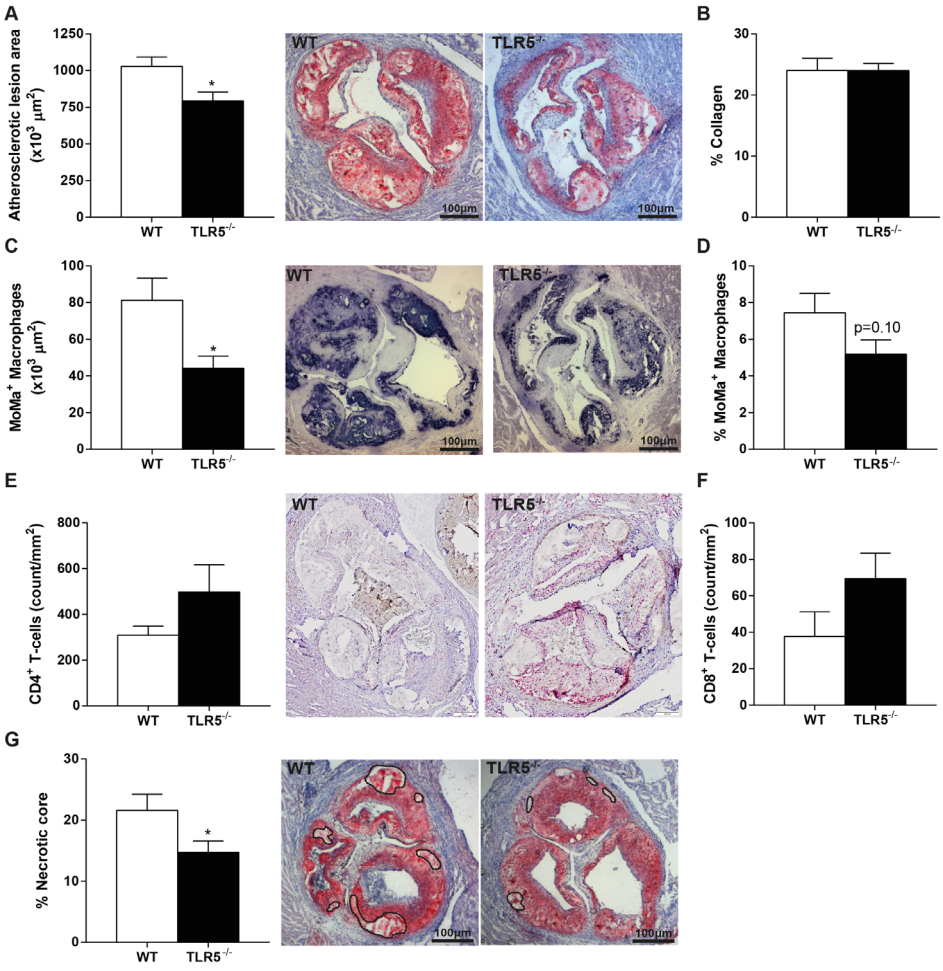

Figure 3. Atherosclerotic plaque size and composition
After 12 weeks of high-fat diet, the atherosclerotic plaque area was significantly larger in WT mice compared to TLR5$^{-/-}$ mice (A). No difference between both groups was observed with respect to collagen content (B), yet the plaque of TLR5$^{-/-}$ mice showed a decrease in macrophage influx (C-D). Although not significant, TLR5$^{-/-}$ mice showed higher numbers of CD4^{+} (E) and CD8^{+} T-cells (F). The necrotic core expressed as a percentage of the plaque was significantly higher in WT mice (G); n=12-13 per group (5-8 for CD4-8 staining). *WT: wildtype, TLR5$^{-/-}$: toll-like receptor 5 knockout, *: p<0.05*

Table 2. Monocyte subsets and their pro-inflammatory and migratory protein levels

	Blood (cells/µl)				Bone Marrow (% of viable cells)			
Cell (sub)type	**Wildtype**	**TLR5$^{-/-}$**		**p**	**Wildtype**	**TLR5$^{-/-}$**		**p**
Monocytes	776 ± 124	621 ± 97	=	0.06	11.4 ± 0.5	9.1 ± 0.5	↓	**<0.0001**
Ly6C^{high} mono	498 ± 75	367 ± 57	↓	**0.01**	10.1 ± 0.7	7.7 ± 0.4	↓	**0.0002**
Ly6C^{low} mono	291 ± 91	274 ± 49	=	0.73	1.3 ± 0.2	1.4 ± 0.1	=	0.54
CCR2^{+} mono	176 ± 36	154 ± 33	=	0.35	7.2 ± 0.4	5.8 ± 0.3	↓	**0.0006**
CCR2+ Ly6C^{high} mono	102 ± 24	90 ± 16	=	0.37	6.5 ± 0.5	5.0 ± 0.3	↓	**0.0005**
Ratio Ly6C$^{hi/low}$	1.83 ± 0.53	1.34 ± 0.04	=	0.08	8.1 ± 1.8	5.7 ± 0.15	↓	**0.02**
IL12^{+} mono	140 ± 55	38 ± 8	↓	**0.003**	n.d.	n.d.		
IL10^{+} mono	307 ± 69	249 ± 51	=	0.16	n.d.	n.d.		
Ratio IL12/IL10	0.45 ± 0.10	0.16 ± 0.05	↓	**0.0003**	n.d.	n.d.		

Mono (=monocytes) were selected as CD11b^{+}, Ly6G^{-}, Ly6C^{+} cells. n.d. = not determined

T-cell subsets were determined in the hematopoietic TLR5$^{-/-}$ mice at the end of the experiment. The number of CD4^{+} T-cells as a percentage of total splenocytes was lower in TLR5$^{-/-}$ mice (32.9±2.2 in WT vs. 22.4±1.0% in TLR5$^{-/-}$; p=0.0013, figure 4A), as was the percentage of activated CD4^{+}CD25^{+} T-cells (32.3±2.1 in WT vs. 21.0±1.2% in TLR5$^{-/-}$; p=0.0018, figure 4B). Similarly, TLR5$^{-/-}$ mice displayed lower percentages of Tregs (13.7±2.4 in WT vs. 6.8±0.6% in TLR5$^{-/-}$; p=0.0087; figure 4C) and a slightly lower percentage of Th1-cells (11.8±3.1 in WT vs. 6.2±0.6% in TLR5$^{-/-}$; p=0.13, figure 4D).

Ex vivo T-cell proliferation was performed to assess complete replacement of T-cells upon bone marrow transplantation (figure 4E). Proliferation under control, non-stimulatory conditions did not differ between WT and TLR5$^{-/-}$ cells (p=1.00). Proliferation upon stimulation with Flagellin alone or Flagellin in combination with αCD3 is displayed as fold induction to control proliferation. Stimulation with Flagellin led to an increased proliferation index in WT mice (3.8±1.1 upon stimulation vs. 1.0±0.3 in non-stimulatory conditions; p=0.03), but did not in TLR5$^{-/-}$ mice (p=0.96). In the presence of both, Flagellin and αCD3, T-cell proliferation was robustly induced in WT (50.4±18.7 upon stimulation vs. 1.0±0.3; p=0.03), but not in TLR5$^{-/-}$ mice (1.2±0.4 upon stimulation vs. 1.0±0.3; p=0.71). Flagellin-independent proliferation was normal in TLR5$^{-/-}$ T-cells as shown by αCD3/αCD28-induced proliferation (proliferation index 85.3±55 in TLR5$^{-/-}$ and 96.7±23 in WT, data not shown).

Hematopoietic TLR5 deficiency influences pro-inflammatory cytokine levels

Luminex was used for the quantification of pro-inflammatory cytokine levels in plasma of WT and TLR5$^{-/-}$ mice at sacrifice. Compared to WT animals, significantly lower levels of IL6 (36.4±5.6 in WT vs. 15.1±2.2 pg/mL in TLR5$^{-/-}$; p=0.0029, figure 5A) and IL17A

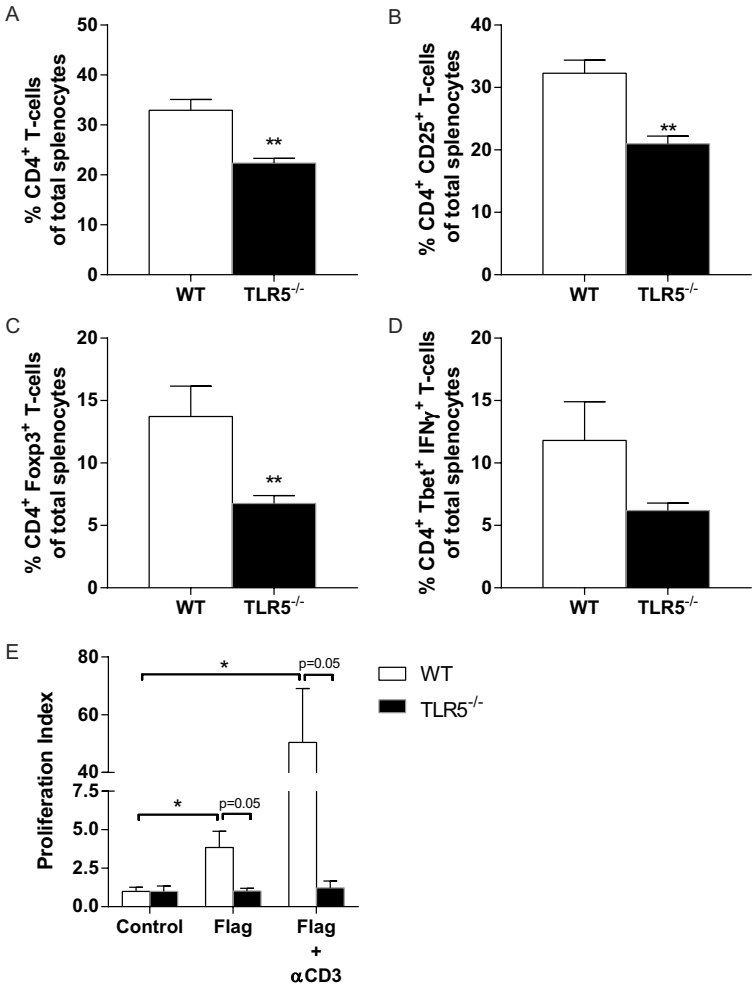

Figure 4. Splenic T-cell numbers, subsets and proliferation indices
The number of $CD4^+$ T-cells as a percentage of total splenocytes was higher in WT mice compared to $TLR5^{-/-}$ mice (A), similar to the percentage of activated $CD4^+CD25^+$ T-cells (B). Tregs expressed as a percentage of total splenocytes were significantly higher in WT mice (C) and, yet insignificantly, so was the percentage of Th1-cells (D). T-cells isolated from the spleen were used for proliferation indices in both groups (E). No differences were observed at baseline. Upon stimulation with Flagellin alone the proliferation index was increased in only the WT T-cells, an effect that was even more pronounced in the presence of αCD3. No such differences were observed with Flagellin either in the presence or absence of αCD3 with the $TLR5^{-/-}$ T-cells; n=4-6 per group. *$TLR5^{-/-}$: toll-like receptor 5 knockout, WT: wildtype, Tregs: regulatory T-cells, Th1-cells: T helper type 1 cells, *: p<0.05, **: p<0.01*

(4.1±1.8 in WT vs. 1.0±0.4 pg/mL in $TLR5^{-/-}$; p=0.028, figure 5B) were detected in plasma of $TLR5^{-/-}$ mice. Plasma IFN-γ levels were relatively low and did not allow us to reliably calculate the concentration. Therefore, we used mean fluorescence intensity (MFI) to

compare both groups, which showed slightly decreased IFN-γ levels in TLR5$^{-/-}$ mice compared WT mice (39.7±9.8 in WT vs. 20.9±5.4 in TLR5$^{-/-}$ MFI; p=0.09, figure 5C).

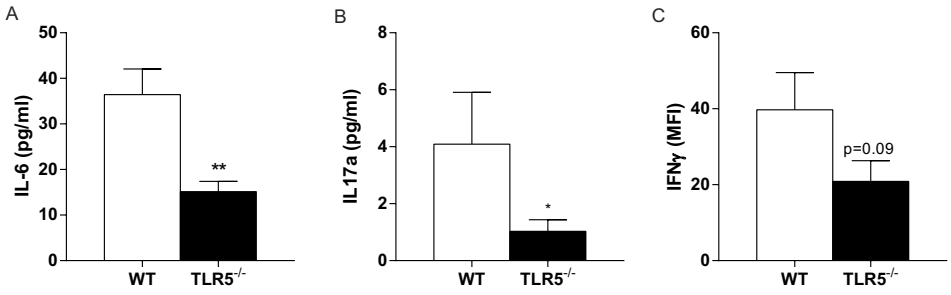

Figure 5. Plasma levels of pro-inflammatory cytokines
Plasma levels of IL6 (A) and IL17A (B) determined by luminex were significantly lower in TLR5$^{-/-}$ mice. Yet insignificant, also the plasma levels of IFN-γ were lower in TLR5$^{-/-}$ compared to WT mice (C); n=8-10 mice per group. *TLR5$^{-/-}$: toll-like receptor 5 knockout, WT: wildtype, IL: interleukin, IFN-γ: interferon γ, *: p<0.05, **: p<0.01*

DISCUSSION

Over the past decades there has been a widespread interest in the role of TLRs in the onset and progression of cardiovascular diseases. In atherosclerosis, TLR2 and TLR4 have been the most prominently studied[9] and evidence for the role of TLR5 has been previously shown.[12,13] In this regard, the current paper is the first to show that hematopoietic TLR5 deficiency attenuates atherosclerosis formation in LDLr$^{-/-}$ mice. In addition, the plaques of these mice contain less macrophages and a smaller necrotic core compared to mice that received WT bone marrow. These findings are in line with previous studies that show the effect of TLR5 in atherosclerotic plaque formation and inflammatory cell accumulation.[12,13] It also confirms the observation that inflammation – and TLRs in particular – are key drivers of atherosclerosis.[3,9,12]

In general, lack of TLRs is believed to decrease atherosclerotic burden through the impairment of pro-inflammatory signaling. In this respect, macrophages from WT mice showed an increased expression of MCP-1 and IL6 upon Flagellin stimulation, whereas no difference was observed upon stimulation of TLR5 deficient macrophages. Also, TLR5$^{-/-}$ mice showed a decrease in circulating and bone-marrow derived Ly6C^{high} monocytes and a decrease in pro-inflammatory cytokine production (IL10, IL12). Correspondingly, plasma levels of several pro-inflammatory cytokines were higher in WT mice than in TLR5$^{-/-}$ bone marrow chimeras.

The fact that we observe a decrease in the Ly6C^{high} monocyte pool in both the bone marrow and circulation suggests that monocyte recruitment to the plaque may be impaired. In addition, CCR2 expression on the bone marrow monocyte pool is significantly decreased in TLR5 deficient mice, which partly reflects previous research showing that CCR2 deficiency attenuates macrophage influx into the plaque.[23] Decreased macrophage CCR2 expression could have had a similar effect in the current manuscript. In addition to the impairment in pro-inflammatory signaling, this may very well be one of the primary mechanisms in the reduction of atherosclerotic plaque formation. These findings are in accordance with previous studies showing that TLR5 stimulation of mouse endothelial cells enhanced the expression of pro-inflammatory molecules and increased the adhesive and migratory capacity for monocytes.[12] In addition, TLR5 inhibition showed decreased serum levels of several pro-inflammatory cytokines.[13] Similarly, ApoE$^{-/-}$TLR4$^{-/-}$ mice on high-cholesterol feeding showed a reduction in serum MCP-1 levels, plaque size and macrophage infiltration when compared to ApoE$^{-/-}$ mice.[24] Again, this emphasizes the importance of migratory proteins (MCP-1, IL6, etc.) in atherogenesis and inflammatory cell deposition.[5,6,23,25]

In addition to TLR5 being abundantly expressed on cells of myeloid origin, we observed expression of TLR5 on CD4^{+} T-cells as well. When exposing T-cells to Flagellin in a non-inflammatory condition, an increase in the number of Tregs and a decrease in Th1-cells were observed. These data are similar to a previous study showing that TLR5 stimulation enhances the suppressive capacity of regulatory T-cells.[26] However, when performing these experiments under more inflammatory conditions by adding αCD3 to simulate antigen-T-cell receptor interaction, the suppressive effect of Tregs was lost and actually proliferation of pro-atherogenic Th1- and Th17-cells was stimulated. This implicates a pro-atherogenic effect of stimulation of TLR5 on T-cells in a pro-inflammatory environment, like observed in atherosclerosis. Indeed, this was reflected *in vivo* by lower numbers of Tregs, activated CD4^{+}CD25^{+} cells and Th1-cells and decreased IL6, IL17A and IFN-γ plasma levels in TLR5$^{-/-}$ bone marrow chimeras. Despite this general effect on CD4^{+} T-cells, no significant reduction in the number of CD4^{+} or CD8^{+} T-cells in the atherosclerotic plaque was observed.

Apart from their importance as pattern recognition receptors (PRR) of exogenous (mostly bacterial) ligands, TLRs can also potently respond to specific disease-associated endogenous ligands.[15] Whereas a broad variety of endogenous ligands have been described for several TLRs[9], an equivalent for TLR5 is lacking. Since many exogenous TLR ligands are expressed in (human) atherosclerotic lesions[16], Flagellin may indeed be (partially) responsible for the results observed in the current study, implicating a role of (subclinical) infection in the development of atherosclerosis.[17] However, this phenomenon may be debated on by accumulating evidence showing that TLR5 also plays an important role in diseases characterized by sterile inflammation, such as cardiac ischemia-reperfusion injury[11] and rheumatoid artritis.[18]

Although it remains unclear which ligand is responsible for the observed effect in the current study, we do show the importance of hematopoietic TLR5 deficiency in the early stage of atherosclerosis formation. Whether this also holds true for a model of atherosclerosis with larger and more complex lesions remains to be elucidated. In this regard, hematopoietic TLR2 deficiency has also been shown to be important in the early stage of atherosclerosis formation, but was not evident when feeding mice a 1.5% instead of a 0.15% cholesterol-enriched diet.[27] Moreover, although baseline TLR5 deficiency was able to attenuate atherosclerotic plaque formation, from a clinical perspective it remains of interest to see whether TLR5 inhibition at a later stage would also be able to reduce or stabilize already manifest atherosclerosis.

CONCLUSION

In conclusion, the present manuscript is one of the first to show that hematopoietic TLR5 deficiency in mice attenuates atherosclerotic plaque development through decreased macrophage accumulation and defective T-cell responsiveness. Still, more knowledge has to be gathered on the possibility to antagonize TLR5 signaling to reduce or stabilize previously established atherosclerotic lesions.

Acknowledgements
The authors gratefully acknowledge Kim Habets and Petra van der Kraak for technical assistance.

Funding
This work was performed within the framework of the Dutch Top Institute Pharma (project: D1-101: S.C.A. de Jager, G.H.M. van Puijvelde, J. Kuiper). This project has been supported by the Foundation *"De Drie Lichten"* in the Netherlands. The funders had no role in study design, data collection and analysis, decision to publish, or preparation of the manuscript.

Conflict of interest
The authors declare no conflict of interest.

REFERENCES

1. GBD 2013 Mortality and Causes of Death Collaborators*. Global, regional, and national age – sex specific all-cause and cause-specific mortality for 240 causes of death, 1990 – 2013: a systematic analysis for the Global Burden of Disease Study 2013. *Lancet*. 2014;385:117–171.
2. Kannel WB, McGee D, Gordon T. A General Cardiovascular Risk Profile: The Framingham Study. *Am J Cardiol*. 1976;36:46–51.
3. Libby P, Ridker PM, Maseri A. Inflammation and atherosclerosis. *Circulation*. 2002;105:1135–1143.
4. Hamirani YS, Pandey S, Rivera JJ, Ndumele C, Budoff MJ, Blumenthal RS, Nasir K. Markers of inflammation and coronary artery calcification: a systematic review. *Atherosclerosis*. 2008;201:1–7.
5. Weber C. Chemokines: Key Regulators of Mononuclear Cell Recruitment in Atherosclerotic Vascular Disease. *Arterioscler Thromb Vasc Biol*. 2004;24:1997–2008.
6. Liehn E a, Zernecke A, Postea O, Weber C. Chemokines: inflammatory mediators of atherosclerosis. *Arch Physiol Biochem*. 2006;112:229–238.
7. Hansson GK, Libby P. The immune response in atherosclerosis : a double-edged sword. *Nat Rev Immunol*. 2006;6:508–519.
8. Medzhitov R. Toll-like receptors and innate immunity. *Nat Rev Immunol*. 2001;1:135–145.
9. Falck-hansen M, Kassiteridi C. Toll-Like Receptors in Atherosclerosis. *Int J Mol Sci*. 2013;14:14008–14023.
10. Blohmke CJ, Park J, Hirschfeld AF, Victor RE, Schneiderman J, Stefanowicz D, Chilvers M a, Durie PR, Corey M, Zielenski J, Dorfman R, Sandford AJ, Daley D, Turvey SE. TLR5 as an anti-inflammatory target and modifier gene in cystic fibrosis. *J Immunol*. 2010;185:7731–8.
11. Parapanov R, Lugrin J, Rosenblatt-Velin N, Feihl F, Waeber B, Milano G, Vergely C, Li N, Pacher P, Liaudet L. Toll-like receptor 5 deficiency exacerbates cardiac injury and inflammation induced by myocardial ischaemia-reperfusion in the mouse. *Clin Sci*. 2015;129:187–198.
12. Kim J, Seo M, Kim SK, Bae YS. Flagellin-induced NADPH oxidase 4 activation is involved in atherosclerosis. *Sci Rep*. 2016;1–16.
13. Zhang Y, Zhang Y. Pterostilbene, a novel natural plant conduct, inhibits high fat-induced atherosclerosis inflammation via NF-κB signaling pathway in Toll-like receptor 5 (TLR5) deficient mice. *Biomed Pharmacother*. 2016;81:345–355.
14. Zarember KA, Godowski PJ, Alerts E. Tissue Expression of Human Toll-Like Receptors and Differential Regulation of Toll-Like Receptor mRNAs in Leukocytes in Response to Microbes, Their Products, and Cytokines. *J Immunol*. 2002;168:554–561.
15. Rifkin IR, Leadbetter EA, Busconi L, Viglianti G, Marshak-Rothstein A. Toll-like receptors, endogenous ligands, and systemic autoimmune disease. *Immunol Rev*. 2005;204:27–42.
16. Monaco C, Cole JE, Georgiou E. The expression and functions of toll-like receptors in atherosclerosis. *Mediators Inflamm*. 2010;
17. Rosenfeld ME, Campbell LA. Pathogens and atherosclerosis: Update on the potential contribution of multiple infectious organisms to the pathogenesis of atherosclerosis. *Thromb Haemost*. 2011;106:858–867.
18. Kassem A, Henning P, Kindlund B, Lindholm C, Lerner UH. TLR5, a novel mediator of innate immunity-induced osteoclastogenesis and bone loss. *FASEB J*. 2015;29:4449–4460.
19. Gewirtz AT, Navas TA, Lyons S, Paul J, Madara JL, Expression PG, Godowski PJ, Madara JL. Cutting Edge: Bacterial Flagellin Activates Basolaterally Expressed TLR5 to Induce Epithelial Proinflammatory Gene Expression. *J Immunol*. 2001;167:1882–1885.
20. Hornung V, Rothenfusser S, Britsch S, Jahrsdörfer B, Giese T, Endres S, Hartmann G. Quantitative Expression of Toll-Like Receptor 1 – 10 mRNA in Cellular Subsets of Human Peripheral Blood Mononuclear Cells and Sensitivity to CpG Oligodeoxynucleotides. *J Immunol*. 2002;168:4531–4537.
21. Okamura Y, Watari M, Jerud ES, Young DW, Ishizaka ST, Rose J, Chow JC, Iii JFS. The Extra Domain A of Fibronectin Activates Toll-like Receptor 4*. *J Biol Chem*. 2001;276:10229–10233.
22. Hayashi F, Smith KD, Ozinsky A, Hawn TR, Yi EC, Goodlett DR, Eng JK, Akira S, Underhill DM, Aderem A. The innate immune response to bacterial flagellin is mediated by Toll-like receptor 5. 2001;410:1099–1103.
23. Boring L, Gosling J, Cleary M, Charo IF. Decreased lesion formation in CCR2-/- mice reveals a role for chemokines in the initiation of atherosclerosis. *Nature*. 1998;394:894–897.
24. Michelsen KS, Wong MH, Shah PK, Zhang W, Yano J, Doherty TM, Akira S, Rajavashisth TB, Arditi M. Lack of Toll-like receptor 4 or myeloid differentiation factor 88 reduces atherosclerosis and alters plaque phenotype in mice deficient in apolipoprotein E. *Proc Natl Acad Sci U S A*. 2004;101:10679–10684.
25. Gu L, Okada Y, Clinton SK, Gerard C, Sukhova GK, Libby P, Rollins BJ. Absence of monocyte chemoattractant protein-1 reduces atherosclerosis in low density lipoprotein receptor-deficient mice. *Mol Cell*. 1998;2:275–281.
26. Crellin NK, Garcia R V, Hadisfar O, Allan SE, Steiner TS, Levings MK. Human CD4+ T cells express TLR5 and its ligand flagellin enhances the suppressive capacity and expression of FOXP3 in CD4+CD25+ T regulatory cells. *J Immunol*. 2005;175:8051–8059.
27. Hasu M, Thabet M, Tam N, Whitman SC. Specific loss of toll-like receptor 2 on bone marrow derived cells decreases atherosclerosis in LDL receptor null mice. *Can J Physiol Pharmacol*. 2011;89:737–42.

SUPPLEMENTAL

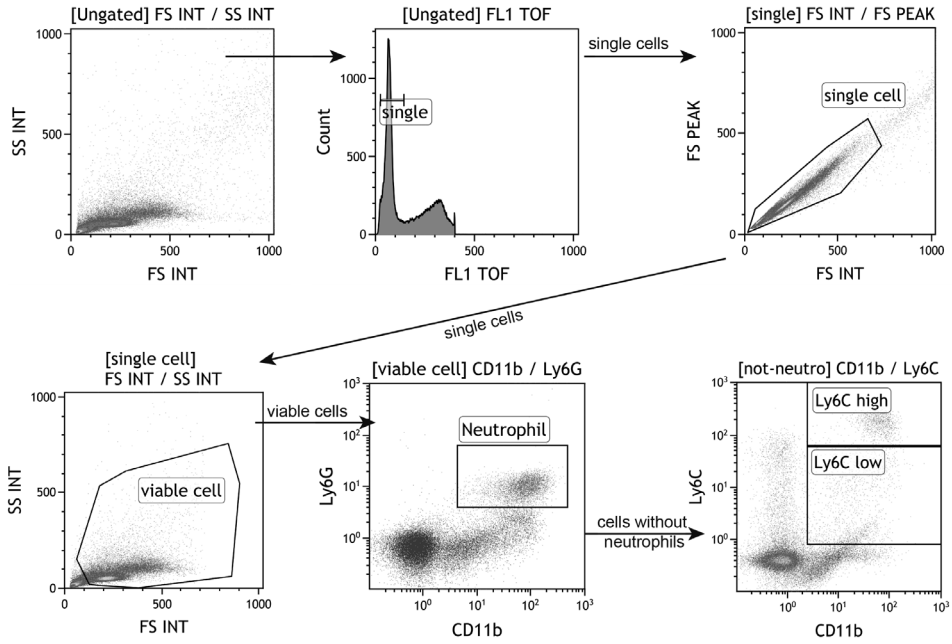

Supplemental Figure 1. Gating strategy for monocytes

CHAPTER 3

Radiofrequency ablation of the atherosclerotic plaque: a proof of concept study in an atherosclerotic model

G.H.J.M. Ellenbroek[1], G.P.J. van Hout[2], S.C.A. de Jager[1], L. Timmers[2], Aryan Vink[3], R. Goldschmeding[3], P.H. van der Kraak[1], G. Pasterkamp[1,4], I.E. Hoefer[1,4], P.A.F.M. Doevendans[2,5], Y. Appelman[6]

[1] Laboratory of Experimental Cardiology, University Medical Center Utrecht, The Netherlands
[2] Department of Cardiology, University Medical Center Utrecht, The Netherlands
[3] Department of Pathology, University Medical Center Utrecht, The Netherlands
[4] Department of Clinical Chemistry and Hematology, University Medical Center Utrecht, The Netherlands
[5] Netherlands Heart Institute, Utrecht, The Netherlands
[6] Department of Cardiology, VU Medical Center, Amsterdam, The Netherlands

Journal of Cardiovascular Translational Research 2017; 2: 221-232

ABSTRACT

Increased plaque vascularization is causatively associated with the progression of unstable atherosclerotic vessel disease. We investigated the safety and efficacy of heat-generating radiofrequency ablation (RFA) in reducing the number of vessels in the plaque and adventitia and its effect on plaque size and composition. To this end, New-Zealand White rabbits were fed a cholesterol-enriched diet and subjected to balloon denudation of the infrarenal aorta to induce atherosclerotic plaque formation. After 13 weeks, the proximal or distal half of the infrarenal aorta was exposed to transluminal RFA. The untreated half served as an intra-individual control. Optical coherence tomography (OCT) was performed directly after RFA. We found that RFA on the rabbit atherosclerotic plaque is safe and leads to decreased intraplaque vessel density and smooth muscle cell content, but does not affect other components of plaque composition or size.

INTRODUCTION

Atherosclerosis is the most prevalent cause of cardiovascular disease (CVD) worldwide and the main cause of death in the Western world.[1] Progression of atherosclerosis may lead to plaque instability and give rise to an acute myocardial infarction (AMI), cerebrovascular accident (CVA) or acute peripheral vascular disease. Increased vasa vasorum density results in a higher influx of inflammatory cells and lipid deposition, culminating in unstable plaque formation.[2] In addition, immature and leaky neovessels originating from the vasa vasorum consequently increase the risk for intraplaque hemorrhage, thereby increasing plaque vulnerability.[3]

Currently, interventional techniques to treat atherosclerotic plaque progression are targeted at increasing and maintaining arterial luminal area by balloon angioplasty, either with or without stent implantation.[4] However, techniques that intervene in the pathophysiological chain of plaque growth and destabilization are scarce.[5] Heat-generating radiofrequency ablation (RFA) has been used to target adventitial sympathetic nerves in treatment-resistant hypertension and has been proven to be safe.[6–8] Like cryotherapy in atherosclerotic vessel disease[9], RFA is known to induce local decellularization and fibrosis formation in healthy arteries[10,11] and could therefore increase plaque stability. Moreover, similar to adventitial nerve degeneration, we hypothesized that this technique may safely be used to reduce vasa vasorum density and subsequent plaque neovascularization, leading to additional plaque stabilization and possibly decreasing plaque size.

MATERIALS AND METHODS

Experimental design

Fourteen male New Zealand white rabbits (Charles River, Chatillon-sur-Chalaronne, R-A, France; 3.0-3.5 kg) were fed a 0.5% cholesterol-enriched diet (Special Diet Services, Essex, UK) for thirteen weeks. After two weeks, balloon denudation of the infrarenal aorta was performed (Figure 1a). Male rabbits were used since large-vessel disease is more common in males[12] and to follow-up on other atherosclerosis studies that are performed in the same gender.[9] Eleven weeks after balloon denudation, half of the atherosclerotic aorta was treated with transluminal RFA. The other half served as an intra-individual control. Tissue was harvested at different time points after RFA. All animal experiments were approved by the Ethical Committee on Animal Experimentation of the University Medical Center Utrecht (Utrecht, the Netherlands) and conform to the 'Guide for the care and use of laboratory animals'.

Balloon denudation

Rabbits were fasted overnight before surgery. As premedication, ketamine (15 mg/kg) and xylazine (1.5 mg/kg) were injected intramuscularly. The right inguinal region was shaven and the ear vein cannulated. Subcutaneous meloxicam (1 mg/kg) was given before surgery as analgesia. Directly prior to and every 15-20 minutes thereafter, a 0.5-1.0mL mixture of ketamine (10 mg/mL) and xylazine (1 mg/mL) was administered intravenously. Povidone-iodium 2% was applied to the right inguinal region and all other parts were covered with sterile sheets. A small incision was made in the direction of the right femoral artery. The fascia and muscles were bluntly separated and heparin (150 IU/kg IV) was injected prior to cannulation of the right femoral artery. A 4F introducer sheath (Terumo, Leuven, Belgium) was inserted and fluoroscopy was used to advance a 3F Fogarty balloon catheter (Edwards Life Sciences, Irvine, CA, USA) in the abdominal aorta. After inflation, the balloon was retracted through the infrarenal aorta three times to induce endothelial denudation. The Fogarty catheter and sheath were removed from the animal, the wound was closed and the rabbit was allowed to recover.

Radiofrequency ablation

Radiofrequency ablation was performed eleven weeks after balloon denudation. Acepromazine and methadone (both 1.5 mg/kg) were injected intramuscularly for premedication. Etomidate (1.5-2 mg/kg) was injected via the ear vein, after which rabbits were intubated and ventilated with a mixture of oxygen/air (1:2) and 1.5% isoflurane. Sufentanil (1 ug/kg/h) was continuously administered intravenously. Subcutaneous meloxicam (1 mg/kg) was given before surgery as analgesia. The right abdominal site was shaven to connect the rabbit to a grounding patch. The neck and inguinal region were then shaven, povidon-iodine 2% was applied and all remaining parts were draped with sterile sheets. Heparin (150 IU/kg IV) was injected prior to cannulation of the left carotid and femoral artery. A 5F and a 4F sheath were inserted in the respective artery. An angiogram of the infrarenal aorta was made by injecting contrast agent through the lumen of an inflated 4F Fogarty balloon catheter (Figure 1b). The balloon was deflated and the Symplicity Spyral Radiofrequency Ablation Catheter (Medtronic, Minneapolis, MN, USA) was advanced from the femoral sheath over a 0.014" Hi-torque Extra S'port guidewire (Abbott Vascular, Libertyville Township, IL, USA) under fluoroscopy. Either the upper or lower half of the infrarenal aorta was randomly selected for treatment with RFA. By slightly retracting the guidewire from the lumen of the RFA catheter, the tip with the electrodes turned to its spiral shape and was firmly positioned to the vascular wall (Figure 1c). Fluoroscopy images were captured in order to determine the boundary between treated and untreated regions for histological processing. The four electrodes on the device were separately and subsequently activated to perform radiofrequency ablation (≈70 °C) for two minutes under

continuous room temperature saline infusion. This was repeated in the adjacent region so that in total 8 points on the aortic wall (half of the infrarenal aorta) were ablated. Afterwards, a control angiogram was performed, the device and sheath were removed from the animal and the wound was closed. The animal was then allowed to recover from surgery. From the day before RFA until termination, rabbits received 10 mg/kg aspirin (Aspro, Bayer, Mijdrecht, the Netherlands) daily, dissolved in 400 mL freshly prepared drinking water.

Optical coherence tomography (OCT)

OCT was performed in 6 of the 14 rabbits directly prior to, after RFA and at the end of the follow-up period. For this purpose, a C7 Dragonfly™ Duo imaging catheter (St. Jude Medical, St. Paul, MN, USA) was advanced through the femoral sheath and positioned in the infrarenal aorta (Figure 1d). In order to temporarily remove signal distorting blood flow from the aorta, contrast agent was injected through the lumen of an inflated 4F Fogarty balloon catheter and a manually triggered pullback was performed using the OCT ILUMIEN™ OPTIS™ OCT-system (St. Jude Medical). The CURAD Vessel Analysis program (Curad B.V., Amsterdam, NH, the Netherlands)[13] was used for the assessment of lumen and vessel wall contours in every frame (n=10/mm). Fluoroscopy images with the OCT catheter in situ and matched vessel wall contours were used to specify the control and RFA-treated regions at index procedure and follow-up. Vascular remodelling was assessed by luminal area ratio, resulting from dividing the luminal area at 28 days follow-up by the luminal area directly prior to intervention. The fibrous cap was defined as the hyperintense signal ranging from the luminal border to the inner border of the lower-intensity lipid pool.[14]

Tissue harvesting

Rabbits were sacrificed 15 minutes (n=2), 60 minutes (n=1), 24 hours (n=2), 7 days (n=3) or 28 days (n=6) after RFA. Similar anesthetic and surgical protocols as during the RFA procedure were used. Heparin (150 IU/kg IV) was injected prior to cannulation of the right carotid artery. An angiogram was performed to visualize the infrarenal aorta. Subsequently, the abdomen was incised. After heparinization (1000 IU/kg IV), catheters were placed in the aorta and caval vein. After sacrifice, the aorta was perfused with 0.9% saline, followed by pressure fixation with 4% formaldehyde. Subsequently, X-ray was used to determine and mark the boundary between treated and untreated regions as could be retrieved from the RFA catheter positioning images. The aorta was amply explanted from the animal and stored in formalin for at least 24 hours. In the rabbit that was sacrificed one hour after RFA, the aorta was marked, explanted, snap-frozen in liquid nitrogen and stored at -80 °C.

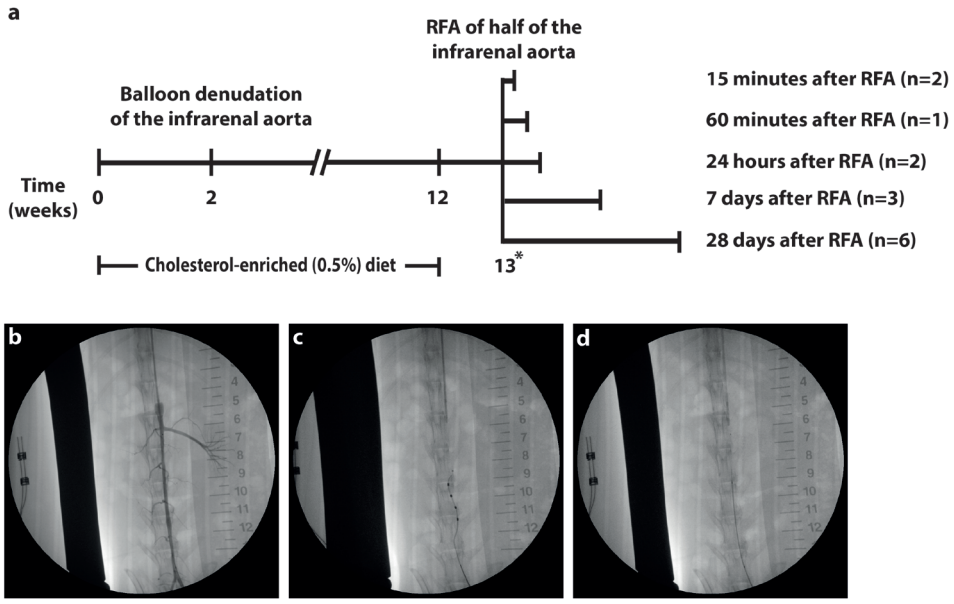

Figure 1. Experimental set-up
Rabbits were fed a 0.5%-enriched cholesterol diet two prior to balloon denudation of the infrarenal aorta and eleven weeks thereafter. One week after cessation of the cholesterol-diet, RFA was performed on half of the infrarenal aorta. Rabbits were then sacrificed at different time points (a). Prior to RFA, directly after and at termination, angiography of the infrarenal aorta was performed (b). In a subset of rabbits, OCT images were acquired (c). RFA catheter positioning was established by slightly retracting the guidewire from the lumen of the catheter to let it return to its original spiral shape and assure stable adherence to the vascular wall (d). **: OCT was performed in a subset of rabbits prior to and directly after RFA.*

Tissue preparation and histological analysis

The treated and untreated region of the infrarenal aorta were each cut axially in 6-8 similar-sized parts and stored at -80 °C (n=1) or embedded in paraffin (n=13). Sections of 4 μm were stained with hematoxylin and eosin (H&E), Elastica van Giesson (EvG) and picrosirius red. In addition, terminal deoxynucleotidyl transferase (TdT) dUTP nick end labeling (TUNEL assay) was performed and immunostains for CD31, alpha-SMA (αSMA) and macrophages.

Cell nuclei in the plaque were stained for H&E and semi-automatically counted using digital histology. EvG staining was used for morphometric analysis. Luminal contours, internal elastic laminae (IEL) and external elastic laminae (EEL) were traced manually using digital histology. Plaque area was calculated by subtracting the luminal area from the IEL area and medial area by substracting the IEL area from the EEL area. Collagen content was quantified in tissue sections stained for picrosirius red and photographed under polarized light. Masson's trichrome staining was used to identify and measure the fibrotic cap area, which

was divided by the luminal perimeter to obtain the average cap thickness per section. Cap thickness was defined as the minimum distance from the luminal border to the inner border of the lipid pool.[14]
TUNEL assay was used to identify double-stranded DNA breaks and performed using a DeadEnd™ Colorimetric TUNEL System (Promega, Madison, WI, USA). Of each tissue section, three random fields of the atherosclerotic plaque were selected at 20x magnification. Nuclei of cells were manually counted and those staining positive for TUNEL expressed as a percentage of the total nuclei in the image. Microvessels in the plaque and adventitia were visualized using a monoclonal mouse anti-CD31 antibody (Clone JC70a, dilution 1:50; Dako). BrightVision poly-AP anti-mouse IgG (Immunologic, Duiven, the Netherlands) was used as a secondary antibody and liquid permanent red (Dako, Glostrup, Denmark) as an enzyme substrate. Only vessels with a lumen smaller than 50 μm in diameter were included in the analysis. Vessel count was corrected for the particular area, with the adventitial area included for analysis extending maximally 200 μm from the EEL. αSMA was used to stain smooth muscle cells. Macrophages were stained using a monoclonal mouse anti-rabbit macrophage antibody (clone RAM-11, dilution 1:800; DAKO). BrightVision poly-AP anti-mouse IgG (Immunologic) was used as a secondary antibody and liquid permanent red (Dako) as an enzyme substrate. Collagen, αSMA and macrophage content are expressed as a percentage of the region of interest (i.e. plaque, media). Images of tissue sections were captured and analysed using CellSens (Olympus Corporation, Tokyo, Japan).

Safety

In both, OCT and histology, we evaluated treated and non-treated regions for dissections, thrombus formation and intraplaque hemorrhage. Dissection was defined as a tear in the wall of the blood vessel that allowed blood to separate the layers. Irregular endoluminal or mural mass on OCT was regarded as thrombus formation. Intraplaque hemorrhage was defined as a fibrin- and/or erythrocyte-rich deposition in the plaque. In addition, attention was paid to clinical symptoms (*i.e.* hindleg problems).

Statistical analysis

In each animal, the individual scores of the tissue sections were averaged per region (i.e. treated vs. untreated, on average 8 slides/region). The averages of the treated and untreated regions of all rabbits were then used to calculate the means and standard deviations. Data distribution was evaluated for normality using the Shapiro-Wilk test. Normally distributed data were compared using a paired-samples T-test, non-normally distributed data were compared using a paired-sample Wilcoxon signed rank test to test for significant differences ($P<0.05$). Statistical analyses were performed using SPSS software, version 21.

RESULTS

Safety assessment by angiography, optical coherence tomography and histology

RFA did not induce any macroscopic effects detectable with angiography. We did not observe vasospasms or oedema at the site of RFA, nor did we detect any adverse events such as dissection or thrombus formation. To increase sensitivity, we performed OCT prior to and directly after RFA in six rabbits (Figure 2a). Again, we could not detect any vessel wall oedema, plaque rupture or dissection. Overall, the vessel wall in RFA-treated regions was not distinguishably different from control regions (Figure 2b-c). Directly after RFA, we observed a decrease in signal intensity in one rabbit (out of six) (Figure 2d). In one rabbit, we detected a small thrombus without evident vessel wall narrowing or dissection (Figure 2e-f). Luminal area ratio showed comparable remodelling in both regions (0.95±0.23 vs. 0.88±0.13; p=0.77, Figure 2g). In addition, cap thickness did not differ between control and RFA-treated regions prior to (271±26 vs. 262±51 μm; p=0.65, Figure 2h) and 28 days after intervention (207±98 vs. 251±115 μm; p=0.08).

On histological examination no evidence was found for dissection, thrombus formation or other adverse events in any of the rabbits. TUNEL assay was used to localize focal ablation points and to allow for identification of blunt ends of double-stranded DNA breaks. Untreated regions showed few to no nuclei staining positive (brown) for TUNEL (Figure 3a-c). On the contrary, treated regions of rabbits sacrificed within 24 hours after RFA showed an increased number of nuclei staining positive for TUNEL, extending from the plaque to the adventitia (Figure 3d-f), without breaching the endothelium. Compared to untreated control regions, the percentage of positive nuclei in the treated region was increased 15 minutes (2.7±3.3 vs. 15.7±10.0%; p=0.22, Figure 3g) and 24 hours after RFA (2.0±2.2 vs. 58.3±51.8%; p=0.38).

Lesion characterization and cellularity

Tissue sections from RFA-treated areas from rabbits sacrificed 24 hours, 7 days or 28 days after RFA showed lesions characterized by (locally) decreased cellularity (Figure 4a-d). As a consequence, a trend towards decreased intimal cellularity 24 hours after RFA was observed (1817±482 vs. 1180±383 nuclei/mm^2; p=0.07, Figure 4e). After 7 or 28 days, ≈20% of the plaque in the treated region remained decellularized and intimal cellularity was no longer different from untreated regions (Figure 4f).

Vessel density

Figure 5a-b shows CD31 staining in both the plaque and adventitia. Plaque vessel density was not different between untreated and treated regions 7 days after RFA (3.0±4.6 vs. 3.9±2.1 vessels/mm^2; p=0.76, Figure 5c). At 28 days, vessel density in the plaque was

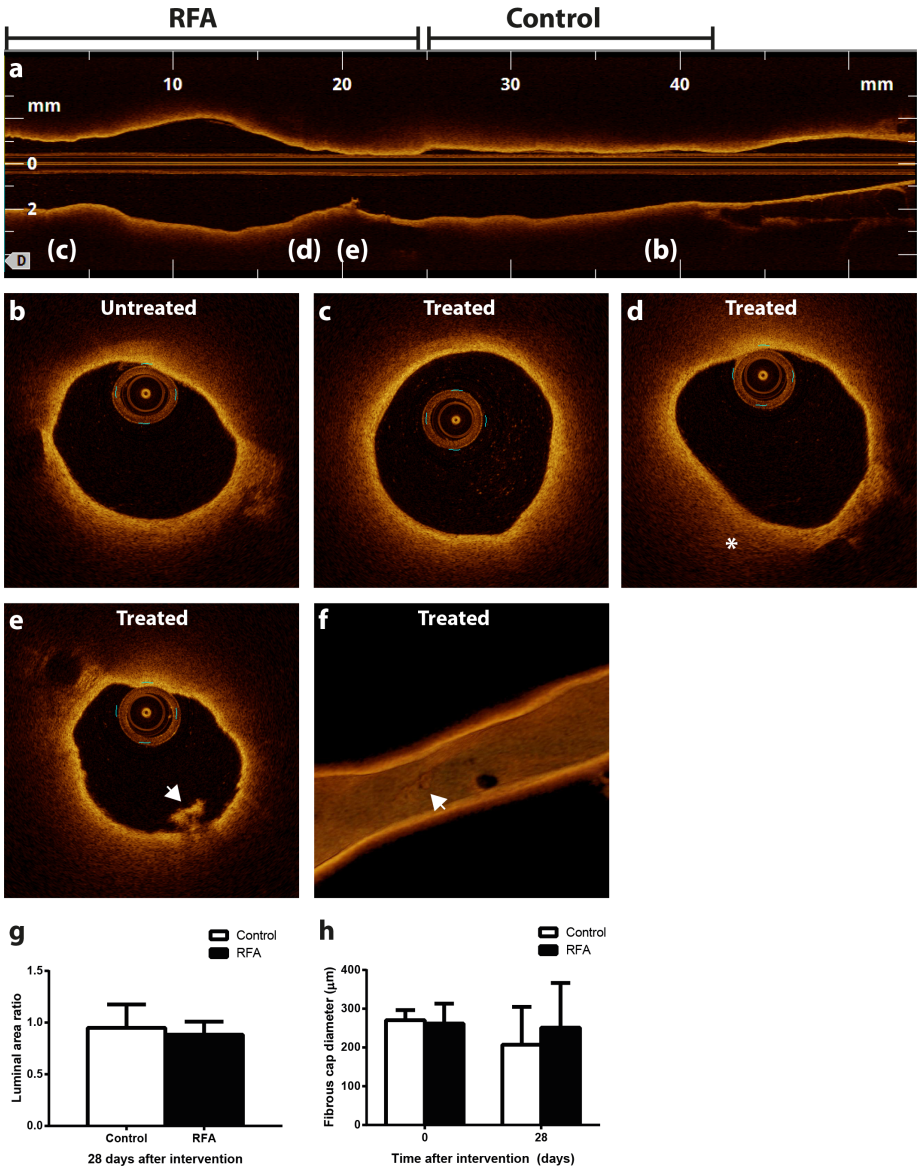

Figure 2. OCT image acquisition

OCT was performed in RFA-treated and control regions of the infrarenal aorta (a). The letters in this longitudinal image indicate respective transverse images (b-e). In the majority of the acquired images, control (b) and ablated regions (c) did not appear to be different. Only incidentally could we observe a slight decrease in signal intensity (*) in the RFA-treated area (d). In one rabbit in one location, we observed thrombus formation without clear dissection (e), with a 3D reconstruction showing the extent of the thrombus formation in the vessel wall (arrow) (f). Luminal area ratio of area at 28 days follow-up divided by area prior to RFA showed no difference in vascular remodelling between control and remote regions (g), nor did fibrouw cap thickness differ at baseline or follow-up (h).

significantly lower in RFA-treated regions (11.6±6.7 vs. 5.4±3.7 vessels/mm^2; p=0.028). With respect to adventitial vessel density, no significant differences were observed 7 days (41.7±8.6 vs. 39.1±11.5 vessels/mm^2; p=0.81, Figure 5d) or 28 days (38.5±6.6 vs. 46.4±13.4 vessels/mm^2; p=0.06) after RFA.

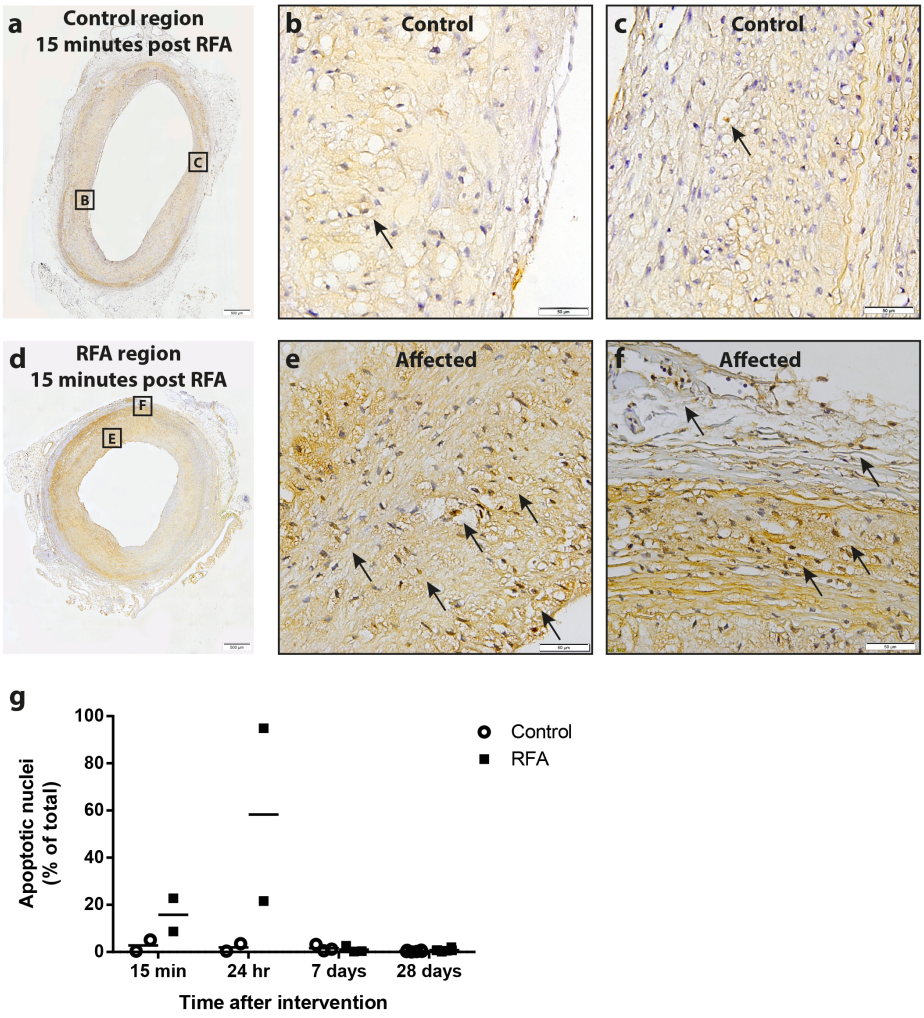

Figure 3. DNA damage in RFA and control regions
TUNEL assay was performed to detect double-stranded DNA breaks as a marker for apoptosis in both control and RFA-treated regions. Control regions showed only few nuclei staining positive (brown) (a-c), whereas in specific RFA-treated regions, a considerable amount of nuclei were shown to stain positive up to the adventitia (d-f). This effect was most apparent 15 minutes and 24 hours after RFA and was abolished at longer term follow-up (g). *Positive nuclei are indicated by arrows.*

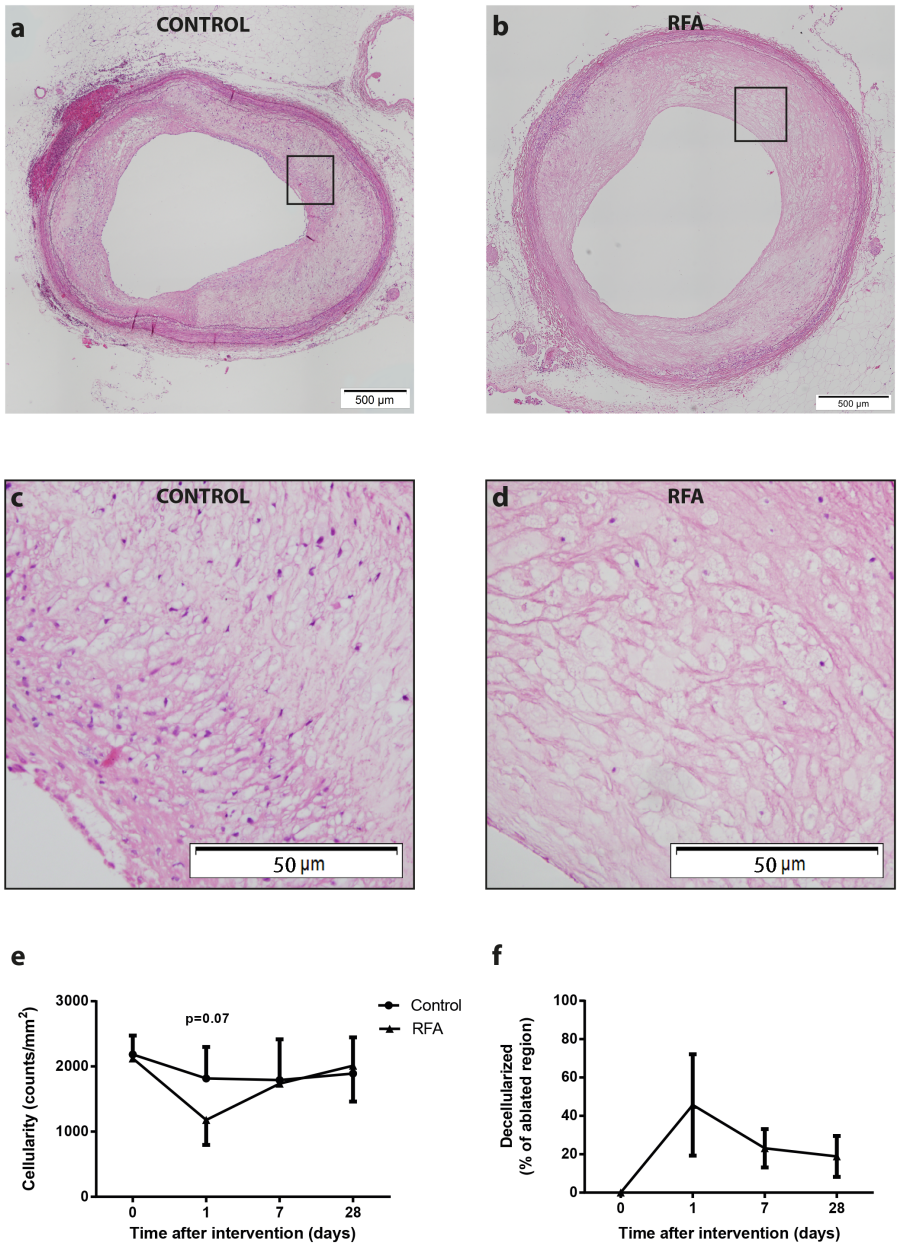

Figure 4. Plaque cellularity and percentage affected region
Representative HE-stained tissue sections of control (a) and treated (b) regions and respective magnifications (c-d) showed that RFA greatly reduced cellular content. This effect was most pronounced 24 hours post-RFA, after which cellularity was normalized at 7 and 28 days (e). The decellularized area was quantified as a percentage of the total region where RFA was performed and showed that the effect of RFA was most apparent after 24 hours (f).

To further explore whether differences existed in the regions due to a local and non-circumferential effect of RFA, we separately quantified vessel density in both the cellularized and decellularized areas in the treated region. We selected the adventitial area extending up to 200 μm from the EEL and directly adjacent to the decellularized plaque and media. This showed that the difference in plaque vessel density after 28 days could be attributed to a decrease in the part of the plaque that remained decellularized (control 10.7±7.1 vs. decellularized area 2.3±3.0 vessels/mm^2; p=0.09, Figure 5e). In contrast, adventitial plaque vessel density was significantly increased in the decellularized region when compared to the control region (control 39.4±6.9 vs. decellularized area 108.9±40.9 vessels/mm^2; p=0.014, Figure 5f).

Atherosclerotic plaque burden and plaque composition

According to the modified AHA Classification, the great majority of the plaques in the current study most closely resembles the fibroatheromatous plaque type without the presence of a necrotic core or calcifications.[15]

Plaque burden by EvG staining (Figure 6a-b) did not differ between untreated and treated regions at 7 days (5.5±1.5 vs. 5.6±1.7 mm^2; p=0.62, Figure 6c) or 28 days (4.3±1.1 vs. 4.6±0.9 mm^2; p=0.46) after RFA. In addition to serial OCT measurements providing luminal area ratio, we also used IEL area at 28 days follow-up as a measure of remodelling.[16,17] Although RFA-treated regions seemed to have slightly more outward remodelling, this difference was not significant (8.7±1.2 vs. 10.3±2.6; p=0.07). Collagen content in the plaque as assessed by picrosirius red staining was comparable between both groups at 7 days (32.7±13.0 vs. 34.6±11.9%; p=0.22, Figure 6d-f) and 28 days (40.3±12.4 vs. 39.2±9.1%; p=0.85) and similarly in the media at 7 days (73.4±3.8 vs. 73.8±7.5%; p=0.89) and 28 days (72.3±14.3 vs. 69.7±11.1%; p=0.72). Representative examples of αSMA stains are displayed in Figure 6g-h. Compared to untreated regions, αSMA content as a percentage of the plaque area was significantly decreased in treated regions at 7 days (18.0±5.9 vs. 9.8±5.3 %; p=0.006, Figure 6i) and a trend was observed at 28 days after RFA (12.0±2.0 vs. 9.1±3.3 %; p=0.06). Moreover, medial αSMA content was decreased 28 days after RFA (27.7±13.6 vs. 15.0±4.6%; p=0.033). Similar to vessel density quantification, we separately quantified αSMA content in both the cellularized and decellularized areas in the treated region. This pointed out that differences between control and treated regions could mainly be explained by decreased αSMA content in the decellularized part of the treated region after 7 days (control 18.0±5.9 vs. decellularized 1.8±0.4%; p=0.038, Figure 6j-l) and 28 days (12.6±1.6 vs. 6.8±3.8%; p=0.020). Similarly, the media of treated decellularized regions was lower in αSMA content after 7 days (23.6±12.7 vs. 2.2±0.7%; p=0.10) and 28 days (32.0±9.7 vs. 6.1±6.4%; p=0.013).

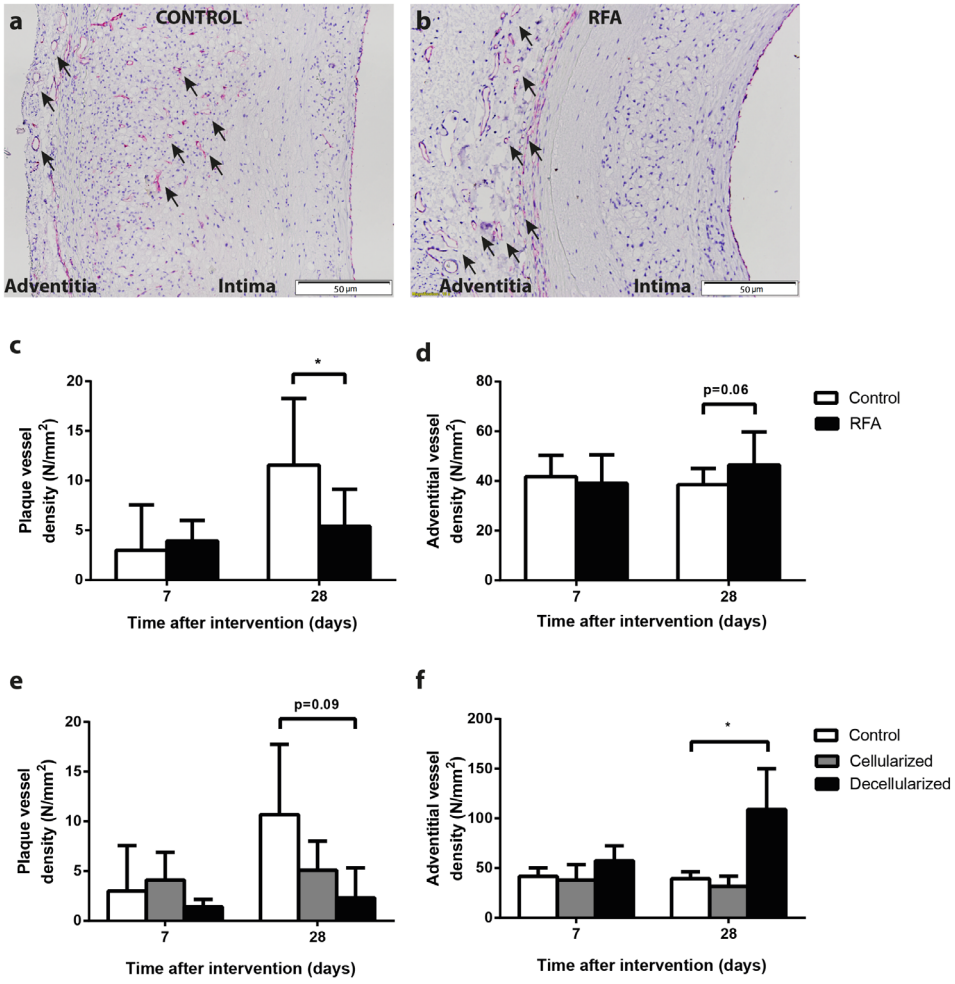

Figure 5. Plaque and adventitial vessel density

Representative images of anti-CD31 staining are shown for control (a) and treated plaques (b). Vessel density in the plaque at 28 days was lower in regions treated by RFA when compared to control regions (c). With respect to adventitial vessel density, no significant differences were observed between both groups (d). Further exploration of cellularized and decellularized areas showed that the difference between treated and untreated regions after 28 days was mainly explained by a decrease in plaque vessel density in the decellularized area (e). With respect to adventitial density, the increase in treated regions after 28 days could be mainly attributed to an increase in decellularized areas (f). *Plaque vessels and vasa vasorum are indicated by black arrowheads. * p<0.05.*

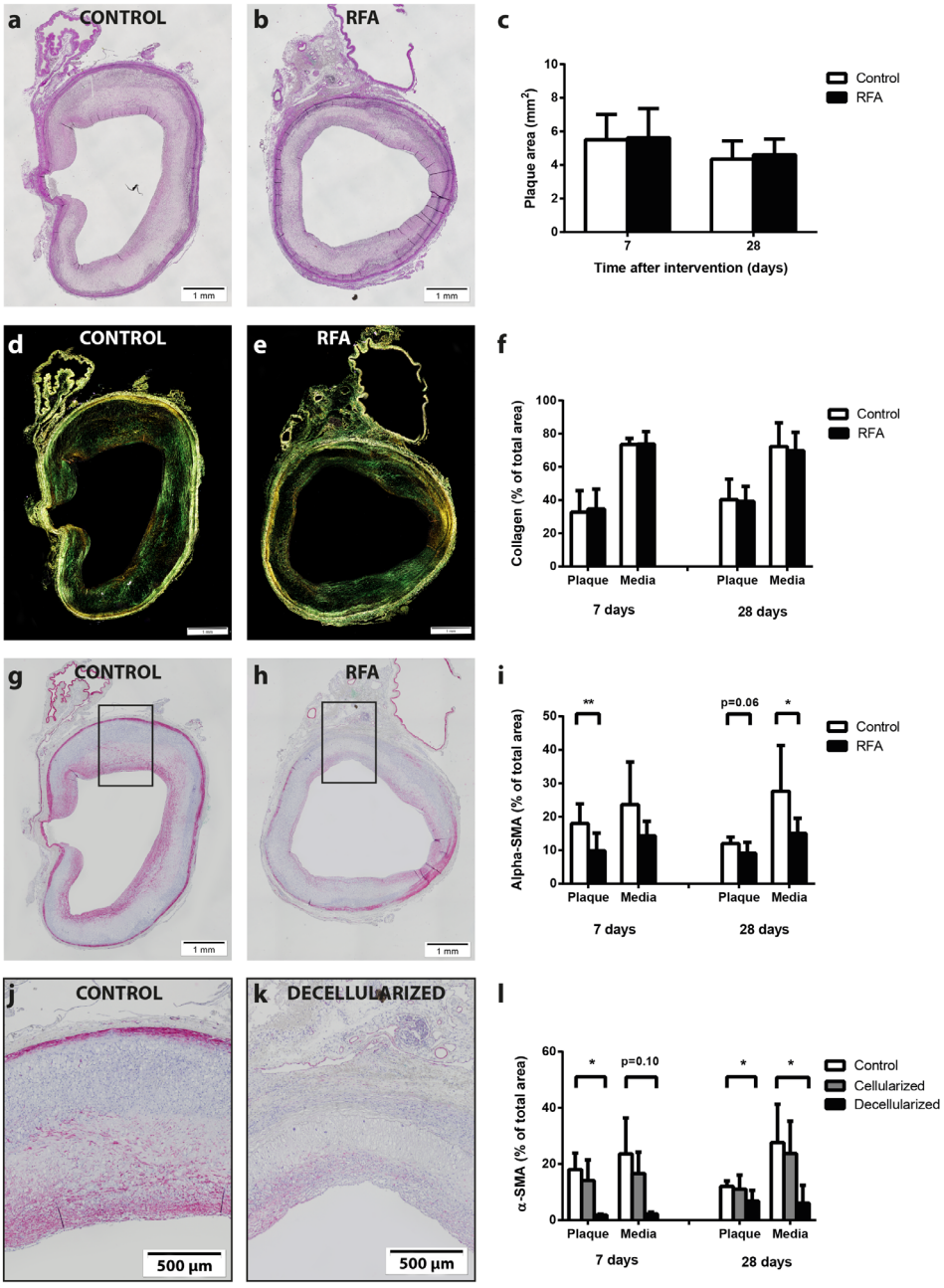

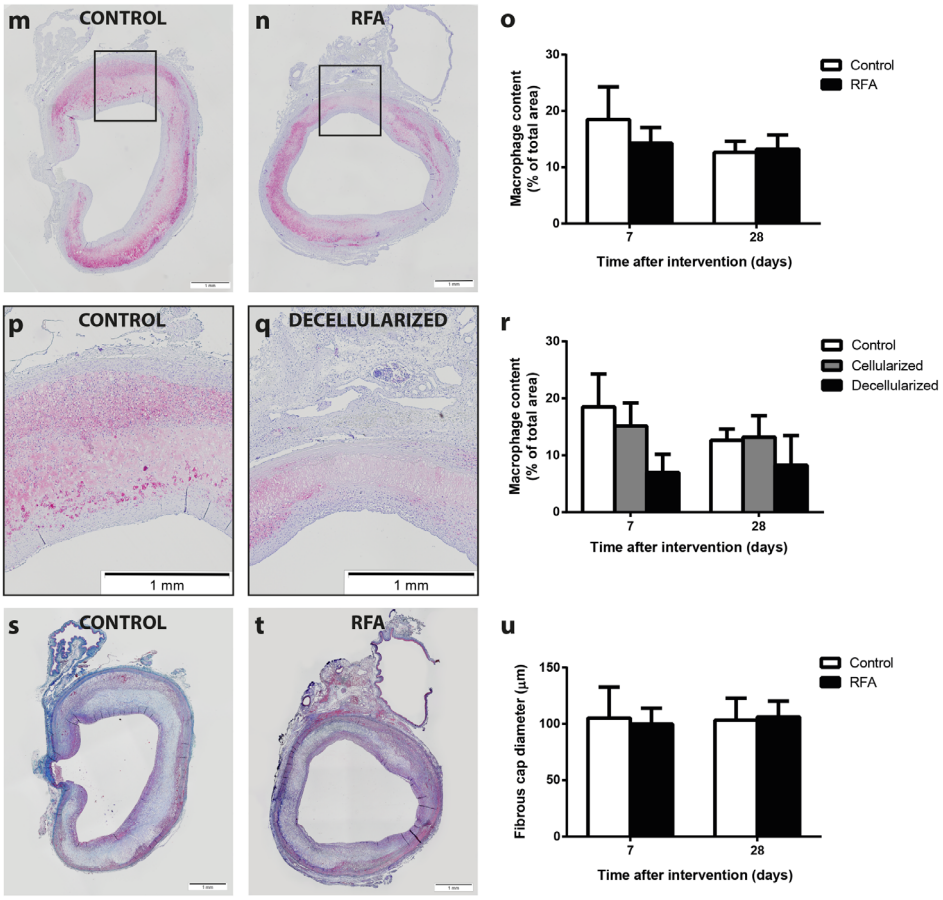

Figure 6. Atherosclerotic plaque burden and plaque composition
An EvG staining was used to quantify plaque burden in control (a) and RFA regions (b). Both, after 7 and 28 days, no difference was observed with respect to atherosclerotic plaque area (c). Collagen content was quantified by picrosirius red staining (d-e) and did not show any differences between either the plaque or media of both regions (f). Smooth muscle cell content assessed by αSMA staining (g-h) showed a major decrease in the plaque and media of regions treated with RFA at either 7 or 28 days (i). Magnified images hereof (j-k) show that this effect could mainly be attributed to areas that remained decellarized after RFA treatment (l). Macrophage content in control (m) and RFA (n) regions was not different (o). Although not significant, decellularized areas showed a trend towards lower macrophage content compared to control regions, mainly after 7 days (p-r). Cap thickness assessed by masson's trichrome staining of control (s) and RFA (t) regions was not different between both regions (u). * *p<0.05, ** p<0.01*

In addition, macrophage area as a percentage of the plaque did not differ between untreated and treated regions at 7 days (18.5±5.8 vs. 14.3±2.8 mm^2; p=0.32, Figure 6n-o) and 28 days (12.6±2.0 vs. 13.2±2.5%; p=0.73). Although not significant, subanalyses indicated that decellularized parts of the treated area were lower in macrophage content than control regions after 7 days (control 18.5±5.8 vs. decellularized area 7.0±3.2%; p=0.11, Figure 6p-r). This difference was not observed after 28 days, when macrophage content was comparable between both areas (12.6±2.0 vs. 8.2±5.2%; p=0.17).
Representative images of cap thickness in both control and RFA-treated regions are shown in Figure 6s-t. No difference was observed between both regions 7 days (105±27 vs. 100±14 μm; p=0.71, Figure 6u) and 28 days after RFA (103±20 vs. 106±14 μm; p=0.72). Similarly, no differences in subanalyses of control, decellularized or cellularized regions were observed after 7 days (control 105±27 vs. decellularized 109±29 μm; p=0.39) and 28 days (control 101±21 vs. decellularized 103±24 μm; p=0.90).

DISCUSSION

To our knowledge this is the first report on radiofrequency ablation (RFA) of atherosclerotic lesions. RFA is safe and modulates plaque vessel density and smooth muscle cell content in a rabbit atherosclerosis model.

Safety
Other than a small thrombus without vessel narrowing in one of the animals after RFA as evidenced by OCT, we did not observe any adverse events after treatment. RFA induced thrombus formation is frequently observed by OCT in preclinical and clinical renal denervation studies without adverse angiographic or clinical relevance[6–8,10,18], whereas this was an incidental finding in our study. We performed RFA under continuous saline irrigation, possibly preventing blood clotting by lowering blood temperature. In addition, coagulation in pig and human blood may differ from rabbit blood[19] and the heparin dose of of 150 IU/kg given is considerably higher than normally administered to patients.
Apoptosis examination by TUNEL assay showed RFA induced double-stranded DNA breaks in all vascular layers without endothelial disruption. The current application of RFA exerted a rather local effect, reflected by persistent decellularization. This corresponds to the tissue ablation and cell depletion observed in previous studies performing RFA on the arterial vessel wall.[10,11]

Vessel density

Although the TUNEL assay confimed that thermal energy indeed reached the adventitia, no significant decrease in vasa vasorum density was observed. In fact, adventitial vessel density was even higher in decellularized regions closest to the applied radiofrequent energy. This could be due to insufficient capillary degradation or a reactive angiogenic response in the adventitia after RFA, as described previously.[10] In contrast, plaque vascularization was significantly decreased in RFA-treated regions 28 days after RFA. Leaky neovessels are the main origin of intraplaque haemorrhage leading to vulnerable plaque phenotypes and worse clinical outcome.[20] Thus, RFA might serve as a means to decrease intraplaque hemorrhage in more advanced plaques. The discrepancy between adventitial and plaque (neo)vascularization may suggest that only more severe tissue ablation results in decellularization, thereby creating an environment that is less susceptible to vascular penetration. This finding is supported by the observation that – although the majority of the plaque was recellularized after RFA – local areas remained decellularized up to 28 days thereafter and showed lower vessel density than recellularized areas in the treated region.

Plaque composition

Although RFA has been shown to increase collagen content and induce fibrosis in healthy arteries[10], this was not observed in the present study. This may be due to the already relatively high collagen plaque content in this model. The unchanged collagen content may also explain the lack of difference in remodelling in both regions, since changes in the extracellular matrix are of key importance in the process of arterial remodelling.[16]

In contrast, RFA-treated regions showed a trend towards reduced overall cellularity after 24 hours and macrophage content up to 7 days. After 28 days, no differences between both regions were observed. Most likely, cell death resulted in a secondary low grade inflammatory reaction to clear the plaque from debris[11], culminating in comparable cellularity and macrophage content at long-term follow-up. Surprisingly however, RFA did not evoke a disproportionate inflammatory response, since macrophage content did not differ between RFA-treated and control regions at 7 days and 28 days follow-up. This finding is in agreement with the considerable proportion of TUNEL positive nuclei, indicating apoptotic cell death.[21,22] These findings suggests that apart from the normally observed thermal coagulation necrosis[23], apoptosis is at least to some extent responsible for cell death in the present study.

In addition, cap thickness was not affected by RFA. Although both methods show comparable cap thickness between the regions, the difference in absolute values can be explained by the observation that – in optical coherence tomography – high-fat plaques have irregular and not well-delineated borders[24], as opposed to human plaques.[14] This increases scattering on OCT images, decreasing the feasibility to clearly delineate the fibrous cap from the inner border of the lipid pool.

Importantly, although RFA treatment did not influence cap thickness, SMC content was decreased 7 and 28 days after RFA in both intima and media. While decreased SMC content could potentially compromise plaque stability[2] and therefore needs to be carefully evaluated, it may hint at a potential benefit in preventing (re)stenosis in peripheral arterial disease (PAD) and coronary artery disease (CAD), where SMC proliferation is a key mechanism. Despite the latest advances in stent design, restenosis rates remain relevant with 10-20% at 12 months follow-up for coronary artery stents and significantly higher rates for peripheral stenting.[5] Since plaque burden is not influenced by the current technique, further studies combining simultaneous radiofrequency energy delivery and balloon angioplasty could offer improved results.

Limitations

Although the current study provides important insight in the effect of RFA on atherosclerotic plaques, we would like to discuss some of its limitations. Due to the limited numbers – especially up to 24 hours after RFA – we were not able to compare vessel density in the subacute phase. Moreover, although serial detection of neovessels using OCT has been described[25], capillaries were rather large (50-300 μm) as opposed to the rabbit neovessels in the current manuscript (~10 μm), hampering their reliable detection. In addition, atherosclerotic animal models, including the present, do not develop advanced atherosclerotic lesions, which limits translation to the human situation. Although it may be interesting to evaluate the effect on a more advanced plaque phenotype, the rabbit model offers us a good alternative approach to appreciate the effects on atherosclerotic plaques. Moreover, a longer follow-up period could be informative to show whether plaque composition (*i.e.* smooth muscle cell content) would eventually normalize and if plaque burden would be affected (*i.e.* would decrease). In this regard, serial morphometric measurements could provide insight into plaque burden over time. Finally, the local effect of RFA might limit its ability to influence plaque burden over the total treated region. Therefore, an approach with a more advanced RFA catheter that targets the whole circumference could be of interest.

CONCLUSION

In conclusion, radiofrequency ablation is safe in moderate atherosclerotic vessel disease. It leads to near-complete plaque decellularization in treated areas in the subacute phase, a decrease in plaque vessel density and a major reduction in local smooth muscle cell content. Yet, 7 and 28 days after intervention it does not reduce vasa vasorum or affect plaque volume, cellularity, cap thickness or collagen content in a rabbit atherosclerotic model.

Therefore, combining this technique with balloon angioplasty could be promising in the treatment of severe (re)stenosis in (peripheral) arterial disease.

Acknowledgements
The authors thank Marlijn Jansen, Joyce Visser, Grace Croft, Martijn van Nieuwburg, Danny Elbersen and Evelyn Velema for their excellent technical support during the animal experiments and Danny Elbersen and Martijn van Nieuwburg for their assistance in histology.

Funding
Direct governmental funding.

Conflict of interest
All listed authors have no conflict of interest to declare.

REFERENCES

1. WHO. The top 10 causes of death, 2000-2012 [Internet]. 2012 [cited 2015 Apr 11];Available from: http://www.who.int/mediacentre/factsheets/fs310/en/
2. Finn A V., Nakano M, Narula J, Kolodgie FD, Virmani R. Concept of vulnerable/unstable plaque. *Arterioscler Thromb Vasc Biol*. 2010;30:1282–1292.
3. Virmani R, Kolodgie FD, Burke AP, Finn A V., Gold HK, Tulenko TN, Wrenn SP, Narula J. Atherosclerotic plaque progression and vulnerability to rupture: Angiogenesis as a source of intraplaque hemorrhage. *Arterioscler Thromb Vasc Biol*. 2005;25:2054–2061.
4. Lee JM, Park J, Kang J, Jeon KH, Jung JH, Lee SE, Han JK, Kim HL, Yang HM, Park KW, Kang HJ, Koo BK, Kim HS. Comparison among drug-eluting balloon, drug-eluting stent, and plain balloon angioplasty for the treatment of in-stent restenosis: A network meta-analysis of 11 randomized, controlled trials. *JACC Cardiovasc Interv*. 2015;8:382–394.
5. Schillinger M, Minar E. Percutaneous treatment of peripheral artery disease: Novel techniques. *Circulation*. 2012;126:2433–2440.
6. Krum H, Schlaich M, Whitbourn R, Sobotka PA, Sadowski J, Bartus K, Kapelak B, Walton A, Sievert H, Thambar S, Abraham WT, Esler M. Catheter-based renal sympathetic denervation for resistant hypertension: a multicentre safety and proof-of-principle cohort study. *Lancet*. 2009;373:1275–1281.
7. Rippy MK, Zarins D, Barman NC, Wu A, Duncan KL, Zarins CK. Catheter-based renal sympathetic denervation: Chronic preclinical evidence for renal artery safety. *Clin Res Cardiol*. 2011;100:1095–1101.
8. Worthley SG, Tsioufis CP, Worthley MI, Sinhal A, Chew DP, Meredith IT, Malaiapan Y, Papademetriou V. Safety and efficacy of a multi-electrode renal sympathetic denervation system in resistant hypertension: The EnligHTN I trial. *Eur Heart J*. 2013;34:2132–2140.
9. Verheye S, Roth L, De Meyer I, Van Hove CE, Nahon D, Santoianni D, Yianni J, Martinet W, Buchbinder M, De Meyer GRY. Cryotherapy increases features of plaque stability in atherosclerotic rabbits. *EuroIntervention*. 2015;11:1–10.
10. Steigerwald K, Titova A, Malle C, Kennerknecht E, Jilek C, Hausleiter J, Nährig JM, Laugwitz K-L, Joner M. Morphological assessment of renal arteries after radiofrequency catheter-based sympathetic denervation in a porcine model. *J Hypertens*. 2012;30:2230–9.
11. Vink EE, Goldschmeding R, Vink A, Weggemans C, Bleijs RLAW, Blankestijn PJ. Limited destruction of renal nerves after catheter-based renal denervation: Results of a human case study. *Nephrol Dial Transplant*. 2014;29:1608–1610.
12. Shaw LJ, Bugiardini R, Merz CNB. Women and Ischemic Heart Disease. Evolving Knowledge. *J Am Coll Cardiol*. 2009;54:1561–1575.
13. Belkacemi A, Agostoni P, Nathoe HM, Voskuil M, Shao C, Van Belle E, Wildbergh T, Politi L, Doevendans PA, Sangiorgi GM, Stella PR. First results of the DEB-AMI (drug eluting balloon in acute ST-segment elevation myocardial infarction) trial: a multicenter randomized comparison of drug-eluting balloon plus bare-metal stent versus bare-metal stent versus drug-eluting stent in primary p. *J Am Coll Cardiol*. 2012;59:2327–37.
14. Kume T, Akasaka T, Kawamoto T, Okura H, Watanabe N, Toyota E, Neishi Y, Sukmawan R, Sadahira Y, Yoshida K. Measurement of the thickness of the fibrous cap by optical coherence tomography. *Am Heart J*. 2006;152:755.e1-755.e4.
15. Virmani R, Kolodgie FD, Burke AP, Farb A, Schwartz SM. Lessons From Sudden Coronary Death. *Arterioscler Thromb*. 2000;20:1262–1275.
16. Pasterkamp G, De Kleijn DP V, Borst C. Arterial remodeling in atherosclerosis, restenosis and after alteration of blood flow: Potential mechanisms and clinical implications. *Cardiovasc Res*. 2000;45:843–852.
17. Ward M, Pasterkamp G, Yeung AC, Borst C. Arterial remodeling: Molecular mechanisms and clinical implications. *Circulation*. 2000;102:1186–1191.
18. Templin C, Jaguszewski M, Ghadri JR, Sudano I, Gaehwiler R, Hellermann JP, Schoenenberger-Berzins R, Landmesser U, Erne P, Noll G, Lüscher TF. Vascular lesions induced by renal nerve ablation as assessed by optical coherence tomography: pre- and post-procedural comparison with the Simplicity catheter system and the EnligHTN multi-electrode renal denervation catheter. *Eur Heart J*. 2013;34:2148b–2148.
19. Vilahur G, Padro T, Badimon L. Atherosclerosis and thrombosis: Insights from large animal models. *J Biomed Biotechnol*. 2011;2011:1–12.
20. Michel JB, Martin-Ventura JL, Nicoletti A, Ho-Tin-Noé B. Pathology of human plaque vulnerability: Mechanisms and consequences of intraplaque haemorrhages. *Atherosclerosis*. 2014;234:311–319.
21. Grasl-Kraupp B, Ruttkay-Nedecky B, Koudelka H, Bukowska K, Bursch W, Schulte-Hermann R. In situ detection of fragmented DNA (tunel assay) fails to discriminate among apoptosis, necrosis, and autolytic cell death: A cautionary note. *Hepatology*. 1995;21:1465–1468.
22. Rock KL, Kono H. The inflammatory response to cell death. *Annu Rev Pathol*. 2008;3:99–126.
23. Chu KF, Dupuy DE. Thermal ablation of tumours: biological mechanisms and advances in therapy. *Nat Rev Cancer*. 2014;14:199–208.
24. Tearney GJ, Regar E, Akasaka T, Adriaenssens T, Barlis P, Bezerra HG, Bouma B, Bruining N, Cho JM, Chowdhary S, Costa MA, De Silva R, Dijkstra J, Di Mario C, Dudeck D, Falk E, Feldman MD, Fitzgerald P, Garcia H, Gonzalo N, Granada JF, Guagliumi G, Holm NR, Honda Y, Ikeno F, Kawasaki M, Kochman J, Koltowski L, Kubo T, Kume

T, Kyono H, Lam CCS, Lamouche G, Lee DP, Leon MB, Maehara A, Manfrini O, Mintz GS, Mizuno K, Morel MA, Nadkarni S, Okura H, Otake H, Pietrasik A, Prati F, Rber L, Radu MD, Rieber J, Riga M, Rollins A, Rosenberg M, Sirbu V, Serruys PWJC, Shimada K, Shinke T, Shite J, Siegel E, Sonada S, Suter M, Takarada S, Tanaka A, Terashima M, Troels T, Uemura S, Ughi GJ, Van Beusekom HMM, Van Der Steen AFW, Van Es GA, Van Soest G, Virmani R, Waxman S, Weissman NJ, Weisz G. Consensus standards for acquisition, measurement, and reporting of intravascular optical coherence tomography studies: A report from the International Working Group for Intravascular Optical Coherence Tomography Standardization and Validation. *J Am Coll Cardiol*. 2012;59:1058–1072.

25. Kume T, Okura H, Yamada R, Koyama T, Fukuhara K, Kawamura A, Imai K, Neishi Y, Uemura S. Detection of Plaque Neovascularization by Optical Coherence Tomography: Ex Vivo Feasibility Study and In Vivo Observation in Patients With Angina Pectoris. *J Invasive Cardiol*. 2016;28:17–22.

CHAPTER 4

The effect of CD34-capturing coronary stents with abluminal sirolimus coating on endothelial coverage

G.H.J.M. Ellenbroek[1], L. Timmers[2], F. Nijhoff[2], E. Ligtenberg[3], S. Rowland[4], J.A. Post[5], G. Pasterkamp[1,6], I.E. Hoefer[1,6]

[1] Laboratory of Experimental Cardiology, University Medical Center Utrecht, The Netherlands
[2] Department of Cardiology, University Medical Center, Utrecht, The Netherlands
[3] OrbusNeich Medical B.V., Hoevelaken, The Netherlands
[4] OrbusNeich Medical Inc., Fort Lauderdale, FL, USA
[5] Cell Biology, Faculty of Science, Utrecht University, The Netherlands
[6] Laboratory of Clinical Chemistry and Hematology, University Medical Center Utrecht, The Netherlands

AsiaIntervention 2016; 2: 132-140

ABSTRACT

Background

Drug-eluting stents (DES) reduce neointimal hyperplasia by inhibition of vascular smooth muscle cell proliferation, concomitantly inhibiting stent endothelialisation and increasing the risk for stent thrombosis. The present study compares a contemporary DES to an endothelial progenitor cell capturing DES (COMBO stent), with regards to intimal hyperplasia and endothelial coverage.

Methods and Results

Twelve New-Zealand White rabbits were subjected to bilateral iliac artery stent placement. Each animal received both an everolimus-eluting stent (EES) and a COMBO stent. Four weeks after implantation, optical coherence tomography (OCT) was performed in six animals and tissue was harvested from the other six animals. Endothelial stent coverage assessed by scanning electron microscopy was significantly higher in COMBO stents than in EES (96.6±3.5% vs. 78.5±16.8%; $p<0.05$). Neointimal hyperplasia by OCT differed significantly (EES: 0.227±0.025 mm^2 vs. COMBO: 0.188±0.044 mm^2; $p<0.05$), but not by histology (EES: 0.823±0.200 mm^2 vs. COMBO: 0.891±0.312 mm^2; p=NS). No differences were observed in late loss between EES and COMBO stent (0.29±0.19 mm^2 vs. 0.29±0.16 mm^2; p=NS).

Conclusion

Endothelialisation is significantly improved in the COMBO stent with equal inhibition of intimal hyperplasia, which may reduce thrombotic events after DES implantation and allow for earlier discontinuation of dual antiplatelet therapy.

INTRODUCTION

Cardiovascular disease remains the leading cause of death in the world with rising numbers especially in non-Western countries.[1] The most frequent treatment for coronary artery disease (CAD) is to restore coronary blood flow by percutaneous coronary intervention (PCI).
Though superior to solo balloon angioplasty[2], coronary stent implantation has two complications: in-stent restenosis and stent thrombosis.[3] In-stent restenosis is driven by the inflammatory response that occurs upon inflation of the balloon catheter to restore the lumen and the accompanying endothelial damage. This triggers vascular smooth muscle cell (VSMC) proliferation, leading to neointimal hyperplasia (NIH) and subsequent luminal narrowing. The advent of drug-eluting stents (DES) that reduce VSMC proliferation has largely solved this problem.[4,5] However, by non-selectively inhibiting endothelial cell proliferation as well, the risk for in-stent thrombosis is increased.
In particular early stent endothelialisation reduces thrombotic complications and decreases neointima formation.[6,7] Endothelial progenitor cell (EPC) capturing stents use anti-CD34 antibody coatings to facilitate colonization of circulating EPCs onto the stent struts. In comparison to bare metal stents (BMS) or DES, they have shown to improve stent endothelialisation and decrease stent thrombosis both in in-vitro and in-vivo studies.[8–11] However, compared to DES, neointima formation and the need for target vessel revascularization were significantly higher due to the lack of anti-proliferative coatings.
It is for these reasons that the COMBO™ Dual Therapy Stent (OrbusNeich; Hong Kong) combines a luminal anti-CD34 antibody coating to improve luminal stent endothelialisation with abluminal antiproliferative drug-elution from a bioresorbable polymer matrix to inhibit VSMC proliferation and intimal hyperplasia. The REMEDEE trial has shown non-inferiority of the COMBO stent compared to paclitaxel eluting stents (PES) with regard to angiographic in-stent late lumen loss.[12]
However, PES belong to the first generation DES, which nowadays have been largely replaced by safer and more effective 2nd generation DES.[13,14] Yet, histological data regarding stent endothelialisation in combination with clinical standard optical coherence tomography (OCT) have not been reported so far. The aim of the current study is to compare these stent types in rabbits, using both histology and OCT to assess endothelial cell coverage and intimal hyperplasia.

MATERIALS AND METHODS

Experimental design

Twelve female New Zealand white rabbits (Charles River, Chatillon-sur-Chalaronne, R-A, France; 3.5-4.0 kg) were subjected to iliac artery stenting. Two different types of stents were implanted in the left and right iliac arteries in an alternating fashion (switching sides). The COMBO™ stent (OrbusNeich, Ft. Lauderdale, FL, USA) combines a sirolimus-eluting bioresorbable coating on the abluminal side with an anti-CD34 antibody coating on the luminal side. The Xience Prime stent (Abbott Vascular, Santa Clara, CA, USA) has a conformal, everolimus-eluting permanent polymer coating with omnidirectional release of the drug.

Data acquisition and measurements were performed by a blinded observer. All animal experiments were approved by the Ethical Committee on Animal Experimentation of the University Medical Center Utrecht (Utrecht, the Netherlands) and conform to the 'Guide for the care and use of laboratory animals'.

Anaesthesia

Rabbits were fasted overnight prior to surgery. From the day before implantation until termination at 28 days, rabbits received 10 mg/kg aspirin (Aspro, Bayer, Mijdrecht, the Netherlands) daily, dissolved in 400 mL freshly prepared drinking water after closely monitoring the average water intake per day. Subcutaneous meloxicam (1 mg/kg) was given before surgery as analgesia.

Acepromazine and methadone (both 1.5 mg/kg) were injected intramuscular for premedication. Etomidate (1.5-2 mg/kg) was injected via the ear vein, after which rabbits were intubated and ventilated with a mixture of oxygen/air (1:2) and 1.5% isoflurane. Sufentanil (1 ug/kg/h) was continuously administered intravenously.

Stent implantation

Heparin (150 IU/kg IV) was injected prior to cannulation of the left carotid artery. A 4F sheath was inserted, through which a 3F Fogarty balloon (Edwards Lifesciences, Irvine, CA, USA) was inserted. After inflation, the balloon was retracted through both iliac arteries twice for approximately 4 cm to induce endothelial denudation. Afterwards, the stents (3.0 x 15.0 mm) were implanted in the iliac artery. Nominal pressure was applied to inflate the balloon to a diameter of 3.0 mm, followed by a second angiogram.

Quantitative angiography

Angiograms of the iliac arteries were obtained before and after stent implantation and at termination. Luminal diameters were measured using Image J. Calibration was performed

on the guiding catheter in the same image. The balloon-to-artery ratio (BAR) was defined as the luminal diameter after stenting/luminal diameter before stenting. Late loss was defined as the difference between the angiographic diameter directly after stenting and the angiographic diameter at 28 days of follow-up.

Optical coherence tomography (OCT)

To avoid detection of iatrogenic endothelial damage in the sEM, OCT was performed in 6 of the 12 rabbits. Four weeks after implantation, rabbits were heparinized with 150 IU/kg heparin prior to cannulation of the right carotid artery. A 6.5F SheathLess Eaucath multipurpose guiding catheter (Asahi Intecc, Aichi, Japan) was inserted and selectively placed in the iliac artery. A C7 Dragonfly™ Duo imaging catheter (St. Jude Medical, St. Paul, MN, USA) was positioned with the proximal and distal marker on both sides of the stent. Pure contrast agent was injected through the guiding catheter to temporarily remove signal distorting blood flow from the iliac artery. A manually triggered pullback was performed using the OCT ILUMIEN™ OPTIS™ OCT-system (St. Jude Medical). Image analysis was performed using dedicated software (Curad B.V., Amsterdam, NH, the Netherlands)[15], including automated contour detection algorithms. For each cross-sectional frame (n=10/mm; n=150/stent), the lumen contour and the stent contour were automatically delineated and manually corrected where needed. Neointima formation was defined as the difference between stent area and luminal area, both expressed as mm^2 and as a percentage of the total stent area (*i.e.* two separate outcome measurements). All 150 cross-sectional frames were used to calculate the average neointimal area and neointimal area as a percentage of total stent area. These were then used to calculate the mean and standard deviation for each group (EES or COMBO). Stent struts were classified into three categories: embedded if buried in the vessel wall, protruding if protruding in the lumen but still in contact with the vessel wall and malapposed if protruding and not in contact with the vessel wall. For the latter, the distance between stent strut and luminal contour was automatically measured and classified malapposed if greater than its strut thickness (EES: 88um; COMBO: 104um).

Tissue preparation, histological analysis and scanning electron microscopy

The remaining six rabbits were also sacrificed after 28 days. After heparinization (1000 IU/kg IV), catheters were placed in the aorta and caval vein under general anesthesia as described above. An angiogram was performed to visualize the stents and surrounding arteries. After sacrifice, the aorta was perfused with Ringers lactate to remove blood cells from the stents, followed by pressure fixation with 4% formalin. Subsequently, the stents and adjacent arteries were dissected. The stent was cut axially so that one part comprised one third of the stent and the other part comprised two thirds of the stents.

The larger part was used for morphometric and inflammation analyses. After an additional formalin fixation for at least 72 hours, the stents were embedded in methyl metacrylate for histological analysis. Sections were cut with a diamond-coated saw at 3 levels. A hematoxylin and eosin (H&E) staining was performed for morphometric analysis. Luminal contours and internal elastic laminae (IEL) were traced manually using pictures made at a 20x magnification using ImageJ. The amount of neointima was calculated by subtracting the luminal area from the IEL area. Inflammation was evaluated as previously described.[16] At 40x magnification, each stent strut in a tissue section was scored for inflammation as follows: 0 = no inflammatory cells surrounding the strut; 1 = very light, non-circumferential cellular infiltrate surrounding the strut; 2 = localized moderate to dense cellular aggregate surrounding the strut non-circumferentially with or without slight expansion into the neointima not in direct contact with the strut; 3 = circumferential dense cellular infiltrate of the strut with extensive expansion into the neointima not in direct contact with the stent strut. The scores of the individual stent struts were averaged per tissue section and tissue sections were averaged per stent. The averages of all the stents in one group (EES or COMBO) were used to calculate the means and standard deviations.

The smaller part was cut longitudinally and used for scanning electron microscopy (sEM). Stents were fixed in a 1.5% glutaraldehyde in 0.1 M cacodylate buffer (pH 7.2). A secondary fixation using 1% osmium tetroxide in 0.1 M cacodylate buffer was performed, followed by dehydration. Liquid was removed from the samples using critical point drying, sprayed with platinum and analyzed using sEM (Phenom desktop sEM, Phenom-World BV, Eindhoven, N-B, the Netherlands). Of each single stent, 8-12 images at 360x magnification were made. Stent strut contours could easily be visualized as slightly elevated areas in the image. In each image, the covered area of the stent strut contour was measured as well as the total area of the stent strut contour, using ImageJ. The covered area was then expressed as a percentage of the total stent strut area. In each animal, the individual scores (*i.e.* percentages) of these 8-12 images were averaged per rabbit. These averages were then used to calculate the mean and standard deviation for each group (EES or COMBO).

Statistical analysis

Values are presented as mean ± standard deviation (SD). Data distribution was evaluated for normality using the Shapiro-Wilk test. All data were normally distributed and a paired-samples T test was performed to test for significant differences ($P<0.05$). Statistical analyses were performed using SPSS software, version 21.

RESULTS

Quantitative angiography

Angiograms were taken before, directly after stent implantation and at 28 days follow-up (figure 1). No differences in vessel diameters, balloon-to-artery ratio or late loss at four weeks follow-up were observed (table 1).

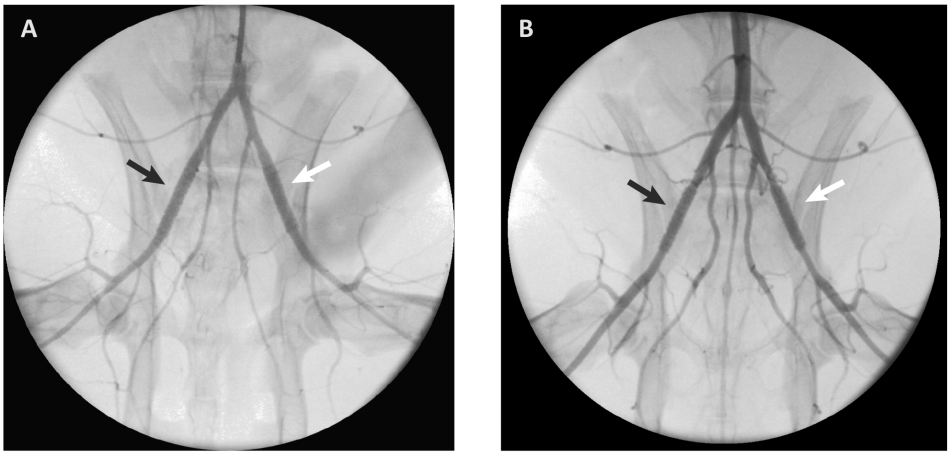

Figure 1. Angiography images
Angiograms obtained directly after implantation (A) and after 28 days of follow-up (B). Stent location is indicated by arrows, black for the everolimus-eluting stent and white for the COMBO stent.

Table 1. Angiography measurements at baseline and 28 days follow-up

Stent	Diameter before stent placement (mm)	Diameter after stent placement (mm)	B:A ratio	Diameter at follow-up (mm)	Late loss
EES (n=12)	2.14±0.23	2.99±0.18	1.42±0.19	2.70±0.20	0.29±0.19
COMBO (n=12)	2.15±0.21	2.91±0.18	1.37±0.16	2.62±0.16	0.29±0.16

Values are represented as mean ± standard deviation (SD). No significant differences were observed between the two groups. B:A ratio: balloon-to-artery ratio.

Stent endothelialisation

Figures 2A-D (left panel) show overview images of the EES and COMBO stent by scanning electron microscopy (sEM). Four weeks after stent implantation, the COMBO stent showed visually improved strut coverage at intermediate (figure 2A-D, upper right panels) and higher magnification (figure 2A-D, lower right panels). Quantification of strut coverage confirmed a lower endothelial coverage in the EES and a significantly improved endothelial coverage in the COMBO stent (78.5±16.8% vs. 96.6±3.5%; p=0.038, figure 2E).

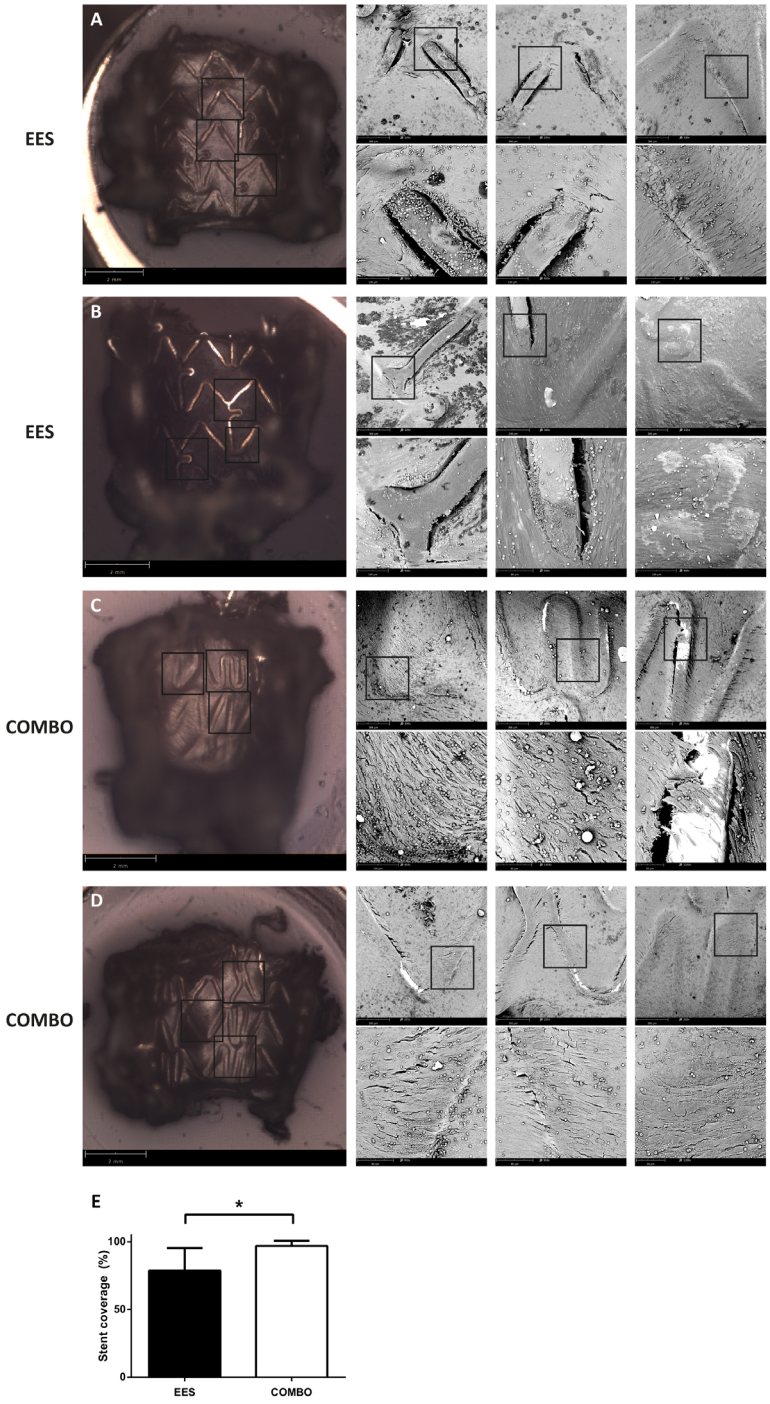

Neointimal hyperplasia and inflammation

Four weeks after stent implantation intravascular OCT was performed in 6 out of 12 animals. All images per stent were semi-automatically analyzed and luminal and stent area were quantified (figure 3A-B). Absolute neointimal area by OCT analysis was significantly higher in EES compared to COMBO stents (0.227±0.025 mm^2 vs. 0.188±0.044 mm^2; p=0.013; figure 3C), but did not differ when expressed as percentage of the total stent area (EES: 3.78±0.45% vs. COMBO: 3.49±0.95%; p=NS; figure 3D). The percentage of protruding stent struts as a measure of the vascular healing response did not significantly differ between the two stent types, shown in figure 3E (EES: 35.1±14.7% vs. COMBO: 29.7±17.1%; p=NS). Neointimal hyperplasia was also assessed in H&E stained tissue sections (figure 4A-B). In contrast to OCT, no significant differences were observed with respect to neointima formation between EES and COMBO stents (0.823±0.200 mm^2 vs. 0.891±0.312 mm^2; p=NS; figure 4C). This may be due to the higher accuracy of histology or the lower number of analyzed sections compared to OCT.

Finally, H&E stained tissue sections were evaluated for inflammation (figure 4D-E). In the majority of stent struts, cellular infiltrate was absent or only minimally present. Hence, average inflammatory scores did not differ significantly between EES and COMBO stents (0.530±0.380 vs. 0.435±0.295; p=NS; figure 4F).

◀ Figure 2. Assessment of stent endothelialisation using scanning electron microscopy (sEM)
Scanning electron microscopy imaging of the luminal surface of the everolimus-eluting stent (EES) (A, B) and the COMBO stent (C, D) at low (left panel), intermediate (upper right panels) and high magnification (lower right panels). At high magnification, the COMBO stent showed confluent stent coverage, whereas the EES struts were not completely endothelialized. Quantification of stent strut coverage showed a significantly improved endothelialisation of the COMBO stent compared to the EES (E). * = p<0.05

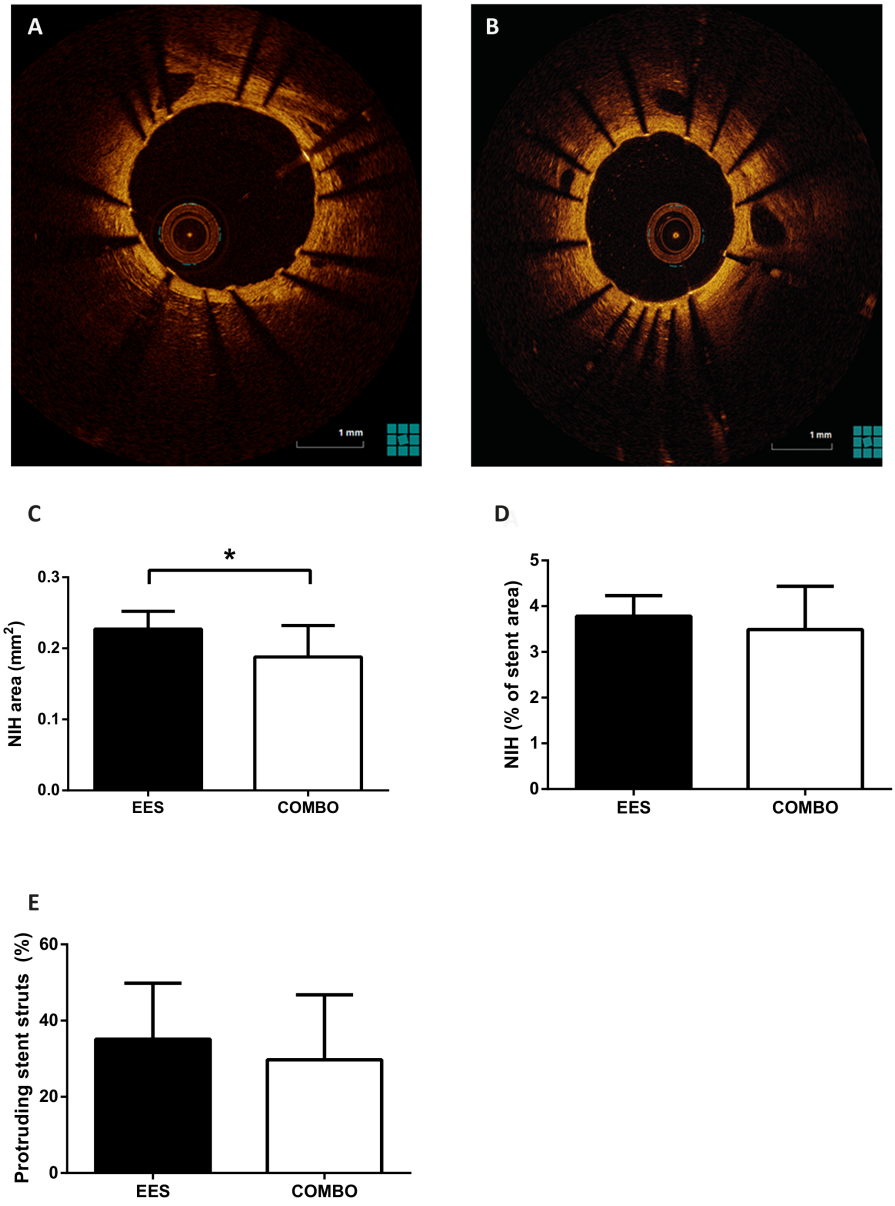

Figure 3. Assessment of neointima formation by optical coherence tomography (OCT)
Representative optical coherence tomography images of the everolimus-eluting stent (EES) (A) and the COMBO stent (B). The difference between stent and lumen contour represents neointima formation, which was significantly decreased in the COMBO stent (C). Neointima formation expressed as a percentage of the total stent area did not differ between both stent types (D). Classification of stent struts as being buried in the vessel wall (embedded) or protruding into the lumen (protruding) was not different between both groups (E). * = $p<0.05$

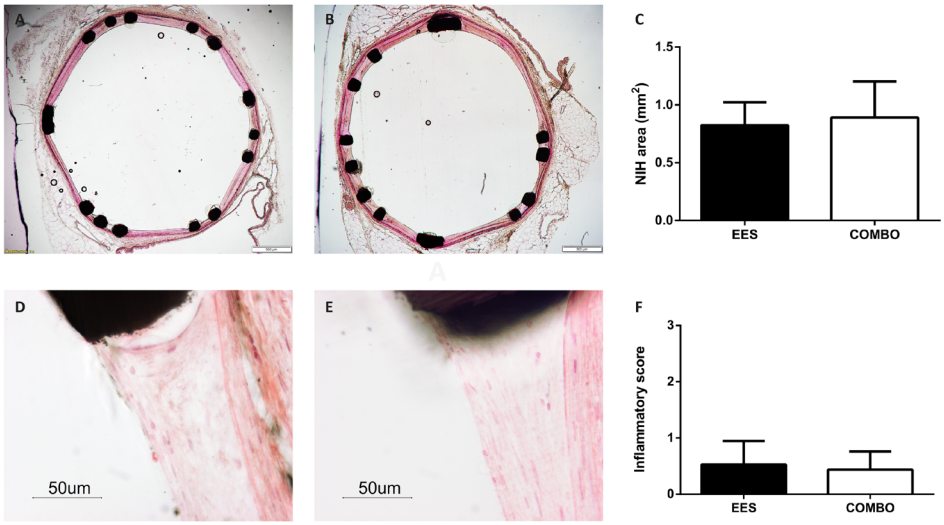

Figure 4. Neo-intima formation assessment by HE-stained tissue sections
Representative images of tissue sections of the everolimus-eluting stent (A) and the COMBO stent (B). The difference between internal elastic membrane (IEL) and lumen area represents neointima formation, which did not differ between both groups (C). Representative high magnification images of both everolimus-eluting (D) and COMBO stent (E) with minor inflammatory cell deposition near the stent strut. Quantification of inflammation on a 0 – 3 scale confirmed no differences between both groups (F).

DISCUSSION

The significant reduction of in-stent restenosis in DES so far came at the expense of reduced endothelialisation and corresponding higher risk for stent thrombosis.[8–11] To overcome these drawbacks, different approaches have been shown to be promising. Amongst these are using a sole abluminal anti-proliferative drug coating[17], seeding stents with human trophoblastic endovascular progenitor cells[18] and using anti-CD34 for endothelial progenitor cell (EPC) capturing.[7] The latter is investigated in the current study, comparing an abluminal sirolimus-eluting stent with luminal anti-CD34 coating (COMBO stent) to a 2nd generation everolimus-eluting stent (EES) with respect to endothelial cell coverage and neointimal hyperplasia. At 28 days, the COMBO stent showed significantly improved endothelial coverage by sEM compared to the EES.

DES are known to interfere with endothelial cell proliferation and function, leading to delayed strut endothelialisation. Strut coverage in our study was decreased in the EES to a comparable degree as previously reported.[19] In contrast, the COMBO stent showed almost complete endothelial coverage. This finding indicates that the anti-CD34 coating accelerates stent coverage, even in the presence of an anti-proliferative component, similar to stents without

anti-proliferative coatings.[20] As stent endothelialisation is a major determinant of stent thrombosis[5], the COMBO stent might therefore reduce stent related thrombotic events. In our previous findings with the anti-CD34 capturing stents (without drug-eluting component) in comparison with BMS we found superior endothelial coverage with the anti-CD34 stent at 7 days (82.21% vs. 77.92%).[21] Our current results with the COMBO stent (96.6% endothelial coverage at 28 days) are largely in line with the earlier findings, suggesting that the abluminal elution of the anti-proliferative drug has no negative effect on stent endothelialisation.

Neointima formation was significantly higher in EES compared to COMBO stents when measured by OCT, whereas histologic measurements did not show significant differences. In histological sections, the internal elastic membrane (IEM) can be easily detected and traced very accurately. In OCT as the clinical standard, the stent strut contour is semi-automatically detected using the endoluminal stent strut reflections. This method excludes the abluminal part of the stent struts and corresponding neointimal area. In situations with very low amounts of neointima as present in the current study, OCT is therefore less accurate than histology. However, the differences between both techniques are very small and therefore clinically not significant.

Previous studies have shown similar underestimation of neointima formation in OCT compared to histology.[22] Moreover, our current results are in line with previous experiments, comparing different DES types with BMS. While BMS showed significantly more neointima formation compared to any DES, there was no difference between DES types.[19,23] The comparable neointimal areas found with EES compared to the COMBO stent suggest that the effect of the improved endothelialisation on VSMC mobilization is relatively small in comparison with the inhibitory action of the anti-proliferative drug. Inflammatory cell deposition was also not affected by accelerated endothelialisation.

Limitations

Because two thirds of each stent was used for morphometric analysis (HE), we were unable to describe the effect of the COMBO stents on endothelialisation in the middle part of the stent. In comparison to most of the contemporary preclinical studies that assessed the entire stent for endothelialisation[10,18,23], the assessment of only one third of the stent limits its translation to stent reendothelialisation in the middle part of the stent. In addition, though the COMBO stent can be expected to reduce neointima formation both by accelerated endothelialisation[24] and by the elution of an antiproliferative drug, our current study was not designed to discriminate between the relative effects of these mechanisms. Moreover, since sEM and histology data on one side and OCT data on the other side were not assessed in the same rabbits, the present study does not allow for direct comparison of stent coverage and neointima formation. Comparisons and associations between OCT and microscopy (i.e. histology or sEM) should therefore interpreted with caution.

CONCLUSION

In summary, when compared to the EES, the COMBO stent shows improved endothelialisation and equal inhibition of neointimal hyperplasia in rabbits at 28 days post-PCI. Large scale clinical trials are warranted to show how the accelerated endothelialisation in the COMBO stent translates into clinical benefit in terms of reduced stent thrombosis and neo-atherosclerosis and the ability to reduce the duration of anti-platelet therapies after PCI.

Impact on daily practice

This study shows that, compared to the everolimus-eluting stent, the COMBO stent shows improved endothelialisation and equal inhibition of neointimal hyperplasia in rabbits at 28 days post-PCI. As stent endothelialisation is an important determinant of stent thrombosis, this finding increases the evidence for preferred use of endothelial cell capturing DES in patients with an increased risk for stent thrombosis or with contra-indications for dual-antiplatelet therapy.

Acknowledgements

The authors thank Marlijn Jansen, Joyce Visser, Danny Elbersen, Melanie van der Kaa and Evelyn Velema for their excellent technical support during the animal experiments and Chris Sneijdenberg for assistance with scanning electron microscopy.

Funding

This research was performed within the framework of the Center for Translational Molecular Medicine, project CIRCULATING CELLS (grant 01C-102), and supported by the Dutch Heart Foundation.

Conflict of interest

E Ligtenberg and S Rowland are employees of OrbusNeich Medical. The authors have no other relevant affiliations or financial involvement with any organization or financial involvement with any organization or entity with a financial interest in or financial conflict with the subject matter or materials discussed in the manuscript apart from those disclosed.

REFERENCES

1. WHO. The top 10 causes of death, 2000-2012 [Internet]. 2012 [cited 2015 Apr 11];Available from: http://www.who.int/mediacentre/factsheets/fs310/en/
2. Fischman DL, Leon MB, Baim DS, Schatz RA, Savage MP, Penn I, Detre K, Veltri L, Ricci D, Nobuyoshi M, Cleman M, Heuser R, Almond D, Teirstein PS, Fish RD, Colombo A, Brinker J, Moses J, Shaknovich A, Hirshfeld J, Bailey S, Ellis S, Rake R, Goldberg S. A randomized comparison of coronary-stent placement and balloon angioplasty in the treatment of coronary artery disease. *N Engl J Med*. 1994;331:496–501.
3. Khan W, Farah S, Domb AJ. Drug eluting stents: developments and current status. *J Control Release*. 2012;161:703–12.
4. Nakazawa G, Finn A V., Virmani R. Vascular pathology of drug-eluting stents. *Herz*. 2007;32:274–80.
5. Joner M, Finn A V., Farb A, Mont EK, Kolodgie FD, Ladich E, Kutys R, Skorija K, Gold HK, Virmani R. Pathology of drug-eluting stents in humans: delayed healing and late thrombotic risk. *J Am Coll Cardiol*. 2006;48:193–202.
6. Aoki J, Serruys PW, van Beusekom H, Ong ATL, McFadden EP, Sianos G, van der Giessen WJ, Regar E, de Feyter PJ, Davis HR, Rowland S, Kutryk MJB. Endothelial progenitor cell capture by stents coated with antibody against CD34: the HEALING-FIM (Healthy Endothelial Accelerated Lining Inhibits Neointimal Growth-First In Man) Registry. *J Am Coll Cardiol*. 2005;45:1574–9.
7. Rotmans JI, Heyligers JMM, Verhagen HJM, Velema E, Nagtegaal MM, De Kleijn DP V, De Groot FG, Stroes ESG, Pasterkamp G. In vivo cell seeding with anti-CD34 antibodies successfully accelerates endothelialization but stimulates intimal hyperplasia in porcine arteriovenous expanded polytetrafluoroethylene grafts. *Circulation*. 2005;112:12–18.
8. Beijk MAM, Klomp M, Verouden NJW, van Geloven N, Koch KT, Henriques JPS, Baan J, Vis MM, Scheunhage E, Piek JJ, Tijssen JGP, de Winter RJ. Genous endothelial progenitor cell capturing stent vs. the Taxus Liberte stent in patients with de novo coronary lesions with a high-risk of coronary restenosis: a randomized, single-centre, pilot study. *Eur Heart J*. 2010;31:1055–64.
9. Damman P, Klomp M, Silber S, Beijk MA, Ribeiro EE, Suryapranata H, Wójcik J, Sim KH, Tijssen JGP, de Winter RJ. Duration of dual antiplatelet therapy and outcomes after coronary stenting with the Genous™ bio-engineered R stent™ in patients from the e-HEALING registry. *Catheter Cardiovasc Interv*. 2012;79:243–52.
10. Nakazawa G, Granada JF, Alviar CL, Tellez A, Kaluza GL, Guilhermier MY, Parker S, Rowland SM, Kolodgie FD, Leon MB, Virmani R. Anti-CD34 Antibodies Immobilized on the Surface of Sirolimus-Eluting Stents Enhance Stent Endothelialization. *J Am Coll Cardiol*. 2010;3:68–75.
11. van Beusekom HMM, Ertaş G, Sorop O, Serruys PW, van der Giessen WJ. The Genous™ endothelial progenitor cell capture stent accelerates stent re-endothelialization but does not affect intimal hyperplasia in porcine coronary arteries. *Catheter Cardiovasc Interv*. 2012;79:231–42.
12. Haude M, Lee SWL, Worthley SG, Silber S, Verheye S, Erbs S, Rosli MA, Botelho R, Meredith I, Sim KH, Stella PR, Tan H-C, Whitbourn R, Thambar S, Abizaid A, Koh TH, Den Heijer P, Parise H, Cristea E, Maehara A, Mehran R. The REMEDEE trial: a randomized comparison of a combination sirolimus-eluting endothelial progenitor cell capture stent with a paclitaxel-eluting stent. *J Am Coll Cardiol Interv*. 2013;6:334–43.
13. Kedhi E, Joesoef KS, McFadden E, Wassing J, van Mieghem C, Goedhart D, Smits PC. Second-generation everolimus-eluting and paclitaxel-eluting stents in real-life practice (COMPARE): a randomised trial. *Lancet*. 2010;375:201–9.
14. Mahmoudi M, Delhaye C, Wakabayashi K, Ben-Dor I, Gonzalez MA, Maluenda G, Gaglia MA, Torguson R, Xue Z, Suddath WO, Satler LF, Kent KM, Pichard AD, Waksman R. Outcomes after unrestricted use of everolimus-eluting stent compared to paclitaxel- and sirolimus-eluting stents. *Am J Cardiol*. 2011;107:1757–62.
15. Belkacemi A, Agostoni P, Nathoe HM, Voskuil M, Shao C, Van Belle E, Wildbergh T, Politi L, Doevendans PA, Sangiorgi GM, Stella PR. First results of the DEB-AMI (drug eluting balloon in acute ST-segment elevation myocardial infarction) trial: a multicenter randomized comparison of drug-eluting balloon plus bare-metal stent versus bare-metal stent versus drug-eluting stent in primary p. *J Am Coll Cardiol*. 2012;59:2327–37.
16. Kornowski R, Hong MK, Tio FO, Bramwell O, Wu H, Leon MB. In-stent restenosis: Contributions of inflammatory responses and arterial injury to neointimal hyperplasia. *J Am Coll Cardiol*. 1998;31:224–30.
17. Zhang H, Deng W, Wang X, Wang S, Ge J, Toft E. Solely abluminal drug release from coronary stents could possibly improve reendothelialization. *Cath Cardiovasc Interv*. 2013;
18. Raina T, Iqbal J, Arnold N, Moore H, Aflatoonian B, Walsh J, Whitehouse S, Kadem A-L, Francis S, Gunn J. Coronary stents seeded with human trophoblastic endovascular progenitor cells show accelerated strut coverage without excessive neointimal proliferation in a porcine model. *EuroIntervention*. 2014;10:709–717.
19. Steigerwald K, Ballke S, Quee SC, Byrne RA, Vorpahl M, Vogeser M, Kolodgie F, Virmani R, Joner M. Vascular healing in drug-eluting stents: differential drug-associated response of limus-eluting stents in a preclinical model of stent implantation. *EuroIntervention*. 2012;8:752–9.
20. Soucy NV, Feyging JM, Tunstall R, Casey MA, Pennington DE, Huibregtse BA, Barry JJ. Strut tissue coverage and endothelial cell coverage: a comparison between bare metal stent platforms and platinum chromium stents with and without everolimus-eluting coating. *EuroIntervention*. 2010;6:630–7.
21. Tersteeg C, Hoefer IE, Ligtenberg E, Rowland S, Mak-Nienhuis EM, Balang V, Jansen MS, Velema E, de Groot PG, Roest M, Pasterkamp G. Fibronectin/fibrinogen/tropoelastin on a stent to promote CD34 + cell growth does not reduce neointima formation. *Interv Cardiol*. 2013;5:359–367.

22. Murata A, Wallace-Bradley D, Tellez A, Alviar C, Aboodi M, Sheehy A, Coleman L, Perkins L, Nakazawa G, Mintz G, Kaluza GL, Virmani R, Granada JF. Accuracy of Optical Coherence Tomography in the Evaluation of Neointimal Coverage After Stent Implantation. *JACC Cardiovasc Imaging*. 2010;3:76–84.
23. Granada JF, Inami S, Aboodi MS, Tellez A, Milewski K, Wallace-Bradley D, Parker S, Rowland S, Nakazawa G, Vorpah M, Kolodgie FD, Kaluza GL, Leon MB, Virmani R. Development of a novel prohealing stent designed to deliver sirolimus from a biodegradable abluminal matrix. *Circ Cardiovasc Interv*. 2010;3:257–266.
24. Kipshidze N, Dangas G, Tsapenko M, Moses J, Leon MB, Kutryk M, Serruys P. Role of the endothelium in modulating neointimal formation: vasculoprotective approaches to attenuate restenosis after percutaneous coronary interventions. *J Am Coll Cardiol*. 2004;44:733–9.

PART TWO
TARGETING INFLAMMATION IN MYOCARDIAL INFARCTION

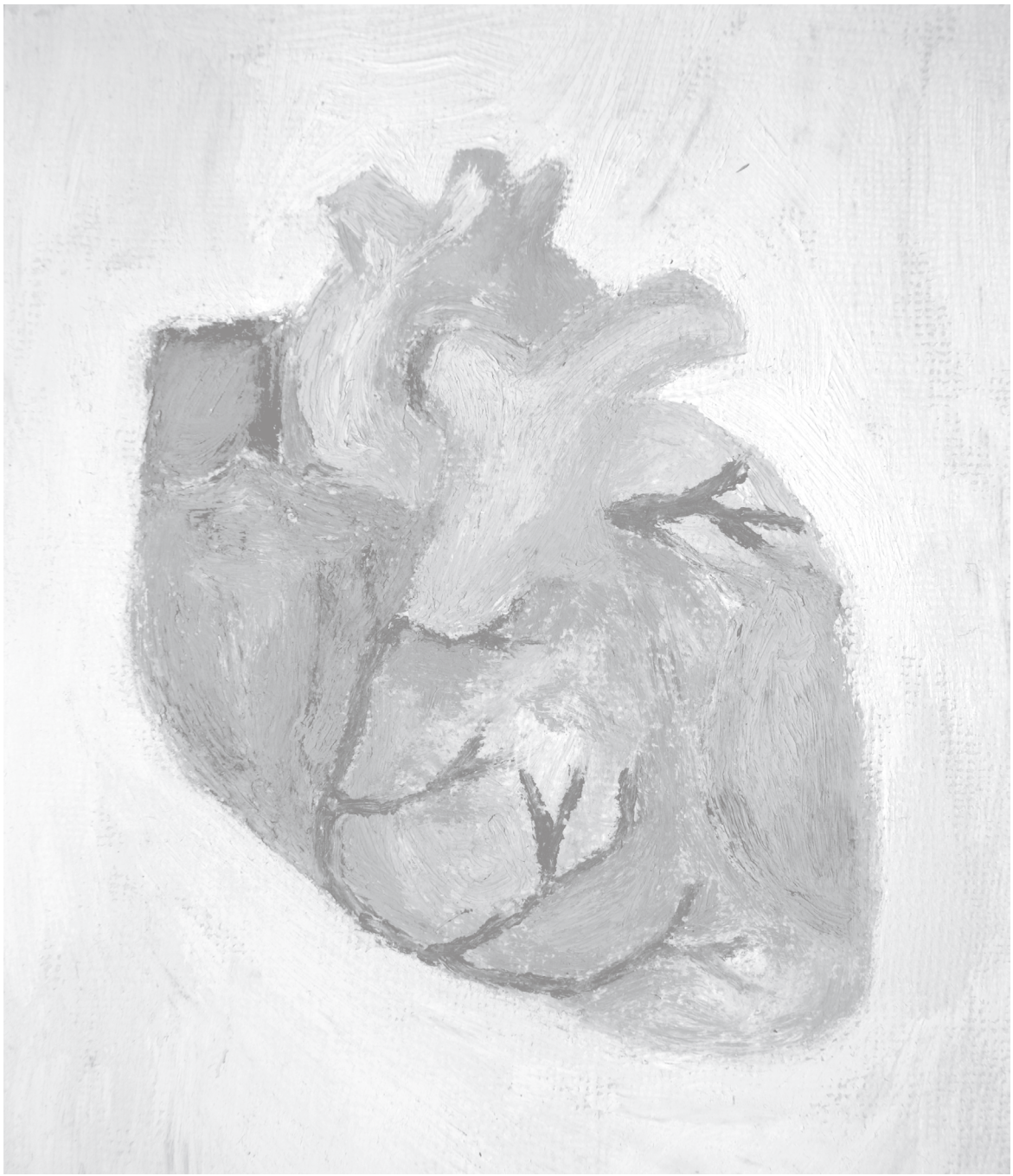

CHAPTER 5

Leukocyte-Associated Immunoglobulin-like Receptor-1 is regulated in human myocardial infarction but its absence does not affect infarct size in mice

G.H.J.M. Ellenbroek*[1], J.J. de Haan*[1], M.A.D. Brans[1], S.M. van de Weg[1], M.B. Smeets[1], S. de Jong[2], F. Arslan[1,3], L. Timmers[3], I.E. Hoefer[1,4], P.A.F.M. Doevendans[3,5], G. Pasterkamp[1,4], L. Meyaard[7], S.C.A. de Jager[1,6]

** Contributed equally to this work*

[1] Laboratory of Experimental Cardiology, University Medical Center Utrecht, The Netherlands
[2] Department of Medical Physiology, University Medical Center Utrecht, The Netherlands
[3] Department of Cardiology, University Medical Center Utrecht, The Netherlands
[4] Department of Clinical Chemistry and Haematology, University Medical Center Utrecht, The Netherlands
[5] Netherlands Heart Institute, Utrecht, the Netherlands
[6] Laboratory of Translational Immunology, Department of Immunology, University Medical Center Utrecht, The Netherlands

Under revision

ABSTRACT

Heart failure after myocardial infarction (MI) depends on infarct size and adverse left ventricular (LV) remodelling, both depending on extent of the inflammatory response. Leukocyte-associated immunoglobulin-like receptor 1 (LAIR-1) is an inhibitory receptor. We investigated the regulation of LAIR-1 leukocyte expression after MI in patients and hypothesized that its absence in a mouse model of MI would increase infarct size and adverse remodelling. In patients, LAIR-1 expression was increased 3 days compared to 6 weeks after MI on circulating monocytes (24.8±5.3 vs. 21.2±5.1 MFI, p=0.008) and neutrophils (12.9±4.7 vs. 10.6±3.1 MFI, p=0.046). In WT and LAIR-1$^{-/-}$ mice, infarct size after ischemia-reperfusion injury was comparable (37.0±14.5 in WT vs. 39.4±12.2% of the area at risk in LAIR-1$^{-/-}$, p=0.63). Remodelling after permanent left coronary artery ligation did not differ between WT and LAIR-1$^{-/-}$ mice (end-diastolic volume 133.3±19.3 vs. 132.1±27.9μL, p=0.91 and end-systolic volume 112.1±22.2 vs. 106.9±33.5μL, p=0.68). Similarly, no differences were observed in inflammatory cell influx or fibrosis formation. In conclusion, LAIR-1 expression on monocytes and neutrophils is increased in the acute phase after MI in patients, but the absence of LAIR-1 in mice does not influence infarct size, inflammation, fibrosis formation or adverse remodelling of the myocardium.

INTRODUCTION

Heart failure (HF) is a complex clinical syndrome and is often caused by reduced cardiac pump function, affecting approximately 1-2% of people in the Western world.[1] The most prevalent cause of HF is an acute myocardial infarction (MI). Despite the significant reduction of early mortality and improved treatment, the prognosis of HF patients remains poor with a 5-year survival of less than 50%[2], stressing the need for a better understanding and treatment of this complex syndrome.

Heart failure after MI is caused by adverse left ventricular remodelling.[3,4] Adverse remodelling is largely depending on infarct size, but also on the quality of cardiac repair, both greatly influenced by the inflammatory response after MI.[5–8] Although inflammatory cells are important in the clearance of debris and necrotic tissue after MI, their pro-inflammatory activity is also responsible for a variety of detrimental effects. In the (sub) acute phase of ischemia-reperfusion injury, neutrophils and monocytes play an important role in the increase in infarct size.[5,9,10] In the chronic phase, activated and pro-inflammatory monocytes and T-lymphocytes increase adverse remodelling, which leads to impaired cardiac function.[11,12] In both processes, leukocyte activation is key and regulated by integration of signals from activating and inhibitory cell-receptors.[13] The majority of immune inhibitory receptors contain intracellular domains that – upon activation – are able to downregulate or inhibit activation signals from stimulating receptors. Thereby, they increase the threshold for leukocytes to become activated and attenuate pro-inflammatory effects. The transmembrane leukocyte-associated immunoglobulin-like receptor 1 (LAIR-1, CD305) is an inhibitory receptor that is expressed on most cells of the immune system.[14] LAIR-1 is activated upon binding of its ligands including collagens or collagen-domain containing proteins such as surfactant protein D.[15,16] LAIR-1 is counteracted by shedding of its ectodomain (sLAIR-1) or by secretion of its antagonist LAIR-2[17], which is why plasma levels of these molecules were also studied.

Though LAIR-1 is capable of regulating immune cell function[18], its role in vivo has been scarcely addressed and evidence for its role in inflammation following acute MI is lacking. Therefore, we compared LAIR-1 expression on leukocytes and circulating levels of sLAIR-s and LAIR2 in patients 3 days and 6 weeks after MI, representing the acute and chronic phase of cardiac remodelling. Moreover, we studied the effect of LAIR-1 deficiency in experimental MI in mice, measuring inflammation, infarct size, cardiac function and adverse left ventricular remodelling.

MATERIALS AND METHODS

Study population

Healthy volunteers and patients (>18 years old) with a first time ST-elevation myocardial infarction (STEMI) and non-STEMI from the DEFI-MI (METC: NL45241.041.13) study were included in the current study. Exclusion criteria were the presence of a chronic inflammatory disease, autoimmune disorder, pregnancy and trauma or surgery in the last six months. The Medical Ethics Committee of the UMC Utrecht approved the study and all patients provided written informed consent. The study conforms to the Declaration of Helsinki.

Patient data collection

In patients, at the moment of inclusion (3 days after MI) and 6 weeks thereafter, venous blood was drawn and collected by the Laboratory of Clinical Chemistry and Haematology of the UMC Utrecht (Figure 1a). Whole blood was directly subjected to flow cytometry and EDTA plasma was stored at -80° Celsius in the UMC Utrecht Biobank and used for ELISA (see below). Similarly, blood was drawn from healthy controls and subjected to flow cytometry.

Animals

Healthy male C57Bl/6 LAIR-1 $^{-/-}$ [19] and C57Bl/6 WT littermates (age 10-12 weeks, weight 25-30 g) received standard chow and water ad libitum. All animals were genotyped prior to the experimental procedure. A blinded researcher performed surgery on randomly assigned animals (random number generation in excel to animal number, which resulted in alternating fashion of operation of WT and LAIR-1 $^{-/-}$ mice). Blinded technicians and observers performed the respective operations, data acquisition and analyses. All animal experiments were approved by the Ethical Committee on Animal Experimentation of the University Medical Center Utrecht (Utrecht, the Netherlands) and conform to the 'Guide for the care and use of laboratory animals'.

Induction of myocardial ischemia-reperfusion injury

The experimental set-up and timeline of myocardial ischemia-reperfusion injury is displayed in Figure 1b. All operations were performed in the morning before noon. In a dedicated mouse operation room, anaesthesia was induced by intraperitoneal (i.p.) injection of medetomidinehydrochloride (1.0 g/kg body weight), midazolam (10.0 mg/kg) and fentanyl (0.1 mg/kg). These anaesthetics were preferred over cardioprotective propofol or volatile anaesthetics (*e.g.* isoflurane).[20] Mice were intubated and connected to a respirator with a 1:1 oxygen-air ratio (times/minute). A core body temperature of 37 °C was maintained during surgery by continuous rectal temperature monitoring and an automatic

heating blanket. The heart was accessed through a left lateral thoracotomy with incision of the pericardium. The left coronary artery was ligated for 30 minutes with an 8-0 Ethilon suture (Ethicon) with a section of polyethylene-10 tubing placed over the left coronary artery (LCA). Ischemia was confirmed by bleaching of myocardium and tachycardia. Reperfusion was initiated by releasing the ligation, resulting in tissue colour recurrence. A piece of the suture was left in place to allow for accurate ligature positioning and determination of the ischemic area and the area at risk at termination. The surgical wounds were closed and subcutaneous atipamezole hydrochloride (3.3 mg/kg), flumazenil (0.5 mg/kg) and buprenorphin (0.15 mg/kg) were used as an antagonist. The evening of the day of operation and every 12 hours thereafter, subcutaneous injection of buprenorphin (0.15 mg/kg) was administered as analgesia.

Infarct size and area at risk quantification after ischemia-reperfusion injury

Twenty-four hours after ischemia/reperfusion injury, mice were euthanized using sodium pentobarbital (60.0 mg/kg) and a left re-thoracotomy was performed. The LCA was ligated at the same location as it was ligated during index ischemia. The thoracic aorta was cannulated and 2% Evans blue was injected upstream in the aorta to perfuse the coronaries, allowing for staining of the remote but not the area at risk (AAR). The heart was then explanted and rinsed with 0.9% saline to remove superfluous dye. The left ventricle (LV) was dissected and a small piece of gauze was inserted in the left ventricular cavity. After one hour at -20° C, the LV was cut into 4 equally sized sections. Sections were placed in 1% 2,3,5-triphenyltetrazolium chloride (TTC) in saline and incubated at 37 °C for 20 minutes. After 10 minutes, sections were turned to allow for adequate reagent contact. Then, sections were placed in formalin and photographs of both sides of each tissue section were captured using a SZH10 Olympus Zoom Stereo Microscope and IC Capture software, version 2.4. The infarct (white), border zone (red) and remote area (blue) were quantified using ImageJ (version 1.48v). Infarct size (IS) was expressed as a percentage of the AAR and as a percentage of the LV.

Induction of myocardial infarction by permanent ligation

Permanent coronary artery ligation was performed as described above for ischemia-reperfusion injury, but leaving the ligature in place, resulting in a permanent occlusion of the left coronary artery. The experimental set-up including the timeline of the mice sacrificed after either 3 days or 28 days is shown in Figure 1c-d.

Survival

Mice that died after MI were thoroughly inspected for the cause of death. Deaths within 48 hours after MI were considered due to perioperative complications or direct complication

of MI. Cardiac rupture was confirmed by massive intrathoracic haemorrhage > 48 hours after operation and ventricular leakage of the myocardium upon perfusion of the heart with 0.9% saline.

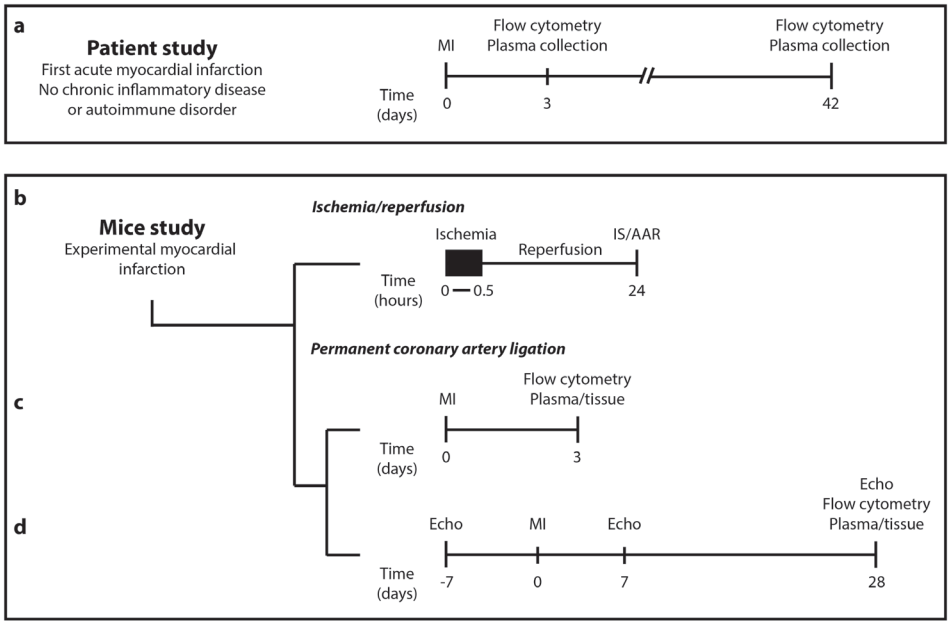

Figure 1. Timeline and experimental set-up
Healthy controls and patients with a first-time MI were included in the current study. Venous blood collection in healthy controls and at 3 days and 6 weeks after MI was used for flow cytometric analyses and to collect plasma (a). Mice were either subjected to ischemia-reperfusion injury or to permanent left coronary artery ligation. In the mice subjected to 30 minutes of ischemia and 24 hours of subsequent reperfusion, IS/AAR staining was performed (b). In the mice subjected to permanent left coronary artery ligation and sacrificed after 3 days, we performed flow cytometric analyses on various tissues and blood (c). In the other mice subjected to left coronary artery ligation, we performed echocardiography at baseline, 7 days and 28 days after MI and performed similar flow cytometric analyses (d – lower panel). *MI: myocardial infarction; IS/AAR: infarct size/area at risk.*

Echocardiography

At baseline, 7 and 28 days after permanent ligation, anaesthesia was induced by inhalation of 2.0% isoflurane in a mixture of oxygen/air (1:1). Echocardiography was used to assess cardiac geometry and function. Heart rate, respiration and rectal temperature were constantly monitored and body temperature was kept between 36.0 and 38.0 ° C using heat lamps. Respiration gating, a 3-dimensional motor and trigger points were used to obtain 300 transversal images of the heart during the expiratory phase, either at the end of systole

or the end of diastole. These images were then used for complete 3D reconstruction of the heart. Image acquisition and analyses were performed using the dedicated Vevo® 2100 System and Software (Fujifilm VisualSonics Inc., Toronto, Canada).

Tissue processing and histological analyses

At the end of the follow-up period, mice were euthanized using sodium pentobarbital (60.0 g/kg). Blood was collected through orbital puncture in EDTA tubes. The inferior caval vein was incised and the vascular system was flushed with 5 mL phosphate-buffered saline (PBS) through right ventricular puncture.

The spleen and the mediastinal lymph nodes posterior to the heart were excised and contained in PBS for flow cytometric analyses afterwards. Then, the heart was explanted and cut in half. One half was dissected further into infarct and remote tissue and used for flow cytometry or snap-frozen in liquid nitrogen. The other half was formalin-fixed for 24 hours, embedded in paraffin and cut into 5 μm thick sections. Neutrophils were stained using a rat monoclonal mouse LY-6G (GR-1) antibody (1:400, Biolegend, 108402, 0.5mg/ml). Rabbit-anti-rat-biotin (1:200, DAKO E0468, 0.84 g/L) was used as a secondary antibody and Streptavidin-AP (1:500, SA-5100) as a tertiary antibody. Liquid permanent red was used as an enzyme substrate. Neutrophils were semi-automatically counted using digital histology.

Collagen content was quantified in tissue sections stained for picrosirius red and photographed under polarized light, and expressed as a percentage of the region of interest (*i.e.* infarct, remote). Images of tissue sections were captured and analysed using CellSens (Olympus Corporation, Tokyo, Japan).

Flow cytometric assays

Fresh human EDTA blood (50 μL) was added to an antibody mixture containing different cell surface markers to identify neutrophils and monocytes (see Supplementary Table S1 online). Cells were incubated for 30 minutes in the dark at room temperature (RT). Before measurement, cells were washed and erythrocytes were lysed using Optilyse C.

To harvest single cells from heart tissue, enzymatic degradation was performed. Infarct and remote tissue were collected 3 days after MI and cut into small pieces of around 1 mm^2. Dissociation solution (10 x 10^2 U/ml DNase I (Roche 04536282001), 10 mM HEPES (Life Technology 15630-080) and 2.6 U/ml Liberase TL (Roche 05401020001)) was added to the tissue and incubated at 37° Celsius for 20 minutes. Single cells of the dissociated myocardial tissue, lymph nodes and spleen were obtained through gentle filtering over a 40 μm cell strainer and subsequently incubated with an antibody mixture containing different cell surface markers to identify neutrophils, monocytes, and T- and B-lymphocytes (see Supplementary Table S2 online) for 30 minutes in the dark at RT. After washing, residual

red blood cells were lysed with erythrocyte-lysis buffer. All samples were measured on a Gallios flow cytometer (10 colour configuration, Beckman Coulter, Marseille, France). Kaluza Analysis Software 1.3 was used for data analysis. The gating strategy is shown in Supplementary Figure S1 online.

ELISA

Plasma levels of soluble LAIR-1 (sLAIR-1) and LAIR-2 were measured in duplo using a respective sLAIR-1 and LAIR-2 sandwich ELISA according to manufacturer's instructions (LifeSpan BioSciences, Seatle, WA, USA). Colorimetric analyses were performed using a spectrophotometer (450 nm). Plasma levels were calculated based on standards.

Statistical analyses

Data distribution was evaluated for normality using the d'Agostino & Pearson normality test. Data are expressed as mean ± standard deviation (SD). Skewed ELISA data were ln-transformed and presented as median with interquartile range (IQR). Normally distributed data were compared using a two-tailed paired (serial measurements) or unpaired t-test (separate groups). Non-normally distributed data were compared using a Wilcoxon (serial measurements) or Mann-Whitney test (separate groups). A log-rank (Mantel-Cox) test was used for survival analysis. A level of $p<0.05$ was considered statistically significant. Statistical analyses were performed using SPSS software, version 21 and GraphPad Prism, version 6.

RESULTS

In patients, LAIR-1 expression on circulating cells and sLAIR-1 and LAIR-2 plasma levels differ between the acute and chronic phase after MI

Out of 22 patients included in this study, 21 patients (96%) suffered from a STEMI and 1 patient (4%) from an nSTEMI. For comparison, 20 healthy volunteers were included as controls. The transmembrane expression of LAIR-1 on monocytes was significantly higher in the acute phase (3 days after MI), compared to the chronic phase (24.8±5.3 at day 3 vs. 21.2±5.1 MFI at 6 weeks post MI, p=0.008; Figure 2a), and both were significantly increased with respect to healthy controls. Subgroup analyses showed that this difference could be attributed to higher LAIR-1 expression on pro-inflammatory classical (25.0±5.4 at 3 days vs. 21.5±5.0 MFI at 6 weeks post MI, p=0.013; Figure 2b) and intermediate monocytes (27.2±7.7 at day 3 vs. 19.9±4.3 MFI at 6 weeks post MI, p=0.001; Figure 2c), but not non-classical monocytes (22.1±9.1 at day 3 vs. 18.9±9.7 MFI at 6 week, p=0.28; Figure 2d). Similar to monocytes, LAIR-1 expression on neutrophils was higher 3 days after MI

compared to 6 weeks after MI (12.9±4.7 vs. 10.6±3.1 MFI, p=0.046; Figure 2e). In general, comparison with healthy controls showed that LAIR-1 expression was increased after MI, either at both 3 days and 6 weeks (monocytes, classical monocytes) or at 3 days only (intermediate monocytes, non-classical monocytes).
Plasma levels of sLAIR-1 were slightly higher 3 days after MI compared to 6 weeks, though this was not significant (2.71 IQR [1.35-3.87] vs. 1.92 IQR [1.01-2.61], p=0.07; Figure 2f). In contrast, LAIR-2 levels were significantly higher after 6 weeks (238.7 IQR [205.2-268.0] vs. 260.3 IQR [223.9-297.7], p=0.049; Figure 2g).

The absence of LAIR-1 does not influence infarct size in mice

Evans blue and TTC staining were used to quantify infarct size (IS), area at risk (AAR) and left ventricular (LV) area in both WT and LAIR-1$^{-/-}$ mice (Figure 3a-b). Reperfusion injury as assessed by IS/AAR, did not differ between WT and LAIR-1 $^{-/-}$ mice (37.0 ±14.5 vs. 39.4±12.2%, p=0.63; Figure 3c). In addition, AAR/LV was comparable between both groups (38.3±14.1 vs. 36.8±10.3%, p=0.75; Figure 3d), as was IS/LV (14.2±7.4 vs. 14.9±7.0, p=0.80; Figure 3e).

Survival, cardiac geometry, and cardiac function are comparable between wild-type and LAIR-1 $^{-/-}$ mice after permanent coronary artery ligation

Within 28 days after permanent ligation, cardiac rupture and subsequent death occurred in 6 out of 18 WT and 9 out of 20 LAIR-1$^{-/-}$ mice (33.3 vs. 45.0%, p=0.38; Figure 4a). In the surviving animals, no differences were observed with respect to end-diastolic volume (EDV) at 7 days (WT 105.6±14.3 vs. LAIR-1$^{-/-}$ 113.0±26.1 µL, p=0.40; Figure 4b) and 28 days (133.3±19.3 vs. 132.1±27.9 µL, p=0.91) after permanent ligation. In addition, end-systolic volume (ESV) was comparable between both groups after 7 days (87.5±16.1 vs. 91.0±29.0 µL, p=0.73; Figure 4c) and 28 days (112.1±22.2 vs. 106.9±33.5 µL, p=0.68). Correspondingly, left ventricular ejection fraction did not differ between WT and LAIR-1$^{-/-}$ mice at 7 days (17.6±4.0 vs. 21.0±9.0%, p=0.25; Figure 4d) and 28 days (16.5±5.1 vs. 20.5±8.5%; p=0.20) after MI.

Wild-type and LAIR $^{-/-}$ mice show no differences in inflammatory responses following myocardial infarction

To confirm LAIR-1 expression on circulating leukocytes, we performed flow cytometry on blood. In WT mice, LAIR-1 was expressed on CD4^{+} T-cells and CD8^{+} T- cells, but most prominent on cells of myeloid origin, amongst which neutrophils, macrophages and Ly6C expressing monocytes (Figure 5a). As expected, LAIR-1 was undetectable on cells from the LAIR-1$^{-/-}$ mice.

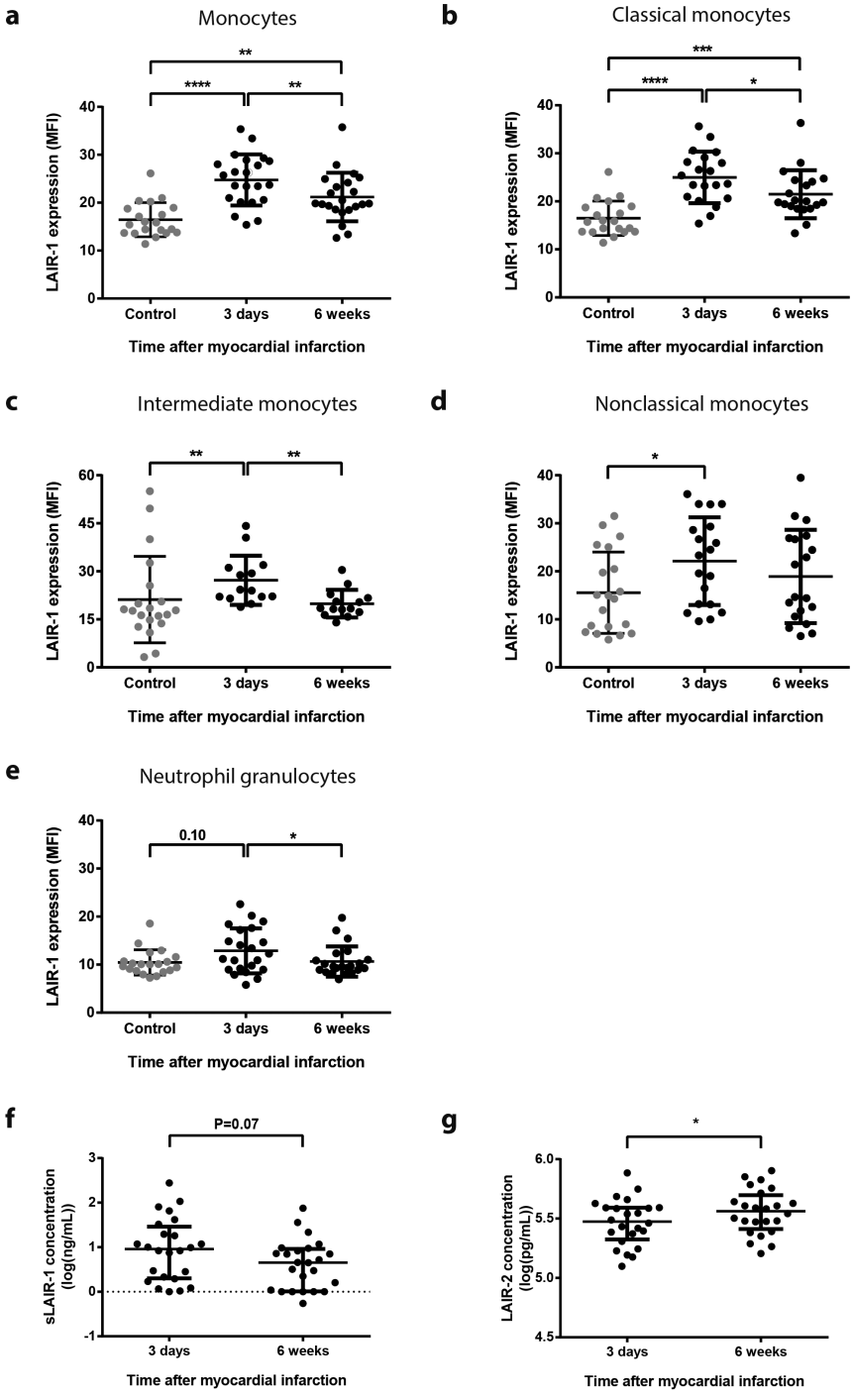

◀ Figure 2. LAIR-1 expression on leukocyte subsets and sLAIR-1 and LAIR-2 plasma levels differ between the acute and chronic phase after myocardial infarction
Flow cytometry showed that LAIR-1 receptor expression on monocytes (a) 3 days after MI was higher than 6 weeks thereafter and than healthy controls, which could be mainly attributed to classical (b) and intermediate monocytes (c), but not to non-classical monocytes (d). Similar to monocytes, also granulocytes showed higher LAIR-1 receptor expression in the acute compared to the chronic phase, but no difference between the chronic phase and healthy controls was observed (e). Though not significant, sLAIR-1 was higher 3 days after MI compared to 6 weeks (f). In contrast, plasma levels of LAIR-2 were lower 3 days after MI compared to 6 weeks (g). N=19-22 (a-b, d-e), 14 (c) and 24 (f-g) patients, 20 healthy controls (a-e). *MI: myocardial infarction; * p<0.05, ** p<0.01, *** p<0.001, **** p<0.0001.*

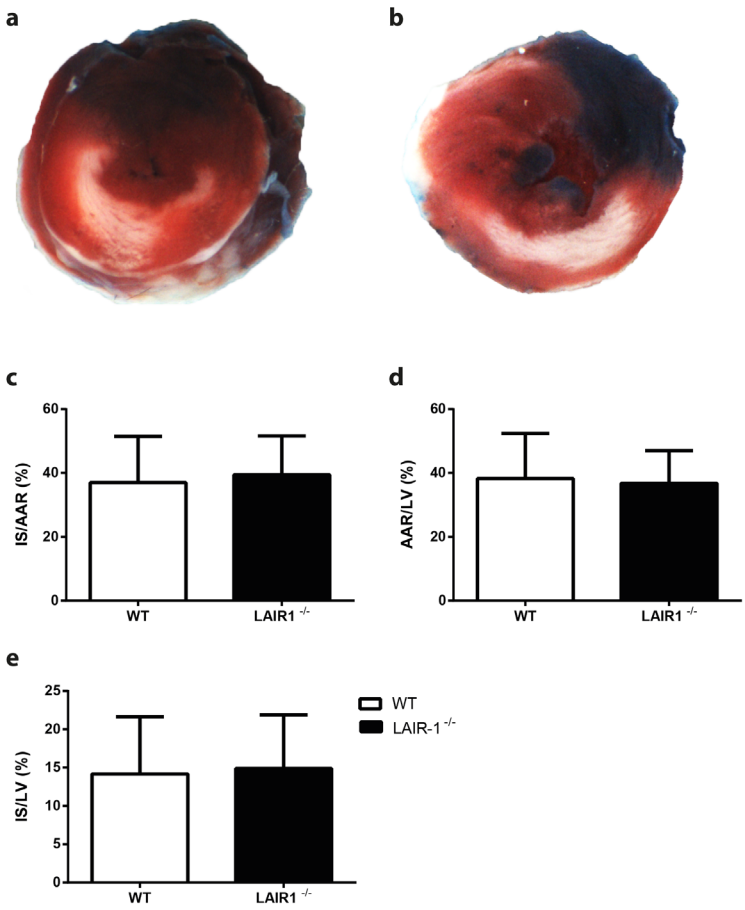

Figure 3. Infarct size and area at risk quantification after ischemia-reperfusion injury
Evans blue and TTC staining of WT (a) and LAIR-1 $^{-/-}$ hearts (b) were used for the quantification of infarct size (IS; white), area at risk (AAR; sum of white and red area) and the left ventricle itself (LV; entire area). Reperfusion injury assessed through IS/AAR% did not differ between both groups (c). Also AAR/LV% (d) and IS/LV% was comparable between both groups. N=13-15 animals per group. *WT: wild-type; LAIR-1 $^{-/-}$: LAIR-1 deficient.*

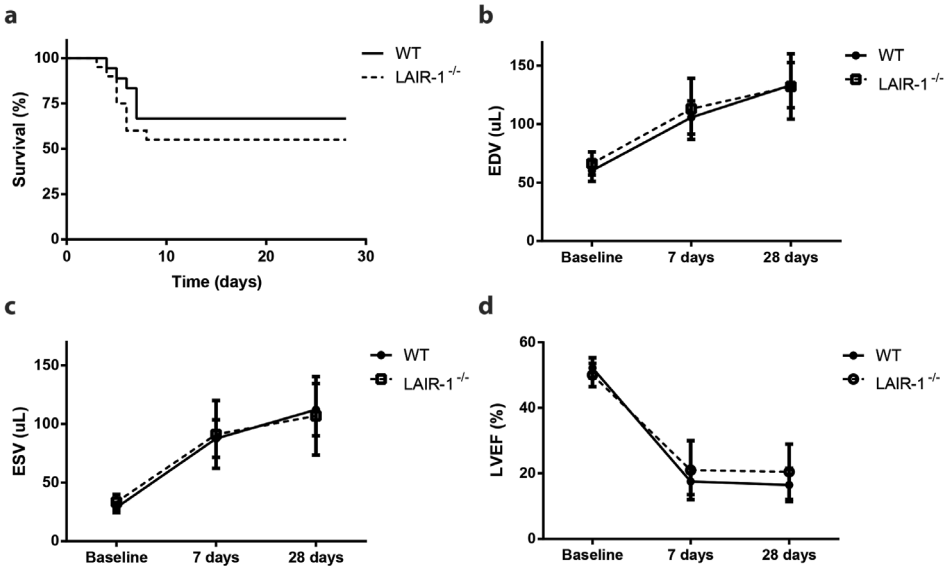

Figure 4. Survival and geometric dimensions by 3D echocardiography
Within the follow-up period of 28 days after permanent occlusion of the left coronary artery, 6 out of 18 WT mice and 9 out of 20 LAIR-1 $^{-/-}$ mice died as a consequence of cardiac rupture (a). In the surviving animals, EDV, ESV and LVEF were comparable 7 and 28 days after ligation (b-d). N=11-12 surviving animals per group. *WT: wild-type; LAIR- $^{-/-}$: LAIR-1 deficient; EDV: end-diastolic volume; ESV: end-systolic volume; LVEF: left ventricular ejection fraction.*

Flow cytometry was performed for the characterization and quantification of leukocytes in the blood, spleen, draining lymph node and heart (see Supplementary Figure S2 online). Three days after MI, a robust leukocyte influx in the heart was observed, that mostly consisted of neutrophils and $CD8^+$ T-cells (Table 1). No difference in white blood cell subtype composition was observed between WT and LAIR-$1^{-/-}$ mice 3 days and 28 days after MI in all studied organs (Table 1 – blood, infarct area; see Supplementary Table S3-4 online – remote area, lymph nodes, spleen).

Since neutrophils are the first to infiltrate the heart in the early phase after MI and notorious for the additional damage they cause to the myocardium, we performed an immunohistochemical neutrophil staining. Three days after MI, neutrophil influx was comparable between WT and LAIR-$1^{-/-}$ mice in both the infarct area (406±167 vs. 405±165 cells/mm^2, p=0.99; Figure 5b-c), border zone (483±245 vs. 539±344 cells/mm^2, p=0.63) and remote area (16±20 vs. 22±23 cells/mm^2, p=0.96).

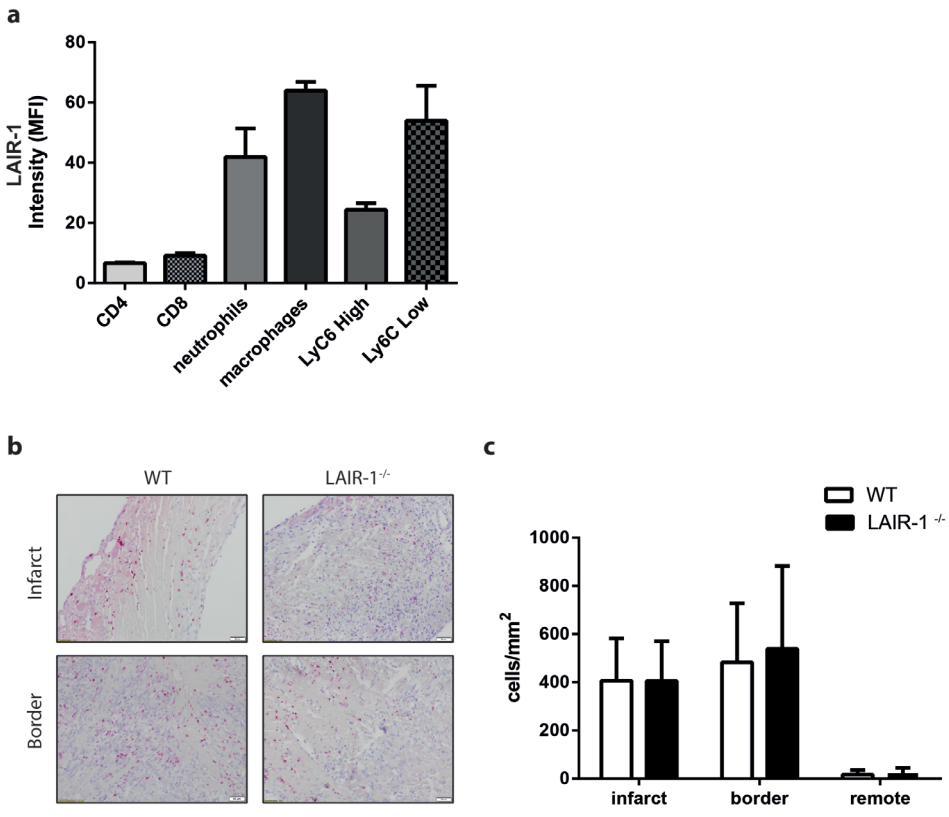

Figure 5. Leukocytes in the heart and blood
LAIR-1 is expressed on T-lymphocytes, but most prominently on cells of myeloid origin (a). Cardiac tissue sections were stained with Ly6G for neutrophil quantification. Representative images of WT and LAIR-1$^{-/-}$ mice of the infarct area and border zone (b) showed no difference in neutrophil influx 3 days after permanent occlusion of the left coronary artery (c). N=6-7 animals per group. *WT: wild-type; LAIR-1 $^{-/-}$: LAIR-1 deficient.*

Table 1. Leukocyte levels in blood and infarct area after 3 days of MI

	Blood		Infarcted myocardium	
	WT	**LAIR-1$^{-/-}$**	**WT**	**LAIR-1$^{-/-}$**
Neutrophils	28.1±23.5%	22.6±8.3%	56.8±11.9%	49.4±14.3%
Macrophages	5.4±4.4%	7.1±4.0%	25.9±8.2%	30.9±8.7%
Ly6C High monocytes	2.0±1.5%	3.0±2.0%	3.0±1.9%	4.5±1.8%
Ly6C Low monocytes	4.5±0.6%	5.0±1.2%	3.9±2.4%	4.6±2.9%
CD4 T-cells	9.0 ± 2.6%	11.4±3.2%	1.9±1.1%	2.0±1.2%
CD8 T-cells	8.7±3.8%	10.9±2.5%	34.3±6.8%	42.5±10%

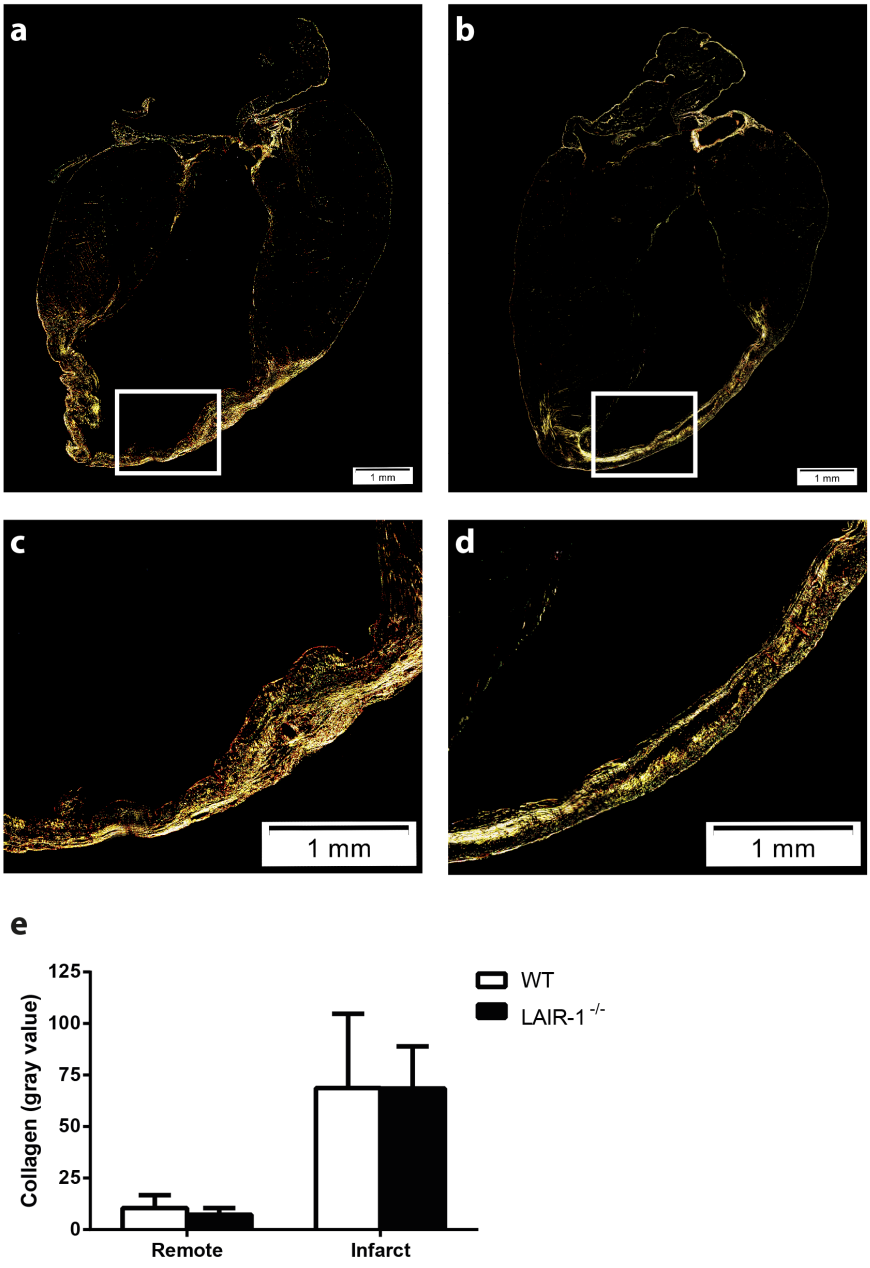

Figure 6. Collagen content 28 days after permanent coronary artery ligation
Cardiac tissue sections were stained with picrosirius red and photographed under polarized light. Representative overview images of WT and LAIR-1$^{-/-}$ mice (a-b) and magnified images of the infarct area (c-d) show no differences in collagen content in both remote and infarct regions 28 days after permanent occlusion of the left coronary artery (E). N=10-11 animals per group. *WT: wild-type; LAIR-1 $^{-/-}$: LAIR-1 deficient.*

Fibrosis formation is not affected by the absence of LAIR-1 after chronic myocardial infarction

As a marker of cardiac fibrosis we stained cardiac tissue sections with picrosirius red of both WT and LAIR-1$^{-/-}$ mice (representative pictures in Figure 6a-b). Magnified images of the infarct area (Figure 6c-d) show no differences in collagen content between both groups 28 days after permanent ligation (WT 68.7±36.1 vs. 68.5±20.4 grey value, p=0.98; Figure 6e).

DISCUSSION

Leukocytes and leukocyte activation, in particular monocytes and neutrophils, have been shown to play an important role in both cardiac ischemia-reperfusion injury and remodelling.[21–24] LAIR-1 is present on a variety of immune cells[14] and important in the regulation of leukocyte activation in response to an inflammatory reaction.[15,25,26] We observed increased LAIR-1 expression on leukocytes of patients compared to healthy controls. More specifically, LAIR-1 expression on circulating monocytes and neutrophils is increased directly after MI and declines after six weeks, suggestive of immune regulation by LAIR-1 in a response to the pro-inflammatory environment of MI. In more detail, LAIR-1 expression differed on pro-inflammatory classical and intermediate monocytes. Although both are necessary for the removal of debris following MI, their effect is generally considered disproportionate and detrimental.[11] Therefore, higher LAIR-1 expression in the acute phase after MI may be beneficial in suppressing pro-inflammatory monocyte activation to limit cardiac damage. Although LAIR-1 expression on monocytes decreases in the chronic phase after MI, the expression levels remain increased when compared to healthy controls. This is most probably linked to ongoing low-grade inflammatory response in the chronic phase of cardiac remodelling after MI.[27] In addition, we observed higher LAIR-1 expression on neutrophils in the acute phase after MI compared to the chronic phase. Considering the observation that pro-inflammatory stimuli lead to the higher LAIR-1 expression on neutrophils[28], this is in agreement with the strong inflammatory response directly after MI.

Next to increased LAIR-1 expression on monocytes and neutrophils, we also observed higher levels of sLAIR-1 in the acute phase after MI, which is in line with the observation that cell activation induces shedding of LAIR-1.[29] Although the source of sLAIR-1 remains to be elucidated, this finding suggests that inflammation in the acute setting of MI increases LAIR-1 expression even more to result in both high expression levels and a high amount of LAIR-1 shedding. Contrarily, the levels of LAIR-2, mainly produced by stimulated CD4$^+$ T-lymphocytes, are lower in the acute phase of MI. This difference might be (partially) explained by the relatively decreased number of circulating CD4$^+$ T-cells in the acute stage

after MI compared to the chronic phase.[30] Though both sLAIR-1 and LAIR-2 are natural antagonists of cell-bound LAIR-1, LAIR-2 has been shown to be far more potent than sLAIR-1.

These findings in patients prompted us to study if LAIR-1 is causally involved in ischemia reperfusion injury in the heart. However, in mice, the absence of LAIR-1, did not affected infarct size or cardiac remodelling after MI. Although leukocyte activating receptors and inflammation are widely recognized as important players in ischemia-reperfusion injury and remodelling after MI[31–33], and despite the regulation in LAIR expression in MI patients, we were not able to establish a causal role for LAIR-1 deficiency in this regard.

The extent of reperfusion injury is in agreement with previously performed experiments in WT mice in our laboratory[33–35] , infarct size after myocardial ischemia-reperfusion did not differ between WT and LAIR-1$^{-/-}$ mice. We anticipated on increased reperfusion injury in the LAIR-1$^{-/-}$ mice as a consequence of enhanced cellular infiltration and inflammation. However, the inflammatory response assessed in various tissues in the acute (3 days) and more chronic (28 days) inflammatory phase after MI did not differ between WT and LAIR-1$^{-/-}$ mice. In addition, the deposition of collagen, as well as the extent of cardiac remodelling at 28 days was comparable to those observed in previously performed experiments[36,37], but did not differ between both groups.

Activating leukocyte receptors[33,38,39] and costimulatory molecules[40] have been shown to play an important role in myocardial reperfusion injury through modulation of the inflammatory response, whereas studies on inhibitory receptors or co-inhibitory molecules are lacking. The inhibitory effect of LAIR-1 may not provide sufficient potency for the extent of tissue damage and severity of the inflammatory response in the present model, as was previously shown *in vitro*.[41] This is in agreement with the observation that LAIR-1 has been shown to be primarily involved in low-grade chronic inflammatory diseases, such as cancer[18,42] and chronic contact dermatitis[43], but not so much in acute, high grade, inflammatory responses as observed in experimental autoimmune encephalitis and LPS injection.[44] Although the chronic phase of myocardial remodelling shows a somewhat less inflammatory response than the acute phase of experimental MI, leukocyte influx is still impressive.[45]

In addition, cell activation starts in the bloodstream[46], whereas inhibition of LAIR-1 is expected to occur predominantly upon the encounter of collagen in the heart. This may either be too late to efficiently inhibit the already initiated pro-inflammatory cascade, or the sheer amount of collagen ligands is too low to induce robust activation of LAIR-1. Moreover, other inhibitory receptors and/or pathways could have compensated for the absence of LAIR-1.

CONCLUSION

In conclusion, LAIR-1 expression on monocytes and neutrophils is increased in patients 3 days after MI. Though, in mice, the absence of LAIR-1 does not influence infarct size, nor does it affect inflammation, fibrosis formation and adverse left ventricular remodelling in mice four weeks after acute MI.

Acknowledgements
The authors gratefully acknowledge Ben van Middelaar for technical assistance and Sjors Fens for logistic support.

Competing Financial Interests Statement
The authors declare no competing financial interests.

Conflict of interest
The authors declare no conflict of interest.

REFERENCES

1. Mosterd A, Hoes AW. Clinical epidemiology of heart failure. *Heart*. 2007;93:1137–46.
2. Roger VL. Epidemiology of heart failure. *Circ Res*. 2013;113:646–659.
3. Konstam MA, Kramer DG, Patel AR, Maron MS, Udelson JE. Left ventricular remodeling in heart failure: Current concepts in clinical significance and assessment. *JACC Cardiovasc Imaging*. 2011;4:98–108.
4. Chareonthaitawee P, Christian TF, Hirose K, Gibbons RJ, Rumberger JA. Relation of initial infarct size to extent of left ventricular remodeling in the year after acute myocardial infarction. *J Am Coll Cardiol*. 1995;25:567–73.
5. Yellon DM, Hausenloy DJ. Myocardial reperfusion injury. *N Engl J Med*. 2007;357:1221–35.
6. Westermann D, Lindner D, Kasner M, Zietsch C, Savvatis K, Escher F, von Schlippenbach J, Skurk C, Steendijk P, Riad A, Poller W, Schultheiss H-P, Tschöpe C. Cardiac inflammation contributes to changes in the extracellular matrix in patients with heart failure and normal ejection fraction. *Circ Hear Fail*. 2011;4:44–52.
7. Seropian IM, Toldo S, Van Tassell BW, Abbate A. Anti-inflammatory strategies for ventricular remodeling following St-segment elevation acute myocardial infarction. *J Am Coll Cardiol*. 2014;63:1593–1603.
8. Hong YJ, Jeong MH, Ahn Y, Yoon NS, Lee SR, Hong SN, Moon JY, Kim KH, Park HW, Kim JH, Cho JG, Park JC, Kang JC. Relationship between peripheral monocytosis and nonrecovery of left ventricular function in patients with left ventricular dysfunction complicated with acute myocardial infarction. *Circ J*. 2007;71:1219–24.
9. Frangogiannis N. The inflammatory response in myocardial infarction. *Cardiovasc Res*. 2002;53:31–47.
10. Vilahur G, Badimon L. Ischemia/reperfusion activates myocardial innate immune response: The key role of the toll-like receptor. *Front Physiol*. 2014;5:1–5.
11. Wrigley BJ, Lip GYH, Shantsila E. The role of monocytes and inflammation in the pathophysiology of heart failure. *Eur J Hear Fail*. 2011;13:1161–71.
12. Hofmann U, Frantz S. Role of lymphocytes in myocardial injury, healing, and remodeling after myocardial infarction. *Circ Res*. 2015;116:354–367.
13. Billadeau DD, Leibson PJ. ITAMs versus ITIMs: Striking a balance during cell regulation. *J Clin Invest*. 2002;109:161–168.
14. Meyaard L. The inhibitory collagen receptor LAIR-1 (CD305). *J Leukoc Biol*. 2008;83:799–803.
15. Lebbink RJ, de Ruiter T, Kaptijn GJA, Bihan DG, Jansen CA, Lenting PJ, Meyaard L. Mouse leukocyte-associated Ig-like receptor-1 (mLAIR-1) functions as an inhibitory collagen-binding receptor on immune cells. *Int Immunol*. 2007;19:1011–1019.
16. Olde Nordkamp MJM, van Eijk M, Urbanus RT, Bont L, Haagsman HP, Meyaard L. Leukocyte-associated Ig-like receptor-1 is a novel inhibitory receptor for surfactant protein D. *J Leukoc Biol*. 2014;96:105–11.
17. Lebbink RJ, Berg MCW van den, Ruiter T de, Raynal N, Roon JAG van, Lenting PJ, Jin B, Meyaard L. The Soluble Leukocyte-Associated Ig-Like Receptor (LAIR)-2 Antagonizes the Collagen/LAIR-1 Inhibitory Immune Interaction. *J Immunol*. 2008;180:1662–1669.
18. Rygiel TP, Stolte EH, de Ruiter T, van de Weijer ML, Meyaard L. Tumor-expressed collagens can modulate immune cell function through the inhibitory collagen receptor LAIR-1. *Mol Immunol*. 2011;49:402–406.
19. Smith CW, Thomas SG, Raslan Z, Patel P, Byrne M, Lordkipanidzé M, Bem D, Meyaard L, Senis YA, Watson SP, Mazharian A. Mice Lacking the Inhibitory Collagen Receptor LAIR-1 Exhibit a Mild Thrombocytosis and Hyperactive Platelets. *Arterioscler Thromb Vasc Biol*. 2017;37:ePub.
20. De Hert SG, Turani F, Mathur S, Stowe DF. Cardioprotection with volatile anesthetics: Mechanisms and clinical implications. *Anesth Analg*. 2005;100:1584–1593.
21. Arslan F, de Kleijn DP, Pasterkamp G. Innate immune signaling in cardiac ischemia. *Nat Rev Cardiol*. 2011;8:292–300.
22. Timmers L, Pasterkamp G, Hoog VC De, Arslan F, Appelman Y, Kleijn DPV De. The innate immune response in reperfused myocardium. *Cardiovasc Res*. 2012;94:276–283.
23. Schofield ZV, Woodruff TM, Halai R, Wu MC-L, Cooper MA. Neutrophils--a key component of ischemia-reperfusion injury. *Shock*. 2013;40:463–70.
24. Glezeva N, Horgan S, Baugh JA. Monocyte and macrophage subsets along the continuum to heart failure: Misguided heroes or targetable villains? *J Mol Cell Cardiol*. 2015;89:136–145.
25. Zocchi MR, Pellegatta F, Pierri I, Gobbi M, Poggi A. Leukocyte-associated Ig-like receptor-1 prevents granulocyte-monocyte colony stimulating factor-dependent proliferation and Akt1/PKB alpha activation in primary acute myeloid leukemia cells. *Eur J Immunol*. 2001;31:3667–75.
26. Maasho K, Masilamani M, Valas R, Basu S, Coligan JE, Borrego F. The inhibitory leukocyte-associated Ig-like receptor-1 (LAIR-1) is expressed at high levels by human naive T cells and inhibits TCR mediated activation. *Mol Immunol*. 2005;42:1521–30.
27. Dick SA, Epelman S. Chronic heart failure and inflammation. *Circ Res*. 2016;119:159–176.
28. Verbrugge A, Ruiter T de, Geest C, Coffer PJ, Meyaard L. Differential expression of leukocyte-associated Ig-like receptor-1 during neutrophil differentiation and activation. *J Leukoc Biol*. 2006;79:828–836.
29. Nordkamp MJMO, Van Roon JAG, Douwes M, De Ruiter T, Urbanus RT, Meyaard L. Enhanced secretion of leukocyte-associated immunoglobulin-like receptor 2 (LAIR-2) and soluble LAIR-1 in rheumatoid arthritis: LAIR-2 is a more efficient antagonist of the LAIR-1-collagen inhibitory interaction than is soluble LAIR-1. *Arthritis Rheum*. 2011;63:3749–3757.

30. Liu L-L, Lu J-L, Chao P-L, Lin L-R, Zhang Z-Y, Yang T-C. Lower prevalence of circulating invariant natural killer T (iNKT) cells in patients with acute myocardial infarction undergoing primary coronary stenting. *Int Immunopharmacol*. 2011;11:480–484.
31. Frangogiannis NG. The inflammatory response in myocardial injury, repair, and remodelling. *Nat Rev Cardiol*. 2014;11:255–265.
32. Timmers L, Sluijter JPG, Van Keulen JK, Hoefer IE, Nederhoff MGJ, Goumans MJ, Doevendans P a., Van Echteld CJ a, Joles J a., Quax PH, Piek JJ, Pasterkamp G, De Kleijn DP V. Toll-like receptor 4 mediates maladaptive left ventricular remodeling and impairs cardiac function after myocardial infarction. *Circ Res*. 2008;102:257–264.
33. Arslan F, Smeets MB, O'Neill LAJ, Keogh B, McGuirk P, Timmers L, Tersteeg C, Hoefer IE, Doevendans PA, Pasterkamp G, De Kleijn DP V. Myocardial ischemia/reperfusion injury is mediated by leukocytic toll-like receptor-2 and reduced by systemic administration of a novel anti-toll-like receptor-2 antibody. *Circulation*. 2010;121:80–90.
34. De Hoog VC, Timmers L, Van Duijvenvoorde A, De Jager SCA, Van Middelaar BJ, Smeets MB, Woodruff TM, Doevendans PA, Pasterkamp G, Hack CE, De Kleijn DP V. Leucocyte expression of complement C5a receptors exacerbates infarct size after myocardial reperfusion injury. *Cardiovasc Res*. 2014;103:521–529.
35. De Hoog VC, Bovens SM, De Jager SCA, Van Middelaar BJ, Van Duijvenvoorde A, Doevendans PA, Pasterkamp G, De Kleijn DP V, Timmers L. BLT1 antagonist LSN2792613 reduces infarct size in a mouse model of myocardial ischaemia-reperfusion injury. *Cardiovasc Res*. 2015;108:367–376.
36. Timmers L, van Keulen K, Hoefer IE, Meijs MFL, van Middelaar B, den Ouden K, van Echteld CJA, Pasterkamp G, de Kleijn DP V. Targeted Deletion of NF-kappaB P50 Enhances Cardiac Remodeling and Dysfunction Following Myocardial Infarction. *Circ Res*. 2009;104:699–706.
37. Arslan F, Smeets MB, Riem Vis PW, Karper JC, Quax PH, Bongartz LG, Peters JH, Hoefer IE, Doevendans PA, Pasterkamp G, De Kleijn DP. Lack of fibronectin-EDA promotes survival and prevents adverse remodeling and heart function deterioration after myocardial infarction. *Circ Res*. 2011;108:582–592.
38. Oyama JI, Blais C, Liu X, Pu M, Kobzik L, Kelly RA, Bourcier T. Reduced Myocardial Ischemia-Reperfusion Injury in Toll-Like Receptor 4-Deficient Mice. *Circulation*. 2004;109:784–789.
39. Yang Z, Day YJ, Toufektsian MC, Ramos SI, Marshall M, Wang XQ, French BA, Linden J. Infarct-sparing effect of A2A-adenosine receptor activation is due primarily to its action on lymphocytes. *Circulation*. 2005;111:2190–2197.
40. Kubota A, Hasegawa H, Tadokoro H, Hirose M, Kobara Y, Yamada-Inagawa T, Takemura G, Kobayashi Y, Takano H. Deletion of CD28 Co-stimulatory Signals Exacerbates Left Ventricular Remodeling and Increases Cardiac Rupture After Myocardial Infarction. *Circ J*. 2016;80:9171–1979.
41. Lebbink RJ, Ruiter T de, Adelmeijer J, Brenkman AB, Helvoort JM van, Koch M, Farndale RW, Lisman T, Sonnenberg A, Lenting PJ, Meyaard L. Collagens are functional, high affinity ligands for the inhibitory immune receptor LAIR-1. *J Exp Med*. 2006;203:1419–1425.
42. Kang X, Lu Z, Cui C, Deng M, Fan Y, Dong B, Han X, Xie F, Tyner JW, Coligan JE, Collins RH, Xiao X, You MJ, Zhang CC. The ITIM-containing receptor LAIR1 is essential for acute myeloid leukaemia development. *Nat Cell Biol*. 2015;17:665–678.
43. Omiya R, Tsushima F, Narazaki H, Sakoda Y, Kuramasu A, Kim Y, Xu H, Tamura H, Zhu G, Chen L, Tamada K. Leucocyte-associated immunoglobulin-like receptor-1 is an inhibitory regulator of contact hypersensitivity. *Immunology*. 2009;128:543–555.
44. Tang X, Tian L, Esteso G, Choi S, Barrow AD, Colonna M, Borrego F, Coligan JE, Tang X, Tian L, Esteso G, Choi S, Barrow AD. Leukocyte-Associated Ig-like Receptor-1 – Deficient Mice Have an Altered Immune Cell Phenotype. *J Immunol*. 2012;188:548–558.
45. Vandervelde S, Van Amerongen MJ, Tio RA, Petersen AH, Van Luyn MJA, Harmsen MC. Increased inflammatory response and neovascularization in reperfused vs. nonreperfused murine myocardial infarction. *Cardiovasc Pathol*. 2006;15:83–90.
46. De Haan JJ, Smeets MB, Pasterkamp G, Arslan F. Danger signals in the initiation of the inflammatory response after myocardial infarction. *Mediators Inflamm*. 2013;2013.

SUPPLEMENTARY

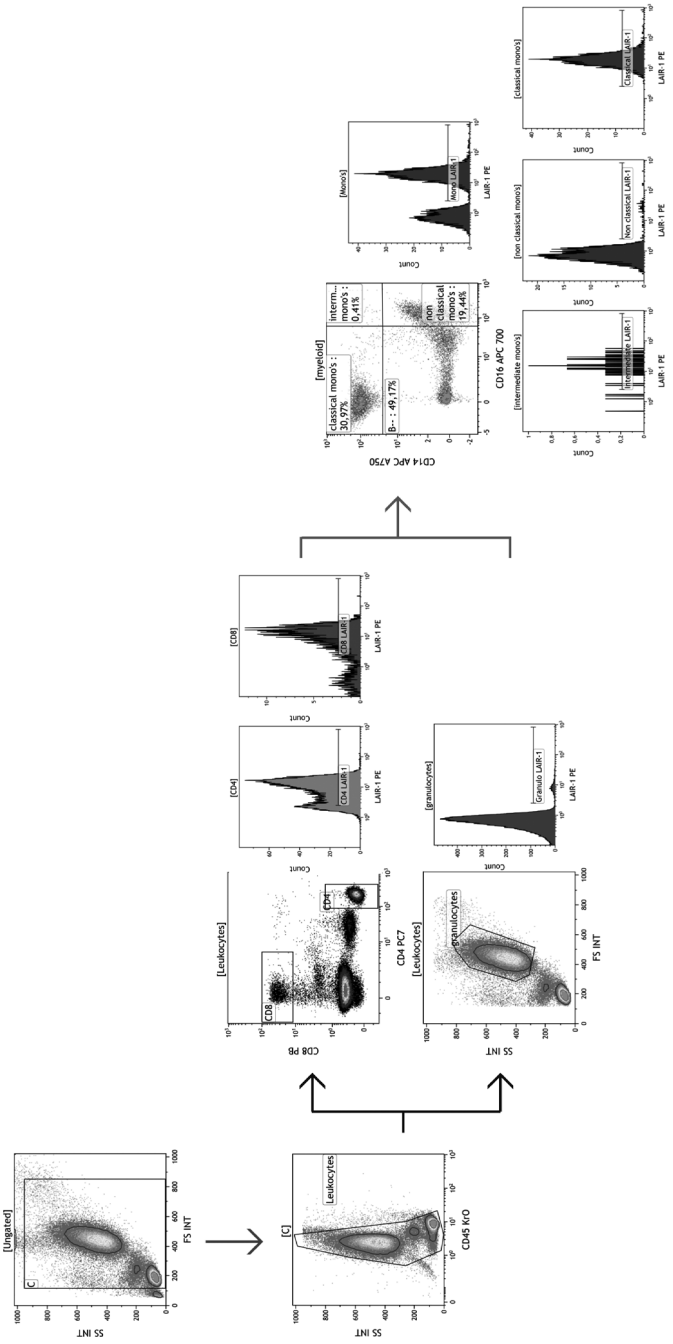

Supplementary Figure S1
Gating strategy of flow cytometry on human blood samples from healthy controls and patients 3 days and 6 weeks after MI. After selection of our cell population on FS/SS scatter, we selected leukocytes defined as $CD45^+$. From this population, granulocytes were selected based on FS/SS scatter. Monocytes were selected based on a Boolean gate (termed Myeloid= ((Leukocytes AND (NOT granulocytes)), and subdivided into classical monocytes ($CD14^+CD16^-$), intermediate monocytes ($CD14^+/CD16^+$) and non-classical monocytes ($CD14^-/CD16^+$). The three monocyte subsets comprise the total monocyte population. LAIR-1 expression by MFI was determined on all leukocytes. *MI: myocardial infarction; MFI: mean fluorescent intensity*

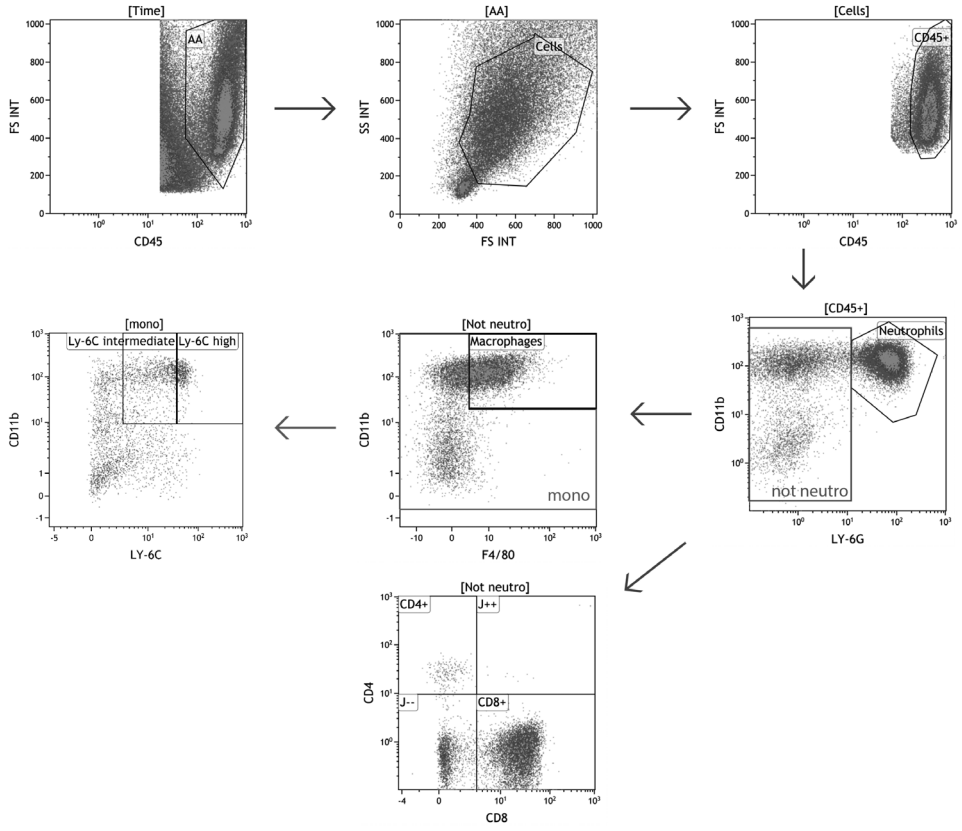

Supplementary Figure S2
Gating strategy of flow cytometry on mouse heart tissue. First CD45$^+$ cells were selected and then, based on FS/SS scatter, the cell population was selected. To further improve purity of only CD45$^+$ cells, an additional gating on CD45$^+$/SSC was performed and cells were termed CD45$^+$. Neutrophils were defined as CD11b$^+$ and Ly6G$^+$ within the CD45$^+$ population. A Boolean gate (termed Not neutro = CD45$^+$ AND (NOT Neutrophils)) was generated to exclude neutrophils from further analysis. Macrophages were defined as CD11b$^+$ and F4/80 positive cells within the 'Not neutro' gate. Monocytes were selected based on a Boolean gate (input gate Mono = "Not neutro" AND (NOT Macrophages)), where Ly6C low and Ly6C high monocytes were defined as CD11b$^+$ and LyC6$^+$ or LyC6^{++} within the monocyte gate. T-cells were analysed in the 'Not neutro' population and defined as CD4$^+$ and CD8$^+$ T-cells.

Supplementary Table S1. Antibody mixture for human blood

Antibody	Flurophore	Clone	Company	µL/sample
LAIR	PE	DX26	BD Pharmingen	5
CD16	APC-A700	3G8	Beckman Coulter	2
CD14	APC-A750	RMO52	Beckman Coulter	2
CD45	Krome Orange	J.33	Beckman Coulter	2

Supplementary Table S2. Antibody mixture for murine blood, spleen and lymph node

Antibody	Flurophore	Clone	Company	Concentration	µL/sample
CD11b	A488	M1/70	eBioscience	0.5 mg/ml	1.25
LAIR-1	PE	113	eBioscience	0.2 mg/ml	3.0
CD3	PE-CF594	145-2C11	BD Bioscience	0.2 mg/ml	0.5
F4/80	PE-CY7	BM8	eBioscience	0.2 mg/ml	2.0
LY-6G	APC	1A8	eBioscience	0.2 mg/ml	1.25
CD4	Alexa Fluor 700	GK1.5	eBioscience	0.2 mg/ml	1.25
CD8	APC-eFluor 780	53-6.7	eBioscience	0.2 mg/ml	1.25
LY-6C	e450	HK1.4	eBioscience	0.2 mg/ml	1.25
CD62L	Briljant Violet510	MEL-14	Biolegend	0.05 mg/ml	2.0

Supplementary Table S3. Antibody mixture for murine myocardial cells

Antibody	Flurophore	Clone	Company	Concentration	µL/sample
CD11b	A488	M1/70	eBioscience	0.5 mg/ml	1.25
CD62L	PE	MEL-14	eBioscience	0.2 mg/ml	2.5
CD45	PE-CF594	30-F11	BD Bioscience	0.2 mg/ml	0.5
F4/80	PE-CY7	BM8	eBioscience	0.2 mg/ml	2
LY-6G	APC	1A8	eBioscience	0.2 mg/ml	1.25
CD4	Alexa Fluor 700	GK1.5	eBioscience	0.2 mg/ml	1.25
CD8	APC-eFluor 780	53-6.7	eBioscience	0.2 mg/ml	1.25
LY-6C	e450	HK1.4	eBioscience	0.2 mg/ml	1.25
Sytox Blue			Life Technology	1 mM solution	0.1

Supplementary Table S4. White blood cell subtype in WT and LAIR-1-/- mice 3 days and 28 days after MI in all studied organs

Myocardium	**Baseline**		**Remote Area (3 days)**		**Infarct Area (3 days)**	
	WT	LAIR-1 $^{-/-}$	WT	LAIR-1 $^{-/-}$	WT	LAIR-1 $^{-/-}$
Neutrophils	7.4±5.9%	2.5±1.8%	38.7±16.6%	38.5±8.6%	56.8±11.9%	49.4±14.3%
Macrophages	28.2±4.2%	23.1±3.2%	38.0±14.0%	41.5±12.6%	25.9±8.2%	30.9±8.7%
Ly6C High monocytes	0.3±0.1%	0.2±0.1%	1.9±2.3%	2.6±3.9%	3.0±1.9%	4.5±1.8%
Ly6C Low monocytes	1.9±0.4%	2.6±1.0%	5.6±2.9%	5.8±2.7%	3.9±2.4%	4.6±2.9%
CD4 T-cells	8.0±1.1%	7.7±0.6%	3.5±2.4%	4.3±3.2%	1.9±1.1%	2.0±1.2%
CD8 T-cells	6.3±0.5%	5.9±0.9%	47.1±19.0%	51.7±12.3%	34.3±6.8%	42.5±1 %
Blood	**Baseline**		**3 days**		**28 days**	
	WT	LAIR-1 $^{-/-}$	WT	LAIR-1 $^{-/-}$	WT	LAIR-1 $^{-/-}$
Neutrophils	24.5±12.3%	10.5±6.9%	28.1±23.5%	22.6±8.3%	4.9±1.2%	20.6±17.0%
Macrophages	7.2±3.3%	7.0±2.5%	5.4±4.4%	7.1±4.0%	3.7±0.9%	5.8±1.9%
Ly6C High monocytes	5.0±3.2%	3.5±1.5%	2.0±1.5%	3.0±2.0%	1.1±0.3%	2.7±2.3%
Ly6C Low monocytes	2.2±0.3%	3.0±0.6%	4.5±0.6%	5.0±1.2%	3.5±0.3%	3.9±0.9%
CD4 T-cells	13.1±3.3%	14.8±1.6%	9.0± 2.6%	11.4±3.2%	8.4±2.5%	9.8±1.6%
CD8 T-cells	9.4±2.2%	10.7±1.5%	8.7±3.8%	10.9±2.5%	8.8±3.0%	10.0±2.4%
Spleen	**Baseline**		**3 days**		**28 days**	
	WT	LAIR-1 $^{-/-}$	WT	LAIR-1 $^{-/-}$	WT	LAIR-1 $^{-/-}$
27,913	17.3±2.7%	15.8±1.0%	13.9±2.8%	11.3±2.1%	17.3±2.4%	16.3±2.0%
Macrophages	72.6±3.2%	73.8±1.5%	66.2±8.8%	71.8±6.7%	66.6±5.7%	77.6±2.4%
Ly6C High monocytes	27.5±3.2%	26.2±1.5%	33.8±8.7%	28.1±6.7%	33.3±5.7%	22.3±2.4%
Ly6C Low monocytes	11.9±1.4%	11.6±0.8%	9.8±2.5%	9.2±2.2%	12.5±1.4%	12.4±0.8%
CD4 T-cells	94.8±0.7%	95.0±0.8%	94.1±1.4%	93.9±1.9%	93.9±2.8%	96.0±0.6%
CD8 T-cells	3.6±1.1%	2.8±0.5%	3.7±1.1%	5.0±1.8%	3.1±0.9%	3.4±1.3%
Lymph node	**Baseline**		**3 days**		**28 days**	
	WT	LAIR-1 $^{-/-}$	WT	LAIR-1 $^{-/-}$	WT	LAIR-1 $^{-/-}$
Neutrophils	21.1±6.2%	17.8±4.9%	11.4±2.8%	11.3±2.8%	16.1±4.5%	15.3±2.9%
Macrophages	86.6±2.6%	86.4±3.0%	78.5±5.4%	82.6±4.2%	65.4±7.1%	76.8±5.4%
Ly6C High monocytes	13.5±2.7%	13.6±3.0%	21.5±5.3%	17.2±4.3%	34.7±7.1%	23.2±5.4%
Ly6C Low monocytes	16.5±4.6%	14.9±5.1%	11.2±2.8%	12.2±3.4%	13.9±3.6%	14.6±2.5%
CD4 T-cells	97.8±0.8%	97.9±0.8%	96.8±0.8%	97.0±1.4%	97.5±0.6%	97.7±0.6%
CD8 T-cells	0.8±0.1%	0.7±0.2%	2.0±0.9%	2.4±1.2%	0.9±0.3%	1.3±0.2%

CHAPTER 6

Primary outcome assessment in a pig model of acute myocardial infarction

G.H.J.M. Ellenbroek[1], G.P.J. van Hout[1,2], L. Timmers[1,2], P.A.F.M. Doevendans[2,3], G. Pasterkamp[1,4], I.E. Hoefer[1,4]

[1] Department of Experimental Cardiology, University Medical Center Utrecht, The Netherlands
[2] Department of Cardiology, University Medical Center Utrecht, The Netherlands
[3] Interuniversity Cardiology Institutes of the Netherlands (ICIN), The Netherlands
[4] Department of Clinical Chemistry and Hematology, University Medical Center Utrecht, The Netherlands

Journal of Visualized Experiments 2016; 116: 1-10

ABSTRACT

Mortality after acute myocardial infarction remains substantial and is associated with significant morbidity, like heart failure. Novel therapeutics are therefore required to confine cardiac damage, promote survival and reduce the disease burden of heart failure. Large animal experiments are an essential part in the translational process from experimental to clinical therapies. To optimize clinical translation, robust and representative outcome measures are mandatory. The present manuscript aims to address this need by describing the assessment of three clinically relevant outcome modalities in a pig acute myocardial infarction (AMI) model: infarct size in relation to area at risk (IS/AAR) staining, 3-dimensional transesophageal echocardiography (TEE) and admittance-based pressure-volume (PV) loops. Infarct size is the main determinant driving the transition from AMI to heart failure and can be quantified by IS/AAR staining. Echocardiography is a reliable and robust tool in the assessment of global and regional cardiac function in clinical cardiology. Here, a method for three-dimensional transesophageal echocardiography (3D-TEE) in pigs is provided. Extensive insight into cardiac performance can be obtained by admittance-based PV loops, including intrinsic parameters of myocardial function that are pre- and afterload independent. Combined with a clinically feasible experimental study protocol, these outcome measures provide researchers with essential information to determine whether novel therapeutic strategies could yield promising targets for future testing in clinical studies.

INTRODUCTION

Heart failure with reduced ejection fraction (HFrEF) accounts for about 50% of all heart failure cases, affecting an estimated 1 - 2% of people in the western world.[1] Its most prevalent cause is acute myocardial infarction (AMI). As acute mortality after AMI has declined significantly due to increased awareness and improved treatment options, emphasis has shifted towards its chronic sequelae; the most prominent being HFrEF.[2,3] Together with increasing health care costs[4], the growing epidemic of heart failure stresses the need for novel diagnostics and therapies, which can be studied in a highly translational porcine model of adverse remodeling after AMI as previously described.[5]

Both, determinants (*e.g.,* infarct size) and functional assessments (*e.g.*, echocardiography) of adverse remodeling are often used for efficacy testing of new therapeutics, indicating the need for reliable and relatively inexpensive methods. The aim of the current paper is to address this need by introducing important and reliable outcome measures for efficacy testing in a pig model of acute myocardial infarction. These include infarct size (IS) in relation to area at risk (AAR), 3D transesophageal echocardiography (3D-TEE) and detailed admittance-based pressure-volume (PV) loop acquisition.

Infarct size is the main determinant of adverse remodeling and survival after AMI.[6] Although timely reperfusion of ischemic myocardium may salvage reversibly injured cardiomyocytes and limit infarct size, reperfusion itself causes additional damage through the generation of oxidative stress and a disproportionate inflammatory response (ischemia-reperfusion injury (IRI)).[7] Hence, IRI has been identified as a promising therapeutic target. The ability of novel therapeutics to decrease infarct size is quantified by assessing infarct size in relation to the area at risk (AAR). AAR quantification is mandatory to correct for inter-individual variability in coronary anatomy of animal models, as a larger AAR leads to a larger absolute infarct size. Since infarct size is directly related to cardiac performance and myocardial contractility, variations in AAR can influence study outcome measures irrespective of treatment modalities.[8]

Three-dimensional transesophageal echocardiography (3D-TEE) is a safe, reliable and, most importantly, clinically applicable inexpensive method to measure cardiac function non-invasively. Whereas transthoracic echocardiography (TTE) images are limited to 2D parasternal long- and short-axis views in pigs[9], 3D-TEE can be used to obtain complete 3-dimensional images of the left ventricle. Therefore, it does not require mathematical approximations of left ventricular (LV) volumes such as the modified Simpson's rule.[10] The latter falls short of correctly estimating LV volumes after LV remodeling due to the lack of cylindrical geometry.[11] Moreover, 3D-TEE is preferable over epicardial echocardiography as it does not require surgical interventions, which have been observed to exert cardioprotective effects in the present model.[12] Although the use of 2D-TEE for the

assessment of myocardial function has been described before[13,14], limitations regarding ventricular geometry are similar to those observed in 2D-TTE and depend on the extent of LV remodeling. Hence, the larger the infarct (and thus the higher the probability of heart failure), the more likely 2D measurements become flawed by incorrect geometrical assumptions and the higher the need for 3D techniques.
Nonetheless, most imaging modalities are limited in their ability to assess intrinsic functional properties of the myocardium. PV loops provide such relevant additional information and their acquisition is therefore described in detail below.

MATERIALS AND METHODS

All animal experiments were approved by the Ethical Committee on Animal Experimentation of the University Medical Center Utrecht (Utrecht, the Netherlands) and conform to the 'Guide for the care and use of laboratory animals'.
NOTE: The protocol to perform a closed-chest balloon occlusion is not part of the current manuscript and is described in detail elsewhere.[5] In short, pigs (60 - 70 kg) are subjected to 75 min transluminal balloon occlusion of the midportion of the left anterior descending artery (LAD).
Both, three-dimensional transesophageal echocardiography (3D-TEE) and pressure-volume (PV) loop measurements can be performed at baseline, short-term and long-term follow-up. Note that these measurements are considered unreliable in the first hours after myocardial infarction due to frequent arrhythmias in this phase. Infarct size (IS) and area-at-risk (AAR) measurements are preferably assessed at short-term follow-up (24 - 72 hr)[15,16], since changes in microvasculature and secondary myocardial scar thinning culminate in less reliable results. Infarct size staining is performed using 2,3,5-triphenyltetrazolium chloride (TTC) (CAUTION, irritant), which is considered highly reproducible and relatively inexpensive. TTC is a white powder that colorlessly dissolves in saline. Upon contact with various dehydrogenases, it is converted to a brick red color. Thereby, it discriminates between viable (red) and dead myocardial tissue (white). For an overview on both invasive and non-invasive infarct size determination, readers are directed to a comprehensive review on this subject.[17]
Figure 1 shows the timeline including anesthesia, surgical preparation and primary outcome measurements used in this study.

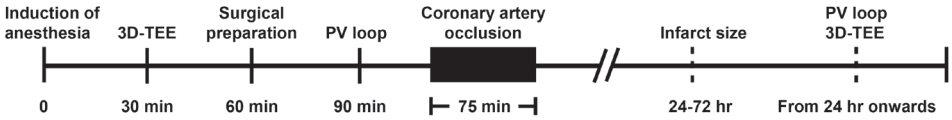

Figure 1. Timeline of the experimental protocol
This timeline provides an overview of the most important experimental steps in the used pig AMI model. Adequate induction of anesthesia is required prior to each measurement. Time indications can be observed under each proceeding. Infarct size is preferably assessed after 24 - 72 hours. 3D-TEE and PV loop data acquisition can be performed at baseline and at short- and long-term follow-up. The first hours after AMI, arrhythmias are frequent and can greatly interfere with cardiac hemodynamics and therefore prevent reliable data acquisition. *AMI: acute myocardial infarction; 3D-TEE: three-dimensional transesophageal echocardiography; PV loop: pressure-volume loop.*

Protocol

1. Medication and anesthesia

1. Ensure that the animal does not eat or drink for at least 5 hours prior to the procedure. Pre-treatment, anesthesia and post-operative pain treatment protocols have been described in detail elsewhere.[5]
2. In short, the day prior to surgery a buprenorfine patch (5 μg/hr) is applied to the skin that is active for seven days to limit post-operative pain. On the day of surgery, sedate pigs by intramuscular injection of 0.4 mg/kg midazolam, 10 mg/kg ketamine and 0.014 mg/kg atropine. Wait for approximately 10 - 15 min. Insert an 18 G cannula in one of the ear veins and administer 5 mg/kg sodium thiopental to induce anesthesia.
3. Intubate the pig using an endotracheal tube (size 8.5 for pigs of 60 - 70 kg). If necessary, perform balloon-ventilation (frequency 12/min) and transport the pig to the operating theater.
4. Upon arrival in the operation theater, start mechanical positive pressure ventilation with FiO_2 0.50, 10 ml/kg tidal volume and a frequency of 12/min using continuous capnography recording.
5. Start balanced anesthesia by continuous intravenous infusion of a combination of midazolam (0.5 mg/kg/hr), sufentanil (2.5 μg/kg/hr) and pancuronium (0.1 mg/kg/hr).
6. Confirm anesthesia by testing the corneal reflex and monitoring the breathing pattern (*e.g.*, spontaneous breathing in combination with mechanical ventilation indicates incomplete anesthesia). Use vet ointment on the eyes to prevent dryness while the animal is under anesthesia.

2. Three-dimensional transesophageal echocardiography (3D-TEE)

1. To allow for heart rate monitoring and data acquisition, connect the animal to the 5 leads ECG on the echocardiography machine.

2. Place the animal in the right lateral position. Make sure the probe is straight and flexible at the tip by unlocking the operating piece.
3. Open the pig's mouth and carefully insert the echo probe in the esophagus. If necessary, use a laryngoscope for visualization. Be careful to avoid ending up in the normal anatomic pharyngeal pouch, resembling a Zenker's diverticulum.[18]
4. Insert the probe for 50 - 60 cm (measure from the tip of the snout). Slowly rotate the probe and flex the head to a left anterolateral position to visualize the heart (Figure 2A - B). Make sure all walls are clearly visible.

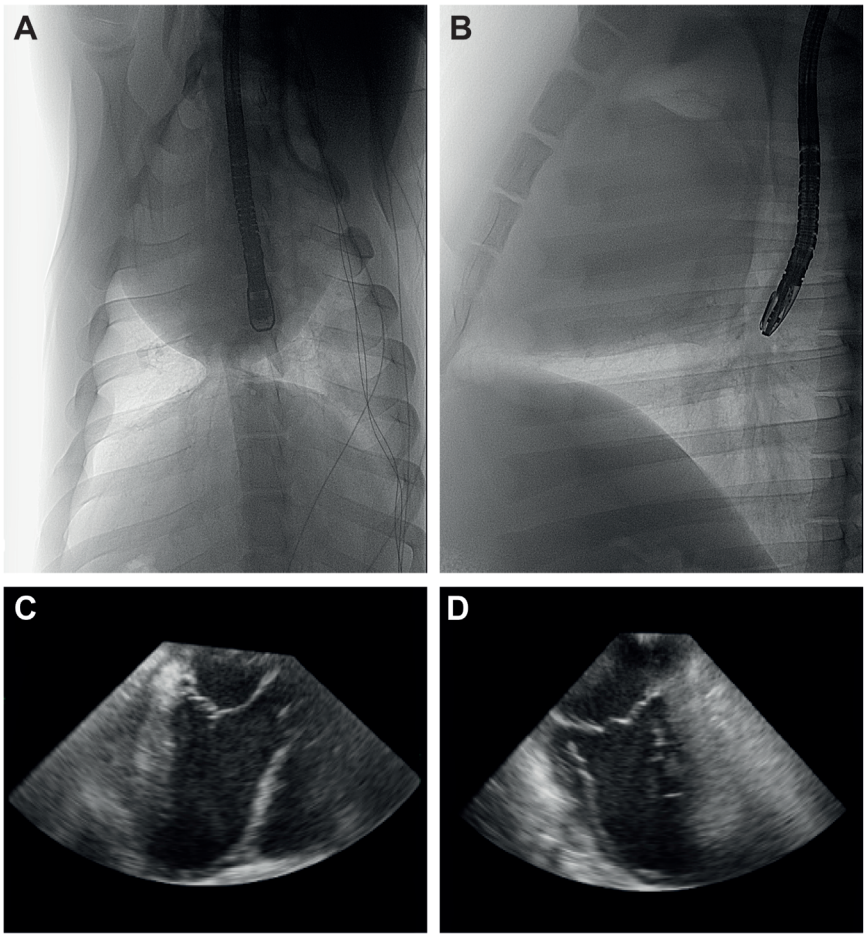

Figure 2. Positioning and acquisition of 3D TEE images
Anteroposterior (**A**) and mediolateral (**B**) X-ray images of the 3D-TEE probe positioning in the esophagus. Image acquisition follows upon correct visualization of the left atrium, left ventricle and aorta (**C**) and a perpendicular image of both left atrium and left ventricle (**D**). *3D-TEE: three-dimensional transesophageal echocardiography.*

5. Use the "3D full volume" option on the display of the echocardiography machine to display two perpendicular images of the left ventricle as shown in Figure 2C - D. Then maximize the sector width that is being acquired by selecting "FV Opt Volume". Pause ventilation by temporarily switching off mechanical ventilation and press "Acquire" to obtain full volume measurements.
6. After echo acquisition, make sure the tip is flexible by unlocking the operating piece. Then slowly remove the probe from the animal.
   NOTE: Do not leave the animal unattended until it has regained sufficient consciousness to maintain sternal recumbency. Do not return an animal that has undergone surgery to the company of other animals until fully recovered.
7. Perform offline analysis with validated software as described previously.[19]

3. Admittance-based pressure-volume loop acquisition

1. Pre-soak the sensing tips of the 7 F tetra-polar admittance catheter in 0.9% saline (room temperature to 37 °C) for a minimum of 20 min to ensure proper hydration and minimal baseline pressure drift during the experiment.[20]
2. Administer medication and anesthesia as described in section 1.
3. Perform surgical preparation and obtain vascular access as described previously.[5]
   1. In short, shave and clean the neck. Disinfect the surgical area with iodine 2% and cover the non-sterile parts of the pigs with sterile surgical drapes.
   2. Make a medial incision in the neck to expose the carotid artery and internal jugular vein. Insert an 8 F sheath into the carotid artery and a 9 F sheath into the jugular vein.
4. Insert a Swan-Ganz (SG) catheter through the 9 F sheath in the jugular vein and wedge it in a small pulmonary artery by inflating the balloon at the tip of the catheter. After adequate placement in the peripheral part of the lung, deflate the balloon. Connect the SG to an external cardiac output device.
5. Attach a 20 ml syringe containing 0.9% sterile saline to the injection port that connects to the lumen with the most proximal debouchment. Measure cardiac output by rapid infusion of 5 ml 0.9% saline (room temperature) and obtain heart rates to calculate stroke volume (SV). Repeat this procedure three times and calculate the average SV.
   NOTE: Cardiac output is (automatically) calculated using the Stewart-Hamilton thermodilution equation and is based on temperature changes in the pulmonary artery upon infusion of room temperature saline.[21]
6. Remove the SG catheter. Insert an 8 F Fogarty catheter through the 9 F sheath in the jugular vein and position it in the inferior vena cava.
7. Calibrate the pressure signal of the PV loop catheter using the "Course" and "Fine" button, while the tip remains in 0.9% saline. Then input the measured SV into the system.

8. Advance the PV loop catheter through the 8 F sheath in the carotid artery and center the tip in the left ventricle (LV) under fluoroscopy.
9. Select the largest adequately placed-segment by plotting the raw conductance signal against the pressure signal. Ensure that the pressure-conductance loops are of rectangle shape. Phase signal is expected to show a sinus trace with values between 3 and 5 degrees. Pause ventilation and perform a baseline scan to convert Conductance to Volume.
    1. Accept the baseline data by pressing "Continue" when the signals are stable (no arrhythmias), heart rate is equal to ECG or pressure derived heart rates and end-systolic (ES) / end-diastolic (ED) conductance are adequately sensed by the system.[20]
    NOTE: The latter can be verified by plotting the raw conductance signal against the pressure signal and comparing ES / ED conductance values derived from the baseline scan to real-time conductance. If any of the requirements above is not met, repeat the procedure.
10. Acquire baseline pressure-volume loops by recording 10 - 12 consecutive beats during apnea by pausing ventilation.
11. Inflate the Fogarty catheter under fluoroscopic guidance to reduce preload and record 10 - 12 consecutive beats as described above. Make sure systolic blood pressure remains >60 mmHg and no arrhythmias interfere with the measurements.
12. Remove the Fogarty and PV loop catheters. Keep recording arterial pressure before and during removal of the PV loop catheter to enable correcting for pressure drift (*i.e.*, *ex vivo* pre- and post-procedural baseline pressure difference).
    NOTE: Do not leave the animal unattended until it has regained sufficient consciousness to maintain sternal recumbence. Do not return an animal that has undergone surgery to the company of other animals until fully recovered.
13. Perform offline analysis of geometrical measurements and functional parameters with validated software.[22]

4. Area at risk (AAR) and infarct size (IS) quantification

1. Dissolve 1.00 g Evans blue (CAUTION[23], toxic) in 50 ml 0.9% saline, fill two 50 ml Luer lock syringes with 20 ml and 30 ml of 2% Evans blue solution respectively and keep at room temperature.
    NOTE: Work in a fume hood and wear a dust mask to limit exposure to hazardous dusts and use gloves and protective glasses to prevent contact from skin and eyes.
2. Taking similar precautions, dissolve 1% 2,3,5-triphenyl-tetrazoliumchloride (TTC) (CAUTION, irritant) in 37 °C 0.9% saline and keep at 37 °C.
3. Surgically prepare the animal to obtain vascular access to both carotid arteries. Perform a sternotomy to allow for direct visualization of the effect of *in vivo* Evans blue infusion.[5]

4. Insert a 7 F and an 8 F introducer sheath in the respective carotid artery. Alternatively, insert both introducer sheaths in one single carotid artery or use one of the femoral arteries for one of both guiding catheters.
5. Connect two standard Y-connectors to a 7 F JL4 and an 8 F JL4 guiding catheter respectively. For a femoral approach, use a JR4 for the right coronary artery (RCA) and a JL4 for the left main coronary artery (LMCA). Connect an additional three-way tap with 10 cm extension to both Y-connectors.
6. Administer 100 IU/kg heparin. Position the 8 F JL4 guiding catheter in the ostium of the LMCA via one of two introducer sheaths.
7. Using a 0.014" guidewire, advance a coronary dilatation catheter through the LCMA catheter and position the balloon at the site where coronary occlusion was performed during MI induction. Do not inflate yet.
8. Position the second 8 F JL4 guiding catheter in the ostium of the RCA via the second introducer sheath.
9. Perform a coronary angiography (CAG) by infusing contrast agent under fluoroscopy to confirm correct positioning of both guiding catheters and the balloon in the coronary arteries, using anteroposterior and LAO 30° views.
10. Attach the two 50 ml syringes containing 30 ml (LMCA) and 20 ml (RCA) 2% Evans blue to the respective three-way taps attached to the Y-connectors on the guiding catheters.
11. Inflate the balloon and confirm occlusion of the coronary artery by CAG. Only when the balloon completely blocks the passage of any contrast agent, inject Evans blue dye through both guiding catheters (5 ml/s) while the balloon is inflated.
12. Directly after the completion of Evans blue infusion, induce ventricular fibrillation by placing a 9 V battery on the non-infarcted part of the heart.
13. Incise the caval vein to release pressure and make sure a suction unit is available to allow for drainage of blood.
14. Deflate the balloon, retract it together with both guiding catheters and explant the heart by dissecting surrounding membranes. A transverse cut through the large vessels (*i.e.*, aorta, pulmonary artery/veins) allows for complete explantation. Rapidly wash off blood and superfluous dye on the exterior surface and in the cardiac cavities using 0.9% saline.
15. Carefully dissect the left ventricle and make cuts in 5 equal 10 mm thick sections from apex to base, in a plane parallel to the atrioventricular (AV) groove.
16. Photograph both sides of all five slices separately under ambient light conditions, as a possible Evans blue washout may occur in the subsequent step. For calibration, make sure a ruler is present in the image.
17. Incubate for 10 min in 1% TTC solution at 37 °C, turning the sections around after 5 min for equal staining.

18. Again, photograph both sides of all five slices separately under ambient light conditions and make sure a ruler is visualized in the image for calibration.
19. Weigh all slices. Use software suitable for the analyses.[5] When using ImageJ (version 1.47), click the "Straight line" button. Now, draw a straight line with a known distance using the ruler in the image (*e.g.*, 5 cm). Click "Analyze" -> "Set scale" and enter the distance in the box "Known distance". This procedure allows for calibration of distance in pixels to SI units of length.
20. Using the "Polygon selections"button, select the total area that corresponds to the LV myocardium in the present image, click "Analyze" -> "Measure" to acquire measurements. Perform this procedure for both sides of each slice of myocardium, and average per slice.
    1. Multiply by the weight of the slice proportional to the total weight of all five slices and average these measurements for all slices.
21. Perform similar measurements for area at risk (AAR) and infarct size (IS). Divide IS/AAR, AAR/LV and IS/LV and multiply by 100% to obtain respective outcome measurements.[5]

RESULTS

3D Transesophageal echocardiography

3D transesophageal echocardiography (3D-TEE) can be used for the assessment of global cardiac function. After AMI, global cardiac function differs from healthy baseline values. In particular, left ventricular ejection fraction (LVEF) decreases from 59 ± 4% to 37 ± 6% after one week of reperfusion.[24] An increase in end-systolic volume (51 ± 7 to 82 ± 13 ml) and decrease in stroke volume (74 ± 11 to 47 ± 8 ml) is also observed, whereas end-diastolic volume does not differ between both time points (125 ± 14 to 129 ± 13 ml). Representative images one week after myocardial infarction (ischemia-reperfusion) are displayed in Figure 3. In our ample experience, we have not encountered any complications related to TEE.

Admittance-based pressure-volume loops

Pressure-volume (PV) loops can be used both to assess global cardiac function and specific intrinsic myocardial muscle properties. Outcome measurements of the former can be easily calculated from the graphs in Figure 4A and include EDV (lower right corner), ESV (upper left corner) and LVEF ((EDV - ESV)/EDV x 100%). Both, ESV and EDV provide important information on left ventricular geometry and LVEF is an important measure for determining left ventricular pump function. A previous study compared admittance-based PV loops to gold-standard cardiac magnetic resonance imaging (CMRI) in a pig model of AMI.[25] After

eight weeks, PV loop measurements significantly overestimated both ESV and EDV. With regard to LVEF however, no significant difference was observed between PV loops and CMRI. In addition, both techniques showed a fairly good correlation of EDV and LVEF. For intrinsic cardiac performance, different measurements can be derived from PV loops, such as end-systolic and end-diastolic pressure-volume relationship (ESPVR; EDPVR).[26] Representative PV loop images with preload reduction and some examples of systolic and diastolic functional parameters are shown in Figure 4B. The ESPVR slope decreases, indicating decreased contractility. Additional valuable functional parameters that can be derived from PV loops are presented in Table 1.

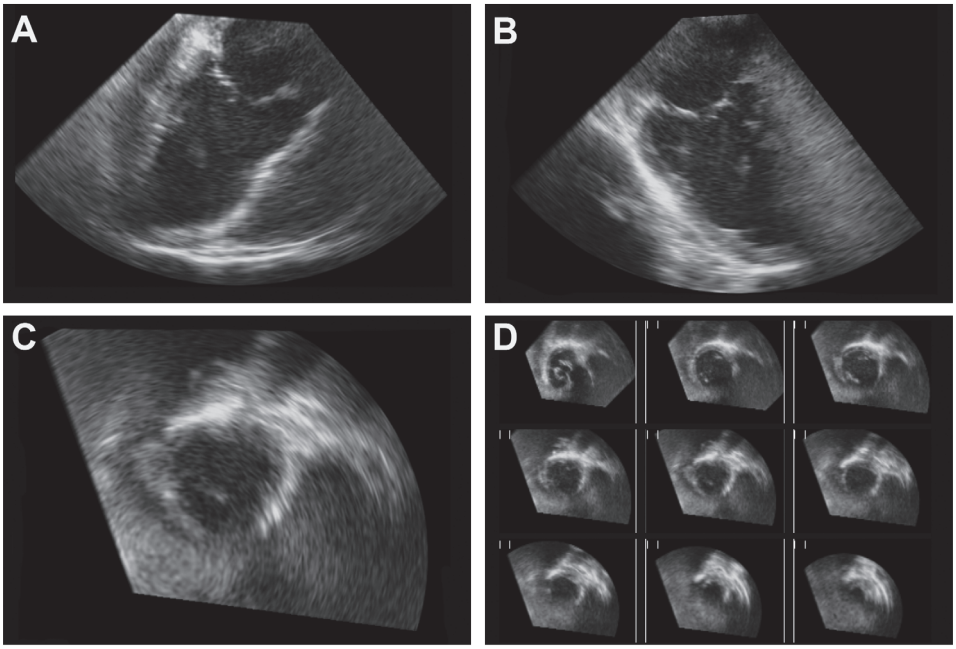

Figure 3. Full volume 3D-TEE images of the left ventricle
3D-TEE recordings of the left ventricle one week after acute myocardial infarction (75 minutes) and reperfusion. Perpendicular long-axis images of the left atrium and left ventricle can be observed in the upper half panel (**A**, **B**). A magnified example (**C**) of multiple cross-sectional images (**D**) of the left ventricle is displayed in the lower half panel. *3D-TEE: three-dimensional transesophageal echocardiography.*

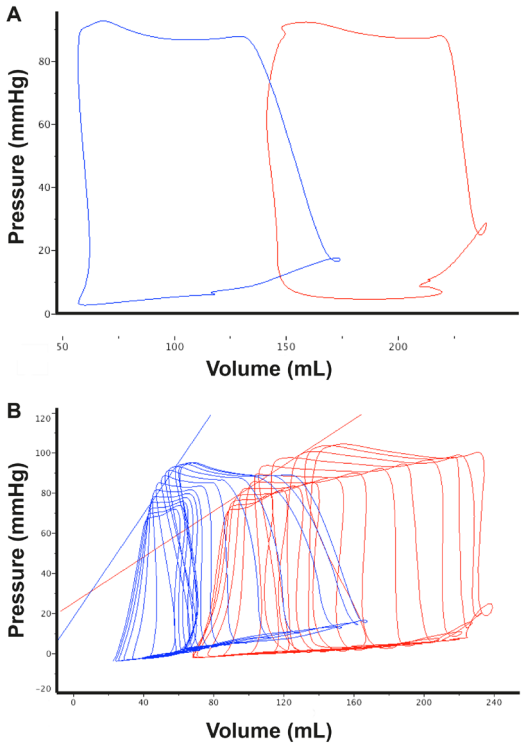

Figure 4. Pressure-volume loop images at baseline and after myocardial infarction
Representative PV loop images during apnea (*i.e.*, pausing ventilation) at baseline (blue) and eight week after AMI (red) (**A**). Increases in EDV and ESV and a decrease in SV can be observed, indicating a decrease in LVEF (%). PV loop images with preload reduction are used to assess intrinsic myocardial function parameters (**B**). Compared to baseline, infarcted myocardium shows a decrease in contractility as derived from the ESPVR (straight blue and red lines). *PV loop: pressure-volume loop; AMI: acute myocardial infarction; EDV: end-diastolic volume; SV: stroke volume; LVEF: left ventricular ejection fraction; ESPVR: end-systolic pressure-volume relationship.*

Table 1. Valuable functional parameters that can be derived from pressure-volume loops

Volume parameters		**Pressure parameters**		**Loading-independent parameters**		**Other**
Systolic	*Diastolic*	*Systolic*	*Diastolic*	*Systolic*	*Diastolic*	*Other*
ESV	EDV	ESP	EDP	ESPVR	EDPVR	HR
		dP/dT	dP/dT	E_{es}	PRSW	SW
Derivatives			_ (tau)	ESV100		PRSW
LVEF, SV, CO			PHT	E_a		dP/dV

Categorized into volume, pressure and loading-independent parameters, this table describes the most commonly used (systolic and diastolic) parameters derived from PV loops. *PV loops: pressure-volume loops; ESV: end-systolic volume; EDV: end-diastolic volume; LVEF: left ventricular ejection fraction; SV: stroke volume; CO: cardiac output; ESP: end-systolic pressure; dP/dT: derivative of pressure; τ (tau): isovolumic relaxation constant; PHT: pressure half-time; ESPVR: end-systolic pressure-volume relationship; E_{es}: end-systolic elastance; ESV100: end-systolic volume corrected for pressure (100 mmHg); E_a: arterial elastance; EDPVR: end-diastolic pressure-volume relationship; PRSW: preload recruitable stroke work; HR: heart rate; SW: stroke work; dP/dV: EDPVR slope (chamber stiffness).*

Infarct size/area at risk quantification

In female Dalland landrace pigs (6 months; 60 - 70 kg), occlusion of the left anterior descending artery (LAD) directly distal to the first septal and first diagonal branch during 75 minutes leads to an area at risk (AAR) of 22 ± 2% of the left ventricle (LV) (n = 5) (GHJM Ellenbroek, 2015). Infarct size constitutes 16 ± 2% of the left ventricle and 73 ± 7% of the AAR. This fairly large IS/AAR has been chosen for as patients with a larger infarct size are more prone to the development of heart failure than patients with a smaller infarct size. In pigs, the greatest therapeutic benefit can therefore be gained when applying 75 minutes of ischemia. Moreover, due to greater infarct size, cardiac function deteriorates, which allows for functional improvement as well. When a shorter period of index ischemia is applied, cardiac infarct size is lower and function is only mildly impaired, which allows for only a very small window of functional improvement. Figure 5 shows a representative example of a TTC and Evans blue staining that allows clear identification of the 3 areas: 1) remote myocardium, 2) AAR, and 3) infarcted myocardium.

Figure 5. Infarct size and area-at-risk staining
Representative image of infarct size and area-at-risk staining of the left ventricle after acute myocardial infarction (75 minutes) and subsequent reperfusion for three days. (Hemorrhagic) infarct tissue can be observed in rosy brown and gray-white, whereas the border zone is stained red. Surrounding blue-stained areas indicate remote myocardium.

DISCUSSION

Cardiac remodeling is largely depending on myocardial infarct size and the quality of myocardial infarct repair.[6,27] To assess the former in a standardized manner, the present manuscript provides an elegant method of *in vivo* infusion of Evans blue combined with *ex vivo* TTC staining, which has been validated and extensively used.[8,16,28,29] This method allows for quantification of the area at risk (AAR) and infarct size in relation to AAR.[16] The current approach reduces the risk of dye diffusion into the AAR, the infarct region or — with malpositioning — papillary muscle, as it does not require myocardial puncture. Moreover, there is no need for external ligation of the coronary artery, which may be imprecise, inaccurate and occasionally damage the myocardium. An alternative method, combining catheter-based Evans blue infusion into the LV and cross-clamping of the ascending aorta[30], is undesirable for different reasons. Clamping occludes the left ventricular guiding catheter, hampering Evans blue infusion into the LV. Besides, compression and traction forces may lead to LMCA catheter and intracoronary balloon malpositioning and inaccurate AAR measurements. Moreover, since balloon occlusion of the LAD requires guiding catheter positioning in the LMCA, coronary filling from the LV is limited, preventing Evans blue entry from the LV into the coronary artery.

However, though superior to myocardial puncture and cross-clamping of the ascending aorta, the technique presented in this manuscript requires some precautions. Complete occlusion of (one of the) coronary arteries through an obstructing guiding catheter needs to be prevented. This can be controlled by monitoring wash-out rates and pressure, and can usually be avoided by slightly retracting the guiding catheter from of the coronary ostium. If inevitable, shorten the time the guiding catheter is positioned in the coronary artery as much as possible by preparation of other parts of the protocol. In addition, make sure the balloon completely occludes the target vessel before Evans blue infusion.

When Evans blue infusion is completed, induce VF and incise the caval vein to release blood pressure before balloon deflation and catheter withdrawal in order to prevent Evans blue diffusion into the AAR. Care should be taken to gently but firmly position the guiding catheter in the coronary ostium, allowing for diffusion of Evans blue in both the LAD and LCx. In addition, Evans blue infusion rates should not be too high since limited flow into the coronary arteries may lead to Evans blue wash-out into the systemic circulation. Although selectively infused into the coronary arteries, Evans blue diffusion into the systemic circulation cannot be completely prevented. Therefore, histologic analysis of other non-cardiac tissue (*e.g.*, spleen, kidney) may still be problematic. Simultaneous TTC co-infusion into the AAR has been described before, but is undesirable in our opinion, as TTC does not reach the part of the AAR obstructed by the balloon. Moreover, previous analyses show that TTC might react with residual intravasal blood in the infarct area and overlap

with the red color in the non-infarct AAR.[31] Future applications of this technique could be to preserve non-cardiac tissues by obstructing blood flow into the systemic circulation. This could be achieved by balloon obstruction of the descending thoracic aorta through a femoral approach.

Echocardiography to date remains a cornerstone for cardiac function assessment in both clinical care and various animal models in cardiovascular research. However, due to the thoracic shape of landrace pigs, transthoracic echocardiography (TTE) is limited to 2-dimensional long- and short-axis views of the LV.[9] Therefore, cardiac volume and LVEF have to be estimated by mathematical approximations such as the modified Simpson's rule, which assumes a cylindrical left ventricular morphology.[10] As a result of LV remodeling after MI however, cardiac dimensions change. Therefore, this particular geometric assumption cannot be made, reducing the accuracy and reliability of such measurements.[32]

This problem can be solved by using 3D echocardiography to obtain 3D images of the complete left ventricle. In pigs, LVEF assessment by epicardial 3D echocardiography shows excellent correlation with gold-standard CMRI.[25,33] However, this requires surgery prior to AMI induction for baseline measurements. Regardless of the approach, *i.e.,* open chest vs. subxiphoidal approach, invasive surgery for epicardial echocardiography has been shown to be cardioprotective.[12,34,35] Concomitant adhesions hinder resternotomy, which renders epicardial echocardiography undesirable for baseline measurements in a closed-chest AMI model.To avoid these drawbacks, 3D images of the heart can be obtained through 3D transesophageal echocardiography (3D-TEE). This technique is portable, widely available and allows for serial measurements and visualization of the entire left ventricular volume. Moreover, it is reliable, relatively inexpensive and safe.

Note that it is important to gently insert the TEE probe into the mouth and esophagus, since ending up in the Zenker's diverticulum and applying too much pressure may lead to esophageal rupture. Moreover, since the anatomical relationship between stomach and heart differs from man, 3D-TEE in pigs does not allow for regional measurements (*e.g.*, strain, tissue Doppler imaging) and is restricted to volume measurements. In the data presented in the manuscript, no increase of EDV 7 days after AMI was observed. A longer follow-up period is needed to extensively drive adverse remodeling, leading to an increased EDV at several weeks follow-up.[11]

In contrast to conventional echocardiography, admittance-based PV loops moderately overestimate LV volumes, both at baseline[36] and after 8 weeks of follow-up.[25] Still, fairly good correlations and high degrees of agreement with CMRI have been found. Although PV loop measurements several weeks after AMI are less precise compared to baseline, LV dimensions and derivatives hereof (LVEF) are useful for the global assessment of cardiac function.[36]

In addition, PV loops provide specific information about intrinsic myocardial properties, such as ESPVR. Since regional functional measurements in TTE and TEE are limited and epicardial echocardiography is undesirable at baseline, PV loops provide an elegant and safe technique for the assessment of intrinsic myocardial function. Both, the decline in ESPVR slope and the typical shift in V_0 can be used to compare different therapeutics. These classical features are validated in *ex vivo* canine heart suffering from pan-ischemia. Hence, in regional ischemia models, like AMI models, these specific characteristics are not always present, which can be attributed to many factors, of which ventricular remodeling and regional ischemia are the most important ones.[26,37,38]

For adequate data acquisition, it is critical to make sure no arrhythmias are present when converting conductance to volume and when acquiring PV loops. If arrhythmias are present, reposition the PV loop catheter so it does not irritate the myocardium. The administration of anti-arrhythmic drugs (*e.g.,* 150 - 300 mg amiodarone) may also help. However, note that PV loop acquisition within several hours after acute myocardial infarction is not reliable due to frequent arrhythmias (*e.g.,* premature ventricular complexes, bigemini).

Slightly advancing or retracting the PV loop catheter into the LV or from the muscular wall may also help to improve the shape of the PV loops. After changing PV loop catheter positioning, always double-check that the largest adequately placed segment is selected.

In conclusion, the current paper introduces three methods for cardiac assessment in a previously described pig AMI model with additional value for the evaluation of new therapeutics to decrease the burden of the ongoing heart failure epidemic.

Acknowledgements

The authors gratefully acknowledge Marlijn Jansen, Joyce Visser, Grace Croft, Martijn van Nieuwburg, Danny Elbersen and Evelyn Velema for their excellent technical support during the animal experiments.

Conflict of interest

The authors have nothing to disclose.

REFERENCES

1. Mosterd A, Hoes AW. Clinical epidemiology of heart failure. *Heart*. 2007;93:1137–46.
2. Nichols M, Townsend N, Luengo-Fernandez R, Leal J, Gray A, Scarborough P, Rayner M. European Cardiovascular Disease Statistics. Brussels: 2012.
3. Krumholz HM, Wang Y, Chen J, Drye EE, Spertus JA, Ross JS, Curtis JP, Nallamothu BK, Lichtman JH, Havranek EP, Masoudi FA, Radford MJ, Han LF, Rap MT, Straube BM, Normand SL. Reduction in Acute Myocardial Infarction Mortality in the United States. *JAMA*. 2010;302:767–73.
4. Go AS, Mozaffarian D, Roger VL, Benjamin EJ, Berry JD, Borden WB, Bravata DM, Dai S, Ford ES, Fox CS, Franco S, Fullerton HJ, Gillespie C, Hailpern SM, Heit JA, Howard VJ, Huffman MD, Kissela BM, Kittner SJ, Lackland DT, Lichtman JH, Lisabeth LD, Magid D, Marcus GM, Marelli A, Matchar DB, McGuire DK, Mohler ER, Moy CS, Mussolino ME, Nichol G, Paynter NP, Schreiner PJ, Sorlie PD, Stein J, Turan TN, Virani SS, Wong ND, Woo D, Turner MB. Heart disease and stroke statistics - 2013 update: A Report from the American Heart Association. 2013.
5. Koudstaal S, Jansen of Lorkeers SJ, Gho JMIH, van Hout GPJ, Jansen MS, Gründeman PF, Pasterkamp G, Doevendans P a, Hoefer IE, Chamuleau S a J. Myocardial infarction and functional outcome assessment in pigs. *J Vis Exp*. 2014;1–10.
6. Chareonthaitawee P, Christian TF, Hirose K, Gibbons RJ, Rumberger JA. Relation of initial infarct size to extent of left ventricular remodeling in the year after acute myocardial infarction. *J Am Coll Cardiol*. 1995;25:567–73.
7. Yellon DM, Hausenloy DJ. Myocardial reperfusion injury. *N Engl J Med*. 2007;357:1221–35.
8. Suzuki Y, Lyons JK, Yeung AC, Ikeno F. In vivo porcine model of reperfused myocardial infarction: In situ double staining to measure precise infarct area/area at risk. *Catheter Cardiovasc Interv*. 2008;71:100–7.
9. Weidemann F, Jamal F, Sutherland GR, Claus P, Kowalski M, Hatle L, De Scheerder I, Bijnens B, Rademakers FE. Myocardial function defined by strain rate and strain during alterations in inotropic states and heart rate. *Am J Physiol Hear Circ Physiol*. 2002;283:H792-9.
10. Mercier JC, DiSessa TG, Jarmakani JM, Nakanishi T, Hiraishi S, Isabel-Jones J, Friedman WF. Two-dimensional echocardiographic assessment of left ventricular volumes and ejection fraction in children. *Circulation*. 1982;65:962–9.
11. de Jong R, van Hout GPJ, Houtgraaf JH, Takashima S, Pasterkamp G, Hoefer I, Duckers HJ. Cardiac Function in a Long-Term Follow-Up Study of Moderate and Severe Porcine Model of Chronic Myocardial Infarction. *Biomed Res Int*. 2015;2015:1–11.
12. van Hout GPJ, Teuben MPJ, Heeres M, de Maat S, de Jong R, Maas C, Kouwenberg LHJ a., Koenderman L, van Solinge WW, de Jager SC a., Pasterkamp G, Hoefer IE. Invasive surgery reduces infarct size and preserves cardiac function in a porcine model of myocardial infarction. *J Cell Mol Med*. 2015;Epub ahead:1–9.
13. Meybohm P, Gruenewald M, Renner J, Maracke M, Rossee S, Hocker J, Hagelstein S, Zacharowski K, Bein B. Assessment of left ventricular systolic function during acute myocardial ischemia: A comparison of transpulmonary thermodilution and transesophageal echocardiography. *Minerva Anestesiol*. 2011;77:132–41.
14. Gruenewald M, Meybohm P, Broch O, Caliebe A, Koerner S, Renner J, Steinfath M, Bein B. Visual evaluation of left ventricular performance predicts volume responsiveness early after resuscitation from cardiac arrest. *Resuscitation*. 2011;82:1553–7.
15. Bolli R, Becker L, Gross G, Mentzer R, Balshaw D, Lathrop DA. Myocardial protection at a crossroads: The need for translation into clinical therapy. *Circ Res*. 2004;95:125–34.
16. Timmers L, Henriques JPS, de Kleijn DP V, Devries JH, Kemperman H, Steendijk P, Verlaan CWJ, Kerver M, Piek JJ, Doevendans PA, Pasterkamp G, Hoefer IE. Exenatide reduces infarct size and improves cardiac function in a porcine model of ischemia and reperfusion injury. *J Am Coll Cardiol*. 2009;53:501–10.
17. Csonka C, Kupai K, Kocsis GF, Novák G, Fekete V, Bencsik P, Csont T, Ferdinandy P. Measurement of myocardial infarct size in preclinical studies. *J Pharmacol Toxicol Methods*. 2010;61:163–70.
18. Law R, Katzka DA, Baron TH. Zenker's Diverticulum. *Clin Gastroenterol Hepatol*. 2014;12:1773–82.
19. Philips Healthcare. QLAB 10.0 Quick Card: 3DQ and 3DQ Adv measurements guide.
20. Transonic. ADV500 Pressure-Volume Measurement System Use and Care Manual, version 5.
21. Schramm W. Is the cardiac output obtained from a Swan-Ganz catheter always zero? *J Clin Monit Comput*. 2008;22:431–3.
22. IWorx. LabScribe 3: Software Manual for Pressure-Volume Analyses.
23. Hueper WC, Ichniowski CT. Toxicopathologic studies on the dye T-1824. *Arch Surg*. 1944;48:17–26.
24. van Hout GPJ, Bosch L, Ellenbroek GHJM, de Haan JJ, van Solinge WW, Cooper MA, Arslan F, de Jager SCA, Robertson AAB, Pasterkamp G, Hoefer IE. The selective NLRP3-inflammasome inhibitor MCC950 reduces infarct size and preserves cardiac function in a pig model of myocardial infarction. *Eur Heart J*. 2016;38:828–836.
25. van Hout GPJ, Jansen Of Lorkeers SJ, Gho JMIH, Doevendans PA, van Solinge WW, Pasterkamp G, Chamuleau SAJ, Hoefer IE. Admittance-based pressure-volume loops versus gold standard cardiac magnetic resonance imaging in a porcine model of myocardial infarction. *Physiol Rep*. 2014;2:1–9.
26. Burkhoff D, Mirsky I, Suga H. Assessment of systolic and diastolic ventricular properties via pressure-volume analysis: a guide for clinical, translational, and basic researchers. *Am J Hear Circ Physiol*. 2005;289:H501-12.
27. Frangogiannis NG. The inflammatory response in myocardial injury, repair, and remodelling. *Nat Rev Cardiol*. 2014;11:255–265.

28. Fishbein M, Meerbaum S, Rit J, Lando U, Kanmatsuse K, Mercier J, Corday E, Ganz W. Early phase acute myocardial infarct size quantification: validation of the triphenyl tetrazolium chloride tissue enzyme staining technique. *Am Hear J*. 1981;101:593–600.
29. Arslan F, Houtgraaf JH, Keogh B, Kazemi K, De Jong R, McCormack WJ, O'Neill L a J, McGuirk P, Timmers L, Smeets MB, Akeroyd L, Reilly M, Pasterkamp G, De Kleijn DP V. Treatment with OPN-305, a humanized anti-toll-like receptor-2 antibody, reduces myocardial ischemia/reperfusion injury in pigs. *Circ Cardiovasc Interv*. 2012;5:279–87.
30. Meyns B, Stolinski J, Leunens V, Verbeken E, Flameng W. Left ventricular support by Catheter-Mountedaxial flow pump reduces infarct size. *J Am Coll Cardiol*. 2003;41:1087–95.
31. Khalil PN, Siebeck M, Huss R, Pollhammer M, Khalil MN, Neuhof C, Fritz H. Histochemical assessment of early myocardial infarction using 2,3,5-triphenyltetrazolium chloride in blood-perfused porcine hearts. *J Pharmacol Toxicol Methods*. 2006;54:307–12.
32. Gardner BI, Bingham SE, Allen MR, Blatter DD, Anderson JL. Cardiac magnetic resonance versus transthoracic echocardiography for the assessment of cardiac volumes and regional function after myocardial infarction: an intrasubject comparison using simultaneous intrasubject recordings. *Cardiovasc Ultrasound*. 2009;7:38.
33. Santos-Gallego C, Vahl T, Gaebelt H, Lopez M, Ares-Carrasco S, Sanz J, Goldman M, Hajjar R, Fuster V, Badimon J. 3D-Echocardiography Demonstrates Excellent Correlation With Cardiac Magnetic Resonance for Assessment of Left Ventricular Function and Volumes in a Model of Myocardial Infarction. *J Am Coll Cardiol*. 2012;59:E1564.
34. Keith Jones W, Fan GC, Liao S, Zhang JM, Wang Y, Weintraub NL, Kranias EG, Schultz J El, Lorenz J, Ren X. Peripheral nociception associated with surgical incision elicits remote nonischemic cardioprotection via neurogenic activation of protein kinase C signaling. *Circulation*. 2009;120:S1-9.
35. Gross GJ, Baker JE, Moore J, Falck JR, Nithipatikom K. Abdominal Surgical Incision Induces Remote Preconditioning of Trauma (RPCT) via Activation of Bradykinin Receptors (BK2R) and the Cytochrome P450 Epoxygenase Pathway in Canine Hearts. *Cardiovasc Drugs Ther*. 2011;25:517–22.
36. van Hout GPJ, de Jong R, Vrijenhoek JEP, Timmers L, Duckers HJ, Hoefer IE. Admittance-based pressure-volume loop measurements in a porcine model of chronic myocardial infarction. *Exp Physiol*. 2013;98:1565–75.
37. Sunagawa K, Maughan WL, Burkhoff D, Sagawa K. Left ventricular interaction with arterial load studied in isolated canine ventricle. *Am J Physiol*. 1983;245:H773-80.
38. Steendijk P, Baan J, Van Der Velde ET, Baan J. Effects of critical coronary stenosis on global systolic left ventricular function quantified by pressure-volume relations during dobutamine stress in the canine heart. *J Am Coll Cardiol*. 1998;32:816–26.

CHAPTER 7

Myeloperoxidase inhibition does not affect reperfusion injury in a pig model of acute myocardial infarction

G.H.J.M. Ellenbroek[1], H. Gremmels[2], L. Timmers[3], E. Michaelsson[4], L-M. Gan[4,5,6], D.P.V. de Kleijn[1,7,8], P.A.F.M. Doevendans[3,7], G. Pasterkamp[1,9], I.E. Hoefer[1,9]

[1] Laboratory of Experimental Cardiology, University Medical Center Utrecht, The Netherlands
[2] Department of Nephrology and Hypertension, University Medical Center Utrecht, Netherlands
[3] Department of Cardiology, University Medical Center Utrecht, The Netherlands
[4] Cardiovascular and Metabolic Diseases, Innovative Medicines and Early Development Biotech Unit, AstraZeneca R&D, Mölndal, Sweden
[5] Department of Cardiology, Institute of Medicine, Sahlgrenska Academy at the University of Gothenburg, Sweden
[6] Department of Molecular and Clinical Medicine, Institute of Medicine, Sahlgrenska Academy at the University of Gothenburg, Sweden
[7] Netherlands Heart Institute, The Netherlands
[8] Departement of Vascular Surgery, University Medical Center Utrecht, the Netherlands & Department of Surgery National University Singapore, Singapore
[9] Department of Clinical Chemistry and Hematology, University Medical Center Utrecht, The Netherlands

In preparation

ABSTRACT

Background

Restoring myocardial blood flow (reperfusion) is essential for myocardial salvage and preservation of cardiac function after acute myocardial infarction (AMI). Reperfusion inherently triggers reactive oxygen species (ROS) production, causing further damage to functional cardiomyocytes. Myeloperoxidase (MPO) is a key enzyme mainly secreted by neutrophils for the production of ROS. We hypothesized that MPO inhibition in a pig AMI model attenuates ischemia-reperfusion injury.

Methods and Results

Pigs underwent left anterior descending coronary artery balloon occlusion for 75 minutes and 72 hours reperfusion. Vehicle or MPO-inhibitor was administered 5 minutes prior to reperfusion and during the complete follow-up period. TTC/Evans blue staining showed comparable infarct size (IS) in vehicle and treated animals as a percentage of the area at risk (73±7% vs. 69±7%, p=0.41) or as a percentage of the left ventricle (16±2% vs. 15±5%, p=0.73). In addition, neutrophil influx did not differ between vehicle and treated animals (455±137 vs. 381±194 per mm^2, p=0.69).

Conclusion

Our small-scaled large animal study does not provide supportive evidence for a beneficial role of MPO inhibition in myocardial ischemia-reperfusion injury.

INTRODUCTION

Restoring myocardial blood flow (reperfusion) is essential for myocardial salvage and preservation of cardiac function in the setting of acute myocardial infarction (AMI). Simultaneously, reperfusion triggers a strong immune response including neutrophil accumulation and reactive oxygen species (ROS) production, causing additional damage to functional cardiomyocytes.[1] Myeloperoxidase (MPO) is a key enzyme mainly secreted by neutrophils for the production of ROS by converting hydrogen peroxide (H_2O_2) and chloride anions into hypochlorous acid (HOCl), responsible for the cytotoxic effects. In addition, MPO is deposited on proteoglycans in the vascular wall, inhibiting vascular function by oxidizing nitric oxide.[2] Elevated MPO levels are not only found in the infarcted area[3], but plasma levels also predict adverse outcome in patients with AMI.[4] We therefore hypothesized that exogenous MPO inhibition (MPOi) in a large animal AMI model attenuates ischemia-reperfusion injury (IRI) and decreases infarct size.

MATERIAL AND METHODS

In vitro inhibition of myeloperoxidase

AZD5904 is a mechanism-based inhibitor of MPO that irreversibly binds to the heme group of the activated enzyme, with a cell free potency of approximately 200 nM.[5] The potency of AZD5904 on MPO activity in leukocytes was determined by stimulating blood from pigs and healthy volunteers with phorbol 12-myristate 13-acetate (PMA). Peroxidase activity in plasma was quantified by luminescence upon restimulation with H_2O_2 in the presence of luminol. Data were normalized towards stimulated controls without compound and expressed as light emission per minute (LPM).

Dose rationale

A separate pharmacokinetic experiment in healthy pigs was performed to quantify the plasma concentration of intravenously administered 14C-labeled AZD5904 (1 μmol/kg) in parallel to intraduodenally administered AZD5904 (20 μmol/kg).

Circulating levels of AZD5904

Plasma concentrations of AZD5904 were quantified using liquid chromatography-tandem mass spectrometry analysis. Plasma samples were protein precipitated with acetonitrile, formic acid and internal standard. A calibration standard curve was prepared in parallel and a lower limit of quantification (LLOQ) of 31.8nmol/L was determined.

Animal study design

All animal experiments were approved by the Ethical Committee on Animal Experimentation of the University Medical Center Utrecht (Utrecht, the Netherlands) and conform to the 'Guide for the care and use of laboratory animals'. Ten female landrace pigs were subjected to closed-chest left anterior descending artery (LAD) balloon occlusion for 75 minutes and 72 hours reperfusion.[6] Blood was collected at various time points during and after MI. Pigs were randomly assigned to receive either vehicle (n=5) or AZD5904 (n=5). On day three, infarct size (IS) and area at risk (AAR) quantification was performed as previously described.[7]

Histology

Tissue was formalin-fixed, embedded in paraffin, cut into 4 μm sections and stained for neutrophils using a mouse anti-pig neutrophil antibody (1:3000, T3503, BMA Biomed, Augst, Switzerland). Similarly, MPO staining was performed using a polyclonal rabbit anti-human MPO antibody (1:3000, A0398, DAKO, Glostrup, Denmark). BrightVision poly-AP anti-mouse or anti-rabbit IgG (Immunologic, Duiven, Netherlands) was used as a secondary antibody and liquid permanent red (DAKO) as an enzyme substrate.

Statistical analyses

Data are expressed as mean±standard deviation (SD) and compared using a Mann-Whitney test (Graphpad Prism 6). $P<0.05$ was considered statistically significant.

RESULTS

AZD5904 reduces pig peroxidase activity in vitro and in vivo

AZD5904 has a potency of approximately 200nM on purified human MPO, whereas the potency on intragranular MPO is considerably lower (>10μM).[8] AZD5904 is equipotent in PMA-stimulated porcine (IC_{50} ~10μM, figure 1A) and human blood (IC_{50} ~27μM, figure 1B), additionally confirming the offset in potency between free and intragranular MPO. PMA-stimulated blood from pigs prior to, 3 and 6 hours after oral administration of AZD5904 demonstrated MPO inhibition of approximately 40% at 6 hours (figure 1C).

Dose rationale

We estimated that a plasma concentration of 2.5μM AZD5904 was required to inhibit 80% of MPO activity, based on the potency of AZD5904 on free MPO and 50% plasma protein binding in the pig. The plasma concentrations obtained in the pharmacokinetic experiment (figure 1D) were used as basis for dosing and infusion rates aiming for an exposure from 5μM (yielding >80% inhibition of free MPO) up to 40μM.

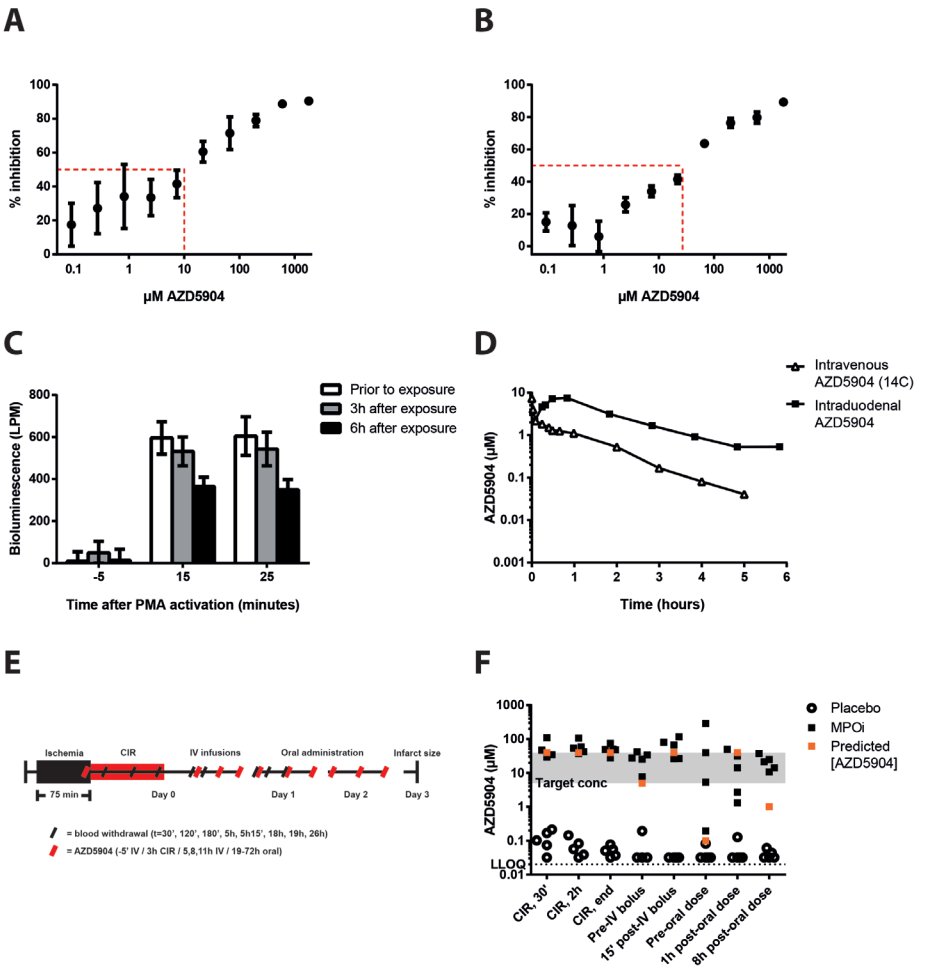

Figure 1. AZD5904 irreversibly inhibits MPO in vitro and in vivo and leads to adequate exposure in vivo
AZD5904 showed a dose-dependent inhibitory effect on MPO in PMA-stimulated porcine (A) and human blood (B). Blood drawn at baseline, 3 and 6 hours after administration of AZD5904 to healthy pigs, was stimulated with PMA and measured at several time points. In particular, blood drawn 6 hours after exposure showed a decrease in bioluminescence (increased MPO inhibition; C). AZD5904 plasma concentration in healthy pigs was measured after intravenous infusion of 14C-labeled AZD5904 or intraduodenal administration (D). The set-up of the AMI pig experiment (E) overall resulted in exposure as predicted (F). *LPM: light emissions per minute; MPO: myeloperoxidase; PMA: Phorbol 12-myristate 13-acetate; AMI: acute myocardial infarction; LLOQ: lower limit of quantification; CIR: continuous infusion regimen; IV; intravenous*

Figure 1E shows a timeline of the experiment. Overall, AZD5904 exposure followed predicted values (figure 1F). The exceptions were high exposure in three pigs before the first peroral administration and low exposure in two pigs one hour following the first peroral dose (decreased appetite).

Infarct size does not differ between vehicle- and AZD5904-treated animals

All pigs survived the procedure. In the vehicle group, one pig was excluded from IS/AAR quantification due to inaccurate staining. Representative examples of IS/AAR staining in the vehicle and MPO inhibition group are shown in figure 2A-B. The AAR/LV% did not differ between vehicle- and MPOi-treated pigs (22±2% vs. 22±6%; p=0.73, figure 1C). There were no differences in infarct size (IS) as percentage of the AAR (73±7% vs. 69±7%, p=0.41; figure 1D) or LV (16±2% vs. 15±5%, p=0.73; figure 1E).

Neutrophil influx (455±137 vs. 381±194/mm^2, p=0.69) and MPO content (0.34±0.16 vs. 0.30±0.09%, p=0.53) was also not different between vehicle- and MPOi-treated animals.

DISCUSSION

The neutrophil effector protein MPO is a major contributor to oxidative stress[9] and correlates with outcome after AMI.[4] Since oxidative stress is considered a key player during IRI[10], we expected MPO inhibition to decrease cell death and reduce infarct size. Despite the established role of oxidative stress in IRI[1], therapeutic approaches targeting oxidative stress have been inconclusive.[11–13] In line with the reported lack of infarct size reduction in MPO$^{-/-}$ mice[14], we did not observe infarct size reduction by MPO inhibition.

Taking into account the beneficial effects of low ROS concentrations, this might imply that the balance between ROS and anti-oxidants is a rather unstable equilibrium. The current inhibition of MPO could have been either too weak or too strong in decreasing radical production which has previously been shown to be important in the case of NADPH oxidase (NOX).[15]

Apart from its role in ROS production, MPO functions as a chemoattractant *in vitro* and *in vivo* in IRI in liver and skeletal muscle.[16] This function does not involve the catalytic activity of MPO and we did indeed not observe any effect of AZD5904 treatment on the number of infiltrating neutrophils. Since neutrophils also have detrimental MPO-independent effects (*e.g.* NOX), the comparable neutrophil influx in the treatment group may as well explain the comparable infarct size in both groups.

It is worth mentioning that the post-reperfusion inflammatory reaction is a highly dynamic process, not only affecting infarct size, but also cardiac function and remodelling.[17] In this regard, delayed MPOi dosing in a murine IRI model ameliorated the inflammatory response and improved LV function.[18] Despite its inability to reduce infarct size in IRI, MPO remains a potential target in myocardial remodelling.

In conclusion, the present results question the role of MPO in ischemia-reperfusion injury.

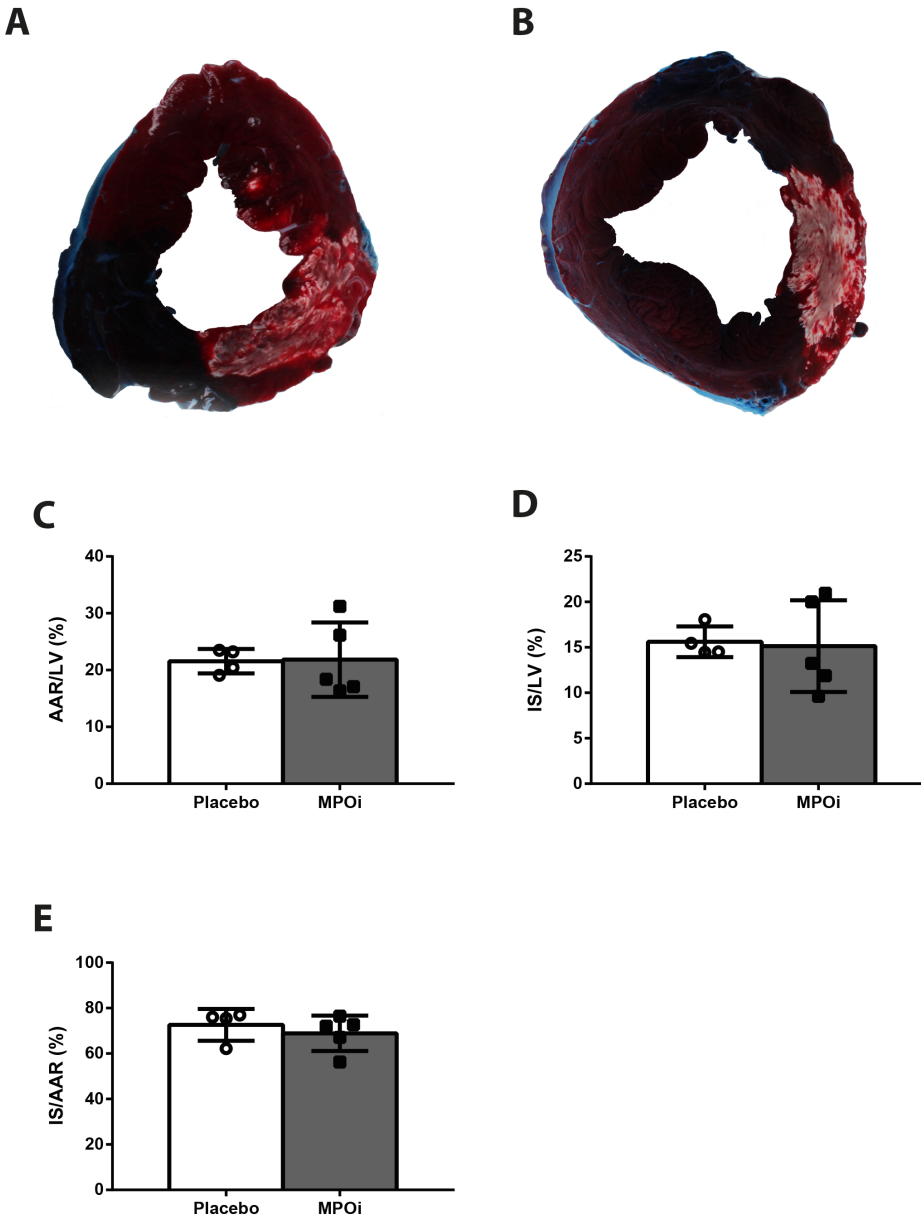

Figure 2. MPO inhibition does not affect infarct size
TTC/Evans blue staining of hearts from vehicle- (A) and MPOi-treated pigs (B) was used for the quantification of infarct size (IS; gray-white area), area at risk (AAR; sum of gray-white and red area) and the left ventricle (LV; entire area). The AAR/LV did not differ between both groups (C). Ischemia-reperfusion injury assessed by IS/AAR was comparable between both groups (D), as was IS/LV (E). *TTC: 2,3,5-triphenyl tetrazolium chloride; MPOi: myeloperoxidase inhibition*

Acknowledgements
The authors gratefully acknowledge Evelyn Velema, Marlijn Jansen, Joyce Visser, Martijn van Nieuwburg, Torbjörn Arvidsson, Daniel Hovdahl and Alexandra Peric for technical assistance. Petra van der Kraak is gratefully acknowledged for expert laboratory assistance and Suzanne Holterman for digital microscopy.

Funding
This research did not receive any specific grant from funding agencies in the public, commercial, or not-for-profit sectors.

Conflict of interest
E. Michaelsson and L. Gan are employees of AstraZeneca. The other authors have no other relevant affiliations or financial involvement with any organization.

REFERENCES

1. Granger DN, Kvietys PR. Reperfusion injury and reactive oxygen species: The evolution of a concept. *Redox Biol*. 2015;6:524–551.
2. Baldus S, Heitzer T, Eiserich JP, Lau D, Mollnau H, Ortak M, Petri S, Goldmann B, Duchstein HJ, Berger J, Helmchen U, Freeman BA, Meinertz T, Münzel T. Myeloperoxidase enhances nitric oxide catabolism during myocardial ischemia and reperfusion. *Free Radic Biol Med*. 2004;37:902–911.
3. Heymans S, Luttun a, Nuyens D, Theilmeier G, Creemers E, Moons L, Dyspersin GD, Cleutjens JP, Shipley M, Angellilo a, Levi M, Nübe O, Baker a, Keshet E, Lupu F, Herbert JM, Smits JF, Shapiro SD, Baes M, Borgers M, Collen D, Daemen MJ, Carmeliet P. Inhibition of plasminogen activators or matrix metalloproteinases prevents cardiac rupture but impairs therapeutic angiogenesis and causes cardiac failure. *Nat Med*. 1999;5:1135–1142.
4. Mocatta TJ, Pilbrow AP, Cameron VA, Senthilmohan R, Frampton CM, Richards AM, Winterbourn CC. Plasma Concentrations of Myeloperoxidase Predict Mortality After Myocardial Infarction. *J Am Coll Cardiol*. 2007;49:1993–2000.
5. Tiden AK, Sjögren T, Svensson M, Bernlind A, Senthilmohan R, Auchère F, Norman H, Markgren PO, Gustavsson S, Schmidt S, Lundquist S, Forbes L V., Magon NJ, Paton LN, Jameson GNL, Eriksson H, Kettle AJ. 2-Thioxanthines are mechanism-based inactivators of myeloperoxidase that block oxidative stress during inflammation. *J Biol Chem*. 2011;286:37578–37589.
6. Koudstaal S, Jansen of Lorkeers SJ, Gho JMIH, van Hout GPJ, Jansen MS, Gründeman PF, Pasterkamp G, Doevendans P a, Hoefer IE, Chamuleau S a J. Myocardial infarction and functional outcome assessment in pigs. *J Vis Exp*. 2014;1–10.
7. Ellenbroek GH, van Hout GP, Timmers L, Doevendans PA, Pasterkamp G, Hoefer IE. Primary Outcome Assessment in a Pig Model of Acute Myocardial Infarction. *J Vis Exp*. 2016;116.
8. Björnsdottir H, Welin A, Michaëlsson E, Osla V, Berg S, Christenson K, Sundqvist M, Dahlgren C, Karlsson A, Bylund J. Free Radical Biology and Medicine Neutrophil NET formation is regulated from the inside by myeloperoxidase-processed reactive oxygen species. *Free Radic Biol Med*. 2015;89:1024–1035.
9. Klebanoff SJ. Myeloperoxidase: friend and foe. *J Leukoc Biol*. 2005;77:598–625.
10. Yellon DM, Hausenloy DJ. Myocardial reperfusion injury. *N Engl J Med*. 2007;357:1221–35.
11. Forman MB, Puett DW, Cates CU, McCroskey DE, Beckman JK, Greene HL, Virmani R. Glutathione redox pathway and reperfusion injury. Effect of N-acetylcysteine on infarct size and ventricular function. *Circulation*. 1988;78:202–213.
12. Yoshida T, Watanabe M, Engelman DT, Engelman RM, Schley J a, Maulik N, Ho YS, Oberley TD, Das DK. Transgenic mice overexpressing glutathione peroxidase are resistant to myocardial ischemia reperfusion injury. *J Mol Cell Cardiol*. 1996;28:1759–1767.
13. Pacher P, Nivorozhkin A, Szabó C. Therapeutic effects of xanthine oxidase inhibitors: renaissance half a century after the discovery of allopurinol. *Pharmacol Rev*. 2006;58:87–114.
14. Vasilyev N, Williams T, Brennan ML, Unzek S, Zhou X, Heinecke JW, Spitz DR, Topol EJ, Hazen SL, Pen MS. Myeloperoxidase-generated oxidants modulate left ventricular remodeling but not infarct size after myocardial infarction. *Circulation*. 2005;112:2812–2820.
15. Matsushima S, Kuroda J, Ago T, Zhai P, Ikeda Y, Oka S, Fong GH, Tian R, Sadoshima J. Broad suppression of NADPH oxidase activity exacerbates ischemia/reperfusion injury through inadvertent downregulation of hypoxia-inducible factor-1 alpha and upregulation of peroxisome proliferator-activated receptor-alpha. *Circ Res*. 2013;112:1135–1149.
16. Klinke A, Nussbaum C, Kubala L, Friedrichs K, Rudolph TK, Rudolph V, Paust HJ, Schröder C, Benten D, Lau D, Szocs K, Furtmüller PG, Heeringa P, Sydow K, Duchstein HJ, Ehmke H, Schumacher U, Meinertz T, Sperandio M, Baldus S. Myeloperoxidase attracts neutrophils by physical forces. 2011.
17. Frangogiannis NG. The inflammatory response in myocardial injury, repair, and remodelling. *Nat Rev Cardiol*. 2014;11:255–265.
18. Ali M, Pulli B, Courties G, Tricot B, Sebas M, Iwamoto Y, Hilgendorf I, Schob S, Dong A, Zheng W, Skoura A, Kalgukar A, Cortes C, Ruggeri R, Swirski FK, Nahrendorf M, Buckbinder L, Chen JW. Myeloperoxidase Inhibition Improves Ventricular Function and Remodeling After Experimental Myocardial Infarction. *JACC Basic to Transl Sci*. 2016;1:633–643.

CHAPTER 8

The selective NLRP3-inflammasome inhibitor MCC950 reduces infarct size and preserves cardiac function in a pig model of myocardial infarction

G.P.J. van Hout*[1], L. Bosch*[1], G.H.J.M. Ellenbroek[1], J.J. de Haan[1], W.W. van Solinge[2], M.A. Cooper[3], F. Arslan[1], S.C.A. de Jager[1], A.A.B. Robertson[3], G. Pasterkamp[1,2], I.E. Hoefer[1,2]

** Contributed equally to this work*

[1] Laboratory of Experimental Cardiology, University Medical Center Utrecht, The Netherlands
[2] Department of Clinical Chemistry and Hematology, University Medical Center Utrecht, The Netherlands
[3] Institute for Molecular Bioscience, The University of Queensland, Brisbane, Australia

European Heart Journal 2017; 38: 828-836

ABSTRACT

Aims

Myocardial infarction (MI) triggers an intense inflammatory response that is associated with infarct expansion and is detrimental for cardiac function. Interleukin (IL)-1β and IL-18 are key players in this response and are controlled by the NLRP3-inflammasome. In the current study, we therefore hypothesized that selective inhibition of the NLRP3-inflammasome reduces infarct size and preserves cardiac function in a porcine MI model.

Methods and Results

Thirty female landrace pigs were subjected to 75 min transluminal balloon occlusion and treated with the NLRP3-inflammasome inhibitor MCC950 (6 or 3 mg/kg) or placebo for 7 days in a randomized, blinded fashion. After 7 days, 3D-echocardiography was performed to assess cardiac function and Evans blue/TTC double staining was executed to assess the area at risk (AAR) and infarct size (IS).

The IS/AAR was lower in the 6 mg/kg group (64.6 ± 8.8%, P = 0.004) and 3 mg/kg group (69.7 ± 7.2%, P = 0.038) compared with the control group (77.5 ± 6.3%). MCC950 treatment markedly preserved left ventricular ejection fraction in treated animals (6 mg/kg 47 ± 8%, P = 0.001; 3 mg/kg 45 ± 7%, P = 0.031; control 37 ± 6%). Myocardial neutrophil influx was attenuated in treated compared with non-treated animals (6 mg/kg 132 ± 72 neutrophils/mm2, P = 0.035; 3 mg/kg 207 ± 210 neutrophils/mm2, P = 0.5; control 266 ± 158 neutrophils/mm2). Myocardial IL-1β levels were dose-dependently reduced in treated animals.

Conclusions

NLRP3-inflammasome inhibition reduces infarct size and preserves cardiac function in a randomized, blinded translational large animal MI model. Hence, NLRP3-inflammasome inhibition may have therapeutic potential in acute MI patients.

INTRODUCTION

Myocardial infarction (MI) is one of the most important causes of death worldwide. Improved treatment strategies for MI, including percutaneous coronary intervention, have led to better survival. However, patients with deteriorated cardiac function are at increased risk for heart failure (HF) and the improved survival of MI patients potentiates its incidence.[1] Heart failure is accountable for a large fraction of cardiovascular deaths, is associated with a poor quality of life and extensive health care costs.[2] Novel therapeutics that prevent HF post-MI through preserving cardiac function are therefore crucial.

Cardiac ischaemia-reperfusion triggers a sterile inflammatory reaction. Though essential for wound healing, this intense inflammatory response expands infarct size and deteriorates cardiac function.[3,4] Infarct size and cardiac function are long-term predictors of adverse remodelling and HF.[5] Immediate damage control by attenuating the post-MI inflammatory response could therefore be of great benefit in MI patients.[6]

Interleukin (IL)-1β and IL-18 are potent mediators in the inflammatory response after MI and have been described to directly impair cardiac contractility in a synergistic way.[7–9] Moreover, their levels predict the occurrence of adverse events in patients after MI[10–12]and attenuation of IL-1β or IL-18 signalling has been shown to reduce infarct size and preserve cardiac function in rodent studies.[13–16]

Interleukin-1β and IL-18 signalling is regulated by the NOD-like-receptor, pyrin containing domain 3 (NLRP3)-inflammasome, an intracellular protein complex activated upon tissue injury.[17] Consequently, NLRP3-inflammasome inhibition leads to pronounced infarct size reduction, attenuation of adverse remodelling, and preservation of cardiac function in small animal MI models.[18–21] Although these studies provide important mechanistic insights, they do not reflect clinical application since they either involved knockout models or pharmacological treatment preceding MI induction.[19,21,22] To successfully translate these findings into clinical applications, preclinical testing in clinically relevant models is mandatory.[23]

Until recently, this was precluded by the lack of selective pharmacological NLRP3-inflammasome inhibitors.[22] MCC950 is a novel, selective small-molecule NLRP3-inflammasome inhibitor with powerful *in vitro* and *in vivo* inhibitory effects[24], enabling clinically relevant testing in large animal models. We therefore hypothesized that pharmacological interference with NLRP3-inflammasome signalling by administration of MCC950 results in infarct size reduction and preservation of cardiac function in a porcine MI model.

METHODS

In vitro assay

To measure MCC950 efficacy in pigs, porcine peripheral blood mononuclear cells (PBMCs) were isolated from baseline blood samples (n = 6) using Ficoll density-gradient centrifugation. Cells were stimulated with 10 μg/mL lipopolysaccharide (LPS) (Sigma-Aldrich, St. Louis, MO, USA). After 1 h, 5 mM adenosine triphosphate (ATP) (Sigma-Aldrich, St. Louis, MO, USA) and different concentrations of MCC950 (0, 0.3, 75, or 450 μM) were added. After 3 h total incubation time, IL-1β release was measured in the supernatant using a luminex immunoassay specific for porcine IL-1β (Procarta™ Simplex, eBioscience, San Diego, CA, USA), according to the manufacturer's protocol.

Animal study design

All animal experiments were approved by the institutional animal welfare committee and were executed conforming to the 'Guide for the Care and Use of Laboratory Animals'. A total of 30 female landrace pigs (body weight 66 ± 4.0 kg) were subjected to transluminal closed-chest left anterior descending (LAD) coronary artery balloon occlusion for 75 min followed by 7 days of reperfusion. One hour prior and 2 h post-occlusion, pigs were subjected to transoesophageal three-dimensional echocardiography (3D TEE). Fifteen minutes before reperfusion, pigs were randomly assigned to intravenous infusion with either a high dose of MCC950 [6 mg/kg in 40 mL phosphate-buffered saline (PBS)], a low dose of MCC950 (3 mg/kg in 40 mL PBS) or PBS alone at a rate of 80 mL/h. Intravenous infusion was repeated daily on Day 1 to Day 6. At the moment of balloon deflation, an additional dose of 6 mg (high dose, in 5 mL PBS), 3 mg (low dose, in 5 mL PBS), or PBS alone (5 mL) was selectively injected into the LAD. On Day 7, animals were again anaesthetized and subjected to 3D TEE and invasive pressure–volume (PV) measurements. This was followed by transthoracic echocardiography and dobutamine stress-echocardiography to assess regional contractility and cardiac reserve capacity. We then performed *in vivo* determination of the area at risk (AAR) through injection of Evans blue. Finally, the heart was explanted for the determination of infarct size and the myocardial inflammatory response. The investigators were blinded to the treatment group during both the experiments and the analysis of results. Detailed methods of echocardiography, PV measurements, and infarct size assessment are described in Supplementary material, Methods.

Circulating levels of MCC950

In vivo MCC950 concentrations were measured in plasma samples using mass-spectrometry. We quantified MCC950 content using negative ionization mode and multiple reaction monitoring on a Waters Xevo TQ mass spectrometer (MRM transition: 403.10 > 204.06).

Neutrophil numbers, interleukin-1β assay, and circulating markers

Circulating leukocyte numbers at different time points after reperfusion were measured by whole-blood analysis using an automated haematological cell-counter (Cell-Dyn Sapphire, Abbott, Santa Clara, CA, USA). Plasma samples were obtained by whole-blood centrifugation at 1850 × *g* and were immediately stored at −80°C. Troponin I, aspartate transaminase (AST), alanine aminotransferase (ALT), and C-reactive protein (CRP) levels were measured using a clinical chemistry analyser (AU5811, Beckman Coulter). Quantification of neutrophils in myocardial tissue is described in Supplementary material, Methods.

Statistics

All data are expressed as mean ± SD unless stated otherwise. In the current study, we performed a complete case analysis. All other outcomes were compared using a one-way ANOVA followed by *post hoc* analysis to compare individual groups. Blood parameters and leukocyte levels in the three treatment groups at different time points were analysed using mixed models. Not normally (Gaussian) distributed parameters were transformed with the natural logarithm. The mixed models include group and time point as fixed factors and a random intercept for each pig. To determine whether the time course of the parameters was different for the groups, the interaction group*time point of measurement was also taken into the model. All statistical analyses were performed in SPSS statistics version 20.0. A two-sided *P*-value of <0.05 was regarded statistically significant in all analyses.

RESULTS

In vitro assay

In vitro stimulation of isolated porcine PBMCs with LPS and ATP led to a pronounced secretion of IL-1β (*Figure 1A*). Administration of 0.3 μM MCC950 significantly attenuated this response (−45 ± 21%, $P = 0.002$). Increasing MCC950 concentrations further reduced IL-1β secretion (75 μM: −51 ± 24%, $P = 0.001$ compared with control, $P = 0.023$ compared with 0.3 μM; 450 μM: −64 ± 21%, $P < 0.001$ compared with control, $P = 0.011$ compared with 75 μM) (*Figure 1A*).

Survival, haemodynamics, and MCC950 levels

Three of 30 pigs died before the follow-up duration of 7 days was completed. Two animals died before reperfusion (1 in control group, 1 in low dose group) due to persistent VF. One pig died on Day 1 after MI induction (high dose group), without preceding clinical signs of acute cardiac failure. Echocardiography prior to MI induction revealed a congenital

anomaly (ventricle septum defect) in 1 pig (low dose group), which was therefore excluded from the study. This allowed analysis of nine animals in the control group, eight animals in the low dose group, and nine animals in the high dose group. Heart rate and mean arterial blood pressure were similar during the first 3 h after the induction of MI and subsequent compound administration (Supplementary material, Table S1).
In vivo levels of MCC950 were measured at 15 min reperfusion, at 4 h reperfusion and just prior to the second intravenous compound administration (24 h reperfusion) (*Figure 1B*, Supplementary material, Table S2).

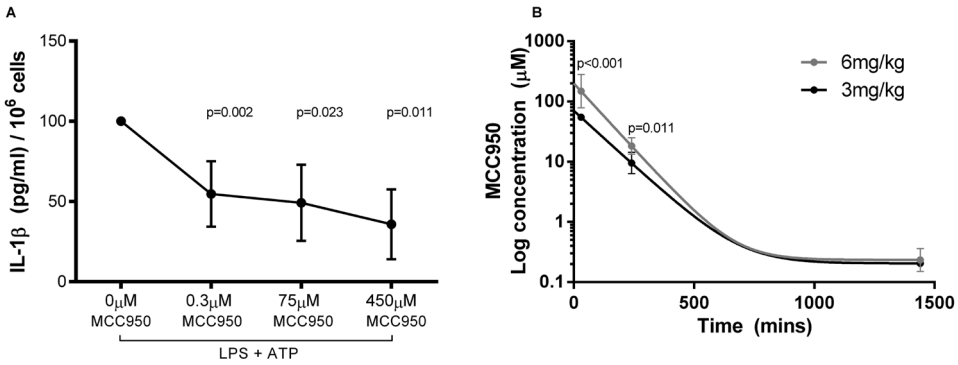

Figure 1. *In vitro* reduction of IL-1β secretion and circulating *in vivo* MCC950 levels
(*A*) Porcine peripheral blood mononuclear cells secrete IL-1β after administration of lipopolysaccharide and adenosine triphosphate *in vitro*. Addition of MCC950 after lipopolysaccharide/adenosine triphosphate stimulation dose-dependently reduced IL-1β release (n = 6). *P*-values represent differences from the previous dosage. (*B*) *In vivo* MCC950 levels during the first 24 h of the experiment were within therapeutic range. MCC950 levels were measured at 15 min, 4 and 24 h of reperfusion (n = 8–9 per group). *P*-values are differences between low and high dose group. Data are depicted as mean ± SD.

Infarct size

At 7 days follow-up, infarct size was assessed by Evans blue/TTC double staining (*Figure 2A*). The AAR as a percentage of the LV (AAR/LV) was similar in all three groups (high dose group 21.3 ± 3.2%, low dose group 23.0 ± 6.9%, control group 22.6 ± 4.4%, P = 0.7) (*Figure 2B*). Infarct size (IS) as percentage of the AAR (IS/AAR) was significantly higher in the control group compared with both treatment groups (high dose group 64.6 ± 8.8%, P = 0.004; low dose group 69.7 ± 7.2%, P = 0.038; control group 77.5 ± 6.3%) (*Figure 2C*). The IS as percentage of the LV (IS/LV) of the control group was significantly higher compared with the high dose group, but not to the low dose group (high dose group 13.7 ± 2.8%, P = 0.023; low dose group 15.8 ± 4.2%, P = 0.5; control group 17.2 ± 3.1%) (*Figure 2D*).

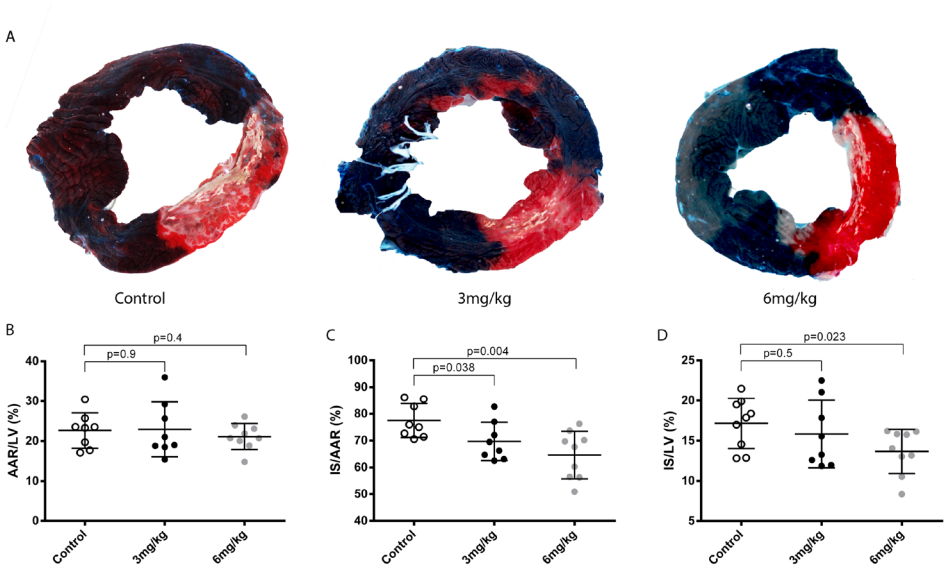

Figure 2. MCC950 administration dose-dependently reduces infarct size
(*A*) Representative pictures of myocardial segments of the three experimental groups. The blue area represents the remote area, the area at risk is stained red and the infarcted myocardium is stained white. (*B*) The area at risk was similar in all groups. (*C*) The infarct size/area at risk was lower in the high dose group and the low dose group compared with the control group. (*D*) The infarct size/left ventricular was lower in the high dose group but not in the low dose group compared with the control group. Data are depicted as mean ± SD.

Global cardiac function

Baseline cardiac function was similar in all groups. At 2 h reperfusion, global cardiac function did not significantly differ among groups (*Table 1*). At 7 days follow-up, no difference in end diastolic volume was observed between the different groups (*Figure 3A*). End systolic volume (ESV) at 7 days was significantly lower in the high dose group. The low dose group also showed a lower, albeit not statistically significant, ESV than the control group (high dose group 69 ± 12 mL, $P = 0.042$; low dose group 70 ± 13 mL, $P = 0.085$; control group 82 ± 13 mL) (*Figure 3B*). Left ventricular ejection fraction (EF) was higher in both the high dose group and the low dose group compared with the control group after 7 days follow-up (high dose group 47 ± 8%, $P = 0.001$; low dose group 45 ± 7%, $P = 0.031$; control group 37 ± 6%) (*Figure 3C*). The end systolic pressure–volume relationship, measured by invasive real-time PV loops, showed a higher contractility for the high dose group, but not for the low dose group at 7 days follow-up high dose group 4.7 ± 2.0 mmHg/mL, $P = 0.043$; low dose group 2.7 ± 1.4 mmgHg/mL, $P = 0.8$; control group 2.5 ± 1.7 mmHg/mL; *Figure 3D*).

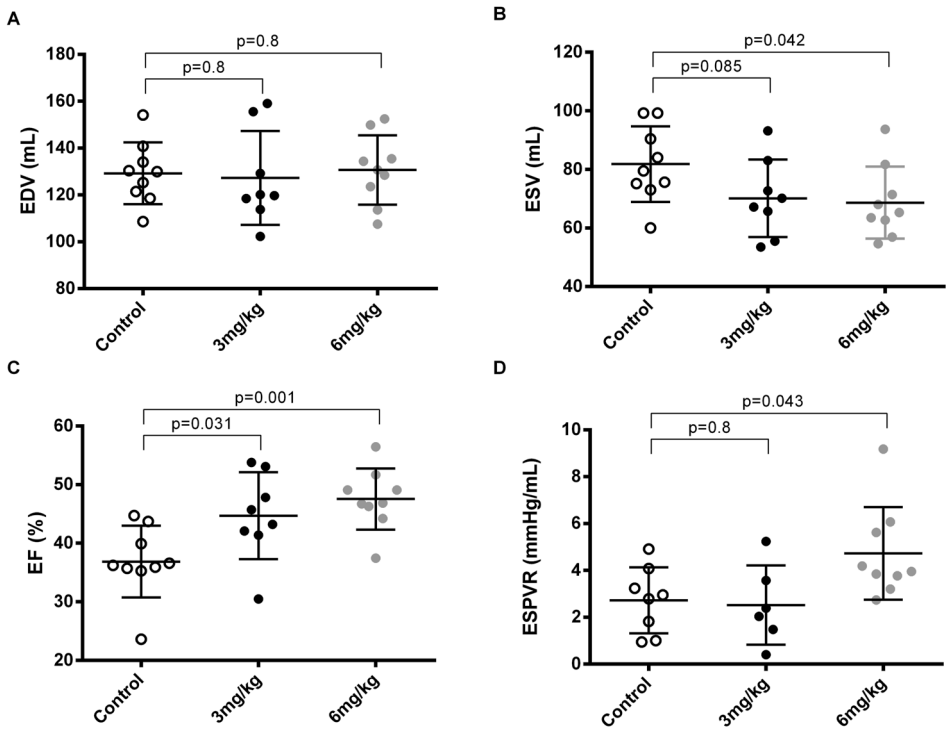

Figure 3. NLRP3-inflammasome inhibition preserves global cardiac function
(*A*) End diastolic volume (EDV) did not differ among the experimental groups. (*B*) End systolic volume (ESV) was lower in the high dose group and a trend was observed for the low dose group compared with the control group. (*C*) Ejection fraction was lower in the high dose group and the low dose group compared with the control group. (*D*) The end systolic pressure–volume relationship (ESPVR) in the high dose group but not the low dose group differed from the control group. Data are depicted as mean ± SD.

Regional cardiac function and dobutamine echocardiography

At 7 days follow-up, regional cardiac function was assessed at a midventricular and apical level by transthoracic echocardiography, before and during dobutamine infusion. Systolic wall thickening (SWT), fractional shortening (FS), and fractional area shortening (FAS) were assessed at the AAR and remote myocardium and MCC950-treated animals showed increased regional cardiac function (*Figure 4A–H*). Dobutamine stress-echocardiography revealed dose-dependent significant differences in cardiac reserve capacity in favour of MCC950-treated animals (*Table 2, Figure 5A–D*).

Serological and histological read-outs

The extent of cardiac damage was also reflected by systemic cardiac marker concentrations. Troponin I levels ($P = 0.047$) within the first 24 h after MI and both AST ($P = 0.049$) and

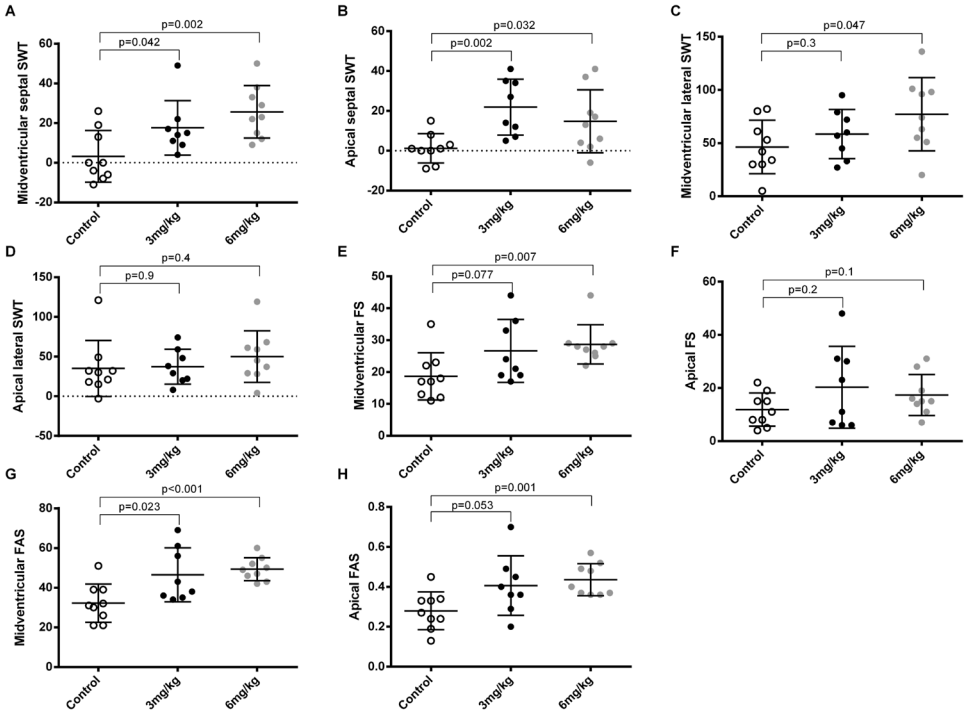

Figure 4. Regional cardiac function is preserved after NLRP3-inflammasome inhibition
Midventricular and apical septal systolic wall thickening were higher in the high and low dose group compared with the control group (*A* and *B*). Lateral systolic wall thickening at a midventricular level was higher in the high dose group while lateral systolic wall thickening at an apical level was equal among groups (*C* and *D*). Fractional shortening at a midventricular level was higher after MCC950 administration while no differences were observed at an apical level (*E* and *F*). Fractional area shortening was higher in MCC950 compared with placebo-treated animals at a midventricular and apical level (G&H). Data are depicted as mean ± SD.

ALT (P = 0.063) levels during the 7-day follow-up period were measured (*Figure 6A–C)*. To assess if inflammasome inhibition also reduced inflammatory markers post-MI, systemic neutrophil numbers (P = 0.056), and CRP (P = 0.030) were measured (*Figure 6D and E*). Circulating lymphocytes and monocytes did not show differences during the 7-day follow-up period (data not shown).

Both active and inactive intra-myocardial IL-1β, but not IL-18 levels were decreased in the treatment group compared with the control group when measured by luminex (high dose group 131 ± 82 pg/mg, P = 0.076; low dose group 156 ± 64 pg/mg, P = 0.2; control group 211 ± 104 pg/mg; *Figure 6F*; Supplementary material, Figure S1A and B). The inhibitory effect of MCC950 on IL-1β activation was confirmed using Western blot for the high dose group (P = 0.015, *Figure 6G and H*). A dose-dependent effect was observed for the infiltration of neutrophils, but not for macrophages into the infarcted myocardium (high

Table 1. Left ventricular geometrical parameters at baseline, 2 h reperfusion, and 7 days reperfusion (mean ± SD)

Parameter	Baseline			2 hours reperfusion			7 days reperfusion		
	Con	3 mg (P-value)	6 mg (P-value)	Con	3 mg (P-value)	6 mg (P-value)	Con	3 mg (P-value)	6 mg (P-value)
EDV (mL)	125 ± 14	122 ± 18 (*P* = 0.7)	121 ± 13 (*P* = 0.5)	96 ± 15	96 ± 16 (*P* = 0.9)	104 ± 19 (*P* = 0.4)	129 ± 13	127 ± 20 (*P* = 0.8)	131 ± 15 (*P* = 0.8)
ESV (mL)	51 ± 7	50 ± 14 (*P* = 0.8)	48 ± 10 (*P* = 0.5)	52 ± 10	53 ± 12 (*P* = 1.0)	57 ± 16 (*P* = 0.5)	82 ± 13	70 ± 13 (*P* = 0.085)	69 ± 12 (*P* = 0.042)
SV (mL)	74 ± 11	72 ± 7 (*P* = 0.7)	73 ± 6 (*P* = 0.8)	44 ± 7	44 ± 7 (*P* = 0.9)	48 ± 11 (*P* = 0.4)	47 ± 8	57 ± 14 (*P* = 0.096)	62 ± 8 (*P* = 0.001)
EF (%)	59 ± 4	60 ± 6 (*P* = 0.8)	61 ± 4 (*P* = 0.5)	46 ± 5	46 ± 6 (*P* = 0.9)	46 ± 8 (*P* = 1.0)	37 ± 6	45 ± 7 (*P* = 0.031)	48 ± 5 (*P* = 0.001)

EDV, end diastolic volume; ESV, end systolic volume; SV, stroke volume; EF, ejection fraction; 6 mg, 6 mg/kg group; 3 mg, 3 mg/kg group; Con, control group. P-values are from post hoc tests, compared with the control group.

Table 2. Left ventricular regional systolic parameters during dobutamine stress-echocardiography (mean ± SD)

Parameters	Mid ventricular			Apex		
	Con	3 mg (P-value)	6 mg (P-value)	Con	3 mg (P-value)	6 mg (P-value)
Septal WT_{ES} (cm)	1.3 ± 0.2	1.6 ± 0.3 (*P* = 0.006)	1.5 ± 0.2 (*P* = 0.005)	1.2 ± 0.3	1.5 ± 0.3 (*P* = 0.076)	1.5 ± 0.2 (*P* = 0.043)
Septal SWT (%)	9 ± 16	24 ± 22 (*P* = 0.1)	26 ± 10 (*P* = 0.024)	7 ± 10	17 ± 16 (*P* = 0.1)	22 ± 12 (*P* = 0.013)
Lateral WT_{ES} (cm)	1.5 ± 0.1	2.0 ± 0.4 (*P* = 0.003)	1.8 ± 0.3 (*P* = 0.010)	1.3 ± 0.3	1.6 ± 0.4 (*P* = 0.1)	1.5 ± 0.2 (*P* = 0.2)
Lateral SWT (%)	39 ± 22	73 ± 36 (*P* = 0.029)	73 ± 38 (*P* = 0.039)	12 ± 14	39 ± 20 (*P* = 0.002)	48 ± 22 (*P* = 0.001)
$LViD_{ES}$ (cm)	3.3 ± 0.7	2.7 ± 0.5 (*P* = 0.042)	2.7 ± 0.5 (*P* = 0.041)	2.3 ± 0.6	2.0 ± 0.4 (*P* = 0.3)	1.8 ± 0.5 (*P* = 0.076)
FS (%)	28 ± 8	40 ± 13 (*P* = 0.043)	38 ± 7 (*P* = 0.015)	29 ± 11	32 ± 9 (*P* = 0.6)	36 ± 11 (*P* = 0.2)
$LVia_{ES}$ (cm^2)	9.9 ± 2.9	6.7 ± 2.2 (*P* = 0.023)	7.0 ± 1.8 (*P* = 0.029)	4.6 ± 1.3	3.2 ± 0.9 (*P* = 0.021)	2.0 ± 1.0 (*P* < 0.001)
FAS (%)	45 ± 9	56 ± 17 (*P* = 0.1)	56 ± 8 (*P* = 0.023)	46 ± 10	53 ± 12 (*P* = 0.2)	63 ± 13 (*P* = 0.007)

WTES, end systolic wall thickness; SWT, systolic wall thickening; LViDES, end systolic left ventricular internal diameter; FS, fractional shortening; LViaES, end systolic left ventricular internal area; FAS, fractional area shortening; 6 mg, 6 mg/kg group; 3 mg, 3 mg/kg group; Con, control group. P-values reported are from post hoc tests, compared with the control group.

dose group 132 ± 72 neutrophils/mm^2, $P = 0.035$; low dose group 207 ± 210 neutrophils/mm^2, $P = 0.5$; control group 266 ± 158 neutrophils/mm^2) (*Figure 6I and J,* Supplementary material, Figure S1C and D). Interestingly, MCC950 administration leads to increased infiltration of CD14$^+$ monocytes and a tendency towards more collagen formation and decreased capillary density (Supplementary material, Figure S1E–J), whereas TGF-β levels were not significantly changed (*data not shown*).

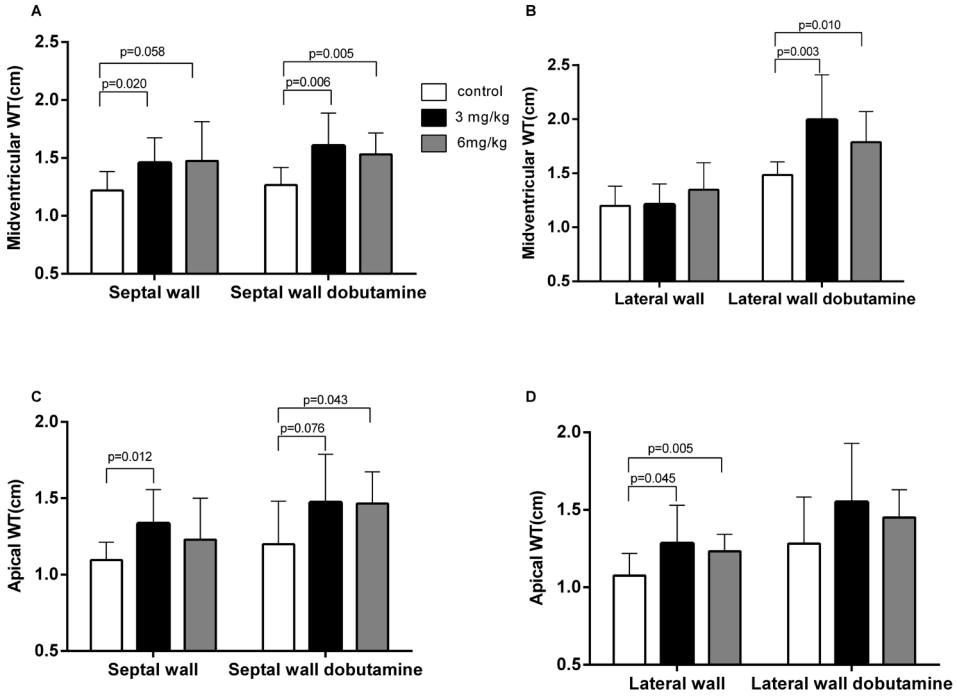

Figure 5. MCC950 administration preserves cardiac reserve capacity
(*A*) Septal wall thickness at a midventricular level was higher prior to dobutamine infusion and remained higher after dobutamine infusion in pigs treated with MCC950 compared with control animals. (*B*). Midventricular lateral wall thickness prior to dobutamine infusion was similar among groups. Dobutamine infusion lead to higher midventricular lateral wall thickness in MCC950-treated animals compared with control animals. (*C*) Apical septal wall thickness after dobutamine infusion was higher in MCC950-treated animals compared with control animals. (*D*) Apical lateral wall thickness was similar after dobutamine infusion among groups. Data are depicted as mean ± SD.

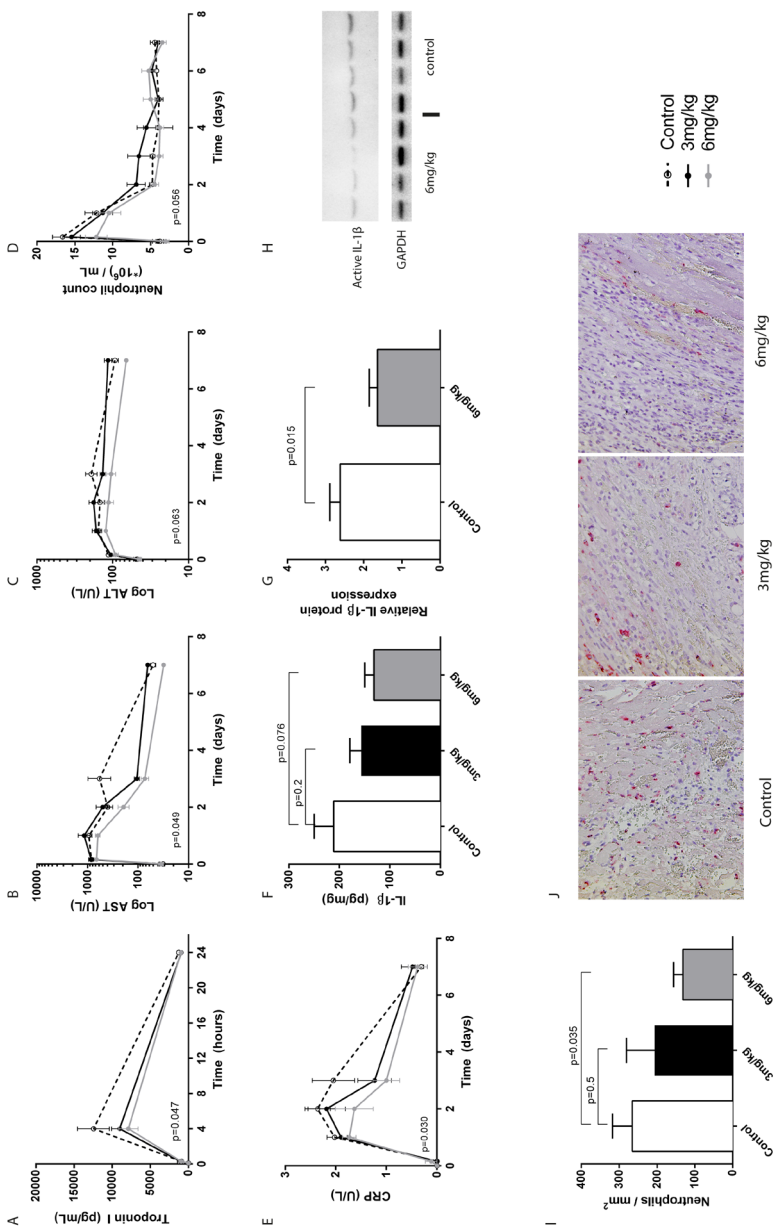

Figure 6. Inhibition of NLRP3-inflammasome signaling reduces inflammation
(*A*) Cardiac troponin levels at the first 24 h of reperfusion. (*B*) Circulating levels of aspartate transaminase. (*C*) Circulating levels of alanine aminotransferase. (*D*) Circulating levels of neutrophils during the 7-day follow-up period in the different experimental groups. (*E*) Circulating levels of C-reactive protein. (*F*) Myocardial IL-1β content 7 days post-myocardial infarction. (*G*) Quantification of active IL-1β levels in the high dose and control group ($n = 7$ for both groups). (*H*) Representative western blot of active IL-1β levels in pigs treated with 6 mg/kg MCC950 and control animals. (*I*). Neutrophils infiltration 7 days after myocardial infarction. (*H*) Representative pictures of neutrophils (in red) in the infarcted myocardium of the different experimental groups. Data are depicted as mean ± SEM.

DISCUSSION

Mechanistic studies have shown an essential role for the NLRP3-inflammasome, not only in IL-18- and IL-1β-driven inflammation in cardiac fibroblasts and circulating inflammatory cells but also caspase-1-dependent cell death (pyroptosis) in cardiomyocytes.[25,26] Both IL-18 and IL-1β signalling and pyroptosis induce amplification of the initial ischaemic damage, culminating in infarct size expansion, and decreased cardiac contractility, thereby increasing the risk of HF.[7,9,27,28] Our study is in line with these findings and for the first time provides *in vivo* efficacy data in a clinically relevant large animal MI model.

MCC950 has recently been shown to selectively inhibit NLRP3-inflammasome formation and reduce pyroptosis, IL-18 and IL-1β signaling.[24] In the current study, we show that daily intravenous administration of MCC950 can maintain pharmacologically active circulating concentrations as evident from our and others' *in vitro* studies.[24] Importantly, we studied for the first time the effect of MCC950 in an animal MI model.

Transgenic mouse models and pre-treatment protocols (pharmacological preconditioning) in rodent studies have elucidated the mechanisms of the post-MI inflammatory response. However, inflammation-related signaling pathways differ between small and larger mammals.[29] Moreover, large animal models allow application of minimally invasive techniques, thereby avoiding major traumatic injury that could confound the possible effect of anti-inflammatory treatment strategies.[30] Hence, large animal model testing is an essential step in bringing NLRP3-inflammasome-targeted therapies from bench into clinical application.[23,31,32]

In the current study, we show that selective inhibition of the NLRP3-inflammasome dose dependently reduces infarct size in a porcine MI model according to a clinically feasible treatment regimen. A pronounced difference in LV function was found in treated compared with non-treated animals at 7 days post-MI. This effect is markedly higher than those in most large animal cardioprotection studies.[32] At 2 h reperfusion, no differences in cardiac function were detected. This is in line with previous reports[33,] indicating that the primary effect of NLRP3-inflammasome inhibition is to attenuate the inflammatory response in the subacute phase after MI. The reserve capacity of the myocardium was higher in MCC950-treated animals compared with placebo-treated animals after dobutamine infusion. This suggests that NLRP3-inflammasome inhibition attenuates the decrease in exercise capacity that is often observed in patients post-MI.[34]

Our study reveals that circulating markers of damage and inflammation were lower in animals treated with a high dose of MCC950. Myocardial infiltration by circulating neutrophils was lower and myocardial IL-1β levels decreased in the high dose group. To our surprise, MCC950-treated animals showed higher monocyte infiltration, which may be related to increased infiltration of anti-inflammatory macrophages. This hypothesis is

supported by a dose-dependent increase in collagen formation (albeit not statistically significant). MCC950-treated animals showed decreased angiogenesis, seemingly contradicting an anti-inflammatory macrophage phenotype. However, this is in line with recent literature on angiogenesis reduction by NLRP3 inhibition or deficiency.[35]

Previous attempts to inhibit inflammation, e.g. by blocking leukocyte transmigration, did not lead to beneficial effects in MI patients. However, the inflammatory response is also necessary for appropriate cardiac wound healing.[3] MCC950 specifically targets cytokines that are notorious for their detrimental effect in cardiac wound healing and cardiac function upon damage. Our observations suggest that MCC950 treatment has more delicate effects in contrast to these previous strategies. Interference of MCC950 with the NLRP3-inflammasome, may fine-tune the inflammatory response rather than completely abolish it and therefore have beneficial effects in MI patients.

Study limitations

NLRP3-inflammasome inhibition could possibly prevent post-MI geometrical changes of the LV. However, we did not observe excessive cardiac dilatation in control animals after 7 days. Since infarct resorption occurs at longer follow-up duration, Evans Blue/TTC double staining becomes less reliable, thereby obscuring any effects on infarct size reduction.[36] Moreover, IL-1β levels are mainly elevated during the (sub)acute phase post-MI.[19] A longer follow-up period would therefore preclude the assessment of myocardial IL-1β content. Hence, we decided to limit the follow-up to 7 days in the current study.

In our model, circulating IL-1β and IL-18 levels after MI were below detection levels. Therefore, we were unable to assess the direct effect of MCC950 on these circulating cytokines. Moreover, due to the lack of reliable porcine-specific techniques that discriminate between the active and inactive form of IL-18 and caspase-1, we were unable to assess their activity in the myocardium. Therefore, no causative link between the known inhibitory properties of MCC950 on caspase-1 or IL-18 levels and the observed cardioprotective effect can be established in the current study. Nonetheless, since we do show that IL-1β levels are effectively reduced in the myocardium, it is conceivable that IL-18 will follow the same pattern.

In conclusion, our study reveals that continuous inhibition of the NLRP3-inflammasome-mediated signaling decreases the post-MI inflammatory response. Daily intravenous infusion of the selective small-molecule NLRP3-inflammasome inhibitor MCC950 for 7 days reduces active myocardial IL-1β levels, culminates in a pronounced cardiac function preservation and infarct size reduction in a randomized, blinded porcine MI study. Interference with NLRP3-inflammasome-mediated signaling therefore has become a promising target to reduce infarct size and preserve cardiac function in MI patients.

Acknowledgements
The authors gratefully acknowledge Marlijn Jansen, Joyce Visser, Martijn van Nieuwburg, Grace Croft, Evelyn Velema, Renée de Rooij, Petra van der Kraak, Arjan Schoneveld, Danny Elbersen, and Ron Stokwielder for their excellent technical support.

Funding
This research forms part of the Project P5.02 CellBeads of the Research Program of the BioMedical Materials Institute, co-funded by the Dutch Ministry of Economic Affairs.

Conflict of interest
None declared.

REFERENCES

1. Steg PG, James SK, Atar D, Badano LP, Lundqvist CB, Borger MA, Di Mario C, Dickstein K, Ducrocq G, Fernandez-Aviles F, Gershlick AH, Giannuzzi P, Halvorsen S, Huber K, Juni P, Kastrati A, Knuuti J, Lenzen MJ, Mahaffey KW, Valgimigli M, Van'T Hof A, Widimsky P, Zahger D, Bax JJ, Baumgartner H, Ceconi C, Dean V, Deaton C, Fagard R, Funck-Brentano C, Hasdai D, Hoes A, Kirchhof P, Kolh P, McDonagh T, Moulin C, Popescu BA, Reiner Z, Sechtem U, Sirnes PA, Tendera M, Torbicki A, Vahanian A, Windecker S, Astin F, Åström-Olsson K, Budaj A, Clemmensen P, Collet JP, Fox KA, Fuat A, Gustiene O, Hamm CW, Kala P, Lancellotti P, Maggioni A Pietro, Merkely B, Neumann FJ, Piepoli MF, Van De Werf F, Verheugt F, Wallentin L. ESC Guidelines for the management of acute myocardial infarction in patients presenting with ST-segment elevation. *Eur Heart J*. 2012;33:2569–2619.
2. Bleumink GS, Knetsch AM, Sturkenboom MCJM, Straus SMJM, Hofman A, Deckers JW, Witteman JCM, Stricker BHC. Quantifying the heart failure epidemic: Prevalence, incidence rate, lifetime risk and prognosis of heart failure - The Rotterdam Study. *Eur Heart J*. 2004;25:1614–1619.
3. Arslan F, de Kleijn DP, Pasterkamp G. Innate immune signaling in cardiac ischemia. *Nat Rev Cardiol*. 2011;8:292–300.
4. Timmers L, Pasterkamp G, Hoog VC De, Arslan F, Appelman Y, Kleijn DPV De. The innate immune response in reperfused myocardium. *Cardiovasc Res*. 2012;94:276–283.
5. Sutton SJ, Sharpe N. Left Ventricular Remodeling After Myocardial Infarction Pathophysiology and Therapy. *Circulation*. 2000;101:2981–2988.
6. Ibáñez B, Heusch G, Ovize M, Van De Werf F. Evolving therapies for myocardial ischemia/reperfusion injury. *J Am Coll Cardiol*. 2015;65:1454–1471.
7. Bujak M, Frangogiannis NG. The role of IL-1 in the pathogenesis of heart disease. *Arch Immunol Ther Exp (Warsz)*. 2009;57:165–176.
8. Sims JE, Smith DE. The IL-1 family: regulators of immunity. *Nat Rev Immunol*. 2010;10:89–102.
9. Toldo S, Mezzaroma E, Brien LO, Marchetti C, Seropian IM, Voelkel NF, Tassell BW Van, Dinarello CA, Abbate A. Interleukin-18 mediates interleukin-1-induced cardiac dysfunction. *Am J Physiol - Hear Circ Physiol*. 2014;306:H1025–H1031.
10. Blankenberg S, Luc G, Ducimetière P, Arveiler D, Ferrières J, Amouyel P, Evans A, Cambien F, Tiret L. Interleukin-18 and the Risk of Coronary Heart Disease in European Men: The Prospective Epidemiological Study of Myocardial Infarction (PRIME). *Circulation*. 2003;108:2453–2459.
11. Hartford M, Wiklund O, Hultén LM, Persson A, Karlsson T, Herlitz J, Hulthe J, Caidahl K. Interleukin-18 as a predictor of future events in patients with acute coronary syndromes. *Arterioscler Thromb Vasc Biol*. 2010;30:2039–2046.
12. Van Tassell BW, Raleigh JMV, Abbate A. Targeting Interleukin-1 in Heart Failure and Inflammatory Heart Disease. *Curr Heart Fail Rep*. 2015;12:33–41.
13. Salloum FN, Chau V, Varma A, Hoke NN, Toldo S, Biondi-Zoccai GGL, Crea F, Vetrovec GW, Abbate A. Anakinra in experimental acute myocardial infarction-does dosage or duration of treatment matter? *Cardiovasc Drugs Ther*. 2009;23:129–135.
14. Abbate A, Salloum FN, Vecile E, Das A, Hoke NN, Straino S, Giuseppe GL, Biondi-Zoccai, Houser JE, Qureshi IZ, Ownby ED, Gustini E, Biasucci LM, Severino A, Capogrossi MC, Vetrovec GW, Crea F, Baldi A, Kukreja RC, Dobrina A. Anakinra, a recombinant human interleukin-1 receptor antagonist, inhibits apoptosis in experimental acute myocardial infarction. *Circulation*. 2008;117:2670–2683.
15. Venkatachalam K, Prabhu SD, Reddy VS, Boylston WH, Valente AJ, Chandrasekar B. Neutralization of interleukin-18 ameliorates ischemia/reperfusion-induced myocardial injury. *J Biol Chem*. 2009;284:7853–7865.
16. Wang M, Tan J, Wang Y, Meldrum KK, Dinarello CA, Meldrum DR. IL-18 binding protein-expressing mesenchymal stem cells improve myocardial protection after ischemia or infarction. *Proc Natl Acad Sci U S A*. 2009;106:17499–17504.
17. Latz E, Xiao TS, Stutz A. Activation and regulation of the inflammasomes. *Nat Rev Immunol*. 2013;13:397–411.
18. Zuurbier CJ, Jong WMC, Eerbeek O, Koeman A, Pulskens WP, Butter LM, Leemans JC, Hollmann MW. Deletion of the innate immune NLRP3 receptor abolishes cardiac ischemic preconditioning and is associated with decreased IL-6/STAT3 signaling. *PLoS One*. 2012;7:1–8.
19. Sandanger O, Ranheim T, Vinge LE, Bliksoen M, Alfsnes K, Finsen A V., Dahl CP, Askevold ET, Florholmen G, Christensen G, Fitzgerald KA, Lien E, Valen G, Espevik T, Aukrust P, Yndestad A. The NLRP3 inflammasome is up-regulated in cardiac fibroblasts and mediates myocardial ischaemia-reperfusion injury. *Cardiovasc Res*. 2013;99:164–174.
20. Mezzaroma E, Toldo S, Farkas D, Seropian IM, Van Tassell BW, Salloum FN, Kannan HR, Menna AC, Voelkel NF, Abbate A. The inflammasome promotes adverse cardiac remodeling following acute myocardial infarction in the mouse. *Proc Natl Acad Sci U S A*. 2011;108:19725–19730.
21. Kawaguchi M, Takahashi M, Hata T, Kashima Y, Usui F, Morimoto H, Izawa A, Takahashi Y, Masumoto J, Koyama J, Hongo M, Noda T, Nakayama J, Sagara J, Taniguchi S, Ikeda U. Inflammasome activation of cardiac fibroblasts is essential for myocardial ischemia/reperfusion injury. *Circulation*. 2011;123:594–604.
22. Marchetti C, Chojnacki J, Toldo S, Mezzaroma E, Tranchida N, Rose SW, Federici M, Van Tassell BW, Zhang S, Abbate A. A novel pharmacologic inhibitor of the NLRP3 inflammasome limits myocardial injury after ischemia-reperfusion in the mouse. *J Cardiovasc Pharmacol*. 2014;63:316–22.

23. Lecour S, Bøtker HE, Condorelli G, Davidson SM, Garcia-Dorado D, Engel FB, Ferdinandy P, Heusch G, Madonna R, Ovize M, Ruiz-Meana M, Schulz R, Sluijter JPG, Van Laake LW, Yellon DM, Hausenloy DJ. ESC working group cellular biology of the heart: Position paper: Improving the preclinical assessment of novel cardioprotective therapies. *Cardiovasc Res*. 2014;104:399–411.
24. Coll RC, Robertson AAB, Chae JJ, Higgins SC, Muñoz-Planillo R, Inserra MC, Vetter I, Dungan LS, Monks BG, Stutz A, Croker DE, Butler MS, Haneklaus M, Sutton CE, Núñez G, Latz E, Kastner DL, Mills KHG, Masters SL, Schroder K, Cooper MA, O'Neill LAJ. A small-molecule inhibitor of the NLRP3 inflammasome for the treatment of inflammatory diseases. *Nat Med*. 2015;21:248–255.
25. Grundmann S, Bode C, Moser M. Inflammasome activation in reperfusion injury: Friendly fire on myocardial infarction? *Circulation*. 2011;123:574–576.
26. Takahashi M. NLRP3 Infl ammasome as a Novel Player in Myocardial Infarction. *Int Heart J*. 2014;55:101–105.
27. O'Brien L, Mezzaroma E. Interleukin-18 as a therapeutic target in acute myocardial infarction and heart failure. *Mol Med*. 2014;20:1.
28. Abbate A, Van Tassell BW, Biondi-Zoccai GGL. Blocking interleukin-1 as a novel therapeutic strategy for secondary prevention of cardiovascular events. *Biodrugs*. 2012;26:217–233.
29. Seok J, Warren HS, Cuenca AG, Mindrinos MN, Baker H V, Xu W, Richards DR, McDonald-Smith GP, Gao H, Hennessy L, Finnerty CC, López CM, Honari S, Moore EE, Minei JP, Cuschieri J, Bankey PE, Johnson JL, Sperry J, Nathens AB, Billiar TR, West M a, Jeschke MG, Klein MB, Gamelli RL, Gibran NS, Brownstein BH, Miller-Graziano C, Calvano SE, Mason PH, Cobb JP, Rahme LG, Lowry SF, Maier R V, Moldawer LL, Herndon DN, Davis RW, Xiao W, Tompkins RG. Genomic responses in mouse models poorly mimic human inflammatory diseases. *Proc Natl Acad Sci U S A*. 2013;110:3507–3512.
30. Gross GJ, Baker JE, Moore J, Falck JR, Nithipatikom K. Abdominal surgical incision induces remote preconditioning of trauma (RPCT) via activation of bradykinin receptors (BK2R) and the cytochrome P450 epoxygenase pathway in canine hearts. *Cardiovasc Drugs Ther*. 2011;25:517–522.
31. Hausenloy D, Yellon D. Myocardial ischemia-reperfusion injury: a neglected therapeutic target. *J Clin Invest*. 2013;123:92–100.
32. Jansen Of Lorkeers SJ, Eding JEC, Vesterinen HM, Van Der Spoel TIG, Sena ES, Duckers HJ, Doevendans PA, Macleod MR, Chamuleau SAJ. Similar effect of autologous and allogeneic cell therapy for ischemic heart disease: Systematic review and meta-analysis of large animal studies. *Circ Res*. 2015;116:80–86.
33. Jong WMC, Leemans JC, Weber NC, Juffermans NP, Schultz MJ, Hollmann MW, Zuurbier CJ. Nlrp3 plays no role in acute cardiac infarction due to low cardiac expression. *Int J Cardiol*. 2014;177:41–43.
34. Mcmurray JJ V, Adamopoulos S, Anker SD, Auricchio A, B??hm M, Dickstein K, Falk V, Filippatos G, Fonseca C, Gomez-Sanchez MA, Jaarsma T, Kober L, Lip GYH, Maggioni A Pietro, Parkhomenko A, Pieske BM, Popescu BA, Ronnevik PK, Rutten FH, Schwitter J, Seferovic P, Stepinska J, Trindade PT, Voors AA, Zannad F, Zeiher A, Bax JJ, Baumgartner H, Ceconi C, Dean V, Deaton C, Fagard R, Funck-Brentano C, Hasdai D, Hoes A, Kirchhof P, Knuuti J, Kolh P, Mcdonagh T, Moulin C, Reiner ??eljko, Sechtem U, Sirnes PA, Tendera M, Torbicki A, Vahanian A, Windecker S, Bonet LA, Avraamides P, Ben Lamin HA, Brignole M, Coca A, Cowburn P, Dargie H, Elliott P, Flachskampf FA, Guida GF, Hardman S, Iung B, Merkely B, Mueller C, Nanas JN, Nielsen OW, Orn S, Parissis JT, Ponikowski P. ESC Guidelines for the diagnosis and treatment of acute and chronic heart failure 2012. *Eur J Heart Fail*. 2012;14:803–869.
35. Weinheimer-Haus EM, Mirza RE, Koh TJ. Nod-like receptor protein-3 inflammasome plays an important role during early stages of wound healing. *PLoS One*. 2015;10:1–13.
36. Holmes JW, Yamashita H, Waldman LK, Covell JW. Scar remodeling and transmural deformation after infarction in the pig. *Circulation*. 1994;90:411–20.
37. van Hout GPJ, Jansen Of Lorkeers SJ, Gho JMIH, Doevendans PA, van Solinge WW, Pasterkamp G, Chamuleau SAJ, Hoefer IE. Admittance-based pressure-volume loops versus gold standard cardiac magnetic resonance imaging in a porcine model of myocardial infarction. *Physiol Rep*. 2014;2:1–9.
38. Soliman OII, Krenning BJ, Geleijnse ML, Nemes A, Van Geuns RJ, Baks T, Anwar AM, Galema TW, Vletter WB, Cate FJT. A comparison between QLAB and tomtec full volume reconstruction for real time three-dimensional echocardiographic quantification of left ventricular volumes. *Echocardiography*. 2007;24:967–74.
39. van Hout GPJ, de Jong R, Vrijenhoek JEP, Timmers L, Duckers HJ, Hoefer IE. Admittance-based pressure-volume loop measurements in a porcine model of chronic myocardial infarction. *Exp Physiol*. 2013;98:1565–75.

SUPPLEMENTAL METHODS

Surgical protocol of infarct induction

Pre-treatment and anesthesia protocols have been described in detail elsewhere.[37] In short, all animals were pre-treated with acetylsalicylic acid for 1 day (320 mg loading dose, 80 mg/day maintenance), clopidogrel for 3 days (75 mg/day) and amiodaron for 10 days (1200 mg loading dose, 800mg/day maintenance). All medication was continued until the end of the 7-day follow-up period. Pre-operatively, animals also received a fentanyl patch (25µg/h). Animals were anesthetized with an intramuscular injection of 0.4 mg/kg midazolam, 10 mg/kg ketamine and 0.014 mg/kg atropine. Venous access was obtained by insertion of an 18G cannula in the ear vein for intravenous administration of 5 mg/kg sodiumthiopental. Anesthesia was maintained with intravenous infusion of 0.5 mg/kg/h midazolam, 2.5 µg/kg/h sufentanyl and 0.1 mg/kg/h pancuronium. Arterial access was obtained by introduction of an 8F sheath into the carotid artery after surgical exposure. A coronary angiogram of the left coronary tree was acquired using a 7F JL4 guiding catheter (Boston scientific, Natick, MA, USA). An adequately sized balloon was placed distal to the first diagonal branch and inflated for 75 minutes. Animals were observed for 3 hours post-reperfusion and a permanent catheter was placed in the jugular vein to allow daily intravenous medication and venous blood sampling. The surgical wound was closed and animals were weaned from anesthesia. Animals were defibrillated in case of ventricular fibrillation (VF). Heart rate and arterial blood pressure were measured continuously and documented every 30 minutes.

Echocardiography, PV measurements and dobutamine stress-echocardiography

3D TEE was performed at baseline, 2 hours post-MI and after 7 days of follow-up. An X7-2t transducer on an iE33 ultrasound device (Philips, Eindhoven, The Netherlands) was used to perform a transesophageal echocardiogram. The depth and sector size were adjusted to fit the complete left ventricle. All data sets were acquired in real time using 7 consecutive cardiac cycles (full volume analysis). Images were analyzed offline using QLab 10.0 (3DQ advanced) analysis software. Ventricle tracing was performed by semi-automatic border detection as described elsewhere.[38]

Pressure-volume measurements were performed after 3D TEE on day 7 as recently described.[37,39] Arterial and venous access was obtained under general anesthesia according to the protocol described above. A 7F tetra-polar admittance catheter (7.0 VSL Pigtail/no lumen, Transonic SciSense, London, Canada) was inserted into the left ventricle (LV) through an 8F sheath in the carotid artery under fluoroscopic guidance. The catheter was connected to the ADVantage system™ (Transonic SciSense, London, Canada) linked to a multi-channel acquisition system (Iworx 404), required for real-time data acquisition. An 8F Fogarty catheter was inserted through a 9F introducer sheath in the jugular vein into

the inferior vena cava. The Fogarty catheter was inflated to induce preload reduction and 10-12 consecutive heartbeats were recorded during apnea. Data were analyzed offline using Iworx analysis software (Labscribe V2.0).

Following PV measurements, grey scale short-axis transthoracic echocardiographic measurements were obtained in parasternal position using a broadband S5-1 transducer (Philips, Eindhoven, The Netherlands). Mid ventricular and apical images were obtained by acquiring three successive cardiac cycles. Regional left ventricular function was analyzed in Xcelera Ultrasound version 4.1 (Philips, Eindhoven, The Netherlands). Systolic wall thickening (SWT) was calculated by measuring end diastolic (ED) and end systolic (ES) wall thickness (WT) ($SWT=(WT_{ES}-WT_{ED})/WT_{ED}*100$) for both the septal and lateral wall. Fractional shortening (FS) was assessed by comparing the ES and ED LV internal diameter (LVid) ($FS=(LVid_{ED}-LVid_{ES})/LVid_{ED}*100$). Fractional area shortening (FAS) was calculated by determining the change in LV ES and ED diastolic internal area (LVia) ($FAS=(LVia_{ED}-LVia_{ES})/LVia_{ED}*100$). After images were obtained, dobutamine was infused through the sheath in the jugular vein at a rate of 2.5ug/kg/min. Once a plateau phase was reached, based on a constant arterial blood pressure, short axis images were again obtained to assess regional contractility.

Area at risk & infarct size

Before exsanguination, an additional 8F introducer sheath was inserted in the ipsilateral carotid artery. After medial sternotomy, an 8F JL4 guiding catheter (Boston Scientific, Natick, MA, USA) was inserted through the first sheath and a coronary angiogram was performed to ensure normal angiographic flow. An adequately sized balloon was placed distal to the first diagonal branch at the same site as the initial occlusion. A 7F JL4 guiding catheter (Boston Scientific, Natick, MA, USA) was placed in the right coronary artery. A 50 mL Luer lock syringe filled with 2% Evans blue dissolved in 30 mL 0.9%NaCl was attached to the 8F guiding catheter and another syringe containing 20 mL Evans blue solution to the 7F guiding catheter. Evans blue was then simultaneously infused at a rate of 10 mL/s in the left and right coronary artery. Immediately following Evans blue infusion, animals were sacrificed by exsanguination under anesthesia by opening the inferior caval vein. The heart was excised and the left ventricle (LV) was cut into 5 equal slices from apex to base. Slices were photographed and then incubated in 1% tetrazolium trichloride (TTC) (Sigma-Aldrich Chemicals, Zwijndrecht, the Netherlands) in 37°C 0.9%NaCl for 10 minutes to discriminate between infarct tissue and viable myocardium. After incubation, slices were again photographed. The remote area, area at risk (AAR) and infarct area were quantified using ImageJ software (NIH, Bethesda, MD, USA). Following quantification, infarcted tissue, tissue from the border zone and tissue from the remote area were collected and either conserved in 4% formaldehyde for histological quantification of neutrophils, or snap frozen in liquid nitrogen for cytokine measurements.

Histology neutrophils, macrophages, monocytes, capillaries and collagen

Neutrophil numbers in myocardial tissue were quantified in paraffin-embedded histological biopsies that were conserved in 4% formaldehyde for at least 7 days with a monoclonal mouse antibody against porcine neutrophils (Clone PM1, BMA Biomedicals, Augst, Switzerland) for 60 minutes and secondary incubation with Brightvision Poly-AP-anti-mouse (ImmunoLogic, Duiven, the Netherlands) for 30 minutes followed by development with liquid permanent red. IL-1β was measured in the myocardium using a luminex immunoassay (Procarta™ Simplex, eBioscience, San Diego, CA, USA) according to the manufacturer's instructions and corrected for total protein concentration.

Macrophages and monocytes were quantified in histological slides of myocardial tissue (paraffin and fresh frozen slides respectively) using a monoclonal mouse anti-pig antibody against CD107a (Clone JM2E5, Bio-Rad, Kidlington, UK) or a mouse monoclonal antibody against CD14 (Ab23919, Abcam, Cambridge, UK). 60 minutes of incubation was followed by Brightvision Poly-AP-anti-mouse (ImmunoLogic, Duiven, the Netherlands) for 30 minutes and development with liquid permanent red. Clustering of CD14 positive cells prevented reliable individual cell counting; monocyte infiltration was therefore quantified by determining the CD14 positive area percentage of the tissue section.

Capillaries (paraffin embedded) were quantified in myocardial tissue slides using a polyclonal rabbit anti-von Willebrand Factor (A0082, Dako, Glostrup, Denmark). Incubation for 60 minutes was followed by Brightvision Poly-AP-anti-mouse (ImmunoLogic, Duiven, The Netherlands) for 30 minutes and development with liquid permanent red. Capillary density was quantified in five random border zone fields per pig. Vessels equal or smaller than 20 μm in diameter were counted. Collagen was stained in paraffin embedded sections using PicroSirius Red. Collagen fibers were visualized using polarized light. Collagen density is expressed as mean grey value.

IL-18 ELISA

Pig IL-18 Platinum ELISA (eBioscience, San Diego, CA, USA) according to manufacturer's protocol, corrected for total protein concentration.

IL-1β Western blotting

Myocardial protein samples were reduced 1:10 with NuPAGE Sample Reducing Agent (Thermo Scientific, Waltham, MA, USA) and boiled for 10 minutes at 70°C. 10 μg of protein was loaded on NuPAGE Bis-Tris Precast gels, and transferred to Polyvinylidene fluoride PVDF membrane with an iBlot Western blotting system (Thermo Scientific, Waltham, MA, USA), according the manufacturer's instructions. 5% BSA in PBS was used as blocking buffer and antibody diluent. Polyclonal rabbit IL-1β antibody was incubated at 1:1000 overnight at 4°C (NB600-633, Novus Biologicals, Littleton, CO, USA) followed by 1:160.000

secondary antibody incubation (Monoclonal Anti-Rabbit IgG A1949, Sigma-Aldrich Chemicals, Zwijndrecht, the Netherlands) for 1 hour at room temperature. Protein bands were visualized using Enhanced Chemiluminescence (ECL) detection (Sigma-Aldrich Chemicals, Zwijndrecht, the Netherlands).
After washing, Horseradish Peroxidase HRP-conjugated secondary antibody was used for enhanced chemiluminescence ECL detection (Sigma-Aldrich, USA).

Sample size calculation
The calculation of the number of animals was based on our primary outcome measures, in particular left ventricular ejection fraction. We aimed for an improvement in LVEF of 5.5% and estimated that the difference in standard deviation would be 3.5%. Together with an alpha of 0.05 and a power of 0.9, 9 animals were needed per group. Based on previous experience with this animal model in our department, we accounted for a mortality of 10%, leading to 10 animals per group and 30 animals in total.

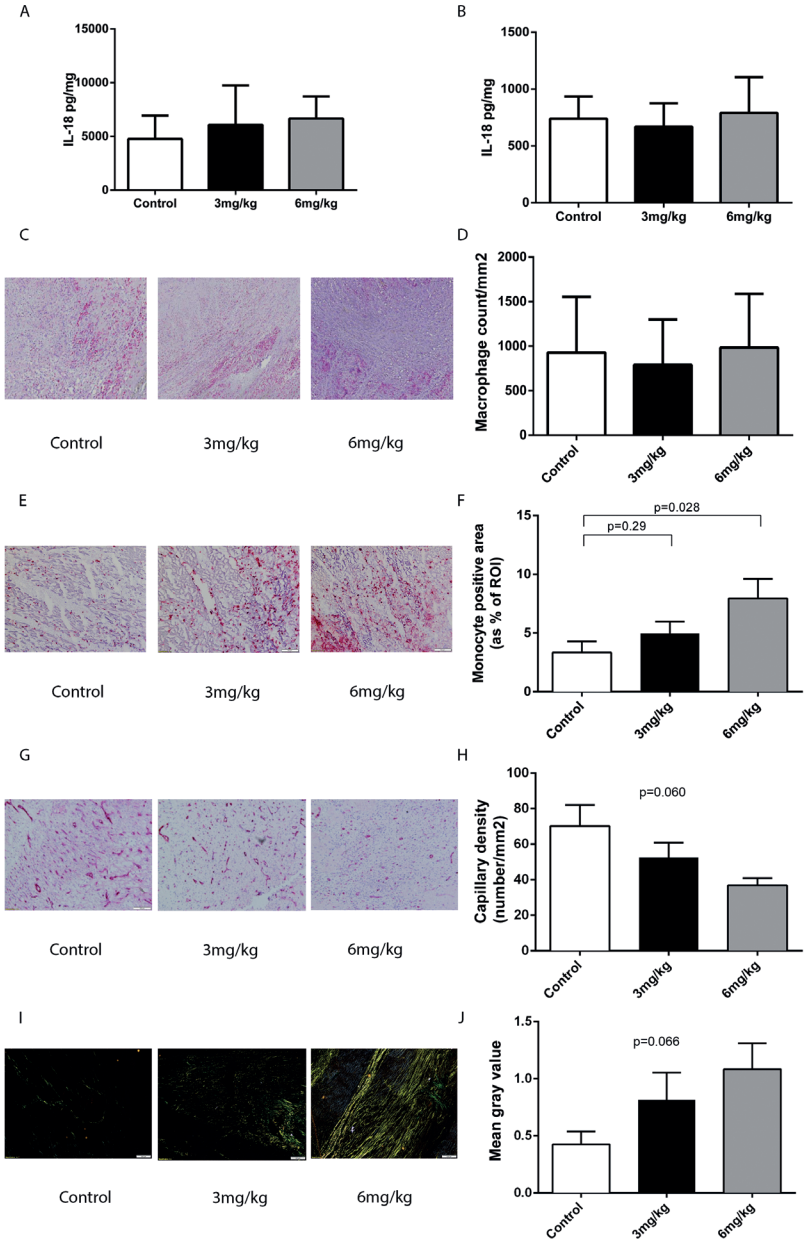

Supplementary Figure S1. Myocardial levels of IL-18, macrophages and monocytes
Myocardial IL-18 levels in the infarcted myocardium (**A**) and the border zone (**B**) of the myocardium are similar. **C.** Representative pictures of macrophage (CD107) staining in the infarcted pig myocardium. **D**. Quantification of macrophage infiltration. **E.** Representative pictures of CD14 monocyte staining in the infarcted pig myocardium. **F**. Quantification of monocyte infiltration. **G.** Representative pictures of capillary density. **H.** Quantification of capillary density. **I.** Representative pictures of collagen formation. **J.** Quantification of collagen expressed in mean gray value.

Supplementary Table 1. Hemodynamic parameters during ischemia and reperfusion among different treatment arms (mean ± SD)

Treatment group	0min		30min		60 min		90 min		120 min		150 min		180 min	
	HR (bpm)	MAP (mmHg)	HR (bpm)	MAP (mmHg)	HR (bpm)	MAP (mmHg)	HR (bpm)	MAP (mmHg)	HR (bpm)	MAP (mmHg)	HR (bpm)	MAP (mmHg)	HR (bpm)	MAP (mmHg)
Control	68±13	84±15	66±8	87±14	64±12	91±18	62±7	103±21	65±9	95±18	74±9	97±16	83±15	96±18
3 mg/kg	69±10	85±10	66±9	89±9	68±11	94±18	59±12	102±17	67±21	87±13	82±25	88±16	75±15	90±18
6 mg/kg	62±9	84±9	67±9	87±21	68±17	89±27	71±17	99±25	72±12	94±21	80±12	90±18	75±11	85±18

HR = heart rate, bpm = beats per minute. MAP = mean arterial blood pressure, mmHg = millimeters mercury

Supplementary Table 2. In vivo levels of MCC950 during the first 24 hours post-MI (mean ± SD).

	15m reperfusion *MCC950 (μM)*	4 hours reperfusion *MCC950 (μM)*	24 hours reperfusion *MCC950 (μM)*
6 mg/kg	101.3±14.6	18.3±6.8	0.24±0.13
3 mg/kg	54.7±6*	9.5±4.8*	0.21±0.29

* Significantly lower than MCC950 levels in 6 mg/kg group ($p<0.05$)

PART THREE
SUMMARY AND DISCUSSION

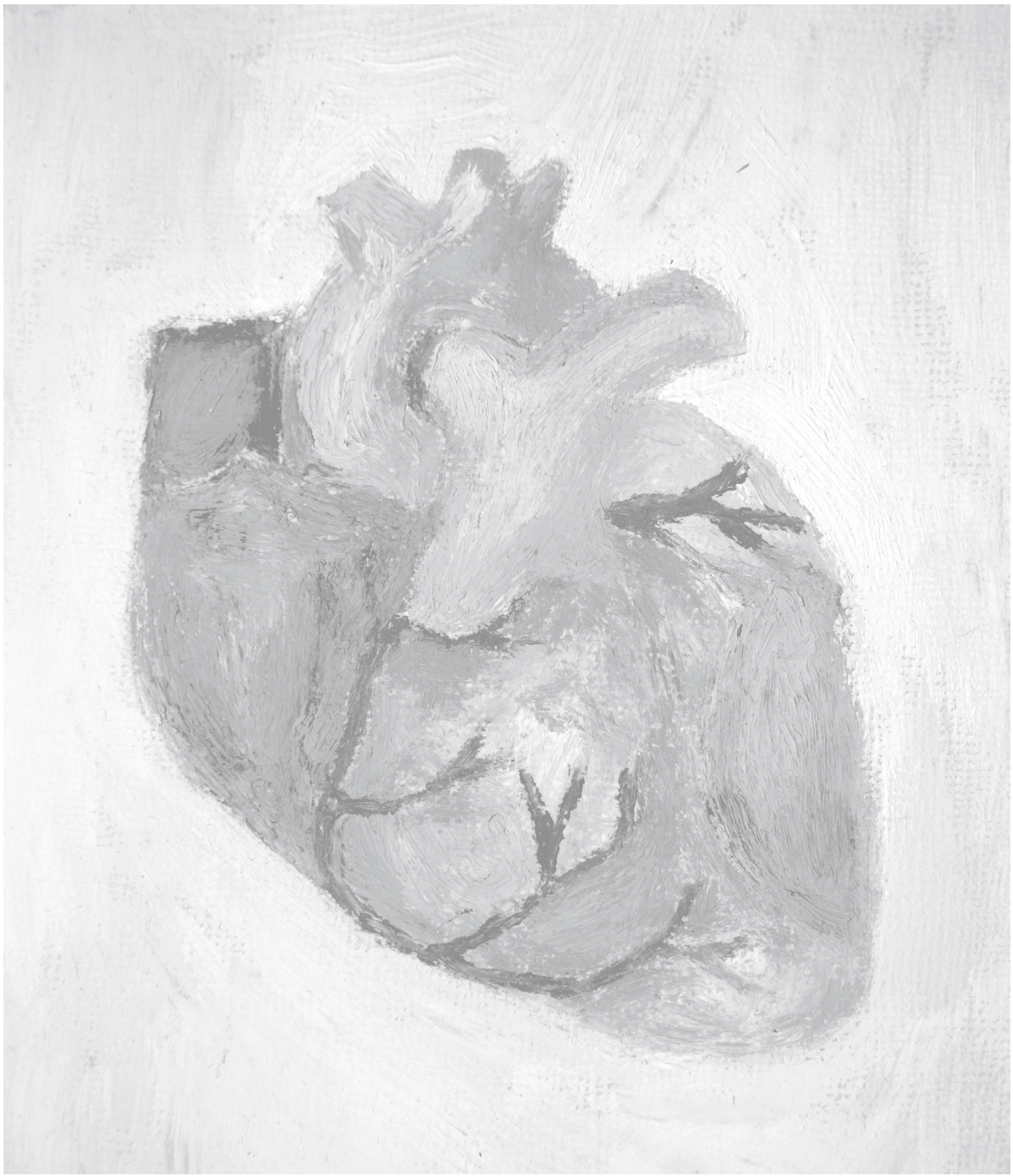

CHAPTER 9

Summary and general discussion

Despite improved prevention, diagnosis and treatment, ischemic heart disease (IHD) remains a leading cause of morbidity and mortality worldwide.[1,2] Two main contributors are atherosclerosis and subsequent myocardial infarction (MI) and inflammation has proven to be key in both.[3] Therefore, the aim of the current thesis was to decrease the burden of IHD by targeting inflammation in atherosclerosis and MI.

Targeting inflammation in atherosclerosis

Initially considered a lipid-laden disease, atherosclerosis has been shown to be greatly affected by inflammation as well.[4] Recruitment and activation of inflammatory cells to the atherosclerotic plaque is initiated at a very early stage and coincides with an increase in plaque burden and instability.[5] Unstable plaques are prone to rupture, amongst others causing acute MI, deteriorated cardiac function and a severely decreased life expectancy.[6] Although several treatments (*e.g.* statins) have been a great aid in plaque stabilization[7], the burden of atherosclerosis, atherosclerotic plaque rupture and their consequences is still eminent, emphasizing the need for novel therapies.

Hematopoietic Toll-like receptor 5 in atherosclerotic plaque formation

In **chapter 2**, we investigated the effect of hematopoietic Toll-like receptor (TLR) 5 deficiency on atherosclerotic plaque formation. Toll-like receptors are the best-known pattern recognition receptors (PRR) that are able to sense pathogen- or danger-associated molecular patterns (PAMPs/DAMPs). Binding of these to TLRs induces a pro-inflammatory response, which is considered to be key in the initiation and progression of atherosclerosis.[8] In agreement with previous research, we showed a decrease in atherosclerotic plaque formation in mice with TLR5 deficient leukocytes. This effect could mainly be attributed to reduced macrophage recruitment and defective T-cell responsiveness *in vitro* and *in vivo*. In line with these observations, treatment with flagellin (TLR5 ligand) increases atherosclerotic plaque formation in $ApoE^{-/-}$ mice.[9]

Both studies confirm the role of TLR5-mediated atherosclerotic plaque formation and are of interest in the mechanism of plaque formation. Further translation to clinical practice warrants investigation of the ability of anti-TLR5 treatment in already manifest atherosclerosis, leading to plaque stabilization or regression. In addition, co-treatment with medication used in standard clinical care will improve translatability.

Radiofrequency ablation in atherosclerosis

The atherosclerotic plaque shows increased vasa vasorum in the adventitia, important for blood and nutrient supply[10], but also for inflammatory cell deposition.[11] Immature and leaky vessels from the vasa vasorum penetrate the plaque and increase intraplaque haemorrhage, leading to plaque destabilization and rupture. Radiofrequency ablation (RFA)

has previously been used to target sympathetic nerves in the adventitia of renal arteries to reduce blood pressure.[12] Similarly, we hypothesized that RFA of the atherosclerotic plaque could safely decrease vasa vasorum and plaque neovessel density. Since RFA also induces fibrosis in the healthy vascular wall[12], additional plaque stabilization could have been of additional value.

Therefore, in **chapter 3**, we performed a proof-of-concept study in a rabbit model of atherosclerosis. We showed that RFA on the plaque is safe and does not lead to severe adverse events. RFA induces transitory decellularization and reduces intraplaque vascularization and contractile smooth muscle cell (SMCs) content, but does not affect plaque burden or other features of plaque stability. Since the current study was intended to evaluate safety and feasibility, it was not powered to detect small differences. Moreover, plaque stabilization could occur over a longer time period, in which case the current study is limited its study period. Nonetheless, RFA remains a safe option to target intraplaque vascularization and SMC proliferation (*e.g.* in restenosis). In this regard, RFA targeting the whole circumference of the vessel wall and/or in combination with balloon angioplasty could be an interesting approach.

Stent endothelialisation

Percutaneous coronary intervention (PCI) has become one of the most performed procedures in the direct treatment of atherosclerotic vessel disease. Although plain old balloon angioplasty (POBA) and bare metal stents (BMS) have improved morbidity and mortality rates, restenosis of the treated vessel remains a major challenge.[13] Drug-eluting stents (DES) with an antiproliferative coating inhibit SMC proliferation and improve restenosis rates, but their aspecific effect also hampers stent endothelialisation, increasing the risk for stent thrombosis.[14] To allow for accelerated endothelialisation, the COMBO stent combines abluminal antiproliferative coating with luminal anti-CD34 coating. Anti-CD34 coating captures endothelial progenitor cells (EPCs) that are able to proliferate and differentiate into endothelial cells to cover the stent surface and to prevent subsequent stent thrombosis. Indeed, in **chapter 4** we showed that, compared to the contemporary everolimus-eluting stent (EES), the COMBO stent improves endothelialisation after 28 days in a rabbit model of restenosis. The current findings are in line with previous preclinical findings on anti-CD34 capturing[15,16] and enhance the evidence for use of this technique to accelerate and improve stent endothelialisation. Despite excellent results in patients with respect to safety and clinical outcomes after 1 year[17], COMBO stents were comparable to EES with respect to stent strut coverage assessed by OCT in the REMEDEE-OCT Study.[18] These findings therefore challenge the efficacy of anti-CD34 in enhancing stent endothelialisation in patients.

Targeting inflammation in myocardial infarction

Atherosclerosis is the most prevalent cause for MI. [2]As early mortality after MI has declined significantly due to increased awareness and improved treatment, emphasis has shifted towards its chronic sequelae; the most prominent being HF. One out of four people develops HF after an MI, and HF affects an estimated 150,000 people in the Netherlands.[27] Although evidence-based medical treatment has been introduced over the last decades, prognosis in HF remains poor with approximately 25% patients deceased within the first year after development of clinical symptoms.[2]

Adverse left ventricular (LV) remodelling causes the development of HF after MI and is dependent on infarct size and the quality of cardiac repair.[28,29] Timely intervention and reperfusion of ischemic myocardium salvages reversibly injured cardiomyocytes and limits infarct size. Paradoxically, reperfusion also leads to increased infarct size through reactive oxygen species (ROS) generation and inflammation.[30] In addition, inflammation has been shown to play an important role in the process of adverse cardiac remodelling through removal of dead tissue and maturation towards the formation of the fibrotic scar.[31]

Leukocyte-associated immunoglobulin-like receptor 1 (LAIR-1) in acute myocardial infarction

In myocardial ischemia-reperfusion injury (IRI) and subsequent adverse remodelling, leukocyte activation is key and regulated by integration of signals from activating and inhibitory cell-receptors.[32] Dampening of the inflammatory response by inhibiting activating leukocyte receptors[33–35] and costimulatory molecules[36] has been shown beneficial in IRI and remodelling, whereas studies on inhibitory receptors or co-inhibitory molecules are lacking. Therefore, in **chapter 5**, we investigated the effect of the inhibitory leukocyte-associated immunoglobulin-like receptor 1 (LAIR-1). Although LAIR-1 expression levels on inflammatory cells are regulated upon MI, we were not able to establish a causal role for LAIR-1 deficiency in the reduction of infarct size and adverse remodelling in a mouse model of acute MI. The contrast between the effect of activating and inhibiting leukocyte receptors may show that the latter may not provide sufficient potency for the extent of tissue damage and severity of the inflammatory response in the present model. In addition, since inhibition by LAIR-1 is established through interaction with collagen, its main ligand, its encounter in the heart may be too late to effectively slow down the already initiated inflammatory response. Therefore, it would be of great interest to investigate the effect of an agonizing LAIR-1 antibody in the setting of MI. Moreover, since leukocyte LAIR-1 expression levels are upregulated upon MI in patients, their relationship with remodelling would be of additional value in understanding the role of LAIR-1.

Primary outcome measurements in a pig model of acute myocardial infarction

Since pigs greatly resemble human myocardial anatomy and physiology, they are key in

safety and efficacy testing of new treatments in MI. To allow for improved translatability, reliable and inexpensive methods to accurately measure clinically important read-outs are key. In **chapter 6**, we provide a detailed protocol for the assessment of infarct size and area at risk staining (IS/AAR), 3-dimensional transesophageal echocardiography (3D-TEE) and pressure-volume (PV) loop acquisition. IS/AAR staining with 2,3,5,-triphenyltetrazolium chloride (TTC) and Evans blue in the current method allows for accurate acquisition, since balloon positioning – and thereby AAR staining – can be performed at the exact same location as during the index operation. It also bypasses the need for myocardial wall puncture and the possible injection of dye into cardiac muscle. Although TTC/Evans blue staining has proven useful[37–39], this technique still requires an invasive approach and necessitates a terminal experiment. Non-invasive techniques (*e.g.* MRI) could be used for the acquisition of IS/AAR at short-term follow-up, while at the same time allowing for long-term assessment of cardiac remodelling. So far however, various MRI modalities to detect IS and AAR remain a topic of debate.[40,41]

With respect to remodelling, the acquisition of myocardial 3D echocardiography images through a transesophageal approach alleviates the need for sternotomy, which has been shown to exert cardioprotection when performed prior to myocardial infarction.[42] Also, it may be clinically less reliable due to changed intrathoracic pressures. To further encourage the use of 3D-TEE for the reliable and accurate assessment of myocardial dimensions and function in pigs, it would be of great interest to compare it to gold standard MRI.

Myeloperoxidase inhibition in ischemia-reperfusion injury

Neutrophils have been shown to be the first to enter the myocardium after reperfusion and are generally considered to be attributing to myocardial IRI.[30,43] Amongst others, they secrete the effector protein myeloperoxidase (MPO), which converts hydrogen peroxide (H_2O_2) to the highly reactive oxygen species (ROS) hypochlorous acid (HOCl).[44] In patients, MPO levels are increased in the infarct area[45] and MPO plasma levels predict adverse outcome in patients with MI.[46] In **chapter 7**, we investigated the effect of MPO inhibition in a highly translational pig model of acute MI. Although we were able to inhibit MPO *in vitro* and achieved good exposure *in vivo*, we did not observe an effect on neutrophil influx or infarct size. This is in line with previous experiments, showing comparable infarct size in wild-type and MPO knockout mice.[47] Together, these studies connect to other inconclusive therapeutic approaches targeting oxidative stress.[48–50] As oxidative stress has been shown to be key in IRI[51], these studies challenge our understanding of the role of ROS in IRI. Inhibition of one enzyme (system) may have been clinically irrelevant and/or compensated for by another system. Also, separate NADPH oxidase (Nox) 2 or 4 knockout reduced ROS formation and infarct size, whereas Nox2/Nox4 double knock-out increased infarct size despite lower ROS formation.[52] The latter emphasizes the beneficial effect of low ROS concentration, which renders optimal therapeutic dosing key in targeting ROS in IRI.

The effect of NLRP3 inflammasome inhibition after acute myocardial infarction in pigs

The NLRP3 inflammasome is an intracellular protein complex that is formed and activated upon cardiac injury, enabling conversion of inactive IL1β and IL18 into their active state.[53] Both, the NLRP3 inflammasome and these pro-inflammatory cytokines induce an extensive inflammatory reaction, which has been shown to be detrimental in mouse models of acute MI.[54–57] To allow for clinical translation, testing of an inhibitor of the NLRP3 inflammasome in a large animal model of acute MI is mandatory. Therefore, we investigated the effect of the small molecule inhibitor MCC950 in a pig model of acute MI in **chapter 8**. We showed that a clinically feasible dosing regimen of NLRP3 inflammasome inhibition dose-dependently decreases infarct size and preserves cardiac function. In addition, markers of inflammation and cardiac damage were lower in treated animals, emphasizing the anti-inflammatory effect of NLRP3 inflammasome inhibition.

As adverse remodelling occurs over weeks to months[58], it would be of additional interest to evaluate the effect of MCC950 in a long-term follow-up study. In addition, considering the association between IL1β levels 2 months after STEMI and adverse remodelling 1 year after the index event[59], delayed treatment with MCC950 could provide information on the treatment effect in already manifest HF. In conclusion, since the current study included a clinically relevant large animal model for MI, NLRP3 inflammasome inhibition by MCC950 suggests a promising therapeutic option.

FUTURE PERSPECTIVES

The first descriptions of inflammatory cell influx in atherosclerotic plaques and infarcted myocardium date back to the second half of the 19th century[4] and the first half of the 20th century[60], respectively. Eventually, it took until the last quarter of the 20th century before substantial investigation of the mechanisms and treatments involving the immune system in cardiovascular disease began to emerge. In the last three decades, we gained important insights in the inflammatory response in this field.[4,30,61–63] Nevertheless, the high complexity of this process in both atherosclerosis and MI remains a major challenge for successful implementation in diagnostic, prognostic and therapeutic applications. The current thesis aimed to contribute to this knowledge and to decrease the burden of ischemic heart disease (IHD) by targeting inflammation in atherosclerosis and myocardial infarction (MI). The first part concerned the improvement of our understanding of the formation and treatment of atherosclerosis. The second part evaluated potential inflammatory targets in myocardial ischemia-reperfusion injury (IRI).

Challenges in the translation of novel therapies to standard clinical care

Over the last decades, the translation of novel findings into potential atherosclerosis and MI therapies has been challenging. Although many therapies provided promising results in animal models, few therapies have been successfully introduced in the clinical setting. In the field of atherosclerosis, several anti-inflammatory treatments in humans were not beneficial or even increased the risk for cardiovascular disease.[62] Similarly, attenuation of the inflammatory response in MI showed no additional benefit or even adversely affected clinical outcome.[64,65] The observation that inflammation has both beneficial and detrimental effects has often been referred to as a double-edged sword.[61,66,67] As an example, the identification of the reparative monocyte subset shows that this cell type could be beneficial in wound healing after MI.[68] Similarly, neutrophils are not unanimously considered detrimental in myocardial IRI.[43,69] The identification of distinct neutrophil subsets with distinct properties[70,71] provides us with a better understanding of which subsets could exert more detrimental or more beneficial effects. Considering the complexity of the inflammatory response, an insufficient understanding of the inflammatory components and their mutual effects might be one of the explanations for the inconclusive results and subsequent translational failure of inflammation-based therapies in cardiovascular diseases.

In addition, many other factors are thought to contribute to our inability to translate novel therapies targeting inflammation from bench to bedside. Amongst these are suboptimal preclinical study design[72,73], insufficient target validation[74], lacking knowledge on the biology of animal models and their similarity to humans, irrelevant surrogate markers for disease and insufficiently powered studies.

To increase the success rate when moving from preclinical studies to clinical testing, optimization of translation is key. Considering the effect of standard clinical therapy on plaque stabilization[62,75] and myocardial repair[76], introduction thereof would only allow further investigation of therapies with additional value. Since the prevalence of risk factors is increasing[2], the same holds true for the introduction of comorbidities. Of particular interest is the relationship between atherosclerosis and MI. Although also in the current thesis these diseases were artificially separated, both change the body's inflammatory status[77] and may be mutually able to influence disease status.[78]

Similarly, increasing translational value of therapies in preclinical animal models of atherosclerosis and MI requires a clinically feasible approach. Indeed, during the last decade, several initiatives have acknowledged these requirements. In the field of cardioprotection, the CAESAR consortium aims to apply the same rigor used in clinical studies to preclinical studies, by performing clinically feasible, blinded, randomized and adequately powered studies.[79] In addition, dose-response analyses with independent data and statistical analysis cores are used to safeguard data quality. These initiatives are perfectly in line with previous research showing that study quality is significantly associated with outcome.[73]

Apart from methodological quality, translational value could improve by an increased understanding of the biological processes involved. Of course, in hindsight, newly available information makes it relatively easy to explain historical results. However, some pitfalls may be avoided by taking a predetermined route.[74,80–82] In this regard, patient studies should be used as a starting point to provide evidence for an association between the target and disease outcome. Additional *in vitro* studies of this specific pathway in humans enhances its biological understanding. Validation thereof in the particular animal model provides an increased understanding of the similarities and differences with humans. In this regard, novel imaging techniques (*e.g.* fluorescent reporters) may prove very helpful to localize and quantify a specific target and to measure the effects of the treatments on the target.[77] Since most established pathways would be targeted by drug administration, optimal *in vitro* and *in vivo* tests are warranted to provide extensive information on pharmacokinetics and pharmacodynamics. In particular, drug selectivity and effectiveness in both species, tissue penetration and exposure are of major concern. To improve selectivity and effectiveness and to avoid side effects, targeted delivery of drugs could be of great additional value.[83]

Old solutions for an old problem: looking forward and backward at the same time

Novel therapies, both medication (*e.g.* statins) and mechanical approaches (*e.g.* PCI) have proven to be beneficial in the treatment of cardiovascular disease (CVD). Numerous patients have benefitted from these treatments and we have been able to increasingly target ischemic heart disease (IHD). Still, IHD remains one of the most important contributors to morbidity and mortality worldwide and imposes a great burden on economy and society.[84] One of the most important contributors is the increasing and unacceptably high prevalence of risk factors such as obesity, physical inactivity, diabetes and smoking.[2] The majority of these have the ability to induce a systemic pro-inflammatory state and targeting these through risk factor control has been proven to reduce the risk for CVD.[85] However, patients with established CVD are largely undertreated, undercontrolled and poorly adhere to treatment regimens.[86–88] Both to reduce the burden of cardiovascular disease and to evaluate novel therapies as a true addition to present therapeutic options, it should be considered of utmost importance to optimize current standard clinical care.

CONCLUSION

Inflammation in cardiovascular disease should be considered as a complex system and a delicate balance between pro- and anti-inflammatory influences. Of these, not all pro-inflammatory responses may be detrimental and conversely not all anti-inflammatory responses beneficial. In this regard, timing and dosage of novel treatments are key in

successful translation. In addition, since interindividual differences in inflammatory activity may limit global anti-inflammatory therapy, biomarker-based strategies could be helpful in identifying high-risk patients with an inadequate inflammatory response. Considering beneficial and detrimental effects of inflammation in cardiovascular disease, research should keep aiming for the golden mean.

REFERENCES

1. WHO. Causes of death, 2000-2012. 2012. Available at: http://www.who.int/mediacentre/factsheets/fs310/en/. Accessed April 11, 2015.
2. Mozaffarian D, Benjamin EJ, Go AS, Arnett DK, Blaha MJ, Das SR, Ferranti S De, Després J, Fullerton HJ, Howard J, Huffman MD, Isasi CR, Jiménez MC, Judd SE, Brett M, Lichtman JH, Lisabeth LD, Liu S, Mackey RH, Magid DJ, Mcguire DK, Mohler ER, Moy CS, Muntner P, Mussolino ME, Nasir K, Neumar RW, Nichol G, Palaniappan L, Pandey DK, Mathew J, Rodriguez CJ, Rosamond W, Sorlie PD, Stein J, Towfighi A, Turan N, Virani SS, Woo D, Yeh RW, Turner MB. Heart Disease and Stroke Statistics—2016 Update: A Report From the American Heart Association. *Circulation* 2016:1–668.
3. Ruparelia N, Chai JT, Fisher EA, Choudhury RP. Inflammatory processes in cardiovascular disease: a route to targeted therapies. *Nat Rev Cardiol* 2016;369:2437–2445.
4. Libby P. History of Discovery: Inflammation in Atherosclerosis. *Arter Thromb Vasc Biol* 2012;32:2045–2051.
5. Libby P, Ridker PM, Maseri A. Inflammation and atherosclerosis. *Circulation* 2002;105:1135–1143.
6. Shibata T, Kawakami S, Noguchi T, Tanaka T, Asaumi Y, Kanaya T, Nagai T, Nakao K, Fujino M, Nagatsuka K, Ishibashi-Ueda H, Nishimura K, Miyamoto Y, Kusano K, Anzai T, Goto Y, Ogawa H, Yasuda S. Prevalence, clinical features, and prognosis of acute myocardial infarction attributable to coronary artery embolism. *Circulation* 2015;132:241–250.
7. Ylä-Herttuala S, Bentzon JF, Daemen M, Falk E, Garcia-Garcia HM, Herrmann J, Hoefer I, Jauhiainen S, Jukema JW, Krams R, Kwak BR, Marx N, Naruszewicz M, Newby A, Pasterkamp G, Serruys PWJC, Waltenberger J, Weber C, Tokgözoglu L. Stabilization of atherosclerotic plaques: An update. *Eur Heart J* 2013;34:3251–3258.
8. Falck-hansen M, Kassiteridi C. Toll-Like Receptors in Atherosclerosis. *Int J Mol Sci* 2013;14:14008–14023.
9. Kim J, Seo M, Kim SK, Bae YS. Flagellin-induced NADPH oxidase 4 activation is involved in atherosclerosis. *Sci Rep* 2016:1–16.
10. Virmani R, Kolodgie FD, Burke AP, Finn A V., Gold HK, Tulenko TN, Wrenn SP, Narula J. Atherosclerotic plaque progression and vulnerability to rupture: Angiogenesis as a source of intraplaque hemorrhage. *Arterioscler Thromb Vasc Biol* 2005;25:2054–2061.
11. Moulton KS, Vakili K, Zurakowski D, Soliman M, Butterfield C, Sylvin E, Lo K-M, Gillies S, Javaherian K, Folkman J. Inhibition of plaque neovascularization reduces macrophage accumulation and progression of advanced atherosclerosis. *Proc Natl Acad Sci U S A* 2003;100:4736–41.
12. Steigerwald K, Titova A, Malle C, Kennerknecht E, Jilek C, Hausleiter J, Nährig JM, Laugwitz K-L, Joner M. Morphological assessment of renal arteries after radiofrequency catheter-based sympathetic denervation in a porcine model. *J Hypertens* 2012;30:2230–9.
13. Costa M a, Simon DI. Molecular basis of restenosis and drug-eluting stents. *Circulation* 2005;111:2257–73.
14. Lüscher TF, Steffel J, Eberli FR, Joner M, Nakazawa G, Tanner FC, Virmani R. Drug-eluting stent and coronary thrombosis: biological mechanisms and clinical implications. *Circulation* 2007;115:1051–8.
15. Nakazawa G, Granada JF, Alviar CL, Tellez A, Kaluza GL, Guilhermier MY, Parker S, Rowland SM, Kolodgie FD, Leon MB, Virmani R. Anti-CD34 Antibodies Immobilized on the Surface of Sirolimus-Eluting Stents Enhance Stent Endothelialization. *J Am Coll Cardiol* 2010;3:68–75.
16. Granada JF, Inami S, Aboodi MS, Tellez A, Milewski K, Wallace-Bradley D, Parker S, Rowland S, Nakazawa G, Vorpah M, Kolodgie FD, Kaluza GL, Leon MB, Virmani R. Development of a novel prohealing stent designed to deliver sirolimus from a biodegradable abluminal matrix. *Circ Cardiovasc Interv* 2010;3:257–266.
17. Woudstra P, Kalkman DN, Heijer P den, Menown IBA, Erglis A, Suryapranata H, Arkenbout KE, Iñiguez A, 't Hof AWJ van, Muller P, Tijssen JGP, Winter RJ de. 1-Year Results of the REMEDEE Registry. *JACC Cardiovasc Interv* 2016;9:1127–1134.
18. Jaguszewski M, Aloysius R, Wang W, Bezerra HG, Hill J, Winter RJ De, Karjalainen PP, Verheye S, Wijns W, Lüscher TF, Joner M, Costa M, Landmesser U. The REMEDEE-OCT Study. *JACC Cardiovasc Interv* 2017;10:489–499.
19. Tearney GJ, Regar E, Akasaka T, Adriaenssens T, Barlis P, Bezerra HG, Bouma B, Bruining N, Cho JM, Chowdhary S, Costa MA, Silva R De, Dijkstra J, Mario C Di, Dudeck D, Falk E, Feldman MD, Fitzgerald P, Garcia H, Gonzalo N, Granada JF, Guagliumi G, Holm NR, Honda Y, Ikeno F, Kawasaki M, Kochman J, Koltowski L, Kubo T, Kume T, Kyono H, Lam CCS, Lamouche G, Lee DP, Leon MB, Maehara A, Manfrini O, Mintz GS, Mizuno K, Morel MA, Nadkarni S, Okura H, Otake H, Pietrasik A, Prati F, Rber L, Radu MD, Rieber J, Riga M, Rollins A, et al. Consensus standards for acquisition, measurement, and reporting of intravascular optical coherence tomography studies: A report from the International Working Group for Intravascular Optical Coherence Tomography Standardization and Validation. *J Am Coll Cardiol* 2012;59:1058–1072.
20. Madjid M, Awan I, Willerson JT, Casscells SW. Leukocyte count and coronary heart disease: Implications for risk assessment. *J Am Coll Cardiol* 2004;44:1945–1956.
21. Lee CD, Folsom AR, Nieto FJ, Chambless LE, Shahar E, Wolfe DA. White blood cell count and incidence of coronary heart disease and ischemic stroke and mortality from cardiovascular disease in African-American and White men and women: atherosclerosis risk in communities study. *Am J Epidemiol* 2001;154:758–64.
22. Kato A, Takita T, Furuhashi M, Maruyama Y, Kumagai H, Hishida A. Blood monocyte count is a predictor of total and cardiovascular mortality in hemodialysis patients. *Nephron - Clin Pract* 2008;110:235–243.

23. Gillum RF, Mussolino ME, Madans JH. Counts of neutrophils, lymphocytes, and monocytes, cause-specific mortality and coronary heart disease: The NHANES-I epidemiologic follow-up study. *Ann Epidemiol* 2005;15:266–271.
24. Guasti L, Dentali F, Castiglioni L, Maroni L, Marino F, Squizzato A, Ageno W, Gianni M, Gaudio G, Grandi AM, Cosentino M, Venco A. Neutrophils and clinical outcomes in patients with acute coronary syndromes and/or cardiac revascularization: A systematic review on more than 34,000 subjects. *Thromb Haemost* 2011;106:591–599.
25. Wang X, Zhang G, Jiang X, Zhu H, Lu Z, Xu L. Neutrophil to lymphocyte ratio in relation to risk of all-cause mortality and cardiovascular events among patients undergoing angiography or cardiac revascularization: a meta-analysis of observational studies. *Atherosclerosis* 2014;234:206–13.
26. Ghattas A, Griffiths HR, Devitt A, Lip GYH, Shantsila E. Monocytes in coronary artery disease and atherosclerosis: where are we now? *J Am Coll Cardiol* 2013;62:1541–1551.
27. Dutch Heart Foundation. *Cijferboek Hart- en Vaatziekten in Nederland*.; 2015.
28. Konstam MA, Kramer DG, Patel AR, Maron MS, Udelson JE. Left ventricular remodeling in heart failure: Current concepts in clinical significance and assessment. *JACC Cardiovasc Imaging* 2011;4:98–108.
29. Chareonthaitawee P, Christian TF, Hirose K, Gibbons RJ, Rumberger JA. Relation of initial infarct size to extent of left ventricular remodeling in the year after acute myocardial infarction. *J Am Coll Cardiol* 1995;25:567–73.
30. Frangogiannis NG. The inflammatory response in myocardial injury, repair, and remodelling. *Nat Rev Cardiol* 2014;11:255–265.
31. Westman PC, Lipinski MJ, Luger D, Waksman R, Bonow RO, Wu E, Epstein SE. Inflammation as a Driver of Adverse Left Ventricular Remodeling After Acute Myocardial Infarction. *J Am Coll Cardiol* 2016;67:2050–2060.
32. Billadeau DD, Leibson PJ. ITAMs versus ITIMs: Striking a balance during cell regulation. *J Clin Invest* 2002;109:161–168.
33. Oyama JI, Blais C, Liu X, Pu M, Kobzik L, Kelly RA, Bourcier T. Reduced Myocardial Ischemia-Reperfusion Injury in Toll-Like Receptor 4-Deficient Mice. *Circulation* 2004;109:784–789.
34. Yang Z, Day YJ, Toufektsian MC, Ramos SI, Marshall M, Wang XQ, French BA, Linden J. Infarct-sparing effect of A2A-adenosine receptor activation is due primarily to its action on lymphocytes. *Circulation* 2005;111:2190–2197.
35. Arslan F, Smeets MB, O'Neill LAJ, Keogh B, McGuirk P, Timmers L, Tersteeg C, Hoefer IE, Doevendans PA, Pasterkamp G, Kleijn DP V De. Myocardial ischemia/reperfusion injury is mediated by leukocytic toll-like receptor-2 and reduced by systemic administration of a novel anti-toll-like receptor-2 antibody. *Circulation* 2010;121:80–90.
36. Kubota A, Hasegawa H, Tadokoro H, Hirose M, Kobara Y, Yamada-Inagawa T, Takemura G, Kobayashi Y, Takano H. Deletion of CD28 Co-stimulatory Signals Exacerbates Left Ventricular Remodeling and Increases Cardiac Rupture After Myocardial Infarction. *Circ J* 2016;80:9171–1979.
37. Suzuki Y, Lyons JK, Yeung AC, Ikeno F. In vivo porcine model of reperfused myocardial infarction: In situ double staining to measure precise infarct area/area at risk. *Catheter Cardiovasc Interv* 2008;71:100–7.
38. Fishbein M, Meerbaum S, Rit J, Lando U, Kanmatsuse K, Mercier J, Corday E, Ganz W. Early phase acute myocardial infarct size quantification: validation of the triphenyl tetrazolium chloride tissue enzyme staining technique. *Am Hear J* 1981;101:593–600.
39. Timmers L, Henriques JPS, Kleijn DP V de, Devries JH, Kemperman H, Steendijk P, Verlaan CWJ, Kerver M, Piek JJ, Doevendans PA, Pasterkamp G, Hoefer IE. Exenatide reduces infarct size and improves cardiac function in a porcine model of ischemia and reperfusion injury. *J Am Coll Cardiol* 2009;53:501–10.
40. Jablonowski R, Engblom H, Kanski M, Nordlund D, Koul S, Pals J Van Der, Englund E, Heiberg E, Erlinge D, Carlsson M, Arheden H. Contrast-Enhanced CMR Overestimates Early Myocardial Infarct Size: Mechanistic Insights Using ECV Measurements on Day 1 and Day 7. *JACC Cardiovasc Imaging* 2015;8:1379–1389.
41. Kim HW, Assche L Van, Jennings RB, Wince WB, Jensen CJ, Rehwald WG, Wendell DC, Bhatti L, Spatz DM, Parker MA, Jenista ER, Klem I, Crowley ALC, Chen EL, Judd RM, Kim RJ. Relationship of T2-Weighted MRI Myocardial Hyperintensity and the Ischemic Area-At-Risk. *Circ Res* 2015;117:254–265.
42. Hout GPJ van, Teuben MPJ, Heeres M, Maat S de, Jong R de, Maas C, Kouwenberg LHJA, Koenderman L, Solinge WW van, Jager SCA de, Pasterkamp G, Hoefer IE. Invasive surgery reduces infarct size and preserves cardiac function in a porcine model of myocardial infarction. *J Cell Mol Med* 2015;19:2655–2663.
43. Baxter GF. The neutrophil as a mediator of myocardial ischemia-reperfusion injury: Time to move on. *Basic Res Cardiol* 2002;97:268–275.
44. Klebanoff SJ. Myeloperoxidase: friend and foe. *J Leukoc Biol* 2005;77:598–625.
45. Heymans S, Luttun a, Nuyens D, Theilmeier G, Creemers E, Moons L, Dyspersin GD, Cleutjens JP, Shipley M, Angellilo a, Levi M, Nübe O, Baker a, Keshet E, Lupu F, Herbert JM, Smits JF, Shapiro SD, Baes M, Borgers M, Collen D, Daemen MJ, Carmeliet P. Inhibition of plasminogen activators or matrix metalloproteinases prevents cardiac rupture but impairs therapeutic angiogenesis and causes cardiac failure. *Nat Med* 1999;5:1135–1142.
46. Mocatta TJ, Pilbrow AP, Cameron VA, Senthilmohan R, Frampton CM, Richards AM, Winterbourn CC. Plasma Concentrations of Myeloperoxidase Predict Mortality After Myocardial Infarction. *J Am Coll Cardiol* 2007;49:1993–2000.
47. Vasilyev N, Williams T, Brennan ML, Unzek S, Zhou X, Heinecke JW, Spitz DR, Topol EJ, Hazen SL, Pen MS. Myeloperoxidase-generated oxidants modulate left ventricular remodeling but not infarct size after

myocardial infarction. *Circulation* 2005;112:2812–2820.
48. Forman MB, Puett DW, Cates CU, McCroskey DE, Beckman JK, Greene HL, Virmani R. Glutathione redox pathway and reperfusion injury. Effect of N-acetylcysteine on infarct size and ventricular function. *Circulation* 1988;78:202–213.
49. Yoshida T, Watanabe M, Engelman DT, Engelman RM, Schley J a, Maulik N, Ho YS, Oberley TD, Das DK. Transgenic mice overexpressing glutathione peroxidase are resistant to myocardial ischemia reperfusion injury. *J Mol Cell Cardiol* 1996;28:1759–1767.
50. Pacher P, Nivorozhkin A, Szabó C. Therapeutic effects of xanthine oxidase inhibitors: renaissance half a century after the discovery of allopurinol. *Pharmacol Rev* 2006;58:87–114.
51. Granger DN, Kvietys PR. Reperfusion injury and reactive oxygen species: The evolution of a concept. *Redox Biol* 2015;6:524–551.
52. Matsushima S, Kuroda J, Ago T, Zhai P, Ikeda Y, Oka S, Fong GH, Tian R, Sadoshima J. Broad suppression of NADPH oxidase activity exacerbates ischemia/reperfusion injury through inadvertent downregulation of hypoxia-inducible factor-1 alpha and upregulation of peroxisome proliferator-activated receptor-alpha. *Circ Res* 2013;112:1135–1149.
53. Latz E, Xiao TS, Stutz A. Activation and regulation of the inflammasomes. *Nat Rev Immunol* 2013;13:397–411.
54. Kawaguchi M, Takahashi M, Hata T, Kashima Y, Usui F, Morimoto H, Izawa A, Takahashi Y, Masumoto J, Koyama J, Hongo M, Noda T, Nakayama J, Sagara J, Taniguchi S, Ikeda U. Inflammasome activation of cardiac fibroblasts is essential for myocardial ischemia/reperfusion injury. *Circulation* 2011;123:594–604.
55. Mezzaroma E, Toldo S, Farkas D, Seropian IM, Tassell BW Van, Salloum FN, Kannan HR, Menna AC, Voelkel NF, Abbate A. The inflammasome promotes adverse cardiac remodeling following acute myocardial infarction in the mouse. *Proc Natl Acad Sci U S A* 2011;108:19725–19730.
56. Zuurbier CJ, Jong WMC, Eerbeek O, Koeman A, Pulskens WP, Butter LM, Leemans JC, Hollmann MW. Deletion of the innate immune NLRP3 receptor abolishes cardiac ischemic preconditioning and is associated with decreased IL-6/STAT3 signaling. *PLoS One* 2012;7:1–8.
57. Sandanger O, Ranheim T, Vinge LE, Bliksoen M, Alfsnes K, Finsen A V., Dahl CP, Askevold ET, Florholmen G, Christensen G, Fitzgerald KA, Lien E, Valen G, Espevik T, Aukrust P, Yndestad A. The NLRP3 inflammasome is up-regulated in cardiac fibroblasts and mediates myocardial ischaemia-reperfusion injury. *Cardiovasc Res* 2013;99:164–174.
58. Jong R de, Hout GPJ van, Houtgraaf JH, Takashima S, Pasterkamp G, Hoefer I, Duckers HJ. Cardiac Function in a Long-Term Follow-Up Study of Moderate and Severe Porcine Model of Chronic Myocardial Infarction. *Biomed Res Int* 2015;2015:1–11.
59. Ørn S, Ueland T, Manhenke C, Sandanger, Godang K, Yndestad A, Mollnes TE, Dickstein K, Aukrust P. Increased interleukin-1β levels are associated with left ventricular hypertrophy and remodelling following acute ST segment elevation myocardial infarction treated by primary percutaneous coronary intervention. *J Intern Med* 2012;272:267–276.
60. Mallory GK, White PD, Salcedo-Salgar J. The speed of healing of myocardial infarction. A study of the pathologic anatomy in seventy-two cases. *Am Heart J* 1939;18:647–671.
61. Hansson GK, Libby P. The immune response in atherosclerosis : a double-edged sword. *Nat Rev Immunol* 2006;6:508–519.
62. Bäck M, Hansson GK. Anti-inflammatory therapies for atherosclerosis. *Nat Rev Cardiol* 2015;12:199–211.
63. Arslan F, Kleijn DP de, Pasterkamp G. Innate immune signaling in cardiac ischemia. *Nat Rev Cardiol* 2011;8:292–300.
64. Dewenter M, Wagner M, El-Armouche A. LATITUDE-TIMI: is there still hope for anti-inflammatory therapy in acute myocardial infaction? *J Thorac Dis* 2016;8:E1047–E1049.
65. Saxena A, Russo I, Frangogiannis NG. Inflammation as a therapeutic target in myocardial infarction: learning from past failures to meet future challenges. *Transl Res* 2017;167:152–166.
66. Braunwald E, Kloner RA. Myocardial reperfusion: A double-edged sword? *J Clin Invest* 1985;76:1713–1719.
67. Liu J, Wang H, Li J. Inflammation and inflammatory cells in myocardial infarction and reperfusion injury: A double-edged sword. *Clin Med Insights Cardiol* 2016;10:79–84.
68. Dutta P, Nahrendorf M. Monocytes in myocardial infarction. *Arterioscler Thromb Vasc Biol* 2015;35:1066–1070.
69. Schofield ZV, Woodruff TM, Halai R, Wu MC-L, Cooper MA. Neutrophils--a key component of ischemia-reperfusion injury. *Shock* 2013;40:463–70.
70. Pillay J, Kamp VM, Hoffen E Van, Visser T, Tak T, Lammers J, Ulfman LH, Leenen LP, Pickkers P, Koenderman L. A subset of neutrophils in human systemic inflammation inhibits T cell responses through Mac-1. *J Clin Invest* 2012;122:327–336.
71. Hout GPJ van, Solinge WW van, Gijsberts CM, Teuben MPJ, Leliefeld PHC, Heeres M, Nijhoff F, Jong S de, Bosch L, Jager SCA de, Huisman A, Stella PR, Pasterkamp G, Koenderman LJ, Hoefer IE. Elevated mean neutrophil volume represents altered neutrophil composition and reflects damage after myocardial infarction. *Basic Res Cardiol* 2015;110:1–11.
72. Macleod MR, Lawson McLean A, Kyriakopoulou A, Serghiou S, Wilde A de, Sherratt N, Hirst T, Hemblade R, Bahor Z, Nunes-Fonseca C, Potluru A, Thomson A, Baginskitae J, Egan K, Vesterinen H, Currie GL, Churilov L, Howells DW, Sena ES. Risk of Bias in Reports of In Vivo Research: A Focus for Improvement. *PLoS Biol* 2015;13:1–12.
73. Hout GPJ Van, Jansen Of Lorkeers SJ, Wever KE, Sena ES, Kouwenberg LHJA, Solinge WW Van, Macleod MR, Doevendans PA, Pasterkamp G, Chamuleau SAJ, Hoefer IE. Translational failure of anti-inflammatory compounds for myocardial infarction: A meta-Analysis of large animal models. *Cardiovasc Res* 2016;109:240–248.

74. Denayer T, Stöhrn T, Roy M Van. Animal models in translational medicine: Validation and prediction. *New Horizons Transl Med* 2014;2:5–11.
75. Yla-Herttuala S, Bentzon JF, Daemen M, Falk E, Garcia-Garcia HM, Herrmann J, Hoefer I, Wouter Jukema J, Krams R, Kwak BR, Marx N, Naruszewicz M, Newby A, Pasterkamp G, Serruys PWJC, Waltenberger J, Weber C, Tokgözoglu L. Stabilisation of atherosclerotic plaques position paper of the european society of cardiology (ESC) working group on atherosclerosis and vascular biology. *Thromb Haemost* 2011;106:1–19.
76. Sutton SJ, Sharpe N. Left Ventricular Remodeling After Myocardial Infarction Pathophysiology and Therapy. *Circulation* 2000;101:2981–2988.
77. Nahrendorf M, Frantz S, Swirski FK, Mulder WJM, Randolph G, Ertl G, Ntziachristos V, Piek JJ, Stroes ES, Schwaiger M, Mann DL, Fayad ZA. Imaging systemic inflammatory networks in ischemic heart disease. *J Am Coll Cardiol* 2015;65:1583–1591.
78. Dutta P, Courties G, Wei Y, Leuschner F, Gorbatov R, Robbins CS, Iwamoto Y, Thompson B, Carlson AL, Heidt T, Majmudar MD, Lasitschka F, Etzrodt M, Waterman P, Waring MT, Chicoine AT, Laan AM van der, Niessen HWM, Piek JJ, Rubin BB, Butany J, Stone JR, Katus HA, Murphy SA, Morrow DA, Sabatine MS, Vinegoni C, Moskowitz MA, Pittet MJ, Libby P, Lin CP, Swirski FK, Weissleder R, Nahrendorf M. Myocardial infarction accelerates atherosclerosis. *Nature* 2012;487:325–9.
79. Jones SP, Tang XL, Guo Y, Steenbergen C, Lefer DJ, Kukreja RC, Kong M, Li Q, Bhushan S, Zhu X, Du J, Nong Y, Stowers HL, Kondo K, Hunt GN, Goodchild TT, Orr A, Chang CC, Ockaili R, Salloum FN, Bolli R. The NHLBI-Sponsored Consortium for preclinicAl assESsment of cARdioprotective Therapies (CAESAR): A new paradigm for rigorous, accurate, and reproducible evaluation of putative infarct-sparing interventions in mice, rabbits, and pigs. *Circ Res* 2015;116:572–586.
80. Marti CN, Gheorghiade M, Kalogeropoulos AP, Georgiopoulou V V., Quyyumi AA, Butler J. Endothelial dysfunction, arterial stiffness, and heart failure. *J Am Coll Cardiol* 2012;60:1455–1469.
81. Cook D, Brown D, Alexander R, March R, Morgan P, Satterthwaite G, Pangalos MN. Lessons learned from the fate of AstraZeneca's drug pipeline: a five-dimensional framework. *Nat Rev drug Discov* 2014;13:419–31.
82. Heusch G. Critical Issues for the Translation of Cardioprotection. *Circ Res* 2017;120:1477–1486.
83. Scott RC, Crabbe D, Krynska B, Ansari R, Kiani MF. Aiming for the heart: targeted delivery of drugs to diseased cardiac tissue. *Expert Opin Drug Deliv* 2008;5:459–70.
84. GBD 2013 Mortality and Causes of Death Collaborators*. Global, regional, and national age – sex specific all-cause and cause-specific mortality for 240 causes of death, 1990 – 2013: a systematic analysis for the Global Burden of Disease Study 2013. *Lancet* 2014;385:117–171.
85. Dong C, Rundek T, Wright CB, Anwar Z, Elkind MS V, Sacco RL. Ideal cardiovascular health predicts lower risks of myocardial infarction, stroke, and vascular death across whites, blacks, and hispanics: The Northern Manhattan study. *Circulation* 2012;125:2975–2984.
86. Benner J, Glynn R, Mogun H, Neumann P, Weinstein M, Avorn J. Long-term persistence in use of statin therapy in elderly patients. *JAMA* 2002;288:455–461.
87. Bhatt DL, Steg PG, Ohman EM, Hirsch AT, Ikeda Y, Mas J-L, Goto S, Liau C-S, Richard AJ, Röther J, Wilson PWF. International Prevalence, Recognition and Treatment of Cardiovascular Risk Factors in Outpatients With Atherothrombosis. *JAMA* 2006;295.
88. Naderi SH, Bestwick JP, Wald DS. Adherence to drugs that prevent cardiovascular disease: Meta-analysis on 376,162 patients. *Am J Med* 2012;125:882–887.

CHAPTER 10

Dutch summary

Ondanks verbeterde preventie, diagnose en behandeling blijven hartziekten door zuurstofgebrek een belangrijke oorzaak van ziekte en sterfte wereldwijd.[1,2] Twee belangrijke bijdragende factoren hierin zijn atherosclerose (slagaderverkalking) en hartinfarcten. In beide processen speelt inflammatie (ontsteking) een essentiële rol[3] en het onderzoek in het huidige proefschrift is verricht met het doel om de ziektelast hiervan te verminderen door aan te grijpen op de ontstekingsreactie die in atherosclerose en hartinfarcten ontstaat.

Beïnvloeding van de ontstekingsreactie bij slagaderverkalking

Initieel werd vooral de vetstofwisseling verantwoordelijk geacht voor het ontstaan en de progressie van atherosclerose, maar de afgelopen decennia is duidelijk geworden dat ook inflammatie een belangrijke rol speelt.[4] De rekrutering en activatie van ontstekingscellen naar en in de verkalkte atherosclerotische plaque begint al heel vroeg in het ziekteproces en gaat samen met een toename van grootte en instabiliteit.[5] Instabiele plaques brengen het risico op plaqueruptuur (scheuren) met zich mee, wat een hartinfarct, een afgenomen hartpompfunctie en een verminderde levensverwachting kan veroorzaken.[6] Ondanks verschillende plaque-stabiliserende therapieën (*e.g.* statines) blijft de ziektelast van atherosclerose, plaqueruptuur en hartinfarcten onacceptabel hoog en de behoefte aan nieuwe therapieën onverminderd groot.

Toll-achtige receptor 5 op circulerende cellen in het bloed en het ontstaan van atherosclerotische plaques

In **hoofdstuk 2** hebben we het effect onderzocht van het wel of niet aanwezig zijn van Toll-achtige receptor (TLR) 5 op circulerende bloedcellen in het ontstaan van atherosclerose in muizen. TLRs zijn de best onderzochte patroonherkenningsreceptoren (PRRs) en zij herkennen moleculaire patronen die geasssocieerd zijn met pathogenen (PAMPs) of gevaar (DAMPs). Binding van deze moleculaire patronen aan TLRs veroorzaakt een ontstekingsreactie die als essentieel wordt beschouwd in de initiatie en progressie van atherosclerose.[8] Overeenkomstig eerder onderzoek laten wij een afname in de grootte van atherosclerotische plaques zien in muizen die TLR5-deficiënte circulerende cellen hebben. Dit effect was voornamelijk het gevolg van verminderde rekrutering van macrofagen en een afgenomen T-celreactie *in vitro* en *in vivo*. In overeenstemming met onze observaties zorgt behandeling met flagelline (een TLR5-stimulator) voor een toename van de grootte van plaques in muizen.[9]

Beide studies bevestigen de rol van TLR5 in het ontstaan van atherosclerotische plaques en zijn belangrijk bij de bestudering van het mechanisme. Voordat een vertaalslag naar de kliniek en patiëntenzorg gemaakt kan worden, is het noodzakelijk om het effect van een anti-TLR5 antilichaam in reeds manifeste atherosclerotische plaques te bestuderen. Evaluatie van het effect van anti-TLR5 therapie bovenop de huidige therapie in

atherosclerose zal zorgen voor een versnelde en verbeterde stap richting klinische toepassing.

Radiofrequente ablatie in atherosclerose

Atherosclerotische plaques kenmerken zich door een verhoogde dichtheid van de vasa vasorum (vaatjes in de adventitia, de buitenste wand van het bloedvat). Deze vaatjes zijn belangrijk voor de toevoer van bloed en voedingsstoffen aan de plaque[10], maar ook voor de instroom van ontstekingscellen.[11] Onvolgroeide en lekkende vasa vasorum monden uit in de plaque en hebben zo een verhoogde kans om daar een bloeding in de plaque te veroorzaken. Deze bloedingen leiden tot oxidatieve stress en een instabielere atherosclerotische plaque, wat uiteindelijk tot plaqueruptuur en een hartinfarct kan leiden. Radiofrequente ablatie (RFA) is voorheen gebruikt om vanuit de nierslagaders de zenuwvezels in de adventitia weg te branden om zo de bloeddruk te verlagen.[12] Overeenkomstig deze benadering was onze hypothese dat RFA op de atherosclerotische plaque op een veilige manier de vasa vasorum in de adventitia zou kunnen verminderen. Op die manier zouden we ook een verminderde vaatdichtheid in de plaque kunnen bewerkstelligen, wat het aantal bloedingen en daarmee de stabiliteit van de plaque gunstig zou kunnen beïnvloeden. Vanwege het feit dat RFA daarnaast ook fibrose (verlittekening) in de gezonde vaatwand veroorzaakt[12], zouden we ook nog via deze weg de plaque stabieler kunnen maken.

In **hoofdstuk 3** hebben we daarom een exploratieve studie verricht in een konijnenmodel met atherosclerose. We laten hier zien dat RFA veilig op deze atherosclerotische laesies kan worden toegepast en dat dit niet leidt tot onvoorziene ernstige complicaties. RFA veroorzaakt een passagère decellularisatie van het behandelde gebied en vermindert het aantal vaatjes in de plaque. Daarnaast vermindert het de hoeveelheid gladde spiercellen, maar het heeft geen effect op de grootte van de plaque of op andere kenmerken van de stabiliteit van de plaque. Omdat we in de huidige studie vooral gericht waren op het beoordelen van de veiligheid en toepasbaarheid, hebben we onvoldoende grote aantallen om kleine verschillen tussen behandelde en niet-behandelde gebieden te evalueren. Daarnaast is het van belang om te noemen dat stabilisatie van de plaque in een langer tijdsbestek zou kunnen optreden, wat impliceert dat onze studie mogelijk gelimiteerd is door een follow-up van slechts vier weken. Desondanks hebben we hier aangetoond dat RFA een veilige optie blijft om de vaatjes in de plaque te reduceren en voor therapeutische beïnvloeding van gladde spiercellen in bijvoorbeeld restenose (dichtgroeien van vaten die eerder zijn gedotterd of gestent). Met deze wetenschap zou het interessant zijn om het effect van een RFA-katheter te evalueren die de gehele omtrek van de vaatwand kan behandelen, eventueel in combinatie met een dotterbehandeling als huidige standaardtherapie.

Stentendothelialisatie

Percutane coronaire interventie (PCI), ook wel bekend als dotteren, is een van de meest uitgevoerde procedures in de directe behandeling van atherosclerose in de kransslagaders. Introductie van de dotterbehandeling met een ballon met of zonder het plaatsen van een metalen stent heeft de ziektelast en sterfte door atherosclerotische plaques enorm verminderd. Toch bleef een groot deel van de patiënten terugkomen vanwege restenose, een proces waarbij het behandelde vat in verloop van tijd opnieuw dichtslibt.[13] Om dit te voorkomen werden de drug-eluting stents geïntroduceerd; stents met een antiproliferatieve coating die de deling en groei van gladde spiercellen – verantwoordelijk voor de restenose – vermindert. Echter, omdat dit effect zowel aan de buitenkant (waar de gladde spiercellen zitten) als aan de binnenkant van het vat (waar het bloed langs stroomt) optreedt, wordt ook de bedekking van de stent met endotheelcellen (endothelialisatie) geremd. Wanneer deze stentendothelialisatie vertraagd optreedt, blijft de stent langer en voor een groter deel in contact staan met langsstromend bloed, wat het risico op stolselvorming op de stent vergroot.[14] Deze stolsels kunenn dan aanleiding geven voor een verstopping in de kransslagaders met chronisch zuurstoftekort en eventueel een hartinfarct tot gevolg.

Om een snellere endothelialisatie te bewerkstelligen, combineert de COMBO stent een antiproliferatieve coating aan de buitenzijde met een anti-CD34 coating aan de binnenzijde van de stent, waar het bloed langs stroomt. Deze anti-CD34 coating vangt als het ware voorlopers van endotheelcellen uit het bloed, die kunnen delen en nadien differentiëren in endotheelcellen om zo de stent te bedekken aan de kant waar het bloed langs stroomt. Op deze manier kan stolselvorming op de stent minder snel optreden of misschien wel voorkomen worden. In **hoofdstuk 4** vergelijken we de COMBO stent met een stent met alleen een antiproliferatieve coating. We laten zien dat de COMBO stent de endothelialisatie verbetert 28 dagen na implantatie in een konijnenmodel van restenose. Dit onderzoek sluit aan bij voorheen gepubliceerde positieve bevindingen met anti-CD34 technology[15,16] en versterkt het bewijs voor het gebruik van deze techniek om endothelialisatie te versnellen en verbeteren. Ook in patiënten werden excellente resultaten gezien met betrekking tot veiligheid en klinische uitkomsten één jaar na stentimplantatie.[17] Echter, een grote klinische studie liet daarna zien dat COMBO stents vergelijkbaar waren met everolimus stents met betrekking tot stentendothelialisatie in de REMEDEE-OCT Study.[18] Juist deze bevindingen trekken de effectiviteit van anti-CD34 in stentendothelialisatie bij patiënten in twijfel, wat verder onderzoek noodzakelijk maakt.

Beïnvloeding van de ontstekingsreactie bij hartinfarcten

Atherosclerose is de meestvoorkomende oorzaak voor het ontstaan van een hartinfarct.[2] Vanwege een verhoogde alertheid en verbeterde behandelingen is de sterfte in de eerste en acute fase van het hartinfarct fors afgenomen, waardoor nu steeds meer aandacht is voor

de gevolgen op lange termijn, waarvan hartfalen het belangrijkste is. Na een hartinfarct ontwikkelt namelijk een op de vier mensen hartfalen, in Nederland zo'n 150.000 in totaal.[27] Ook al verloopt behandeling steeds meer volgens door wetenschappelijk onderzoek getoetste richtlijnen, de prognose in hartfalen blijft slecht: ongeveer 25% van de patiënten overlijdt in het eerste jaar na ontwikkeling van klinische symptomen.[2]
Hartfalen na een hartinfarct wordt veroorzaakt door ongunstige remodellering van het linkerventrikel, wat afhankelijk is van de grootte van het infarct en de kwaliteit waarmee het beschadigde hartweefsel door het lichaam hersteld wordt.[28,29] Tijdige interventie en herstel van de bloedstroom (reperfusie) naar het gebied dat bij een hartinfarct geen bloed krijgt, is belangrijk om hartspiercellen te redden die beschadigd maar nog wel in leven zijn. Paradoxaal genoeg heeft reperfusie ook een keerzijde: het leidt in eerste instantie tot een uitbreiding van de infarctgrootte vanwege oxidative stress en ontsteking.[30] Daarbij komt dat ontsteking heeft laten zien een belangrijke rol in het proces van remodellering te spelen vanwege het opruimen van dood weefsel en maturatie van het getroffen gebied richting een volwaardig verbindweefseld litteken.[31]

Leukocyten-geassocieerde immunoglubline-achtige receptor-1 (LAIR-1) in het acute hartinfarct

De activatie van leukocyten (witte bloedcellen) ten tijde van ischemie- (zuurstoftekort) en reperfusieschade en daaropvolgend ongunstig remodelleren wordt beïnvloed door signalen van activerende en remmende celreceptoren.[32] Het dempen van deze ontstekingsreactie door het remmen van activeren leukocytenreceptoren[33–35] en costimulatoire moleculen[36] is voordelig gebleken in ischemie-reperfusie schade en remodellering. Echter, de rol van remmende leukocytenreceptoren in dezen is tot op heden onbestudeerd gebleven. Dat was voor ons de reden om in **hoofdstuk 5** het effect van de Leukocyt-geassocieerde immunoglubline-achtige receptor 1 (LAIR-1) te onderzoeken. Ondanks het feit dat LAIR-1 expressie op inflammatoire cellen gereguleerd wordt in patiënten met een hartinfarct, konden we geen oorzakelijk verband aantonen voor LAIR-1 deficiëntie in de grootte van het infarct en de mate van herstel van het hartspiefweefsel in muizen met een hartinfarct. Dit contrast tussen het effect van activerende en remmende leukocytenreceptoren zou mogelijkerwijs kunnen betekenen dat laatstgenoemde onvoldoende krachtig is om de hoeveelheid weefselschade en de ernst van de ontstekingsreactie in het huidige model te beïnvloeden. Daarnaast is het mogelijk dat de remming van de ontstekingsreactie door het binden van LAIR-1 aan collageen te laat is, gezien het feit dat deze binding pas in het hart tot stand wordt gebracht. Leukocyten zouden dan mogelijkerwijs al lang en breed geactiveerd kunnen zijn, aangezien dat voornamelijk vóór instroom in het hart gebeurt. Vanwege deze reden zou het van grote waarde zijn om het effect te evalueren van een stimulerend LAIR-1 antilichaam in de setting van een acuut hartinfarct, dat al reeds in het

bloed werkzaam zou kunnen zijn. Daarnaast zou het interessant zijn om expressielevels van LAIR-1 te relateren aan de mate van remodellering in patiënten om zo een beter begrip te krijgen van de rol van LAIR-1 in de mens.

Primaire uitkomstmaten in een varkensmodel van het acute hartinfarct

Vanwege het feit dat varkens qua anatomie en fysiologie van hart en bloedvaten vergelijkbaar zijn met de mens, worden zij niet zelden gebruikt in studies die de effectiviteit en veiligheid van nieuwe behandelingen van het acute hartinfarct testen. Om ervoor te zorgen dat de overstap van het varken naar de mens zo goed mogelijk verloopt, zijn betrouwbare en kostenefficiënte onderzoeksmethoden voor het meten van klinisch belangrijke uitkomstmaten essentieel. **In hoofdstuk 6** verstrekken we daarom een gedetailleerd protocol voor het meten van infarctgrootte en het gebied dat tijdens het hartinfarct risico loopt omdat het geen zuurstof krijgt. Daarnaast bespreken we 3-dimensionele slokdarmechocardiografie (3D-TEE) en druk-volume curves.

De kleuring van het infarct en het gebied zonder zuurstof tijdens het infarct wordt verricht met 2,3,5,-triphenyltetrazolium chloride (TTC) en Evans blauw. Deze methode is zeer accuraat omdat het positioneren van de ballon – en daarmee het gebied met zuurstofgebrek – op exact dezelfde locatie plaatsvindt bij terminatie als tijdens de operatie waarbij het hartinfarct geïnduceerd werd. Daarnaast is het niet meer nodig om de hartwand te doorboren voor het inspuiten van Evans blauw, waarbij de mogelijke injectie van kleurstof in de hartspier voorkomen wordt. Ook al is deze kleuring bewezen effectief en bruikbaar[37–39], het is nog steeds noodzakelijk om een invasieve procedure en een terminaal experiment te verrichten. Non-invasieve technieken (bijv. MRI) zouden uitkomst kunnen bieden voor het meten van de infarctgrootte en het gebied zonder zuurstof op korte termijn na het hartinfarct, en tegelijk de mogelijkheid bieden voor metingen van remodellering van het hart op lange termijn. Tot nog toe echter zijn de verschillende modaliteiten van de MRI om deze metingen te verrichten nog steeds onderwerp van debat.[40,41]

Met betrekking tot remodellering is het grote voordeel van de acquisitie van 3-dimensionele echocardiografie via de slokdarm dat een sternotomie (open-hart operatie) overbodig is. Dit is van belang omdat juist deze open-hart operatie vóór het hartinfarct een beschermend effect op het hart heeft[42], iets dat bij patiënten niet van toepassing is en daarom ook bij voorkeur niet in varkens wordt gedaan. Daarnaast zou echocardiografie direct op het hart na een open-hart operatie ook mogelijk minder representatieve beelden geven, gezien het feit dat de drukken in de borstholte veranderd zijn. Om bewijs voor het gebruik van slokdarmecho nog verder uit te bouwen, is het van het grootste belang dat de huidige methode van 3D-slokdarmecho wordt vergeleken met de gouden standaard (MRI). Bij positieve resultaten zou de 3D-slokdarmecho dan een praktisch en kosteneffectief alternatief zijn.

Remming van myeloperoxidase in ischemie-reperfusie schade

Neutrofiele granulocyten zijn de eerste ontstekingscellen die het hart binnendringen bij reperfusie van het voorheen ischemische (van zuurstof verstoken) gebied.[30,43] In zijn algemeenheid worden neutrofielen gezien als bijdragend aan ischemie-reperfusie schade. Ze scheiden onder andere het eiwit myeloperoxidase (MPO) uit, een enzym dat waterstofperoxide (H_2O_2) omzet in het zeer reactieve zuurstofradicaal hypochloor zuur (HOCl).[44] Daarnaast zijn MPO-concentraties in het infarctgebied van patiënten met een hartinfarct verhoogd[45] en voorspellen verhoogde plasmaconcentraties van MPO een nadelige uitkomst.[46] In **hoofdstuk 7** bestuderen we het effect van de remming van MPO in een klinisch relevant model van het acute hartinfarct in varkens. Ondanks de remming van MPO *in vitro* en de goede blootstelling *in vivo*, zagen we geen effect op de instroom van neutrofielen in het infarctgebied, noch zagen we een effect op infarctgrootte. Deze resultaten sluiten aan bij eerder onderzoek, waarin ook in muizen een vergelijkbare infarctgrootte gezien werd tussen wild-type en MPO-deficiënte muizen.[47] Tezamen zijn deze studies in overeenstemming met de niet eenduidige resultaten ten aanzien van het beïnvloeden van oxidatieve stress.[48–50] Ondanks onze aanname dat oxidatieve stress een sleutelrol speelt in ischemie-reperfusie schade[51], benadrukken deze studies dat ons begrip het mechanisme nog steeds onvoldoende is. Remming van een enzym(systeem) zou mogelijk klinische irrelevant kunnen zijn en/of zou gecompenseerd kunnen worden door een ander enzym(systeem). Tegelijkertijd zou oxidatieve stress tot op zekere hoogte een fysiologisch belangrijke functie kunnen vervullen. In dit opzicht is het niet verwonderlijk dat bij muizen deficiënt in NADPH oxidase (Nox) 2 óf Nox4 verminderde oxidatieve stress en gereduceerde infarctgrootte werden gezien, terwijl bij muizen die deficiënt waren in zowel Nox2 als Nox4 juist een groter infarct werd gezien, ondanks verminderde oxidatieve stress.[52] Deze bevindingen illustreren het voordelige effect van lage concentraties van zuurstofradicalen en benadrukt dat de optimale dosering om oxidatieve stress te beïnvloeden essentieel is voor een eventuele behandeling.

Het effect van de remming van het NLRP3 inflammasoom na een acuut hartinfarct in varkens

Het NLRP3 inflammasoom is een intracellulair eiwitcomplex dat gevormd en geactiveerd wordt bij hartspierschade en dat de omzetting van inactief IL1β en IL18 in hun actieve vorm mogelijk maakt.[53] Zowel het NLRP3 inflammasoom als deze pro-inflammatoire cytokines induceren een uitgebreide inflammatoire reactie die heeft laten zien zeer nadelig te zijn in de genezing na een hartinfarct in muizen.[54–57] Om een zo goed mogelijke overstap naar de patiëntenzorg te maken is het noodzakelijk om een medicijn dat het NLRP3 inflammasoom remt te testen in grote proefdieren met een acuut hartinfarct. Daarom hebben we in **hoofdstuk 8** het effect van de NLRP3 inflammasoomremmer MCC950 in

varkens met een acuut hartinfarct geëvalueerd. De resultaten lieten zien dat een klinisch toepasbaar doseringsschema van remming van het NLRP3 inflammasoom resulteert in een dosisafhankelijke afname in infarctgrootte en behoud van hartfunctie. Daarnaast bleken parameters van ontsteking en hartschade lager in behandelde dieren, wat het anti-inflammatoire effect op het NLRP3 inflammasoom benadrukt.
Gezien het feit dat nadelige remodellering van het hart zich ontwikkelt gedurende weken tot maanden na een hartinfarct[58], zou het interessant zijn om het effect van MCC950 ook in een studie met een langdurig vervolg te evalueren. Gezien de positieve relatie tussen IL1β concentraties twee maanden na het hartinfarct en het optreden van ongunstige remodellering van het hart een jaar nadien[59], zou daarnaast evaluatie van latere behandeling met MCC950 meer informatie kunnen verschaffen voor wat betreft het behandeleffect in mensen met reeds bestaand hartfalen. Concluderend lijkt remming van het NLRP3 inflammasoom een veelbelovende behandeloptie in patiënten met een hartinfarct.

TOEKOMSTPERSPECTIEF

De eerste beschrijvingen van ontstekingscellen in de atherosclerotische plaque en geïnfarceerd hartspierweefsel komen respectievelijk uit de tweede helft van de 19e eeuw[4] en de eerste helft van de 20e eeuw.[60] Uiteindelijk heeft het tot het laatste kwart van de 20e eeuw geduurd voordat onderzoek naar de mechanismen en behandelingen betreffende het immuunsysteem in hart- en vaatziekten vaste vorm begon aan te nemen. In de laatste decennia hebben we belangrijke inzichten verkregen in de immuunrespons in dit veld.[4,30,61–63] Desondanks blijft de complexiteit van dit proces in zowel atherosclerose als hartinfarcten een grote uitdaging voor wat betreft de implementatie in diagnostische, prognostische en therapeutische toepassingen. Dit proefschrift heeft zich ten doel gesteld om bij te dragen aan deze kennis en zo de ziektelast van ischemische hartziekten te reduceren door beïnvloeding van de ontstekingsreactie. Het eerste deel betrof een toename van ons begrip van het ontstaan en de behandeling van atherosclerose. Het tweede deel had ten doel potentiële anti-inflammatoire therapieën in ischemie-reperfusie schade van het hart te evalueren.

Uitdagingen betreffende de implementatie van nieuwe behandelingen in de patiëntenzorg
De vertaling van nieuwe bevindingen in het (dieren)laboratorium naar potentiële behandelingen voor atherosclerose en hartinfarcten in de mens is de laatste drie decennia een uitdaging gebleken. Ook al laten behandelingen veelbelovende resultaten zien in diermodellen, er zijn er weinig die ook daadwerkelijk succesvol in de klinische setting (*i.e.* patiëntenzorg) worden geïntroduceerd. Voor wat betreft atherosclerose zijn veel anti-

inflammatoire behandelingen niet voordelig of zelfs risicoverhogend gebleken.[62] Evenzo liet remming van de inflammatoire respons na een hartinfarct geen betere resultaten zien of zorgde juist voor een meer nadelige effecten.[64,65] De observatie dat ontsteking zowel voor- als nadelige effecten kent, wordt vaak gezien als een dubbelrol.[61,66,67] Bij wijze van voorbeeld heeft de identificatie van de helende monocyten subpopulatie laten zien dat dit celtype voordelig zou kunnen zijn in de wondheling na een hartinfarct, in tegenstelling tot de eerdere gedachte voor wat betreft de monocyten in zijn algemeenheid.[68] Ditzelfde geldt voor neutrofielen, die niet door iedereen als nadelig of bijdragend worden beschouwd in ischemie-reperfusie schade.[43,69] Juist de identificatie van een aparte groep neutrofielen met onderscheidende functies[70,71] geeft ons beter inzicht in welke onderdelen van de ontstekingsreactie voor- en welke nadelig zouden kunnen zijn. Gezien de complexiteit van de inflammatoire reactie zou onvoldoende begrip hiervan een van de verklaringen kunnen zijn voor het gebrek aan eenduidige resultaten en het falen van de translatie van anti-inflammatoire behandelingen in hart- en vaatziekten.

Daarnaast zijn er tal van andere factoren die mogelijkerwijs bijdragen aan ons onvermogen om nieuwe behandelingen betreffende de ontstekingsreactie te vertalen van het (dieren) laboratorium naar de patiëntenzorg. Dit zijn onder andere een suboptimaal preklinische studie-opzet[72,73], onvoldoende validatie van het betreffende target[74], onvoldoende kennis betreffende de biologie van de gebruikte proefdiermodellen en hun gelijkenis met mensen, irrelevante surrogaatparameters voor ziekte en onvoldoende grote studies.

Om de slagingskans van de overstap van preklinische studies naar de patiëntenzorg te vergroten, is optimalisatie van deze vertaalslag essentieel. Gezien het effect van reeds bestaande medicijnen op stabilisatie van de plaque[62,75] en herstel van hartweefsel na een hartinfarct[76], zou standaard gebruik hiervan naast het nieuwe te testen medicijn ervoor zorgen dat alleen nieuwe middelen met toegevoegde waarde verder onderzocht worden. Dit geldt eveneens voor het meenemen van comorbiditeiten in preklinische modellen, gezien het feit dat de prevalentie van risicofactoren stijgende is.[2] Van uitzonderlijk belang is de relatie tussen atherosclerose en een hartinfarct. Ook al zijn deze ook in dit proefschrift artificieel gescheiden, beide veranderen de inflammatoire status van het lichaam[77] en zouden daarom mogelijkerwijs elkaars ziekteproces en de reactie op nieuwe medicatie kunnen beïnvloeden.[78]

Daarnaast is het voor de vertaling naar de patiëntenzorg van belang om juist bij preklinische proefdiermodellen een zo klinisch mogelijk toepasbare setting na te streven. Dit heeft zich het laatste decennium vertaald in verschillende initiatieven en richtlijnen. In het veld van cardioprotectie (ischemie-reperfusie schade) heeft het CAESAR consortium zich ten doel gesteld om gelijk klinische studies ook bij preklinische studies eenzelfde strenge en robuuste evaluatie van de nieuwe behandeling toe te passen. Dit doet ze door studies van voldoende grote, geblindeerd, gerandomiseerd en volgens een klinisch toepasbare opzet uit te voeren.[79]

Verschillende doseringen worden geëvalueerd en alle data en statistische analyses worden in een onafhankelijk centrum verwerkt en uitgevoerd om zo de kwaliteit ervan veilig te stellen. Deze initiatieven sluiten perfect aan bij voorgaand oorzaak dat heeft laten zien dat de kwaliteit van een studie zeer belangrijk is voor de uitkomsten daarvan.[73]
Naast methodologische kwaliteit zou ook een verbeterd begrip van de relevante biologische processen voor een betere vertaling van laboratorium naar patiëntenzorg kunnen zorgen. Uiteraard is het met de kennis van nu relatief makkelijk om historische en tegenvallende resultaten te verklaren. Echter, sommige van deze valkuilen zouden vermeden kunnen worden door een vooraf bepaalde route te nemen.[74,80–82] Ten eerste zouden patiëntenstudies gebruikt moeten worden als startpunt voor het aantonen van een relatie tussen het target en de uitkomstmaat. Daarnaast kunnen *in vitro* studies van dit specifieke proces ons helpen het biologisch proces beter te begrijpen. Vervolgens zou validatie hiervan in het betreffende diermodel ons voorzien van een beter begrip van de gelijkenissen en verschillen met mensen. In dezen zouden nieuwe beeldvormingstechnieken (*e.g.* fluorescente reporters) erg behulpzaam kunnen zijn om het specifieke target te kwantificeren en lokaliseren en om het effect van de nieuwe behandeling te evalueren.[77]
Voor wat betreft nieuwe medicatie is het erg belangrijk om goede *in vitro* en *in vivo* proeven uit te voeren om zo uitgebreide informatie over de farmacokinetiek en –dynamiek te verkrijgen. Hierbij zijn selectiviteit, effectiviteit, weefselpenetratie en halfwaardetijd van het nieuwe middel van groot belang. Om selectiviteit en effectiviteit te verbeteren en zo bijwerkingen te verminderen zou medicatie die specifiek is voor bepaald weefsel of bepaalde cellen van grote toegevoegde waarde kunnen zijn.[83]

Oude trucs voor een oud probleem: vooruit- en terugblikken op hetzelfde moment
Nieuwe behandelingen, zowel medicijnen (*e.g.* statines) als mechanische behandelingen (*e.g.* dotterbehandelingen) hebben laten zien voordelig te kunnen zijn in de behandeling van hart- en vaatziekten. Talloze patiënten hebben hiervan reeds geprofiteerd en we hebben meer en meer laten zien hartziekten door zuurstofgebrek te kunnen behandelen. Toch blijft deze ziekte een van de belangrijkste oorzaken voor ziektelast en sterfte in de wereld en heeft zo een enorme impact op de economie en de samenleving.[84] Een van de belangrijkste bijdragende factoren hierin is de toenemende en onaanvaardbaar hoge prevalentie van risicofactoren zoals obesitas, fysieke inactiviteit, suikerziekte en roken.[2] Vrijwel allemaal veroorzaken ze een systemische pro-inflammatoire toestand en het behandelen hiervan door het controleren ervan is bewezen effectief in de vermindering van hart- en vaatziekten.[85] Echter, patiënten blijven voor een groot deel on(der)behandeld, onvoldoende gecontroleerd en niet therapietrouw.[86–88] Om zowel de ziektelast van hart- en vaatziekten te verminderen en om nieuwe behandelingen te evalueren die daadwerkelijk van toegevoegde waarde zijn op de huidige behandelingen, is het daarom van het grootste belang om de huidige behandeling van patiënten te optimaliseren.

CONCLUSIE

Ontsteking in hart- en vaatziekten dient te worden beschouwd als een complex proces en een delicate balans tussen pro- en anti-inflammatoire invloeden. Hierbij zijn niet alle pro-inflammatoire invloeden nadelig en omgekeerd niet alle anti-inflammatoire invloeden voordelig. Vanwege deze reden is timing en dosering essentieel om een succesvolle vertaalslag te maken naar de patiëntenzorg.
Interindividuele verschillen in inflammatoire activiteit tussen patiënten zouden onderdeel kunnen zijn van het tegenvallende resultaat van globale anti-inflammatoire behandelingen. Dit zou opgelost kunnen worden door het gebruik van biomarkers in het identificeren van patiënten met over- of onderactieve pro-inflammatoire activiteit. Concluderend, gezien de voordelige én nadelige effecten van inflammatie in hart- en vaatziekten zal onderzoek altijd moeten blijven streven naar het gulden midden.

REFERENCES

1. WHO. Causes of death, 2000-2012. 2012. Available at: http://www.who.int/mediacentre/factsheets/fs310/en/. Accessed April 11, 2015.
2. Mozaffarian D, Benjamin EJ, Go AS, Arnett DK, Blaha MJ, Das SR, Ferranti S De, Després J, Fullerton HJ, Howard J, Huffman MD, Isasi CR, Jiménez MC, Judd SE, Brett M, Lichtman JH, Lisabeth LD, Liu S, Mackey RH, Magid DJ, Mcguire DK, Mohler ER, Moy CS, Muntner P, Mussolino ME, Nasir K, Neumar RW, Nichol G, Palaniappan L, Pandey DK, Mathew J, Rodriguez CJ, Rosamond W, Sorlie PD, Stein J, Towfighi A, Turan N, Virani SS, Woo D, Yeh RW, Turner MB. Heart Disease and Stroke Statistics—2016 Update: A Report From the American Heart Association. *Circulation* 2016:1–668.
3. Ruparelia N, Chai JT, Fisher EA, Choudhury RP. Inflammatory processes in cardiovascular disease: a route to targeted therapies. *Nat Rev Cardiol* 2016;369:2437–2445.
4. Libby P. History of Discovery: Inflammation in Atherosclerosis. *Arter Thromb Vasc Biol* 2012;32:2045–2051.
5. Libby P, Ridker PM, Maseri A. Inflammation and atherosclerosis. *Circulation* 2002;105:1135–1143.
6. Shibata T, Kawakami S, Noguchi T, Tanaka T, Asaumi Y, Kanaya T, Nagai T, Nakao K, Fujino M, Nagatsuka K, Ishibashi-Ueda H, Nishimura K, Miyamoto Y, Kusano K, Anzai T, Goto Y, Ogawa H, Yasuda S. Prevalence, clinical features, and prognosis of acute myocardial infarction attributable to coronary artery embolism. *Circulation* 2015;132:241–250.
7. Ylä-Herttuala S, Bentzon JF, Daemen M, Falk E, Garcia-Garcia HM, Herrmann J, Hoefer I, Jauhiainen S, Jukema JW, Krams R, Kwak BR, Marx N, Naruszewicz M, Newby A, Pasterkamp G, Serruys PWJC, Waltenberger J, Weber C, Tokgözoglu L. Stabilization of atherosclerotic plaques: An update. *Eur Heart J* 2013;34:3251–3258.
8. Falck-hansen M, Kassiteridi C. Toll-Like Receptors in Atherosclerosis. *Int J Mol Sci* 2013;14:14008–14023.
9. Kim J, Seo M, Kim SK, Bae YS. Flagellin-induced NADPH oxidase 4 activation is involved in atherosclerosis. *Sci Rep* 2016:1–16.
10. Virmani R, Kolodgie FD, Burke AP, Finn A V., Gold HK, Tulenko TN, Wrenn SP, Narula J. Atherosclerotic plaque progression and vulnerability to rupture: Angiogenesis as a source of intraplaque hemorrhage. *Arterioscler Thromb Vasc Biol* 2005;25:2054–2061.
11. Moulton KS, Vakili K, Zurakowski D, Soliman M, Butterfield C, Sylvin E, Lo K-M, Gillies S, Javaherian K, Folkman J. Inhibition of plaque neovascularization reduces macrophage accumulation and progression of advanced atherosclerosis. *Proc Natl Acad Sci U S A* 2003;100:4736–41.
12. Steigerwald K, Titova A, Malle C, Kennerknecht E, Jilek C, Hausleiter J, Nährig JM, Laugwitz K-L, Joner M. Morphological assessment of renal arteries after radiofrequency catheter-based sympathetic denervation in a porcine model. *J Hypertens* 2012;30:2230–9.
13. Costa M a, Simon DI. Molecular basis of restenosis and drug-eluting stents. *Circulation* 2005;111:2257–73.
14. Lüscher TF, Steffel J, Eberli FR, Joner M, Nakazawa G, Tanner FC, Virmani R. Drug-eluting stent and coronary thrombosis: biological mechanisms and clinical implications. *Circulation* 2007;115:1051–8.
15. Nakazawa G, Granada JF, Alviar CL, Tellez A, Kaluza GL, Guilhermier MY, Parker S, Rowland SM, Kolodgie FD, Leon MB, Virmani R. Anti-CD34 Antibodies Immobilized on the Surface of Sirolimus-Eluting Stents Enhance Stent Endothelialization. *J Am Coll Cardiol* 2010;3:68–75.
16. Granada JF, Inami S, Aboodi MS, Tellez A, Milewski K, Wallace-Bradley D, Parker S, Rowland S, Nakazawa G, Vorpah M, Kolodgie FD, Kaluza GL, Leon MB, Virmani R. Development of a novel prohealing stent designed to deliver sirolimus from a biodegradable abluminal matrix. *Circ Cardiovasc Interv* 2010;3:257–266.
17. Woudstra P, Kalkman DN, Heijer P den, Menown IBA, Erglis A, Suryapranata H, Arkenbout KE, Iñiguez A, 't Hof AWJ van, Muller P, Tijssen JGP, Winter RJ de. 1-Year Results of the REMEDEE Registry. *JACC Cardiovasc Interv* 2016;9:1127–1134.
18. Jaguszewski M, Aloysius R, Wang W, Bezerra HG, Hill J, Winter RJ De, Karjalainen PP, Verheye S, Wijns W, Lüscher TF, Joner M, Costa M, Landmesser U. The REMEDEE-OCT Study. *JACC Cardiovasc Interv* 2017;10:489–499.
19. Tearney GJ, Regar E, Akasaka T, Adriaenssens T, Barlis P, Bezerra HG, Bouma B, Bruining N, Cho JM, Chowdhary S, Costa MA, Silva R De, Dijkstra J, Mario C Di, Dudeck D, Falk E, Feldman MD, Fitzgerald P, Garcia H, Gonzalo N, Granada JF, Guagliumi G, Holm NR, Honda Y, Ikeno F, Kawasaki M, Kochman J, Koltowski L, Kubo T, Kume T, Kyono H, Lam CCS, Lamouche G, Lee DP, Leon MB, Maehara A, Manfrini O, Mintz GS, Mizuno K, Morel MA, Nadkarni S, Okura H, Otake H, Pietrasik A, Prati F, Rber L, Radu MD, Rieber J, Riga M, Rollins A, et al. Consensus standards for acquisition, measurement, and reporting of intravascular optical coherence tomography studies: A report from the International Working Group for Intravascular Optical Coherence Tomography Standardization and Validation. *J Am Coll Cardiol* 2012;59:1058–1072.
20. Madjid M, Awan I, Willerson JT, Casscells SW. Leukocyte count and coronary heart disease: Implications for risk assessment. *J Am Coll Cardiol* 2004;44:1945–1956.
21. Lee CD, Folsom AR, Nieto FJ, Chambless LE, Shahar E, Wolfe DA. White blood cell count and incidence of coronary heart disease and ischemic stroke and mortality from cardiovascular disease in African-American and White men and women: atherosclerosis risk in communities study. *Am J Epidemiol* 2001;154:758–64.
22. Kato A, Takita T, Furuhashi M, Maruyama Y, Kumagai H, Hishida A. Blood monocyte count is a predictor of total and cardiovascular mortality in hemodialysis patients. *Nephron - Clin Pract* 2008;110:235–243.

23. Gillum RF, Mussolino ME, Madans JH. Counts of neutrophils, lymphocytes, and monocytes, cause-specific mortality and coronary heart disease: The NHANES-I epidemiologic follow-up study. *Ann Epidemiol* 2005;15:266–271.
24. Guasti L, Dentali F, Castiglioni L, Maroni L, Marino F, Squizzato A, Ageno W, Gianni M, Gaudio G, Grandi AM, Cosentino M, Venco A. Neutrophils and clinical outcomes in patients with acute coronary syndromes and/or cardiac revascularization: A systematic review on more than 34,000 subjects. *Thromb Haemost* 2011;106:591–599.
25. Wang X, Zhang G, Jiang X, Zhu H, Lu Z, Xu L. Neutrophil to lymphocyte ratio in relation to risk of all-cause mortality and cardiovascular events among patients undergoing angiography or cardiac revascularization: a meta-analysis of observational studies. *Atherosclerosis* 2014;234:206–13.
26. Ghattas A, Griffiths HR, Devitt A, Lip GYH, Shantsila E. Monocytes in coronary artery disease and atherosclerosis: where are we now? *J Am Coll Cardiol* 2013;62:1541–1551.
27. Dutch Heart Foundation. *Cijferboek Hart- en Vaatziekten in Nederland*.; 2015.
28. Konstam MA, Kramer DG, Patel AR, Maron MS, Udelson JE. Left ventricular remodeling in heart failure: Current concepts in clinical significance and assessment. *JACC Cardiovasc Imaging* 2011;4:98–108.
29. Chareonthaitawee P, Christian TF, Hirose K, Gibbons RJ, Rumberger JA. Relation of initial infarct size to extent of left ventricular remodeling in the year after acute myocardial infarction. *J Am Coll Cardiol* 1995;25:567–73.
30. Frangogiannis NG. The inflammatory response in myocardial injury, repair, and remodelling. *Nat Rev Cardiol* 2014;11:255–265.
31. Westman PC, Lipinski MJ, Luger D, Waksman R, Bonow RO, Wu E, Epstein SE. Inflammation as a Driver of Adverse Left Ventricular Remodeling After Acute Myocardial Infarction. *J Am Coll Cardiol* 2016;67:2050–2060.
32. Billadeau DD, Leibson PJ. ITAMs versus ITIMs: Striking a balance during cell regulation. *J Clin Invest* 2002;109:161–168.
33. Oyama JI, Blais C, Liu X, Pu M, Kobzik L, Kelly RA, Bourcier T. Reduced Myocardial Ischemia-Reperfusion Injury in Toll-Like Receptor 4-Deficient Mice. *Circulation* 2004;109:784–789.
34. Yang Z, Day YJ, Toufektsian MC, Ramos SI, Marshall M, Wang XQ, French BA, Linden J. Infarct-sparing effect of A2A-adenosine receptor activation is due primarily to its action on lymphocytes. *Circulation* 2005;111:2190–2197.
35. Arslan F, Smeets MB, O'Neill LAJ, Keogh B, McGuirk P, Timmers L, Tersteeg C, Hoefer IE, Doevendans PA, Pasterkamp G, Kleijn DP V De. Myocardial ischemia/reperfusion injury is mediated by leukocytic toll-like receptor-2 and reduced by systemic administration of a novel anti-toll-like receptor-2 antibody. *Circulation* 2010;121:80–90.
36. Kubota A, Hasegawa H, Tadokoro H, Hirose M, Kobara Y, Yamada-Inagawa T, Takemura G, Kobayashi Y, Takano H. Deletion of CD28 Co-stimulatory Signals Exacerbates Left Ventricular Remodeling and Increases Cardiac Rupture After Myocardial Infarction. *Circ J* 2016;80:9171–1979.
37. Suzuki Y, Lyons JK, Yeung AC, Ikeno F. In vivo porcine model of reperfused myocardial infarction: In situ double staining to measure precise infarct area/area at risk. *Catheter Cardiovasc Interv* 2008;71:100–7.
38. Fishbein M, Meerbaum S, Rit J, Lando U, Kanmatsuse K, Mercier J, Corday E, Ganz W. Early phase acute myocardial infarct size quantification: validation of the triphenyl tetrazolium chloride tissue enzyme staining technique. *Am Hear J* 1981;101:593–600.
39. Timmers L, Henriques JPS, Kleijn DP V de, Devries JH, Kemperman H, Steendijk P, Verlaan CWJ, Kerver M, Piek JJ, Doevendans PA, Pasterkamp G, Hoefer IE. Exenatide reduces infarct size and improves cardiac function in a porcine model of ischemia and reperfusion injury. *J Am Coll Cardiol* 2009;53:501–10.
40. Jablonowski R, Engblom H, Kanski M, Nordlund D, Koul S, Pals J Van Der, Englund E, Heiberg E, Erlinge D, Carlsson M, Arheden H. Contrast-Enhanced CMR Overestimates Early Myocardial Infarct Size: Mechanistic Insights Using ECV Measurements on Day 1 and Day 7. *JACC Cardiovasc Imaging* 2015;8:1379–1389.
41. Kim HW, Assche L Van, Jennings RB, Wince WB, Jensen CJ, Rehwald WG, Wendell DC, Bhatti L, Spatz DM, Parker MA, Jenista ER, Klem I, Crowley ALC, Chen EL, Judd RM, Kim RJ. Relationship of T2-Weighted MRI Myocardial Hyperintensity and the Ischemic Area-At-Risk. *Circ Res* 2015;117:254–265.
42. Hout GPJ van, Teuben MPJ, Heeres M, Maat S de, Jong R de, Maas C, Kouwenberg LHJA, Koenderman L, Solinge WW van, Jager SCA de, Pasterkamp G, Hoefer IE. Invasive surgery reduces infarct size and preserves cardiac function in a porcine model of myocardial infarction. *J Cell Mol Med* 2015;19:2655–2663.
43. Baxter GF. The neutrophil as a mediator of myocardial ischemia-reperfusion injury: Time to move on. *Basic Res Cardiol* 2002;97:268–275.
44. Klebanoff SJ. Myeloperoxidase: friend and foe. *J Leukoc Biol* 2005;77:598–625.
45. Heymans S, Luttun a, Nuyens D, Theilmeier G, Creemers E, Moons L, Dyspersin GD, Cleutjens JP, Shipley M, Angellilo a, Levi M, Nübe O, Baker a, Keshet E, Lupu F, Herbert JM, Smits JF, Shapiro SD, Baes M, Borgers M, Collen D, Daemen MJ, Carmeliet P. Inhibition of plasminogen activators or matrix metalloproteinases prevents cardiac rupture but impairs therapeutic angiogenesis and causes cardiac failure. *Nat Med* 1999;5:1135–1142.
46. Mocatta TJ, Pilbrow AP, Cameron VA, Senthilmohan R, Frampton CM, Richards AM, Winterbourn CC. Plasma Concentrations of Myeloperoxidase Predict Mortality After Myocardial Infarction. *J Am Coll Cardiol* 2007;49:1993–2000.

47. Vasilyev N, Williams T, Brennan ML, Unzek S, Zhou X, Heinecke JW, Spitz DR, Topol EJ, Hazen SL, Pen MS. Myeloperoxidase-generated oxidants modulate left ventricular remodeling but not infarct size after myocardial infarction. *Circulation* 2005;112:2812–2820.
48. Forman MB, Puett DW, Cates CU, McCroskey DE, Beckman JK, Greene HL, Virmani R. Glutathione redox pathway and reperfusion injury. Effect of N-acetylcysteine on infarct size and ventricular function. *Circulation* 1988;78:202–213.
49. Yoshida T, Watanabe M, Engelman DT, Engelman RM, Schley J a, Maulik N, Ho YS, Oberley TD, Das DK. Transgenic mice overexpressing glutathione peroxidase are resistant to myocardial ischemia reperfusion injury. *J Mol Cell Cardiol* 1996;28:1759–1767.
50. Pacher P, Nivorozhkin A, Szabó C. Therapeutic effects of xanthine oxidase inhibitors: renaissance half a century after the discovery of allopurinol. *Pharmacol Rev* 2006;58:87–114.
51. Granger DN, Kvietys PR. Reperfusion injury and reactive oxygen species: The evolution of a concept. *Redox Biol* 2015;6:524–551.
52. Matsushima S, Kuroda J, Ago T, Zhai P, Ikeda Y, Oka S, Fong GH, Tian R, Sadoshima J. Broad suppression of NADPH oxidase activity exacerbates ischemia/reperfusion injury through inadvertent downregulation of hypoxia-inducible factor-1 alpha and upregulation of peroxisome proliferator-activated receptor-alpha. *Circ Res* 2013;112:1135–1149.
53. Latz E, Xiao TS, Stutz A. Activation and regulation of the inflammasomes. *Nat Rev Immunol* 2013;13:397–411.
54. Kawaguchi M, Takahashi M, Hata T, Kashima Y, Usui F, Morimoto H, Izawa A, Takahashi Y, Masumoto J, Koyama J, Hongo M, Noda T, Nakayama J, Sagara J, Taniguchi S, Ikeda U. Inflammasome activation of cardiac fibroblasts is essential for myocardial ischemia/reperfusion injury. *Circulation* 2011;123:594–604.
55. Mezzaroma E, Toldo S, Farkas D, Seropian IM, Tassell BW Van, Salloum FN, Kannan HR, Menna AC, Voelkel NF, Abbate A. The inflammasome promotes adverse cardiac remodeling following acute myocardial infarction in the mouse. *Proc Natl Acad Sci U S A* 2011;108:19725–19730.
56. Zuurbier CJ, Jong WMC, Eerbeek O, Koeman A, Pulskens WP, Butter LM, Leemans JC, Hollmann MW. Deletion of the innate immune NLRP3 receptor abolishes cardiac ischemic preconditioning and is associated with decreased IL-6/STAT3 signaling. *PLoS One* 2012;7:1–8.
57. Sandanger O, Ranheim T, Vinge LE, Bliksoen M, Alfsnes K, Finsen A V., Dahl CP, Askevold ET, Florholmen G, Christensen G, Fitzgerald KA, Lien E, Valen G, Espevik T, Aukrust P, Yndestad A. The NLRP3 inflammasome is up-regulated in cardiac fibroblasts and mediates myocardial ischaemia-reperfusion injury. *Cardiovasc Res* 2013;99:164–174.
58. Jong R de, Hout GPJ van, Houtgraaf JH, Takashima S, Pasterkamp G, Hoefer I, Duckers HJ. Cardiac Function in a Long-Term Follow-Up Study of Moderate and Severe Porcine Model of Chronic Myocardial Infarction. *Biomed Res Int* 2015;2015:1–11.
59. Ørn S, Ueland T, Manhenke C, Sandanger, Godang K, Yndestad A, Mollnes TE, Dickstein K, Aukrust P. Increased interleukin-1β levels are associated with left ventricular hypertrophy and remodelling following acute ST segment elevation myocardial infarction treated by primary percutaneous coronary intervention. *J Intern Med* 2012;272:267–276.
60. Mallory GK, White PD, Salcedo-Salgar J. The speed of healing of myocardial infarction. A study of the pathologic anatomy in seventy-two cases. *Am Heart J* 1939;18:647–671.
61. Hansson GK, Libby P. The immune response in atherosclerosis : a double-edged sword. *Nat Rev Immunol* 2006;6:508–519.
62. Bäck M, Hansson GK. Anti-inflammatory therapies for atherosclerosis. *Nat Rev Cardiol* 2015;12:199–211.
63. Arslan F, Kleijn DP de, Pasterkamp G. Innate immune signaling in cardiac ischemia. *Nat Rev Cardiol* 2011;8:292–300.
64. Dewenter M, Wagner M, El-Armouche A. LATITUDE-TIMI: is there still hope for anti-inflammatory therapy in acute myocardial infaction? *J Thorac Dis* 2016;8:E1047–E1049.
65. Saxena A, Russo I, Frangogiannis NG. Inflammation as a therapeutic target in myocardial infarction: learning from past failures to meet future challenges. *Transl Res* 2017;167:152–166.
66. Braunwald E, Kloner RA. Myocardial reperfusion: A double-edged sword? *J Clin Invest* 1985;76:1713–1719.
67. Liu J, Wang H, Li J. Inflammation and inflammatory cells in myocardial infarction and reperfusion injury: A double-edged sword. *Clin Med Insights Cardiol* 2016;10:79–84.
68. Dutta P, Nahrendorf M. Monocytes in myocardial infarction. *Arterioscler Thromb Vasc Biol* 2015;35:1066–1070.
69. Schofield ZV, Woodruff TM, Halai R, Wu MC-L, Cooper MA. Neutrophils--a key component of ischemia-reperfusion injury. *Shock* 2013;40:463–70.
70. Pillay J, Kamp VM, Hoffen E Van, Visser T, Tak T, Lammers J, Ulfman LH, Leenen LP, Pickkers P, Koenderman L. A subset of neutrophils in human systemic inflammation inhibits T cell responses through Mac-1. *J Clin Invest* 2012;122:327–336.
71. Hout GPJ van, Solinge WW van, Gijsberts CM, Teuben MPJ, Leliefeld PHC, Heeres M, Nijhoff F, Jong S de, Bosch L, Jager SCA de, Huisman A, Stella PR, Pasterkamp G, Koenderman LJ, Hoefer IE. Elevated mean neutrophil volume represents altered neutrophil composition and reflects damage after myocardial infarction. *Basic Res Cardiol* 2015;110:1–11.
72. Macleod MR, Lawson McLean A, Kyriakopoulou A, Serghiou S, Wilde A de, Sherratt N, Hirst T, Hemblade R, Bahor Z, Nunes-Fonseca C, Potluru A, Thomson A, Baginskitae J, Egan K, Vesterinen H, Currie GL, Churilov L, Howells DW, Sena ES. Risk of Bias in Reports of In Vivo Research: A Focus for Improvement. *PLoS Biol* 2015;13:1–12.

73. Hout GPJ Van, Jansen Of Lorkeers SJ, Wever KE, Sena ES, Kouwenberg LHJA, Solinge WW Van, Macleod MR, Doevendans PA, Pasterkamp G, Chamuleau SAJ, Hoefer IE. Translational failure of anti-inflammatory compounds for myocardial infarction: A meta-Analysis of large animal models. *Cardiovasc Res* 2016;109:240–248.
74. Denayer T, Stöhrn T, Roy M Van. Animal models in translational medicine: Validation and prediction. *New Horizons Transl Med* 2014;2:5–11.
75. Yla-Herttuala S, Bentzon JF, Daemen M, Falk E, Garcia-Garcia HM, Herrmann J, Hoefer I, Wouter Jukema J, Krams R, Kwak BR, Marx N, Naruszewicz M, Newby A, Pasterkamp G, Serruys PWJC, Waltenberger J, Weber C, Tokgözoglu L. Stabilisation of atherosclerotic plaques position paper of the european society of cardiology (ESC) working group on atherosclerosis and vascular biology. *Thromb Haemost* 2011;106:1–19.
76. Sutton SJ, Sharpe N. Left Ventricular Remodeling After Myocardial Infarction Pathophysiology and Therapy. *Circulation* 2000;101:2981–2988.
77. Nahrendorf M, Frantz S, Swirski FK, Mulder WJM, Randolph G, Ertl G, Ntziachristos V, Piek JJ, Stroes ES, Schwaiger M, Mann DL, Fayad ZA. Imaging systemic inflammatory networks in ischemic heart disease. *J Am Coll Cardiol* 2015;65:1583–1591.
78. Dutta P, Courties G, Wei Y, Leuschner F, Gorbatov R, Robbins CS, Iwamoto Y, Thompson B, Carlson AL, Heidt T, Majmudar MD, Lasitschka F, Etzrodt M, Waterman P, Waring MT, Chicoine AT, Laan AM van der, Niessen HWM, Piek JJ, Rubin BB, Butany J, Stone JR, Katus HA, Murphy SA, Morrow DA, Sabatine MS, Vinegoni C, Moskowitz MA, Pittet MJ, Libby P, Lin CP, Swirski FK, Weissleder R, Nahrendorf M. Myocardial infarction accelerates atherosclerosis. *Nature* 2012;487:325–9.
79. Jones SP, Tang XL, Guo Y, Steenbergen C, Lefer DJ, Kukreja RC, Kong M, Li Q, Bhushan S, Zhu X, Du J, Nong Y, Stowers HL, Kondo K, Hunt GN, Goodchild TT, Orr A, Chang CC, Ockaili R, Salloum FN, Bolli R. The NHLBI-Sponsored Consortium for preclinicAl assESsment of cARdioprotective Therapies (CAESAR): A new paradigm for rigorous, accurate, and reproducible evaluation of putative infarct-sparing interventions in mice, rabbits, and pigs. *Circ Res* 2015;116:572–586.
80. Marti CN, Gheorghiade M, Kalogeropoulos AP, Georgiopoulou V V., Quyyumi AA, Butler J. Endothelial dysfunction, arterial stiffness, and heart failure. *J Am Coll Cardiol* 2012;60:1455–1469.
81. Cook D, Brown D, Alexander R, March R, Morgan P, Satterthwaite G, Pangalos MN. Lessons learned from the fate of AstraZeneca's drug pipeline: a five-dimensional framework. *Nat Rev drug Discov* 2014;13:419–31.
82. Heusch G. Critical Issues for the Translation of Cardioprotection. *Circ Res* 2017;120:1477–1486.
83. Scott RC, Crabbe D, Krynska B, Ansari R, Kiani MF. Aiming for the heart: targeted delivery of drugs to diseased cardiac tissue. *Expert Opin Drug Deliv* 2008;5:459–70.
84. GBD 2013 Mortality and Causes of Death Collaborators*. Global, regional, and national age – sex specific all-cause and cause-specific mortality for 240 causes of death, 1990 – 2013: a systematic analysis for the Global Burden of Disease Study 2013. *Lancet* 2014;385:117–171.
85. Dong C, Rundek T, Wright CB, Anwar Z, Elkind MS V, Sacco RL. Ideal cardiovascular health predicts lower risks of myocardial infarction, stroke, and vascular death across whites, blacks, and hispanics: The Northern Manhattan study. *Circulation* 2012;125:2975–2984.
86. Benner J, Glynn R, Mogun H, Neumann P, Weinstein M, Avorn J. Long-term persistence in use of statin therapy in elderly patients. *JAMA* 2002;288:455–461.
87. Bhatt DL, Steg PG, Ohman EM, Hirsch AT, Ikeda Y, Mas J-L, Goto S, Liau C-S, Richard AJ, Röther J, Wilson PWF. International Prevalence, Recognition and Treatment of Cardiovascular Risk Factors in Outpatients With Atherothrombosis. *JAMA* 2006;295.
88. Naderi SH, Bestwick JP, Wald DS. Adherence to drugs that prevent cardiovascular disease: Meta-analysis on 376,162 patients. *Am J Med* 2012;125:882–887.

PART FOUR
ADDENDUM

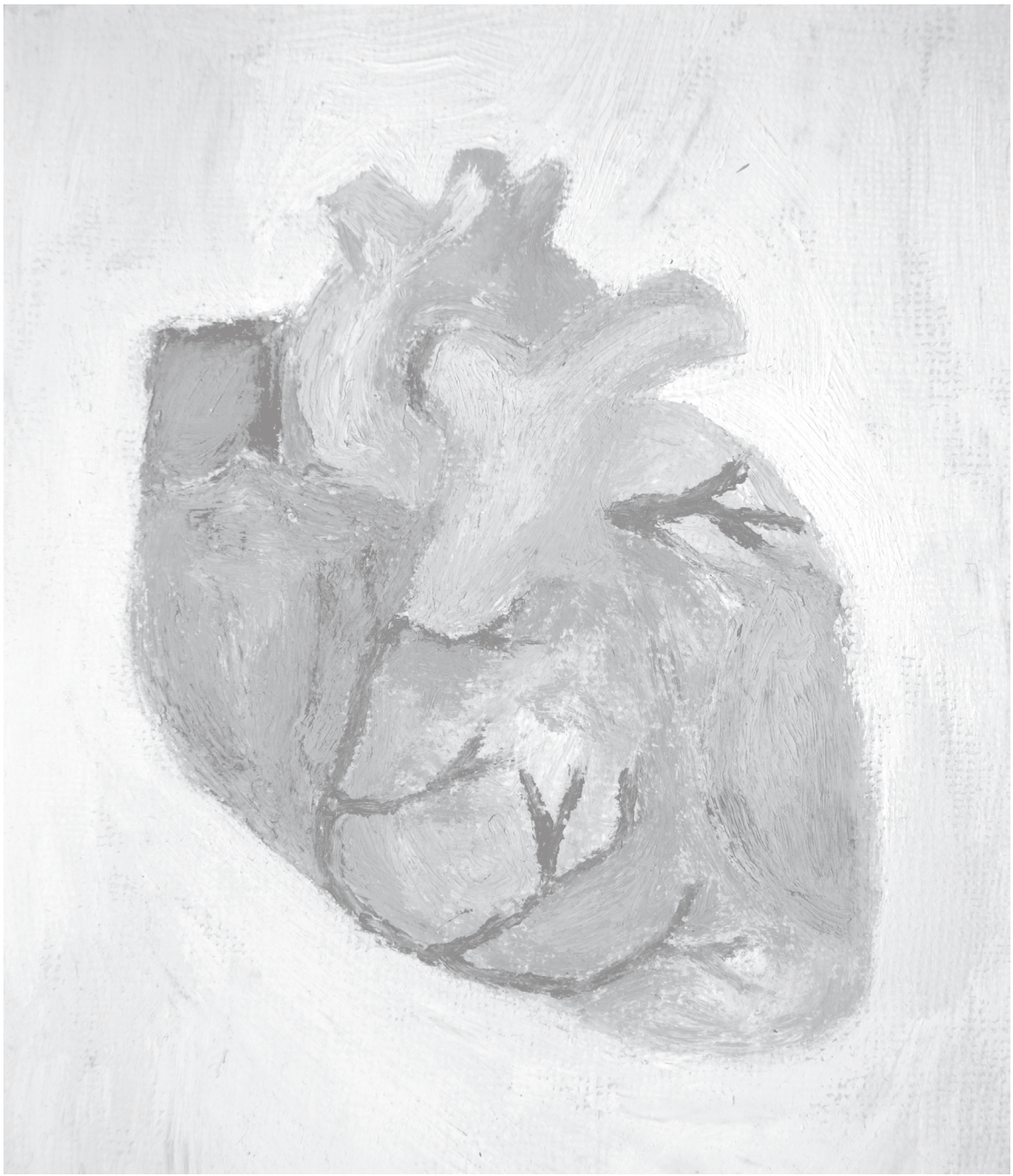

REVIEW COMMITTEE

Prof. dr. D.P.V. de Kleijn
Prof. dr. S.A.J. Chamuleau
Prof. dr. D. Duncker
Prof. dr. P.A. de Jong
Prof. dr. W.W. van Solinge

LIST OF ABBREVIATIONS

*	P<0.05
**	P<0.01
***	P<0.001
****	P<0.0001
2D	2-dimensional
3D	3-dimensional
3D-TEE	3-dimensional transesophageal echocardiography
AAR	area at risk
AMI	acute myocardial infarction
αSMA	alpha-smooth muscle actin
A.U.	arbitrary units
BA ratio	balloon-to-artery ratio
BMS	bare-metal stent
bpm	beats per minute
CAD	coronary artery disease
CCR	C-C chemokine receptor
CD	cluster of differentiation
CMRI	cardiac magnetic resonance imaging
CRP	C-reactive protein
CVA	cerebrovascular accident
CVD	cardiovascular disease
DAMP	danger-associated molecular patterns
DES	drug-eluting stent
dP/dT	derivative of pressure
E_a	arterial elastance
E_{es}	end-systolic elastance
EC	endothelial cell
ED	end-diastolic
EDP	end-diastolic pressure
EDPVR	end-diastolic pressure-volume relationship
EDV	end-diastolic volume
EEL	external elastic laminae
EES	everolimus-eluting stent
EF	ejection fraction
EPC	endothelial progenitor cell
ES	end-systolic

ESP	end-systolic pressure
ESPVR	end-systolic pressure-volume relationship
ESV	end-systolic volume
EvG	Elastica van Giesson (EvG)
F	French
FAS	fractional area shortening
Fig.	figure
FS	fractional shortening
H_2O_2	hydrogen peroxide
HE	hematoxylin and eosin
H&E	hematoxylin and eosin
HF	heart failure
HFrEF	heart failure with reduced ejection fraction
$HOCl^-$	hypochlorous acid
HR	heart rate
IEL	internal elastic laminae
IHD	ischemic heart disease
IL	interleukin
iNOS	inducible nitric oxide synthase
IFN-γ	interferon γ
IM	intramuscular
IV	intravenous
IQR	interquartile range
IRI	ischemia-reperfusion injury
IS	infarct size
LAD	left anterior descending
LAIR	leukocyte-associated immunoglobulin-like receptor
LCA	left coronary artery
LL	late loss
LMCA	left main coronary artery
LPM	light emissions per minute
LPS	lipopolysaccharide
LV	left ventricle
LVEF	left ventricular ejection fraction
$LVia_{ES}$	end systolic left ventricular internal area
$LViD_{ES}$	end systolic left ventricular internal diameter
MACE	major adverse cardiovascular events
MAP	mean arterial pressure

MCP	monocyte chemoattractant protein-1
MFI	mean fluorescent intensity
MI	myocardial infarction
MMP	matrix metalloproteinases
Mono	Monocytes
MPO	myeloperoxidase
MRI	magnetic resonance imaging
NFκB	nuclear factor kappa B
NOX	NADPH oxidase
NS	not significant
NIH	neointimal hyperplasia
NLR	NOD-like receptor
OCT	optical coherence tomography
PAMP	pathogen-associated molecular patterns
PBS	phosphate-buffered saline
PCI	percutaneous coronary intervention
PES	paclitaxel-eluting stent
PHT	pressure half-time
PMA	phorbol 12-myristate 13-acetate
PMN	polymorphonuclear leukocytes
POBA	plain old balloon angioplasty
PRR	pattern recognition receptors
PRSW	preload recruitable stroke work
PV	pressure-volume
RFA	radiofrequency ablation
ROS	reactive oxygen species
RT	room temperature
RT-PCR	real-time polymerase chain reaction
SD	standard deviation
sEM	scanning electron microscopy
SEM	standard error of the mean
SES	sirolimus-eluting stent
SG	Swan-Ganz
sLAIR-1	soluble leukocyte-associated immunoglobulin-like receptor-1
SMC	smooth muscle cell
STEMI	ST-elevation myocardial infarction
SV	stroke volume
SW	stroke work

SWT	systolic wall thickening
τ (tau)	isovolumic relaxation constant
TEE	transesophageal echocardiography
Th	T-helper
TLR	Toll-like receptors
TNF-α	Tumour necrosis factor alpha
Treg	regulatory T-cells
TTC	2,3,5-triphenyl tetrazolium chloride
TTE	transthoracic echocardiography
TUNEL	terminal deoxynucleotidyl transferase (TdT) dUTP nick end labeling
VF	ventricular fibrillation
VSMC	vascular smooth muscle cell
WT	wild-type
WT_{ES}	end systolic wall thickness

ACKNOWLEDGEMENTS / DANKWOORD

De afgelopen drieënhalf jaar heb ik met veel plezier en enthousiasme onderzoek gedaan naar de beïnvloeding van ontstekingsprocessen gedurende slagaderverkalking en na een hartinfarct. Het uiteindelijke resultaat – dit proefschrift – zou niet mogelijk geweest zijn zonder de hulp van collega's, vrienden en familie. Ik wil dan ook deze gelegenheid aangrijpen om iedereen die op enige manier hieraan heeft bijgedragen te bedanken, in het bijzonder de volgende personen.

Prof. dr. **Pasterkamp**, beste Gerard, bedankt voor het vertrouwen en de gelegenheid om op jouw afdeling een bijzonder gevarieerd en leerzaam promotietraject te doen. Tijdens ons eerste gesprek gaf je aan dat ik met ieder voorstel en plan bij je op de proppen kon komen, maar als ik het wilde uitvoeren moest ik wel met valide argumenten komen. Juist deze manier van denken waarbij de beargumentering telt, heb ik enorm gewaardeerd en heeft me op een andere manier naar veel dingen leren kijken, waarvoor dank.

Prof. dr. **Doevendans**, beste professor, het was een eer om onder uw directe supervisie een vernieuwend project te mogen opzetten. Uw manier van aanpakken en superviseren heeft me doen inzien dat er voor (bijna) alles een oplossing is en dat doorzetten, kritisch nadenken en buiten de gebaande paden gaan daarbij essentieel is.

Dr. **Höfer**, beste Imo, van een vrij formele kennismaking in het begin tot aan de borrel in New Orleans afgelopen jaar; ik kijk met veel plezier terug op mijn tijd met jou als copromotor. De afgelopen jaren heb ik veel van je geleerd wat betreft het schrijven van wetenschappelijke artikelen, het uitvoeren van experimentele dierstudies en cynisme als een vak op zichzelf. Je bent niet bang om je promovendi te laten zwemmen, maar houdt de voortgang in de gaten en zorgt er uiteindelijk voor dat het voltooien van het proefschrift niet in gevaar komt. Ik ben je enorm dankbaar voor je hulp op onverwachte momenten en je bijdrage aan alle projecten. Ik zal de telefoontjes missen (nu ook figuurlijk).

Dr. **Timmers**, beste Leo, al toen ik nog aan mijn laatste coschap Orthopaedie bezig was en je alleen van gezicht kende, sprak jij me terloops aan in het ziekenhuis over een prachtig promotietraject bij de Experimentele Cardiologie. De afgelopen drieënhalf jaar bewees jij dat je het bij het rechte eind had. Ondanks je druk werkzaam en sociaal leven maak je tijd wanneer dat nodig, belangrijk, of gewoon gezellig is. Je bent kritisch, behulpzaam en een bijzonder prettig iemand in de omgang en ik hoop dan ook dat we elkaar in de toekomst in de kliniek, wetenschap of gewoon met een goed glas wijn opnieuw zullen treffen.

Dr. **De Jager**, beste Saskia, als pleegmoeder en derde (officieuze) copromotor ben ook jij van grote waarde geweest voor de totstandkoming van dit proefschrift. Met de supervisie van twee projecten en de constructieve feedback op een groot deel van de andere, wil ik je bedanken voor je hulp, betrokkenheid en gezelligheid. Ik heb bewondering voor jouw persoonlijk contact met en de hulp aan eigen en andermans promovendi, en ik besef dat dit niet vanzelfsprekend is. Ik ben blij onderdeel te hebben uitgemaakt van de "Inflammatory cells group" en hoop van harte dat die nog lang en succesvol blijft voortbestaan.

De leden van de leescommissie, prof. dr. **De Kleijn**, prof. dr. **Chamuleau**, prof. dr. **Duncker**, prof. dr. **De Jong**, prof. dr. **Van Solinge**, hartelijk dank voor uw interesse in mijn proefschrift en uw bereidheid om zitting te nemen in de beoordelingscommissie.

Alle **coauteurs** wil ik hartelijk danken voor hun kritische opmerkingen en constructieve bijdragen aan de publicaties in dit proefschrift. In het bijzonder **Yolande**, bedankt voor je prettige en betrokken begeleiding, ik bewonder je gedrevenheid en je aandacht voor de persoon achter het werk. Misschien dat ook zonder rolstoel een koffie in de zon er een keertje in zit. **Dominique**, dank voor de samenwerking, het samen schrijven van de Dekker en de sporadische borrels. Jammer dat ik niet in Singapore heb kunnen komen werken, maar we komen elkaar in de wetenschappelijke wereld en daarbuiten vast nog weleens tegen. **Hester**, bedankt voor de epidemiologische input en je down-to-earth humor. **The Portland Group**, voor het verschaffen van de mogelijkheid om een van mijn projecten op een gedegen en goede manier uit te voeren.

Dr. **Arslan**, beste Fatih, nadat **Niek** op de Eerste HartHulp in het Meander hoorde dat ik op zoek was naar een wetenschappelijk onderzoeksproject, twijfelde hij geen moment en bracht me met je in contact. Na werktijd in het Diak en daarna bij vele broodjes Tricolore heb je me geïntroduceerd in de wetenschap en vele andere zaken daarbuiten. Je enthousiasme werkt aanstekelijk en ik bewonder je blijvende optimisme en doorzettingsvermogen. Ik kijk er dan ook naar uit om met je samen te werken in de kliniek.

Mirjam, ook al heb je altijd beweerd dat ik me de Western blots snel eigen maakte tijdens mijn stage, je moet toch af en toe hard gelachen hebben om mijn eerste (en misschien ook latere) stappen in het lab. Ik wil je enorm bedanken voor deze leuke tijd en alles dat je me geleerd hebt, zowel tijdens mijn stage als daarna.

Petra, nooit had ik gedacht dat we na die ene ijzerkleuring tijdens m'n wetenschappelijke stage nog zoveel zouden samenwerken en dat dat zo goed zou klikken. Ik bewonder je (vrijwel) altijd aanwezige enthousiasme, jouw gewoon-doen-mentaliteit en ook wel een

beetje hoe jij chaos in de orde weet te scheppen, en vice versa. Ik zal de vele gezellige uren snijden, kleuren, organiseren en praten over vanalles en nog wat missen!

Arjan, jij bent in het lab als een rots in de branding. Onvermurwbaar, helder, standvastig. Ik heb een mooie tijd gehad en zal met plezier terugdenken aan je hulp, droge humor en (vaak terechte) strenge blik. Daarnaast wil ik **Corina, Daniek**, **Esther, Julie, Loes, Noortje** en **Sander** bedanken voor de fijne manier waarop jullie tijd maken om iedere keer weer nieuwe PhDs (zeker artsen zoals ikzelf) op weg te helpen!

Ineke, bedankt voor de hulp bij de speciale verzoeknummers voor mijn ongebruikelijke projecten. Je regelt alles tot in de puntjes en je afwisselende reisverhalen maakten de bezoekjes meer dan de moeite waard. **Joukje** en **Irene**, bedankt voor het runnen van het secretariaat en jullie hulp!

Graag wil ik mijn (ex)collega-onderzoekers bedanken voor hun wetenschappelijke input, de vrijdagmiddagborrels, uitjes en weekendjes weg. Om te beginnen de **Toren**, mijn werkplek, een onuitputbare bron van inspiratie. **Geert**, m'n voorganger, voor het me wegwijs maken in het GDL en je inzichten in translationeel onderzoek. Ik heb je leren kennen als serieus, nauwgezet en professioneel, toch mooi om te zien dat ook jij in Barcelona je studentikoze flair nog niet helemaal kwijt was. **Crystel**, twee jaar naast elkaar werken met hetzelfde arbeidsethos en (bij vlagen) zwartgallige humor; ik heb veel gelachen, wil je bedanken voor je epi hulp en hoop dat we elkaar in de toekomst nog zullen treffen. **Jonne**, back-to-back op werk, ananas-muziek aan de mijn en opzwepende muziek aan jouw kant, wat kan ik nog meer zeggen? Je bent een schat van een mens en een supercollega! **Aisha**, na een wat onwennig begin volgde een prachtige tijd met flauwe grappen en van die tijd heb ik genoten; Nederland is zo slecht nog niet toch?! **Ingrid**, je bent een principieel, hartelijk en leuk persoon en dat maakt je tot een fijne collega. De tijd in de Toren was mooi, laten we dat doorzetten in het Antonius! **Ian**, door Imo gesuperviseerde borrels op vrijdagmiddag, op stap bij congres en de Ford Mustang op Miami Beach; drank was nooit ver weg, en bijkomend plezier ook niet. Sommige dingen ben ik vergeten, misschien is dat maar beter ook. De andere (ex)Torenbewoners: **Vince** (wijn, zeilen en werken, je combineert het altijd met gevoel), **Sander v/d Laan** (nee, genetica vind ik nog steeds moeilijk), **Saskia** (discussies en behulpzaamheid, en altijd enthousiast en opgewekt!), **Gideon** (meestal op vakantie, een prima eigenschap), **Marten** (filosofische discussies) en **Quirina** (trouw geadopteerd, altijd gezellig). Daarnaast in het UMC **Eveline** en **Gerdien**, zonder jullie epidemiologische kwaliteiten waren statistische verantwoording van beursaanvragen en het opvragen en traceren van een deel van de data veel minder vanzelfsprekend geweest.

Naast de Toren was ook het lab bij tijd en wijle mijn thuisbasis. **Judith**, ik heb veel geleerd van jouw kritische blik op wetenschappelijk onderzoek en wil je bedanken voor de serieuze en minder serieuze tijden in het lab, ons avontuur in Nice, Leiden, themafeesten en Thanksgiving in huis en op het dakterras. Je bent een goede onderzoekster en bovenal een leuke collega! **Lena**, voor de gezelligheid tijdens borrels en congressen in Nice en Parijs. **Peter-Paul** (vlotte, gezellige praatjes, privé en op het werk), **Erik** (een mooi begin), **Marian** (borrels en nooit uitgevoerde salsa), **John** (flauwe grappen), **Robin** (jouw monsterlijk gevoel voor feeding en sarcasme), **Daniëlle** (PCR, wat is dat?), **Dennie** (wereldproblematiek en wetenschap), **Frederieke** (neutrofielen en tequila) en **Hendrik** (samen kennis en bier slurpen, New Orleans was mooi!), **Danny** (altijd opgewekt en een fijne samenwerking!). Daarnaast **Alain**, **Emma** en **Patricia** voor de gezellige tijd in het lab. In het bijzonder wil ik mijn opvolgster **Evelyne** veel plezier en succes wensen met de prachtige combi grootproefdieronderzoek en labonderzoek!

Niet te vergeten, dank aan de Villa en alle klinische onderzoekers, in het bijzonder **René** voor de technische inzichten in onderzoek en alles wat het nachtleven in New Orleans te bieden heeft. Daarnaast **Freek,** voor de goede gesprekken, borrels op het dakterras en never-ending stapavonden.

Het grootste deel van mijn onderzoeksdata heb ik vergaard in het dierenlab. Dat zou niet mogelijk geweest zijn zonder de uitstekende kwaliteiten van **Evelyn**, **Grace**, **Joyce**, **Marlijn** en **Tinus**. Jullie zijn toppers in het vak en een prachtig team om mee samen te werken. Deze paar regels zijn niet genoeg om alle onmogelijke, grappige en onvoorspelbare situaties die zich voordeden tijdens en buiten onze experimenten om te beschrijven, maar ik heb mijn tijd met plezier met jullie doorgebracht en wil jullie bedanken voor de intensieve en mooie samenwerking. Ik zal het missen. Daarnaast wil ik graag **Maike** en **Ben** bedanken voor jullie hulp en het meedenken bij alle experimenten op afdeling Klein. **Paul**, jij benadert technische problemen via een alternatieve route en dat heeft me in mijn promotietijd op een andere manier naar zaken leren kijken, waarvoor dank. Ook alle andere medewerkers van het GDL en in het bijzonder **Jeroen**, **Koen**, **Harry** en **Fred**, wil ik bedanken voor jullie hulp en input, die ervoor heeft gezorgd dat dierexperimenten met een goede opzet en zo proefdiervriendelijk mogelijk werden uitgevoerd.

Alle **arts-assistenten** en **cardiologen** in **Amersfoort**, bedankt voor de prettige en leerzame omgeving waarin ik als semi-arts en nu als arts-assistent mag werken. Jullie zijn een leuk team met aandacht voor onderwijs en met liefde voor het vak. De tijd in Amersfoort vóór mijn promotieonderzoek is de reden dat ik nu zo enthousiast ben voor de cardiologie, en jullie zijn daar zonder meer debet aan.

Robert, ik denk met plezier terug aan de introductie in de cardiologie tijdens mijn studie. Je relativering, advies in lastige situaties, gevoel voor humor en kosmopolitische gedachtegoed tijdens telefoontjes, lunches en borrels maken je tot een waardevolle vriend.

De Leuvenclub, **Arian**, **Frank**, **Guido**, **Koos**, **Jan-Thijs**, **Lianne**, **Loes** en **Maria**, wat kan er in een paar jaar veel veranderen. De borrels en BBDs zijn niet meer zo frequent als tijdens de studie, maar de borrels en de weekenden die er zijn blijven als vanouds gezellig! Mijn **medisch dispuut**, wat me doet beseffen hoe onbezorgd het leven kan en af en toe ook moet zijn. **Pieter**, ook jaren na de middelbare school blijft een borrel en etentje als vanouds vertrouwd, mooi dat we nog steeds bevriend zijn! **Lisanne**, van het begin van geneeskunde tot samen promoveren, bedankt voor de gezelligheid bij etentjes en borrels. Bedankt **Rob**, voor de ontspannen ongedwongen avonden praten, wat drinken en soms een spel, dat simpel zo leuk kan zijn. **Nicoline**, ik ben je steun en hulp in het begin van mijn toch wel onvoorspelbare promotietraject niet vergeten en wil je daar nogmaals enorm voor bedanken. Ik ben ervan overtuigd dat jij – sympathiek, ambitieus en met een open blik – een prachtige promotie zult neerzetten en wens je veel plezier en succes met het vervolg.

Mijn jaarclub, **Bas**, **Gijs**, **Heuf**, **Hompus**, **Jan**, **Leenders**, **Ruit**, **Mike**, **TT**, **Vink**. Jullie zijn collectief verantwoordelijk voor mijn niet-geneeskundig bewustzijn, waarvoor dank, en het verlies van ettelijke hersencellen daarnaast, wat ik heb geaccepteerd. Een goede afleiding van mijn promotieonderzoek waren de borrels, etentjes, weekenden, lustrumreis en alles daarnaast. In het bijzonder wil ik nog bedanken **Gijs** en **Jan**, als advocaten van de duivel houden jullie me scherp door aangenomen waarheden in twijfel te trekken. Daarnaast dank voor de etentjes, borrels en minivakanties; we kunnen wellicht een vriendschap overwegen.

Koos, samen promoveren betekent ook het delen van frustraties, successen en ontspanning. Ik denk met plezier terug aan de tijd dat we samen in huis woonden, beiden promoverend. Ik waardeer de avonden, borrels, feestjes en de onverwachte dingen die we op de een of andere manier altijd meemaken. Door jou realiseer ik me dat meer doen op hoger tempo niet altijd beter is, en een ontspannen tijd is met jou als vriend nooit ver weg.

Medard en **Wouter**, met eenzelfde instelling, loyaliteit en gevoel voor humor zijn jullie dit promotietraject verantwoordelijk geweest voor ontspannen Skype-sessies, borrels, feestjes en vakanties. Serieuze en minder serieuze gesprekken, een etentje hier of weekend in Edinburgh, ik wil jullie bedanken voor de onvoorwaardelijke en goede vriendschap. De mooie tijden samen gedurende mijn promotietraject zullen zeker vervolg vinden in wat we ook gaan doen en ik kijk dan ook uit naar wat de toekomst zal brengen.

Mien femilie vaan alletwie de kante, veur de intresse en belangstèlling in mien oonderzeuk en de oongedwonge verjaordege en viziete. In het bezunder **Jo** & **Hanny**, aoch al zeet geer neet altied op de väörgroond aonwezeg, iech weet dat geer 't ganse trajèk höb gevolleg en iech höb 't altied leuk gevonde um uuch weer te zien en te spreke. **Opa**, veur eur onverminderd en altied aonwezege belangstèlling veur wat veer dege of oetgespook hadde. Iech weet zeker dat geer hei op de ierste rij had gezete en gruutser es eder aander waort gewees.

Yannick, Bruder, wie versjèllend veer aoch waore, iech dènk dat v'r mier gemeinsjappelek höbbe es dat v'r oets gedach hadde. Iech bewoonder de meneer wie ste diech ontwikkels en dien zake veur mekaar krijgs. Iech bin gruuts op wee stiech bis en boe se veur steis en wil diech bedaanke veur 't feit dat stiech – ondaanks mien grille – altied veerdeg steis. Aoch al is d'n tied beperk, iech weit zeker dat eus kontak allein mer beter zal weure.

Ariana, me alegre mucho que estamos juntos, un resultado directo de esta PhD trayectoria. No llevamos bien juntos y contigo yo puedo hablar y descansar, discutir y pasear, disfrutir y reír. Sé que la distancia no es siempre facil, pero me haces feliz y yo confio en la futura! TQB!

Pap & **mam**, zoonder uuch zou iech hei noets gestande höbbe. Iech wil uuch vaanoet de groond vaan mien hart bedaanke veur 't veurrech um in zoeë werm gezin op te greuje. Geer zeet 'n oetzunderlek gooj kombinasie en höb miech altied de käös en de kans gegeve um te doen wat iech leuk vond en miech te ontwikkele. Iech wil uuch bedaanke veur alles wat geer miech gelierd höb, veur uuch vertrouwe en uuche onveurwaardeleke steun. Veur alles wat heet gemaak dat iech bin wee iech noe bin.

LIST OF PUBLICATIONS

Gijsberts CM, Gohar A, **Ellenbroek GH**, Hoefer IE, de Kleijn DP, Asselbergs FW, Nathoe HM, Agostoni P, Rittersma SZ, Pasterkamp G, Appelman Y, den Ruijter HM. Severity of stable coronary artery disease and its biomarkers differ between men and women undergoing angiography. *Atherosclerosis. 2015;241(1):234-240*

Gijsberts CM, **Ellenbroek GH**, Ten Berg MJ, Huisman A, van Solinge WW, Asselbergs FW, den Ruijter HM, Pasterkamp G, de Kleijn DP, Hoefer IE. Routinely analyzed leukocyte characteristics improve prediction of mortality after coronary angiography. *Eur J Prev Cardiol. 2016;23(11):1211-1220*

Ellenbroek GH, Timmers L, Nijhoff F, Ligtenberg E, Rowland S, Post JA, Pasterkamp G, Hoefer IE. Improved Endothelial Coverage On CD34 Capturing Coronary Stents With Abluminal Sirolimus Coating. Ellenbroek, GHJM; Timmers, L; Nijhoff, F; Ligtenberg, E.; Rowland, S.; Post, J.; Pasterkamp, G; Höfer, IE. *AsiaIntervention. 2016;2(2):132-140*

Ellenbroek GH, van Hout GP, Timmers L, Doevendans PA, Pasterkamp G, Hoefer IE. Primary Outcome Assessment in a Pig Model of Acute Myocardial Infarction. *J Vis Exp. 2016;116;1-10*

Ellenbroek GH, van Puijvelde GH, Anas AA, Bot M, Asbach M, Schoneveld A, van Santbrink PJ, Foks AC, Timmers L, Doevendans PA, Pasterkamp G, Hoefer IE, van der Poll T, Kuiper J, de Jager SC. Leukocyte TLR5 deficiency inhibits atherosclerosis by reduced macrophage recruitment and defective T-cell responsiveness. *Sci Rep. 2017;7:1-10*

Ellenbroek GH, van Hout GP, de Jager SC, Timmers L, Vink A, Goldschmeding R, van der Kraak P, Pasterkamp G, Hoefer IE, Doevendans PA, Appelman Y. Radiofrequency Ablation of the Atherosclerotic Plaque: a Proof of Concept Study in an Atherosclerotic Model. *J Cardiovasc Transl Res. 2017*

van Hout GP, Bosch L, **Ellenbroek GH**, de Haan JJ, van Solinge WW, Cooper MA, Arslan F, de Jager SC, Robertson AA, Pasterkamp G, Hoefer IE. The selective NLRP3-inflammasome inhibitor MCC950 reduces infarct size and preserves cardiac function in a pig model of myocardial infarction. *Eur Heart J. 2017;38(11):828-836*

Gijsberts CM, **Ellenbroek GH**, ten Berg MJ, Huisman A, van Solinge WW, Lam CS, Asselbergs FW, den Ruijter HM, Pasterkamp G, Hoefer IE, de Kleijn DP. Effect of Monocyte-

to-Lymphocyte Ratio on Heart Failure Characteristics and Hospitalizations in a Coronary Angiography Cohort. *Am J Cardiol; accepted*

Ellenbroek GH, de Haan JJ, Brans MAD, van de Weg SM, Smeets MB, de Jong S, Arslan F, Timmers L, Hoefer IE, Doevendans PA, Pasterkamp G, Meyaard L, de Jager SCA. Leukocyte-Associated Immunoglobulin-like Receptor-1 is regulated in human myocardial infarction but its absence does not affect infarct size in mice. *Under revision*

Ellenbroek GH, Gremmels H, Timmers L, Michaelsson E, Gang L-M, de Kleijn DP, Doevendans PA, Pasterkamp G, Hoefer IE. Myeloperoxidase inhibition does not affect reperfusion injury in a pig model of acute myocardial infarction. *In preparation*

CURRICULUM VITAE

Jelte Ellenbroek was born on the 20th of December 1988 in Heerlen, The Netherlands. After graduating secondary school cum Laude at the St. Maartenscollege in Maastricht, he moved to Utrecht to start his medical studies. His last year's internship Cardiology in the Meander Medical Centre in Amersfoort initiated his fascination for the heart. He came into contact with dr. F. Arslan, who supervised and enthused him for scientific research through a scientific internship in the Laboratory of Experimental Cardiology. Subsequently, he worked as a research fellow in translational cardiology under supervision of prof. dr. G. Pasterkamp, prof. dr. P.A.F.M. Doevendans, dr. I.E. Höfer and dr. L. Timmers, focusing on inflammation in ischemic heart disease. This research resulted in the publication of multiple peer-reviewed articles and the composition of the present thesis. In June 2017, he started working at the department of Cardiology in the Meander Medical Centre in Amersfoort under supervision of dr. B.J.G.L. de Smet.